Helsinki University of Technology Control Engineering Laboratory

Espoo 2004 Report 142

RADIO RESOURCE SCHEDULING AND SMART ANTENNAS IN CELLULAR CDMA COMMUNICATION SYSTEMS

Mohammed S. Elmusrati

TEKNILLINEN KORKEAKOULU
TEKNISKA HÖGSKOLAN
HELSINKI UNIVERSITY OF TECHNOLOGY
TECHNISCHE UNIVERSITÄT HELSINKI
UNIVERSITE DE TECHNOLOGIE D´HELSINKI

Helsinki University of Technology Control Engineering Laboratory

Espoo August 2004 Report 142

RADIO RESOURCE SCHEDULING AND SMART ANTENNAS IN CELLULAR CDMA COMMUNICATION SYSTEMS

Mohammed S. Elmusrati

Dissertation for the degree of Doctor of Science in Technology to be presented with due permission of the Department of Automation and Systems Technology, for public examination and debate in Auditorium AS1 at Helsinki University of Technology (Espoo, Finland) on the 30th of August, 2004, at 12 noon.

Helsinki University of Technology

Department of Automation and Systems Technology

Control Engineering Laboratory

Distribution:
Helsinki University of Technology
Control Engineering Laboratory
P.O. Box 5500
FIN-02015 HUT, Finland
Tel. +358-9-451 5201
Fax. +358-9-451 5208
E-mail: control.engineering@hut.fi
http://www.control.hut.fi/

ISBN 951-22-7219-9 (printed)
ISBN 951-22-7220-2 (pdf)
ISSN 0356-0872

Picaset Oy
Helsinki 2004

Available on net at http://lib.hut.fi/Diss/2004/isbn9512272202

HELSINKI UNIVERSITY OF TECHNOLOGY P.O. BOX 1000, FIN-02015 HUT http://www.hut.fi	ABSTRACT OF DOCTORAL DISSERTATION

Author Mohammed Salem Elmusrati

Name of the dissertation

Radio Resource Scheduling and Smart Antennas in Cellular CDMA Communication Systems

Date of manuscript April 1, 2004	Date of the dissertation August 30, 2004
☑ Monograph	☐ Article dissertation (summary + original articles)

Department	Automation and Systems Technology
Laboratory	Control Engineering Laboratory
Field of research	Control Engineering
Opponent(s)	Professor Sven-Gustav Häggman and Professor Tapani Ristaniemi
Supervisor	Professor Heikki Koivo
(Instructor)	

Abstract

This thesis discusses two important subjects in multi-user wireless communication systems, radio resource scheduler (RRS) and smart antenna. RRS optimizes the available resources among users to increase the capacity and enhance the system performance. The RRS optimization procedure is based on the network conditions (link gain, interference,…) and the required quality of service (QoS) of each user. The CDMA system capacity and performance can be greatly enhanced by reducing the interferences. One of the techniques to reduce the interferences is by exploiting the spatial structure of the interferences. This could be done by using smart antennas which are the second subject of this thesis. The joining procedures of the smart antennas and RRS are discussed as well.

Multi-Objective optimization approach is proposed to solve the radio resource scheduler problems. New algorithms are derived namely the Multi-Objective Distributed Power Control (MODPC) algorithm, Multi-Objective Distributed Power and Rate Control (MODPRC) algorithm, and Maximum Throughput and Minimum Power Control (MTMPC) algorithm. Other modified versions of these algorithms have been obtained such as Multi-Objective Totally Distributed Power and Rate Control (MOTDPRC) algorithm, which can be used when only one-bit quantized Carrier to Interference Ratio (CIR) is available.

Kalman filter is proposed as a second technique to solve the RRS problem. The motivation to use Kalman filter is the known fact that Kalman filter is the optimum linear tracking device on the basis of second order statistics. The RRS is formulated in state space form. Two different formulations are introduced.

New simple and efficient estimation of the CIR is presented. The method is used to construct a novel power control algorithm called Estimated Step Power Control (ESPC) algorithm.

The smart antenna concepts and algorithms are discussed. New adaptation algorithm is proposed. It is called General Minimum Variance Distortionless Response (GMVDR) algorithm.

The joining of MIMO smart antennas and radio resource scheduler is investigated. Kalman filter is suggested as a simple algorithm to join smart antenna and multi-rate power control in a new way. The performance of the RRS of CDMA cellular communication systems in the presence of smart antenna is studied.

Keywords CDMA, power control, RRS, smart antennas, multi-objective optimization, Kalman filters

UDC	Number of pages 178
ISBN (printed) 951-22-7219-9	ISBN (pdf) 951-22-7220-2
ISBN (others)	ISSN 0356-0872

Publisher Helsinki University of Technology, Control Engineering Laboratory

Print distribution Helsinki University of Technology, Control Engineering Laboratory

☑ The dissertation can be read at http://lib.hut.fi/Diss/ 2004/isbn9512272202

This work is dedicated to the nearest persons to my heart my father ***Salem Elmusrati*** *and in loving memory of my mother,* ***Zakia Mohamed*** *(1947-1998)*

Preface

I joined Helsinki University of Technology, Control Engineering Laboratory in August 1999 as a postgraduate student. I started with postgraduate courses. In January 2001 I started the research work for Licentiate degree. I obtained the Licentiate degree in August 2002. In September 2002 I continued the research work presented in this thesis.

First of all I would like to thank my lord Allah who has helped me to complete this work. O my Lord! Guide me to the successful way that allows me to succeed in this life and in the hereafter.

I could not have completed my dissertation without the support and help from several people. First, my sincere appreciation goes to my advisor, Professor Heikki Koivo who has provided an invaluable support and encouragement over the past years.

I would like to thank all my Libyan friends here in Helsinki as well as in Libya and Canada for their care and encouragement.

My warm thanks for the reviewers of this thesis, Dr. Hassan El-Sallabi and Professor Tapani Ristaniemi for their constructive comments.

I wish to express my gratitude to all my friends and colleagues in the Control Engineering Laboratory, for creating a friendly and stimulating atmosphere. My especial thanks for Professor Riku Jäntti, Lic.Tec. Naser Tarhuni, Lic.Tec. Abdalla Abouda, Lic.Tec. Vesa Hasu and Lic.Tec. Matti Rintämäki for the fruitful scientific discussions about topics related to this thesis.

My deep appreciations are for all my family and relatives especially my brother Dr. Ahmed Elmusrati, for their support and encouragement.

This work would not have been achieved without the ultimate support, the great generosity, and the big lovingness of my wife *Nagat* and my daughters *Aia* and *Zakia*. I would like to say that no words can express my cordiality feeling towards them.

This thesis has been supported by a grant from Garyounis University – Benghazi-Libya and partially from Exsite project. The author has received grants that are gratefully acknowledged, from NOKIA FOUNDATION and ELLA JA GEORG EHRNROOTIN Foundation.

ABBREVIATIONS

3G	Third Generation
B-BPC	Bang-Bang Power Control Algorithm
BS	Base Station
CDF	Cumulative Distribution Function
CDMA	Code Division Multiple Access
CIR	Carrier to Interference Ratio
CN	Core Network
CPC	Centralized Power Control
CMTTP	Centralized Minimum Total Transmitted Power Algorithm
CSN	Circuit Switched Network
CSOPC	Constrained Second Order Power Control Algorithm
DBA	Distributed Balancing Algorithm
DCPC	Distributed Constrained Power Control Algorithm
DPC	Distributed Power Control Algorithm
DS-CDMA	Direct Sequence – CDMA
EN	External Network
ESPC	Estimated Step Power Control
FDMA	Frequency Division Multiple Access
FDPC	Fully Distributed Power Control Algorithm
FMA	Foschini's and Miljanic's Algorithm
FSPC	Fixed Step Power Control
GSM	Global System for Mobile Communication
IP	Internet Protocol
ISDN	Integrated Services Digital Network
QoS	Quality of Service
LMS	Least Mean Square
LS-DRMTA	Least Square De-spread Re-spread Multi-target Array

LRPC	Lagrangian Multiplier Power Control
MC-CDMA	Multi-Code-CDMA
MIMO	Multiple Input Multiple Output
MMSE	Minimum Mean Square Error
MS	Mobile Station
MO	Multi-Objective
MODPC	Multi-Objective Distributed Power Control Algorithm
MOTDPC	Multi-Objective Totally Distributed Power Control Algorithm
MODPRC	Multi-Objective Distributed Power and rate Control Algorithm
MOTDPRC	Multi-Objective Totally Distributed Power and rate Control Algorithm
MTMPC	Maximum Throughput and Minimum Power Control
MTPC	Maximum Throughput Power Control
MVDR	Minimum Variance Distortionless Response
GMVDR	General Minimum Variance Distortionless Response
Pdf	Probability density function
PSN	Packet Switched Network
PSTN	Public Switched Telephone Network
RNC	Radio Network Controller
RLS	Recursive Least Square Algorithm
RRM	Radio Resource Management (or Manager)
RRS	Radio Resource Scheduler
SINR	Signal to Interference and Noise Ratio
SPC	Selective power control algorithm
TDMA	Time Division Multiple Access
VSL-CDMA	Variable-spreading length-CDMA
UMTS	Universal Mobile Telecommunication System
UTRAN	UMTS Terrestrial Radio Access Network
UE	User Equipment
WCDMA	Wideband Code Division Multiple Access

CONTENTS

CHAPTER ONE

INTRODUCTION

Less than fifteen years ago, the main challenges in mobile communications were how to connect people wherever they were and providing cheap services as well as cheap and small handsets. Since ambition is one of human characteristics, these challenges have gradually been met and surpassed. The current challenges are how to provide multimedia communication, exploring the unlimited information of the Internet, watching TV channels, and many other services on small and handy mobile phones. The services to the customers should be cheap and of high quality. To reach these novel services, the first step is to use a multiple access method that can support high data rate transmission over wireless and mobile channels. Wideband Code Division Multiple Access (WCDMA) has been chosen to be the multiple access technique for the 3G mobile communication system. The reasons of selecting WCDMA will be discussed in section 1.3.

To achieve cheap services, the mobile communication systems should be able to support a large number of users simultaneously. The users in WCDMA systems are usually sending messages at the same time and with the same bandwidth but with different codes. The main noise source of each user is the interference signals from other users due to the imperfect orthogonalization of the spreading codes and the channel dispersion characteristics such as multi-path and Doppler shift. This interference limits the capacity of the mobile communication system. To increase the capacity and to enhance the system performance one should optimize the usage of the available radio resources. The system performance can further be enhanced by exploiting the spatial distribution of users to reduce the interference using smart antennas.

In CDMA cellular systems, the base stations (BS) represent the access points of the mobile stations (MS). The communication from the BS to the MS is called downlink (DL) and from MS to BS is uplink (UL). Without loss of generality only the uplink communication is considered in this thesis. The radio resource management is very important in multi-user communication systems. It regulates the sharing of the radio resource between users. There are two main controllable radio resources: the transmitted

power and data rate. The transmitted power should be adjusted to the minimum power required to achieve the target Quality of Service (QoS). The target QoS is a list of conditions which should be fulfilled to obtain successful communication. The transmitted data rate, maximum packet delay, and the packet loss probability are examples of the QoS list. The adjusting process of power is called power control. Power control is not an easy task due to the time-varying fluctuations in the channel gain as well as the lag in information about the total channel situation. If the data rate can be adjusted as well, we should use a combined power and rate control algorithm. S*patial filtering* is an important interference management item which can considerably enhance the communication system performance. The transmitted signals from mobile stations arrive to the base station antenna in multi-path fashion and in different directions of arrivals (DoA). The DoA of each multipath component of each MS depends on its location as well as the multi-path characteristics. Using spatial filtering, one can enhance the reception of the receiving antenna from certain DoAs and attenuate the others. This means, if the DoA of the required user can be estimated, we can enhance the Signal to Interference Ratio (SIR) by reducing the interference signals which have different DoAs. Spatial filtering is possible by using multi-antenna arrays with adaptive weights (smart antennas). *Multi-user detection methods* are utilized as well to further enhance the system performance. The code structures of the users are employed to reduce the co-channel interference. It should be noticed that for a large number of users the optimum multi-user detection method is computationally very intensive.

In this thesis, we will focus on the radio resource management and smart antennas. Although the topics are treated in a general way, more attention is given to the UMTS standards.

1.1 Network Architecture of 3G mobile communication system

A simplified network architecture of the Universal Mobile Telecommunication System (UMTS) is shown in Figure 1.1 [64]. As seen in Figure 1.1 the UMTS Terrestrial Radio Access Network (UTRAN) has two interfaces. The first interface is with User Equipment (UE) using WCDMA. The second interface is with the Core Network (CN). The UTRAN consists of Base Stations (BS) and Radio Network Controllers (RNC). The core network is the interface between UTRAN and the External Network (EN). It consists of two

networks, the Circuit Switched Network (CSN), which is the same as the old GSM switching network and the packet switched network (PSN), which is based on Internet Protocol (IP) address. The CSN is connected to the conventional switching systems, such as Public Switched Telephone Network (PSTN) and Integrated Services Digital Network (ISDN).

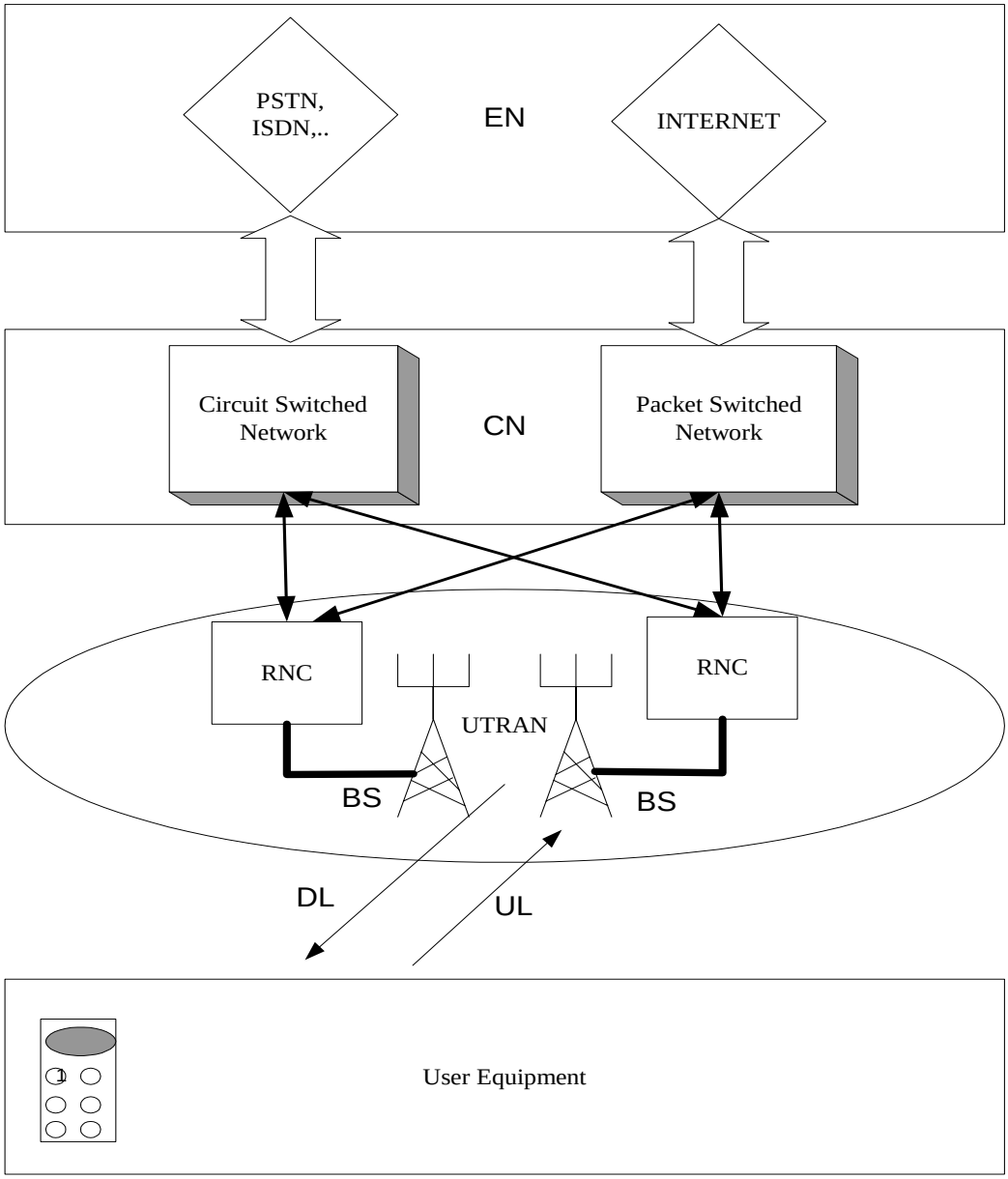

Figure 1.1 UMTS network architecture

The PSN, on the other hand, is connected to the Internet network [64]. The transmitted power controls in uplink and downlink are very important issues in CDMA systems. Two main types of power control are used with UMTS networks. The closed (fast) loop power control regulates the transmitted power of all UE to minimize the interference between them. The control command is updated at the rate of 1500 Hz. The outer (slow) loop power control updates the target Signal to Interference and Noise Ratio (SINR), which is determined by Radio Network Controller (RNC). Detailed description of the power control concept and algorithms will be introduced in Chapter 2. The data rate can be updated as well as explained in Chapter 3.

1.2 Radio Resource Management (RRM)

In the UMTS architecture, each BS has a radio resource management module that attempts to preserve the traffic's QoS requirements across the radio access network (RAN) [82]. The QoS attributes are usually specified in terms of bit error rate (BER), data rate, delay, and so on. The main role of the RRM is to assign resources to users according to their QoS requirements. As shown in Figure 1.2, the RRM mission starts by performing connection admission control (CAC). Since the decision is based on resource availability, CAC consults the Radio Resource Scheduler (RRS) before accepting or rejecting the requested call [82]. Upon call acceptance, the traffic classifier (TC), another RRM component, categorizes the incoming traffic according to its QoS specification, which is typically included in each packet header. Data flows are then directed to a corresponding queue according to its QoS field. Each QoS class (QoSc) is represented by at least one queue. Finally, the traffic dispatcher (TD) drains the multiple queues according to some priority logic after getting the assigned radio resources from the RRS, which relies on the channel conditions and the requested QoS in its response. Based on the above, it is evident that RRS bears a great responsibility in having a successful RRM [82].

In a CDMA network the RRM has two important radio resources to control: MS transmitting power and data rate. Combining the transmitted power control and data rate control in an optimum way is a very important issue as will be shown in Chapter 3. One of the important goals of the multiple access systems, such as in the UMTS, is to maximize the number of simultaneous users. If each MS is assigned the minimum resources necessary for meeting or exceeding its QoS requirements, the capacity of the

system will be maximized [82]. Another important goal for non-voice users is to maximize their data rates. All these issues will be discussed in more details in Chapters 2 and 3.

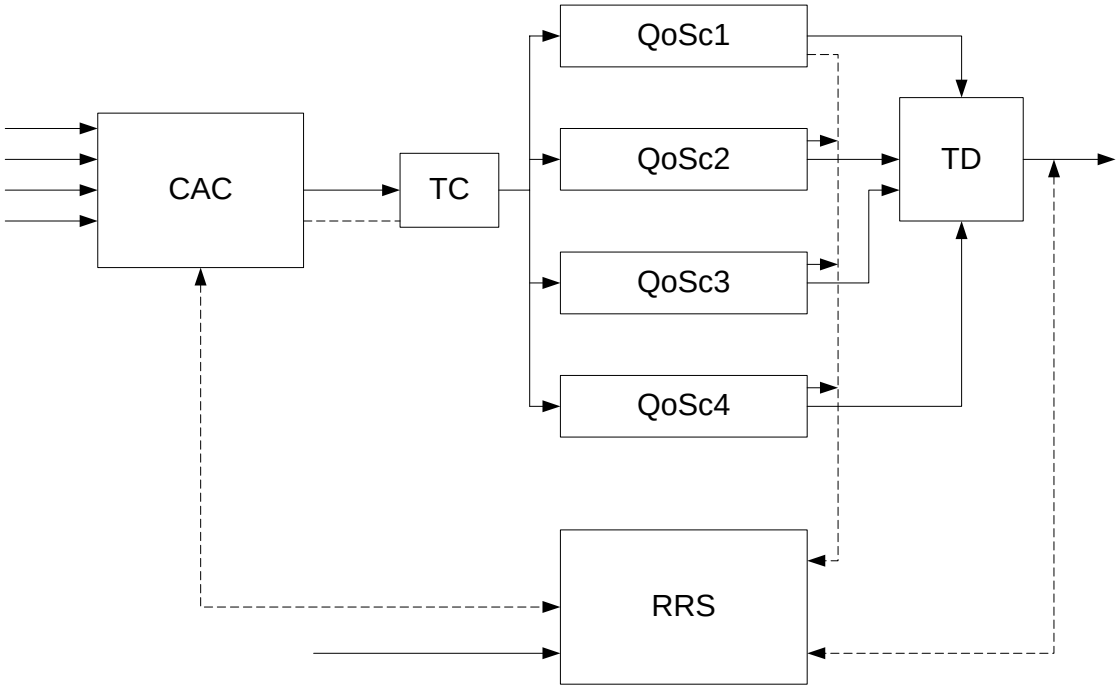

Figure 1.2. Block diagram of the Radio Resource Manager [82].

1.3 Wideband Code Division Multiple Access

In multi-user environment, it is very important to separate the users, so that they are not interfering with one another. For example, users of Frequency Division Multiple Access (FDMA) are separated by allocating certain frequency bands for each user. In Time Division Multiple Access (TDMA), each user has a repeated time slot. In CDMA all users share simultaneously the same bandwidth, but with different codes, as is illustrated in Figure 1.3. CDMA has many advantages over TDMA or FDMA technologies. CDMA techniques are wideband in the sense that the entire transmission bandwidth is shared between all users at all times. This is accomplished by spreading the baseband signals onto a bandwidth much larger than its actual bandwidth. This spreading is achieved by using spreading codes. The spreading leads to simpler statistical multiplexing without the explicit scheduling of time or frequency slots, universal frequency reuse between cells, and graceful degradation of quality near congestion. It exploits the frequency selectivity of the channel (which uses a rake receiver that resolves individual multi-path components

and then coherently combines them) to avoid the harmful effects of deep fades that afflict narrowband systems, and the exploitation of silence periods in voice conversations.

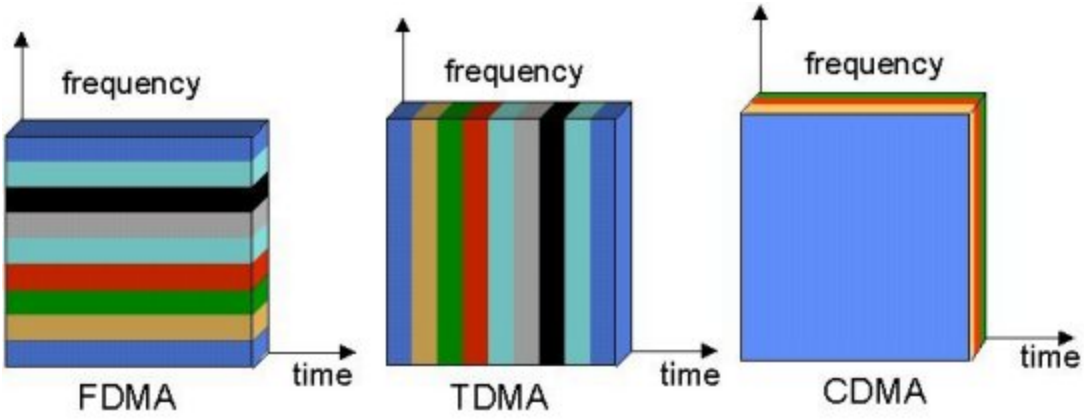

Figure 1.3. Principle time and frequency division in FDMA, TDMA and CDMA.

It is then possible in the CDMA environment to provide unique benefits for cellular applications [61], [63]. There is no single, universally accepted, definition of Wideband CDMA [41]. In fact, one may find two commonly accepted definitions. One is based on system parameters such as *chip rate*, or bandwidth expressed as a fraction of the center frequency; and the other is based on the characteristics of the channel. If the bandwidth of the signal exceeds the coherence bandwidth of the channel, the term Wideband CDMA is used. Yet there is no distinct bandwidth threshold that separates the narrowband CDMA from the Wideband CDMA [41]. Currently the term WCDMA is used for the UMTS standard.

1.4 Channel characteristics of mobile radio systems

The modulation type, the carrier frequency and the coding/decoding methods depend on the characteristics of the channel. The channel is the media between the transmitter and the receiver. We need to know, or at least to estimate, its behaviour to design successful communication system. Unfortunately, most of radio channels have characteristics that vary over time, i.e. they are *time-varying channels*. This complicates channel parameter estimation. The problem is much more acute in mobile channels due to the nature of the

mobility of the mobile terminals. Figure 1.4 shows an overview of fading channel manifestations [65]. From Figure 1.4, the large-scale fading manifestation is shown in blocks 1, 2, and 3. This phenomenon is affected by prominent terrain contours (hills, forests, billboards, buildings, etc.) between the transmitter and the receiver. The receiver is often represented as being *shadowed* by such obstacles. This phenomenon can be modelled as a mean-power loss using a *path loss exponent n*, and a *random variable with log-normal distribution*. The small-scale fading refers to a rapid fluctuation in the received signal due to very small movement of the mobile. The reason is that the received signal is usually coming through different paths. Every path causes a time delay, which changes the phase. The received signal is the complex sum of the signals from all paths. Then if the path signals are in-phase, the received signal power will achieve its highest value. If the path signals are out of phase, the received signal power will be at the lowest value. The received signal power may vary as much as 40 dB, when the mobile moves only a fraction of a wavelength [12]. A more detailed description of Figure 1.4 is presented in [65].

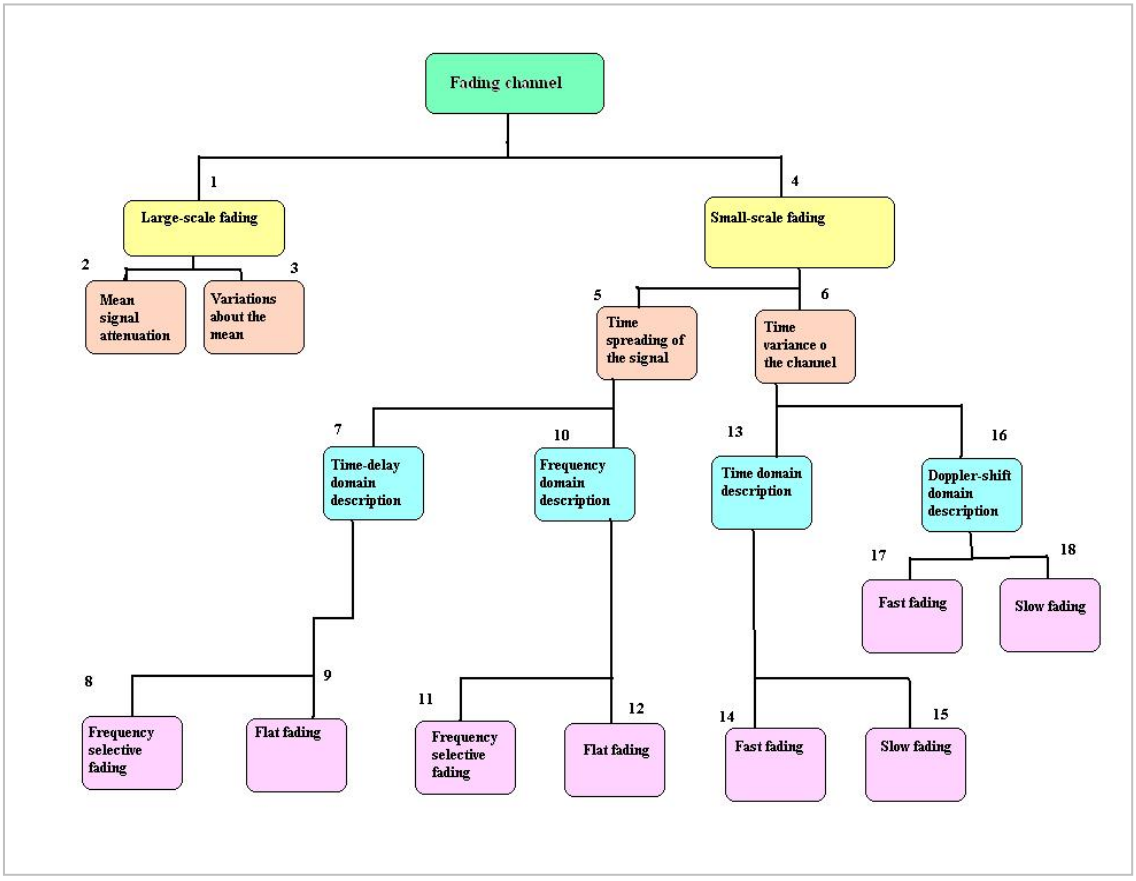

Figure 1.4. Overview of fading channel.

1.5 Contributions

In this thesis we focus on power control algorithms, combined power and rate control, smart antennas and joining radio resource scheduler and smart antenna. The contributions can be classified from the methodology point of view under three main categories as follows:

A. The Multi-Objective Optimization

I. **Multi-objective distributed power control (MODPC) algorithm.** Power control problem is first formulated in a new way, as a multi-objective (MO) optimization problem. In the formulation, dynamical behaviour of the mobile communication channel is also taken into consideration. The problem is then transformed into a single-objective optimization problem and solved. Certain properties of the convergence are proved. Simulation studies show the superiority of the proposed power control algorithm over several other well-known power control algorithms. These topics are presented in Section 2.4.8

II. **Mathematical formulation of the RRM problem in Multi-Objective framework.** New mathematical formulation of the RRM problem is proposed. In the literature the RRM problem is treated as a single optimization problem with constraints. We propose to use multi-objective optimization to solve the RRM. More flexible and sophisticated solutions can be obtained. These topics are covered in Section 3.8.

III. **Multi-Objective distributed power and rate control (MODPRC) algorithm.** This topic is an application of the MO optimization in RRM. The (MODPRC) algorithm is a distributed algorithm and the simulations show that its performance outperforms many other combined power and rate control algorithms. The algorithm is based on minimizing a multi-objective definition of an error function. Three objectives are defined. The objectives are 1) minimizing the transmitted power, 2) achieving at least the target CIR which is defined at the minimum data rate, and 3) achieving the maximum CIR which is defined at the maximum data rate. The topic is covered in Section 3.8.1.

IV. **Centralized algorithm for the tradeoff between total throughput maximization and total power minimization (MTMPC) algorithm.** This algorithm is another application of the MO optimization in RRM field. Power control algorithm for total throughput maximization is proposed in [74]. In the proposed algorithm, we use the same throughput maximization objective, but an added objective for power minimization is used. The Multi-objective optimization problem is solved using the *weighting method*. A centralized power control algorithm is obtained. This topic is treated in Section 3.8.3.

V. **Multi-Objective Totally Distributed Power Control (MOTDPC) algorithm.** In reality, only a quantized version of the estimated CIR is available at the mobile station. Therefore, MODPC is modified to take into consideration the quantized CIR. This algorithm uses the concept of ESPC algorithm to estimate the CIR. The topic is presented in Section 2.4.8.1

VI. **Multi-objective totally distributed power and rate control (MOTDPRC) algorithm.** This algorithm is the same as MODPRC algorithm but with estimated CIR. We use the same concept as in ESPC to estimate the CIR from the ON-OFF commands of power control. The performance of the system is investigated by simulations. The topic is covered in Section 3.8.2

VII. **Soft dropping power control.** If the CIR target cannot be achieved for every user, then power control becomes infeasible. In this case some connections should be dropped from the current link. The MODPC is modified to be used for connection dropping. The topic is presented in Section 2.4.8.2

VIII. **Joining algorithms for smart antenna and RRS.** The main concept of joining smart antenna and RRS using MO optimization is summarized in Section 5.3.

B. Kalman Filters

IX. **Kalman distributed power control.** Kalman filter is proposed to be used in power control of CDMA mobile communication systems. The motivation to use Kalman filter is the known fact that Kalman filter is the optimum linear tracking device on the basis of second order statistics [20]. The topic is presented in Section 2.4.9.

X. **Multi-rate distributed power control using Kalman filters.** We propose a new multi-rate distributed power control algorithm based on Kalman filter. The algorithm is a direct extension of the Kalman power control algorithm. This topic is treated in Section 3.9

XI. **Minimum variance distributed power and rate control.** This algorithm is a different formulation to solve the RRM problem using Kalman filters. The topic is discussed in Section 3.9.1.

XII. **Joining smart antenna and RRS using Kalman filters.** Simple method to join smart antenna and power control using Kalman filter is proposed in Section 5.3.1.

C. Others

XIII. **Estimated step power control (ESPC) algorithm.** We propose a new method to estimate the uplink Carrier to Interference Ratio (CIR) using the power control ON-OFF commands at the MS. The estimated CIR is used to adjust the transmitted power from the mobile terminal using the Distributed Constrained Power Control (DCPC) algorithm. The main advantage of the proposed algorithm is that it can improve the performance of power control without any increase in power control signalling. This method has been used with other algorithms throughout this thesis. The algorithm is explained in Section 2.4.7

XIV. **General MVDR algorithm for frequency selective channels.** The minimum variance distortionless response (MVDR) is a very well known algorithm to obtain the optimum weight vector which maximizes the output signal to interference and noise ratio (SINR) of multiple antennas. In this part we generalize the algorithm to be used in multi-path and frequency selective channels to capture the different path signal components. The topic is covered in Section 4.3.1. Also the influence of using GMVDR algorithm on the upper channel capacity is treated in Section 4.4.4.

XV. **Convergence speed comparison of power control algorithms.** The convergence speed is an important factor in the selection of the optimum power control algorithm for a wireless communication system. In this part we introduce

a simple method to compare the convergence speed of power control algorithms. So far most of the studies on power control have used spectral radius of the corresponding iteration matrix as a convergence speed measure. However, this method is only applicable to linear algorithms. In addition, although always possible, finding the spectral radius can sometimes be tedious. We show in Section 2.5 that a simple differentiation of the power control algorithm can be used to compare the convergence speed of algorithms.

XVI. **Influence of smart antenna systems on the performance of radio resource scheduling in CDMA cellular systems.** In this part the joining procedure between the RRS and the adaptive antenna is explained. A pseudo-code algorithm to join the smart antenna with RRS is introduced. Chip level simulations are performed to evaluate the influence of a smart antenna on CDMA cellular systems. More details are given in Section 5.3.2.

1.6 Outline of the thesis

The concepts of power control theory in cellular communication systems are explained in Chapter 2. Different algorithms from literature as well as the new proposed algorithms and intensive simulations are presented also in Chapter 2. Combined algorithms of power and rate control are presented in Chapter 3. The smart antenna concept and different adaptation algorithms are introduced in Chapter 4. The joining procedures of radio resource scheduler algorithms and smart antennas are discussed in Chapter 5. Finally, our conclusions and remarks are given in Chapter 6. Appendix 1 summarizes basics of multi-objective optimization. Some extra proofs for the spectral radius comparisons are presented in Appendix 2.

CHAPTER TWO

POWER CONTROL ALGORITHMS

2.1 Introduction

Power control is essential in mobile communication systems, because it can mitigate the near-far problem, increase the system capacity, improve the quality of service, increase the battery life of the mobile terminal, and decrease the biological effects of electromagnetic radiation.

The objective of the power control algorithm is to keep the transmitted power (for the mobile station in the uplink power control and for base-station in downlink power control) at the minimum power required to achieve the target Quality of Service (QoS) in the system.

The QoS of a communication system is a list of requirements to be fulfilled by the operator. Some of these terms are the bit error rate (BER) , the data rate, the packet delay, the outage probability, etc. In this Chapter we will consider only the BER as an indication of the QoS. The BER is directly mapped (depends on modulation type) to the CIR. The mapping of fixed CIR to BER is well known and can be found in classical digital communication books such as [24] and [50]. For more real situation when the CIR is random variable, one should average the BER over the probability density function (pdf) of the CIR. The resultant mapping is usually rather difficult [107]. There are different approximations for CDMA channels [107],[111]. To generalize as well as to simplify the analysis we will use CIR as an indication of the QoS. Multi-rate power control will be covered in the next Chapter.

Before giving a precise mathematical formulation for the optimum power control problem, some notations and definitions are given. Let the *transmitted power control* vector be a Q-dimensional column vector $\mathbf{P} = [P_1, P_2, .., P_Q]'$, where P_i is the transmitted power of user i. CIR of user i is denoted by Γ_i .

Mathematically the power control problem is formulated as follows:

Find the power control vector **P** that minimizes the cost function

$$J(\mathbf{P}) = \mathbf{1}'\mathbf{P} = \sum_{i=1}^{Q} P_i \tag{2.1}$$

subject to

$$\Gamma_{ki} = \frac{P_i G_{ki}}{\sum_{\substack{j=1 \\ j \neq i}}^{Q} P_j G_{kj} + N_i} \geq \Gamma_{\min},\ i = 1,...,Q,\ k = 1,...,M, \tag{2.2}$$

and

$$P_{\min} \leq P_i \leq P_{\max},\quad \forall i = 1,\cdots,Q, \tag{2.3}$$

where

$\mathbf{1}'$ = [1, …, 1] ,

Q = Number of mobile stations.

M = Number of base stations.

G_{kj} = Channel gain between mobile station *j* and base-station *k*, as shown in Figure 2.1.

N_i = The average power of the additive noise at receiver *i*. Because it results from many sources, it is convenient to represent it as Gaussian white noise with zero mean.

P_{max} = Maximum power, which can be handled by the transmitter.

P_{min} = Minimum power, which can be handled by the transmitter.

$\Gamma_{\min}$ = Minimum predefined CIR.

For simplicity, we will refer to user *i* without using the subscript of its assigned base station. For example, we will use Γ_i instead of Γ_{ki}. If the CIR of user *i*, $\Gamma_i < \Gamma_{\min}$, and the transmitted power $P_i = P_{max}$, then user *i* (or some other users) has to be dropped from this link. Another important factor is the target CIR $\left(\Gamma^T\right)$. It should be noted that the superscript (*T*) means (Target). The dash (′) is used to indicate transpose operation. The difference between the target CIR and the minimum predefined CIR is called CIR margin. The target CIR value is determined by the outer-loop power control to achieve certain QoS in the cell. The target CIR could be different from user to user because it depends on the type of service requested by the user. The multi-services power control will be covered in the next chapter.

The optimization problem of (2.1)-(2.3) seems to be a simple linear programming problem, but this is not totally true due to the fact that the channel gain G_{kj} and the additive noise N_i are not accurately known. The parameters, such as the channel gain, the noise and the number of users are time varying, and they change in a random manner. Since the power control algorithm should be able to regulate the transmitted power in real time, it should be fast convergent and robust. Power control subject is classified in the literature into open-loop and closed-loop power control, signal-strength based and CIR-based power control, centralized and distributed power control, deterministic and stochastic power control, and so on. A brief review of the most well-known power control algorithms is given next.

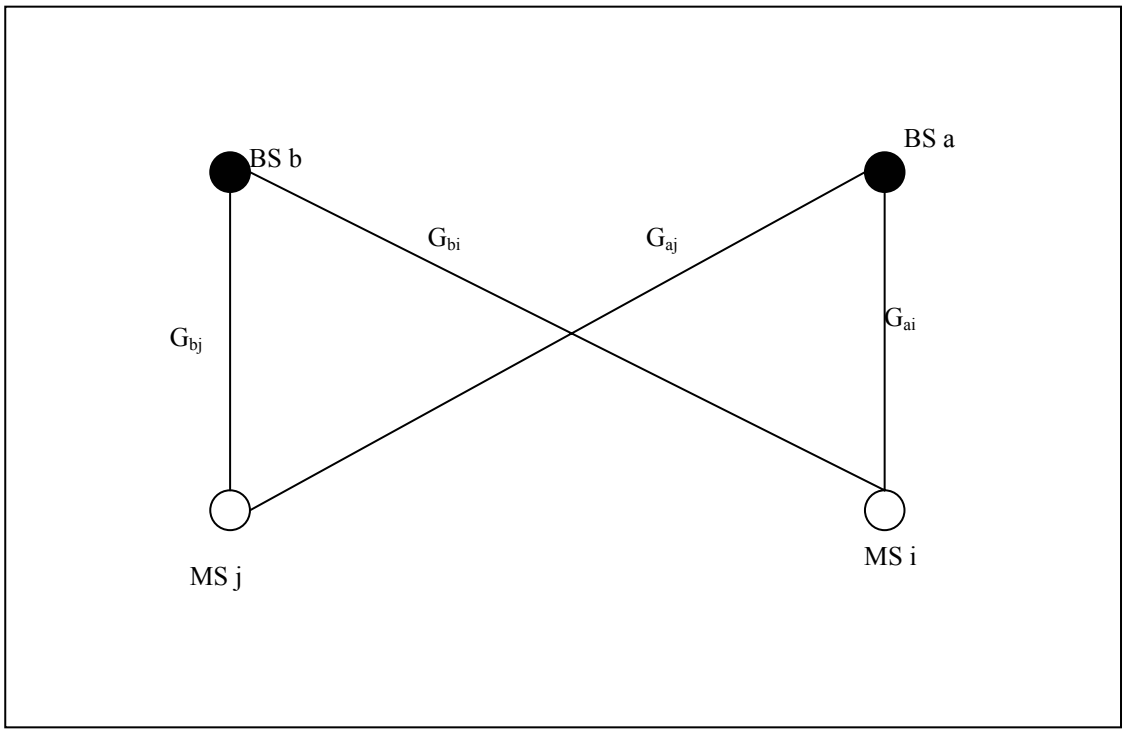

Figure 2.1. Link geometry and link gain model

2.2 Centralized power control

If the information of the link gains and the noise levels are available for all users, then the centralized power control algorithm can be applied to solve the power control problem given in (2.1)-(2.3) perfectly [56]. For noiseless case, $N_i = 0$, (2.2) becomes

$$\Gamma_i = \frac{P_i G_{ki}}{\sum_{\substack{j=1 \\ j \neq i}}^{Q} P_j G_{kj}} \geq \Gamma_{\min}, \quad i = 1,...,Q, \quad k = 1,...,M. \tag{2.4}$$

Equation (2.4) can be written in a matrix form as

$$\mathbf{P} \geq \Gamma_{\min} \mathbf{H} \mathbf{P} \tag{2.5}$$

where **H** is a nonnegative matrix with the following elements

$$(\mathbf{H})_{ij} = \begin{cases} 0 & \text{i} = \text{j} \\ \dfrac{G_{kj}}{G_{ki}} > 0 & \text{i} \neq \text{j} \end{cases} \tag{2.6}$$

The problem is how to find the power vector **P>0** such that (2.5) is satisfied. Equation (2.5) can be written as

$$\left[\frac{1}{\Gamma_{\min}} \mathbf{I} - \mathbf{H} \right] \mathbf{P} = \mathbf{0} \tag{2.7}$$

The inequality is dropped in (2.7), since equality sign holds for the minimum power vector. It is known from linear algebra that a nontrivial solution of (2.7) exists if and only if $\left[\frac{1}{\Gamma_{\min}} \mathbf{I} - \mathbf{H} \right]$ is a singular matrix. It is seen from (2.7) that this happens, if $\frac{1}{\Gamma_{\min}}$ is an eigenvalue of **H,** and the optimum power vector **P** is the corresponding eigenvector. The power vector **P** should be positive. Perron-Frobenius theorem [5] says that for a nonnegative and irreducible QxQ matrix **H** there exists a positive vector **P** associated with the maximum eigenvalue

$$\lambda^* = \rho(\mathbf{H}) = \max_i |\lambda_i|, \quad i = 1,...,Q, \tag{2.8}$$

where λ_i is the i^{th} eigenvalue of the matrix **H**, and $\rho(\mathbf{H})$ is the *spectral radius* of matrix **H.** Based on this the maximum achievable CIR can be expressed as

$$\gamma^* = \frac{1}{\lambda^*} = \frac{1}{\rho(\mathbf{H})} \tag{2.9}$$

Now by considering the additive white noise at the receivers, (2.2) can be written in a matrix form as

$$[\mathbf{I} - \Gamma^T \mathbf{H}]\mathbf{P} \geq \mathbf{u} \tag{2.10}$$

where **u** is a vector with positive elements u_i specified by

$$u_i = \frac{\Gamma^T N_i}{G_{ki}}, \quad \text{i} = 1, \ldots, \text{Q}, \text{k} = 1, \ldots, \text{M}. \tag{2.11}$$

It can be shown [5] that if $\Gamma^T < \frac{1}{\rho(\mathbf{H})}$, then the matrix $[\mathbf{I} - \Gamma^T \mathbf{H}]$ is invertible and positive.

In this case, the power vector **P***

$$\mathbf{P}^* = \left[\mathbf{I} - \Gamma^T \mathbf{H}\right]^{-1} \mathbf{u} \tag{2.12}$$

is the solution of the optimization problem posed in (2.1)-(2.3).

There are neither guarantees that $\Gamma^{\mathrm{T}} \geq \gamma^*$ nor guarantees that the power vector $\mathbf{P}^*$ is within the constraints (2.3). In this case *a removal algorithm* will be needed to reduce the number of users in the cell like the *Stepwise Removal Algorithm* (SRA) [1].

Power control in CDMA mobile communication system will be illustrated by the following example. In the example we assume additive Gaussian white noise radio channel with propagation loss and shadowing. The received signal power at base station *j* due to user *i* is assumed to follow power law

$$\hat{P}_{ji} = P_i \frac{10^{S_{ji}}}{d_{ji}^{\alpha}}, \tag{2.13}$$

where S_{ji} is the shadowing variable in the path from *i*-th mobile station to *j*-th base station and it is assumed to be a random variable with log-normal distribution and 5 dB variance. d_{ji} is the distance between user i and base station *j*. We assume that all the users are uniformly distributed in a circular cell with radius of *r* = 500 m. The loss factor α is assumed to be constant for all users with α=4. Also the variance of the additive white noise is assumed to be -120dBm. In the simulations we have calculated the number of users, which can achieve the specified CIR. Figure 2.2 shows the number of users (y-axis) with the achieved CIR (x-axis) in two cases. In the first case centralized power control and in the second case no power control is used. The improvement in the channel capacity is clear, when power control has been used. If the target CIR is –15 dB in Figure 2.2, then the number of users, which can be supported using centralized power control, is 33. Only 3 users can be supported, when no power control is used.

The result of this example can not be generalized because it shows one scenario of the mobile communication system. It gives only a general impression of the importance of using power control in CDMA cellular communication systems.

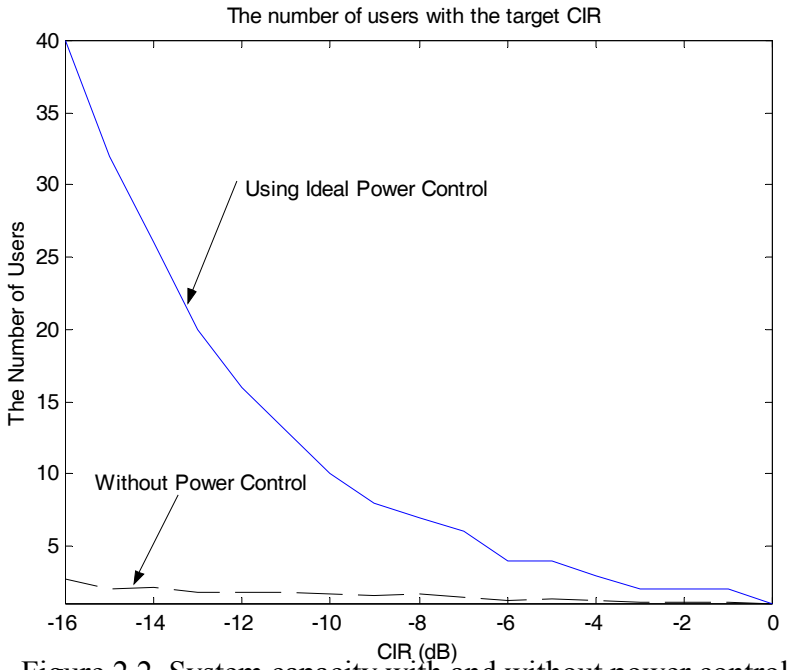

Figure 2.2. System capacity with and without power control

The computation of the optimum power vector using the centralized power control algorithm needs the link gains of all users. This is computationally intensive; moreover it is not feasible particularly in multi-cell cases. Therefore it is common in practice to use a distributed power control technique. Centralized power control can be applied to test the upper bound performance using a distributed technique in simulation.

2.3 Two-User power control

The power control problem can be described graphically for a simple case. Consider two users within one cell. The first user has the link gain $G_1(t)$ and the second user the link gain $G_2(t)$. The link gains are functions in time due to the dynamical behavior of the mobile communication system. Assume that N is the average noise power. Recall the optimum power control problem (2.1)-(2.3). The problem is to determine the minimum transmitted power vector that satisfies the required QoS. Then, we can write

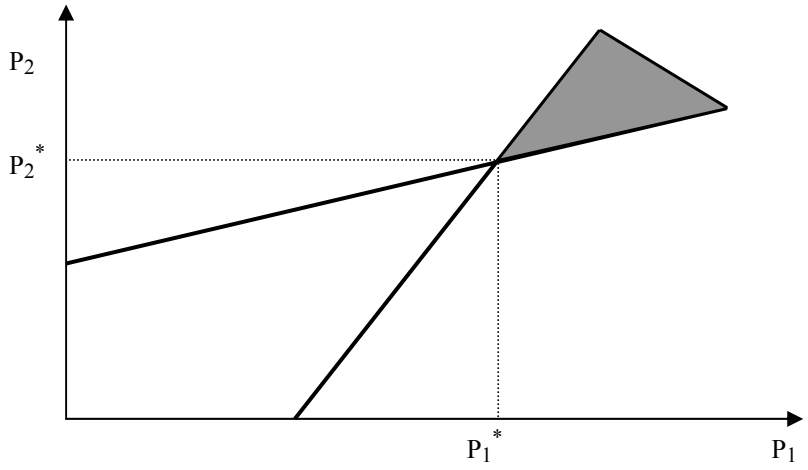

Figure 2.3. Black area consists of feasible power pair values satisfying QoS.

$\frac{P_1(t)G_1(t)}{P_2(t)G_2(t)+N} \geq \Gamma^T$ for the first user and $\frac{P_2(t)G_2(t)}{P_1(t)G_1(t)+N} \geq \Gamma^T$ for the second user.

Solving the previous inequalities we obtain

$$\begin{aligned} P_1(t) &\geq \Gamma^T \frac{G_2(t)}{G_1(t)} P_2(t) + \frac{N\Gamma^T}{G_1(t)} \\ P_2(t) &\geq \Gamma^T \frac{G_1(t)}{G_2(t)} P_1(t) + \frac{N\Gamma^T}{G_2(t)} \end{aligned} \tag{2.14}$$

In practice, the gains are random variables due to slow fading, and fast fading behavior.

To solve the system of linear equations (2.14), it is easier to assume that the gains are constant, i.e. they are frozen at time t. This is termed *snapshot* assumption. With that assumption the problem can be solved by centralized or distributed linear techniques, as we will describe later. Figure 2.3 illustrates the graphical interpretation of power control with the snapshot assumption. The shaded area shows the set of feasible power pair values to achieve the required QoS.

2.4 Distributed Power Control Algorithms

For distributed power control, only local information is needed for a specific transmitter to transmit the optimum power. The transmitted power of all users can be described mathematically as

$$\mathbf{P}(t+1) = \mathbf{\Psi}(\mathbf{P}(t)) \qquad t=0,1,\ldots \tag{2.15}$$

where $\mathbf{\Psi}(\mathbf{P}(t)) = \left[\Psi_1(\mathbf{P}(t)),...,\Psi_Q(\mathbf{P}(t))\right]'$ is the interference function. There are different types of interference functions in the literature as we will see later.

The interference function $\mathbf{\Psi}(\bullet)$ is called standard when the following properties are satisfied for all components of the nonnegative power vector **P** [7]:

- Positivity $\mathbf{\Psi}(\mathbf{P}) > 0$;
- Monotonicity, if $\mathbf{P} \geq \bar{\mathbf{P}}$ then $\mathbf{\Psi}(\mathbf{P}) \geq \mathbf{\Psi}(\bar{\mathbf{P}}) > 0$;
- Scalability, for all $\alpha > 1$, $\alpha\mathbf{\Psi}(\mathbf{P}) > \mathbf{\Psi}(\alpha\mathbf{P})$.

Theorem (1)

If the standard power control algorithm (2.15) has a fixed point, then that fixed point is unique.

Proof: See [7].

Theorem (2)

If $\mathbf{\Psi}(\mathbf{P})$ is feasible, then for any initial power vector $\mathbf{P_o}$, the standard power control algorithm converges to a unique fixed point $\mathbf{P}^*$.

Proof: See [7].

Theorem (3)

If $\mathbf{\Psi}(\mathbf{P})$ is feasible, then from any initial power vector $\mathbf{P_o}$, the asynchronous standard power control algorithm converges to a unique fixed point $\mathbf{P}^*$.

Proof: See [7].

2.4.1 Distributed Balancing Algorithm (DBA)

Zander has proposed a Distributed Balancing Algorithm [1]. The method is based on the power method for finding the dominant eigenvalue (spectral radius) and its corresponding eigenvector.

The DBA algorithm is as follows

$$\begin{aligned} &\mathbf{P}(0) = \mathbf{P_0} \qquad \mathbf{P_0} > \mathbf{0} \\ &P_i(t+1) = \beta P_i(t)\left(1 + \frac{1}{\Gamma_i(t)}\right), \qquad \beta > 0,\ \text{t=0,1,...,}\ \text{i=1,...,Q} \end{aligned} \tag{2.16}$$

The algorithm starts with an arbitrary positive vector **P**(0). The CIR level $\Gamma_i(t)$ is

measured in link *i*. If the power control is for downlink, then the measurement of the CIR is made at the mobile. The result is to be reported back to the base station. The transmitter power at the base station is then adjusted according to the DBA in (2.16). If the power control is for uplink, then the measurement of the CIR has to be made at the base station. The result has to be reported back to the mobile, and each mobile station will adjust its transmitted power according to the DBA. Practically, to reduce the feedback bandwidth as well as the signaling data, only quantized (one or few bits) CIR is reported. We call power control algorithms based on the quantized CIR as totally distributed power control algorithms. These types of algorithms will be discussed later.

Proposition (2.1)

Using the DBA algorithm (2.16) the system will converge to CIR balance with probability one, i.e.,

$$\begin{aligned} &\lim_{t\to\infty} \mathbf{P}(t) = \mathbf{P}^* \qquad t = 0,1,... \\ &\lim_{t\to\infty} \Gamma_i(t) = \gamma^* \qquad i = 1,...,Q \end{aligned} \tag{2.17}$$

where γ^* is the maximum achievable CIR, which is equal to $1/\lambda^*$. As before, λ^* is the spectral radius of the nonnegative matrix **H**, and $\mathbf{P}^*$ is the corresponding eigenvector representing the optimum transmitted power.

Proof: See [1]

It is clear that the DBA uses only local CIR information and utilizes an iterative scheme to control the transmitted power. The main disadvantage of the DBA is that its convergence speed is not satisfactory. If the allowed speed of the iterations is not high enough, then the distributed algorithm may result in an outage probability much greater than the optimum value [3].

The DBA requires a normalization procedure after each iteration (in noiseless case) to determine the transmitted power; hence it is not fully distributed [3].

2.4.2 The Distributed Power Control (DPC)

It has been shown that the distributed power control scheme for satellite systems can be applied to cellular systems [2]. The results presented in [2] indicate that the DPC scheme has the potential to converge faster than the DBA scheme at high CIR's.

The power adjustment made by the i^{th} mobile at the t^{th} time slot is given by

$$P_i(t+1) = \beta(t)\frac{P_i(t)}{\Gamma_i(t)} \qquad \text{i=1,...,Q,} \quad \text{t} = 0,1,... \tag{2.18}$$

where β(t) is some positive coefficient chosen to achieve the proper power control vector (not too large or too small). In additive noise environment, it is very common to select $\beta(t)=\Gamma^T$.

Proposition (2.2)

For a system with M ≥ 3 (necessary condition for convergence) that uses the DPC scheme of (2.18) with β(t), t ≥ 0 chosen so that

$$\lim_{t\to\infty}\left(\lambda^*\right)^t \prod_{k=0}^{t}\beta(k) < \infty, \tag{2.19}$$

we have

$$\lim_{t\to\infty}\mathbf{P}(t) = \mathbf{P}^* b \lim_{t\to\infty}\left(\lambda^*\right)^t \prod_{k=0}^{t}\beta(k) \tag{2.20}$$

$$\lim_{t\to\infty}\Gamma_i(t) = \gamma^*, \qquad \text{i} = 1,\cdots,\text{Q}, \tag{2.21}$$

where b is a positive constant determined by $\mathbf{P}(0)$.

Proof : See [2]

We can see from proposition (2.2) that as t increases we approach the optimum power control $\mathbf{P}^*$ multiplied by a common factor. It is clear that $\mathbf{P}^*$ is the eigenvector of the gain matrix associated with the largest eigenvalue. β(t) can be selected as follows (in noiseless case)

$$\beta(\text{t}) = \frac{1}{\max\left\{\text{P}_\text{i}\ (\text{t})\right\}_{\text{i=1}}^{\text{Q}}} \tag{2.22}$$

Equation (2.22) further shows that the DPC algorithm is not a fully distributed algorithm.

2.4.3 Distributed Constrained Power Control (DCPC)

The transmitted power of a mobile station or a base station is limited by some maximum value P_{max}. The constrained power control generally takes the following form

$$P_i(t+1) = \min\left\{P_{\max}, \Psi_i\left(\mathbf{P}(t)\right)\right\}, \quad t = 0,1,2,...; \quad i = 1,...,Q \tag{2.23}$$

where $\Psi_i(\cdot),\ i = 1,...,Q$ is the standard interference function. The distributed constrained power control DCPC algorithm suggested in [6] has the following form

$$P_i(t+1) = \min\left\{P_{\max}, \Gamma^T \frac{P_i(t)}{\Gamma_i(t)}\right\}, \quad t = 0,1,2,...; \quad i = 1,...,Q \tag{2.24}$$

Proposition (2.3)

Starting with any nonnegative power vector **P**(0), the DCPC scheme described in (2.24) converges to the fixed point $\mathbf{P}^*$ of

$$\mathbf{P}(t+1) = \min\left\{\mathbf{P}_{\max}, \Gamma^T\left(\mathbf{HP}(t) + \mathbf{u}\right)\right\}, \quad t = 0,1,2,... \tag{2.25}$$

where **u** is a vector with positive elements u_i specified by (2.11). If the target CIR is greater than the maximum achievable CIR, i.e., $\Gamma^T \geq \gamma^*$ then the fixed point $\mathbf{P}^*$ will converge to P_{max}.

Proof : see [6].

2.4.4 Fully Distributed Power Control (FDPC) Algorithm

The Fully Distributed Power Control (FDPC) has been proposed in [3]. The FDPC algorithm can be specified as follows:

$$\mathbf{P}(0) = 1$$
$$P_i(t+1) = \frac{\min\left(\Gamma_i(t), \xi\right)}{\Gamma_i(t)} P_i(t) \qquad 0 < \xi < \infty,\ \text{t=0,1,...} \tag{2.26}$$

Note that there is one parameter ξ in the above FDPC algorithm.

Clearly, when $\xi \to \infty$, the FDPC algorithm becomes the fixed power control algorithm (i.e., without power control). For very small values of ξ the proposed FDPC reduces to the distributed power control DPC algorithm (in noiseless case). The main advantage of this algorithm is that no normalization is required as is the case in the other distributed algorithms. In simulation part we show that the FDPC fails to converge in dynamical channel environment.

Proposition (2.4)

If $\xi \leq \gamma^*$, then $\lim_{t\to\infty} \Gamma_i(t) = \gamma^*$ for all *i*.

Proof: See [3].

2.4.5 Foschini's and Miljanic's Algorithm (FMA)

Foschini and Miljanic have proposed a simple and efficient distributed power control algorithm [4]. The proposed algorithm is based on the following continuous time differential equation:

$$\dot{\Gamma}_i(\tau) = -\beta[\Gamma_i(\tau) - \Gamma^T] \quad , \beta > 0, \quad \tau \geq 0 \tag{2.27}$$

The steady state solution of the above differential equation for user *i* is $\Gamma_i = \Gamma^T$.

The speed of the convergence depends on the coefficient β.

Define the *total interference of user i*:

$$I_i(\tau) = \sum_{j \neq i}^{Q} G_{kj}(\tau) P_j(\tau) + N(\tau) \tag{2.28}$$

Then Γ_i from (2.2) becomes

$$\Gamma_i(\tau) = \frac{G_{ki}(\tau) P_i(\tau)}{\sum_{j \neq i}^{Q} G_{kj}(\tau) P_j(\tau) + N(\tau)} = \frac{G_{ki}(\tau) P_i(\tau)}{I_i(\tau)}, \; i = 1,...,Q, \; k = 1,...,M. \tag{2.29}$$

Assuming that $I_i(\tau)$ and $G_{ki}(\tau)$ are constant, substituting (2.29) into (2.27) gives

$$\frac{G_{ki}\dot{P}_i(\tau)}{I_i} = -\beta\left[\frac{G_{ki}P_i(\tau)}{I_i} - \Gamma^T\right], \quad i = 1,...,Q, \; k = 1,...,M. \tag{2.30}$$

Using (2.28) becomes

$$\dot{P}_i(\tau) = -\beta\left[P_i(\tau) - \frac{\Gamma^T}{G_{ki}}\left(\sum_{j \neq i}^{Q} G_{kj}(\tau) P_j(\tau) + N\right)\right], \; i = 1,...,Q, \; k = 1,...,M. \tag{2.31}$$

Using matrix notation one can write (2.31) as

$$\dot{\mathbf{P}}(\tau) = -\beta[\mathbf{I} - \Gamma^T \mathbf{H}]\mathbf{P}(\tau) + \beta \, \mathbf{u}. \tag{2.32}$$

At the steady state, we have

$$\mathbf{P}^* = \left[\mathbf{I} - \Gamma^T \mathbf{H}\right]^{-1} \mathbf{u}. \tag{2.33}$$

Proposition (2.5)

If there is a power vector $\mathbf{P}^*$, for which the target Γ^T values are attained, then no matter what is the initial $\mathrm{P_i}(0)$, each of the $\mathrm{P_i}(\tau)$ evolving according to (2.31) will converge to $\mathbf{P}^*$ of (2.33).

Proof: see [4].

The discrete form of (2.31) is

$$\mathbf{P}(t+1)=\beta\left[\left(\frac{1}{\beta}-1\right)\mathbf{I}+\mathbf{\Gamma}^{T}\mathbf{H}\right]\mathbf{P}(t)+\beta\ \mathbf{u},\quad t=0,1,... \tag{2.34}$$

and the iterative power control for each user i is

$$P_i\ (t+1)=(1-\beta)P_i\ (t)\left[1+\frac{\beta}{(1-\beta)}\left(\frac{\Gamma^{T}}{\Gamma_i\ (t)}\right)\right],\quad t=0,1,2,...;\quad i=1,...,Q \tag{2.35}$$

Proposition (2.6)

Whenever a centralized "genie" can find a power vector $\mathbf{P}^{*}$ meeting the desired criterion, then for $\beta\in(0,1]$, the solution of (2.35) starting from any initial vector $\mathrm{P_i}(0)$, converges to $\mathbf{P}^{*}$.

Proof: See [4]

Actually, the Foschini and Miljanic algorithm is a special case of the general linear iterative method of numerical linear algebra, which has been used to solve the distributed power control problem [56].

The power control problem with considerable additive white noise can be described as

$$[\mathbf{I}-\mathbf{\Gamma}^{T}\mathbf{H}]\mathbf{P}=\mathbf{u} \tag{2.36}$$

Now define

$$\left[\mathbf{I}-\mathbf{\Gamma}^{T}\mathbf{H}\right]=\mathbf{M}-\mathbf{N}, \tag{2.37}$$

where **M** and **N** are Q×Q matrices, **M** nonsingular. Then (2.37) could be solved iteratively as

$$\mathbf{P}(t+1)=\mathbf{M}^{-1}\mathbf{N}\mathbf{P}(t)+\mathbf{M}^{-1}\mathbf{u}. \tag{2.38}$$

This leads to

$$\mathbf{P}(t)=\left(\mathbf{M}^{-1}\mathbf{N}\right)^{t}\mathbf{P}(t)+\sum_{\mathbf{k=0}}^{t-1}\left(\mathbf{M}^{-1}\mathbf{N}\right)^{k}\mathbf{M}^{-1}\mathbf{u}. \tag{2.39}$$

If $\rho\left(\mathbf{M}^{-1}\mathbf{N}\right)<1$ then $\lim_{\mathrm{t}\to\infty}\left(\mathbf{M}^{-1}\mathbf{N}\right)^{t}\to\mathbf{0}$ and since $\lim_{t\to\infty}\sum_{k=0}^{t-1}\left(M^{-1}N\right)^{k}\to\left(I-M^{-1}N\right)^{-1}$,

then

$$\mathbf{P}(t) \to \left(\mathbf{I} - \mathbf{M}^{-1}\mathbf{N}\right)^{-1} \mathbf{M}^{-1}\mathbf{u} = \left(\mathbf{I} - \mathbf{\Gamma}^{T}\mathbf{H}\right)^{-1} \mathbf{u}\,, \tag{2.40}$$

which is the solution of power control problem.

The foregoing analysis shows that for any initial power vector $\mathbf{P}(0)$, the linear iterative method converges with probability one to the fixed point solution $\mathbf{P}^{*}$, providing that the spectral radius of $\left(\mathbf{M}^{-1}\mathbf{N}\right)$ is less than one, and that there is a feasible positive solution $\left(i.e., \Gamma^{T} < \frac{1}{\rho(\mathbf{H})}\right)$.

Setting

$$\mathbf{M} = \frac{1}{\beta}\mathbf{I},\ \ \mathbf{N} = \left(\frac{1}{\beta} - 1\right)\mathbf{I} + \mathbf{\Gamma}^{T}\mathbf{H} \tag{2.41}$$

in (2.38) results in FMA in (2.34).

2.4.6 Constrained Second Order Power Control (CSOPC)

Jäntti and Kim have proposed a second order algorithm, which significantly enhances the convergence speed of power control [9]. The algorithm is based on the framework of the general iterative method shown in (2.38). What differs of the existing algorithms, however, is that it has a second –order iterative form given by

$$P_i(t+1) = \min\left\{P_{\max}, \max\left\{0, a(t)\frac{\Gamma_i^{T}}{\Gamma_i(t)}P_i(t) + \left(1 - a(t)\right)P_i(t-1)\right\}\right\}, \quad t = 1, 2, \ldots \tag{2.42}$$

where $P_i(0)$ and $P_i(1)$ are chosen arbitrarily in the range $[0, P_{\max}]$. The term a(t) is a nonincreasing sequence of control parameters, where $1 < a(1) < 2$ and $\lim_{t\to\infty} a(t) = 1$. In simulations of [9], the following relaxation factor is employed

$$a(t) = 1 + \frac{1}{1.5^{t}} \tag{2.43}$$

Proposition (2.7) If the system is feasible, CSOPC converges to $\mathbf{P}^{*}$.

Proposition (2.8) If the system is feasible, CSOPC is asymptotically faster than DCPC.

Proofs: See [9].

2.4.7 Estimated Step Power Control Algorithm (ESPC)

Perfect estimation of the mobile's CIR at the base station is assumed in the previous distributed power control algorithms. In the existing cellular communication system only quantized version of the CIR is available at the mobile station. To reduce the bandwidth of the feedback channel only one bit is used to represent the CIR (two or three bits are used as repetitive code). In the existing CDMA cellular system, the power control is performed as follows:

1) Measure and estimate the CIR of user *i* at its assigned BS.
2) Compare the estimated CIR with the target.
3) If the estimated CIR is less than the target CIR, then send (+) command to ask the mobile to increase its transmitted power by one step.
4) If the estimated CIR is larger than the target CIR, then send (-) command to ask the mobile to decrease its transmitted power by one step.

From the above steps, it is clear that the MS does not know the actual CIR value at the BS. The MS transmitted power follow the instructions of the BS blindly. This type of power control is called bang-bang power control or Fixed Step Power Control (FSPC). Mathematically, this is represented as (all the values are in dB)

$$P_{i,FSPC}(t+1) = P_{i,FSPC}(t) + \delta sign\left(\Gamma^T - \Gamma_i(t)\right), \quad t = 0,1,2,...; \quad i = 1,...,Q \qquad (2.44)$$

where $P_{\min} \le P_{FSPC}(t) \le P_{\max}$ is the transmitted power at time slot *t*, $P_{\min}$ and $P_{\max}$ are the minimum and maximum transmitted powers respectively, δ is the step size of the power update, Γ^T is the target CIR which is determined by the outer loop power control, and $\Gamma(t)$ is the measured CIR at time slot *t*. The sign function is given by

$$sign(x) = \begin{cases} +1, & x \ge 0 \\ -1, & x < 0 \end{cases} \qquad (2.45)$$

It is clear from (2.44) that the MS is commanded to increase or decrease its transmitted power without detailed information about the channel situation, i.e., the MS does not know how large is the difference between the target CIR and the measured CIR. If the measured CIR is much greater than the target CIR then it will take a relatively long time to adjust the transmitted power to the proper value to make the actual CIR close to the target CIR. This can reduce the performance and the capacity of the system.

The DCPC algorithm (2.24) can be rewritten in dB scale as

$$P_{i,DPC}(t+1) = P_{i,DPC}(t) + \left(\Gamma^T - \Gamma_i(t)\right), \quad t = 0,1,2,...; \quad i = 1,...,Q \tag{2.46}$$

where $P_{\min} \le P_{i,DPC}(t) \le P_{\max}$, and all the values are in decibels.

It is clear that the DCPC algorithm assumes no quantization distortion so more information about the channel is available. For this reason the DCPC performance is better than the FSPC algorithm. In this section we introduce a new power control algorithm based on the estimation of the difference $\left(\Gamma^T - \Gamma_i(t)\right)$ by using one bit signaling. We call it Estimated Step Power Control (ESPC) algorithm [93]-[94].

In what follows we consider only uplink, but the proposed method is applicable also to downlink. The ESPC algorithm is based on a simple tracking method, which uses one memory location for the previous BS power command.

Define for all users i=1,…,Q, and t=0,1,2,…

$$e_i(t) = \Gamma^T - \Gamma_i(t), \tag{2.47}$$

$$v_{tr,i}(t) = \text{sign}\left(e_i(t)\right), \tag{2.48}$$

$$v_i(t) = v_{tr,i}(t) E_{PC,i}(t), \tag{2.49}$$

where $E_{PC,i}(t)$ is 1 with probability $P_{PCE,i}(t)$ and -1 with probability $1 - P_{PCE,i}(t)$. $P_{PCE,i}(t)$ is the probability of bit error in power control command transmission at time t.

Let the estimate of the error signal $e_i(t)$ be $\tilde{e}_i(t)$. We propose a simple form for the estimate:

$$\tilde{e}_i(t) = \frac{1}{2}\left[1 + v_i(t)v_i(t-1)\right] \; \tilde{e}_i(t-1) + \delta_i v_i(t), \tag{2.50}$$

where δ_i is the adaptation step size of user i. The ESPC algorithm is given by

$$P_{ESPC,i}(t+1) = P_{ESPC,i}(t) + \tilde{e}(t), \tag{2.51}$$

where $P_{\min} \le P_{ESPC,i}(t) \le P_{\max}$, and all the values are in decibels. Figure 2.4 shows the block diagram of the suggested algorithm.

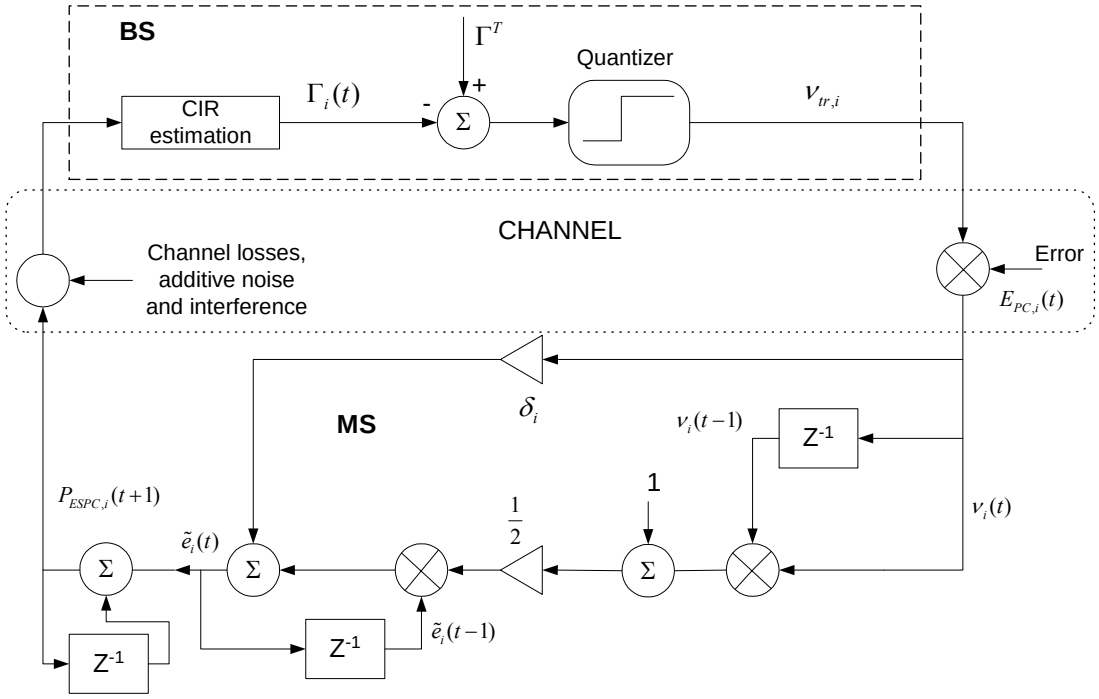

Figure 2.4. Block diagram of the ESPC algorithm

If we define

$$a_i(t) = \frac{1}{2}\left[1 + v_i(t)v_i(t-1)\right] = \begin{cases} 1, & v_i(t) = v_i(t-1) \\ 0, & v_i(t) \neq v_i(t-1) \end{cases} \tag{2.52}$$

then, solving (2.50) recursively, we obtain

$$\tilde{e}_i(t) = \prod_{m=1}^{t} a_i(m)\tilde{e}_i(0) + \delta_i \sum_{k=1}^{t-1} v_i(t-k) \prod_{n=0}^{k-1} a_i(t-n) + \delta_i v_i(t). \tag{2.53}$$

It is clear that the first term will be zero (after any zero crossing of $e_i(t)$ or if $\tilde{e}_i(0) = 0$). Then (2.53) can be rewritten as

$$\tilde{e}_i(t) = \delta_i \left[\sum_{k=1}^{t-1} v_i(t-k) \prod_{n=0}^{k-1} a_i(t-n) + v_i(t) \right] \tag{2.54}$$

Define

$$c_i(t,k) = \prod_{n=0}^{k-1} a_i(t-n) \tag{2.55}$$

Substitute (2.55) in (2.54) to obtain

$$\tilde{e}_i(t) = \delta_i \left[\sum_{k=1}^{t-1} v_i(t-k) c_i(t,k) + v_i(t) \right] \tag{2.56}$$

The first part of (2.56) can be seen as the convolution between the input $v_i(t)$ and a time-varying system $c_i(t,k)$. The statistical properties of $\tilde{e}_i(t)$ depend on the statistical

properties of the channel, interference and the additive noise. The performance of the ESPC algorithm can be further improved by using variable step size. The idea is to increase the step size if the same command is received 3 consequence times. The algorithm is called modified ESPC or ESPC-M. To show the performance of our algorithm we introduce the following simulation example.

2.4.7.1 Simulation Example

As an example, Figure 2.5 shows the estimated error signal versus the actual error signal. It is clear that the estimated error signal is close enough to the actual, keeping in mind that this estimation is after one bit quantization. More simulations will be given in Section 2.6.

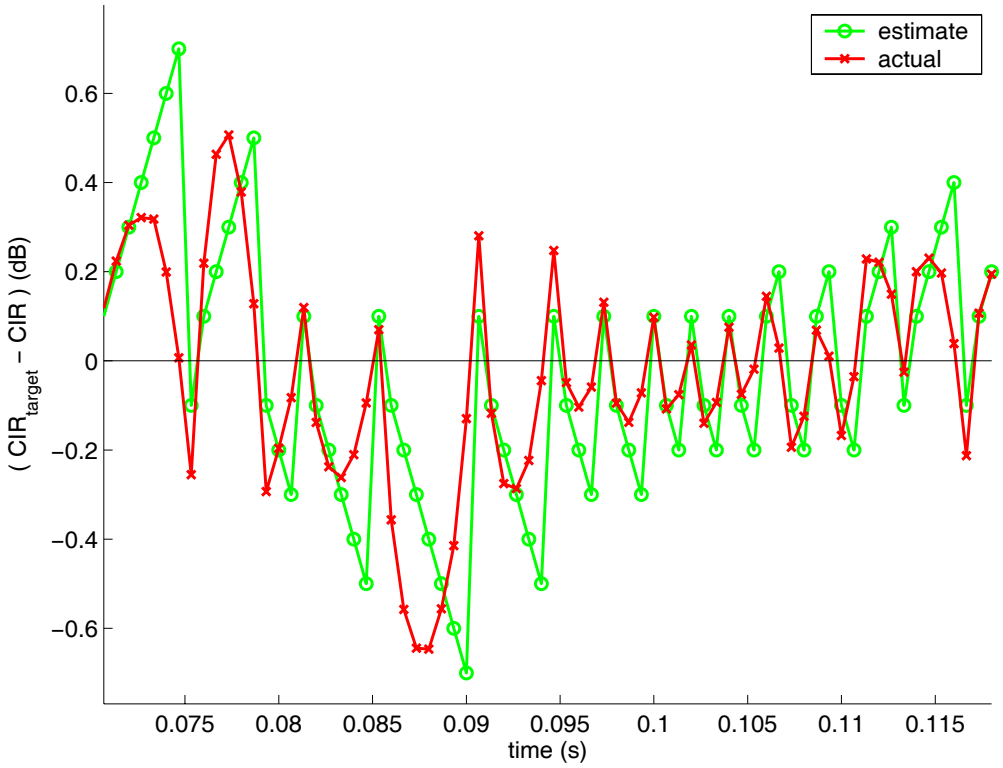

Figure 2.5. Estimated error signal versus actual error signal.

2.4.8 Multi-Objective Distributed Power Control Algorithm (MODPC)

One of the main contributions in this thesis is a novel power control algorithm based on multi-objective optimization in the radio resource management. A brief overview of the

multi-objective optimization and its application to fixed rate power control will be given in this Section.

The MO optimization technique is a method to optimize between different (usually) conflicting objectives. In the MO optimization problem we have a vector of objective functions instead of one scalar objective. Each objective function is a function of the decision (variable) vector. The mathematical formulation of a MO optimization problem becomes [77]:

Find **x** which achieves

$$\begin{aligned} &\min\left\{f_1(\mathbf{x}), f_2(\mathbf{x}), ..., f_m(\mathbf{x})\right\}, \\ &\text{subject to } \mathbf{x} \in \mathbf{S}, \end{aligned} \tag{2.57}$$

where we have m (≥ 2) objective functions $f_i : \Re^n \to \Re$, **x** is the decision (variable) vector, $\mathbf{x} \in \mathbf{S}$, **S** is (nonempty) feasible region (set). The abbreviation $\min\{.\}$ means that we want to minimize all the objectives simultaneously. Since usually the objectives are at least partially conflicting and possibly incommensurable then there is no single vector **x** minimizing all the objectives. In the MO optimization we have different optimal solutions in different sense, and they are called Pareto optimal solutions (see the Appendix for more details).

Definition 1 [77]

A decision vector $\mathbf{x}^\bullet \in S$ is Pareto optimal if there does not exist another decision vector $\mathbf{x} \in S$ such that $f_i(\mathbf{x}) \leq f_i(\mathbf{x}^*)$ for all i=1,2,..,m and $f_j(\mathbf{x}) < f_j(\mathbf{x}^*)$ for at least one index j.

The *Pareto optimal set* is the set of all possible Pareto optimal solutions. This set can be nonconvex and nonconnected.

After the generation of the Pareto set, we are usually interested in one solution of this set. This solution is selected by a decision maker. There are different techniques to solve the MO optimization problems. One way to solve this kind of problems is to use soft-computing methods such as genetic algorithms [89]. In this thesis we will concentrate on the analytical solutions of the MO optimization problems. One of the techniques to solve the MO optimization problem is to convert it to a single objective optimization problem as in the *Weighting Method* [77]. The weighting method transforms the problem posed in (2.57) into

$$\begin{aligned} &\min \sum_{i=1}^{m} \lambda_i f_i(\mathbf{x}), \\ &\text{subject to } \mathbf{x} \in \mathbf{S}, \end{aligned} \tag{2.58}$$

where the tradeoff factors $\lambda_i \geq 0$, $\forall$i=1,..,m and $\sum_{\mathrm{i}=1}^{\mathrm{m}} \lambda_i = 1$.

The Pareto set can be obtained by solving the single objective (SO) optimization problem (2.58) for different tradeoff factor values [77].

Another important method which is of special interest in the applications of MO optimization in RRS is the method of *Weighted Metrics* [77]. If the optimum solution of each objective is known in advance then problem (2.57) can be formulated as

$$\begin{aligned} &\min \left(\sum_{i=1}^{m} \lambda_i \left| f_i(\mathbf{x}) - z_i^* \right|^p \right)^{1/p}, \\ &\text{subject to } \mathbf{x} \in \mathbf{S}, \end{aligned} \tag{2.59}$$

where $1 \leq \mathrm{p} \leq \infty$, z_i^* is the desired solution of the objective *i*, and the tradeoff factors $\lambda_\mathrm{i} \geq 0$, $\forall$i=1,..,m and $\sum_{\mathrm{i}=1}^{\mathrm{m}} \lambda_\mathrm{i} = 1$.

In this section, we propose to use the MO optimization techniques to solve the single rate power control problem (2.1)-(2.3).

The power control algorithms, which have been described so far are based on a snapshot assumption, i.e. the channel parameters as well as the mobile location are assumed to be fixed. This assumption is not valid for mobile communication systems due to their dynamic behavior. Actually, studying the convergence behavior and the performance of the distributed power control algorithms based on the snapshot assumption does not give enough information about their behavior in real systems. The reason is that for dynamical systems channel parameters, "simply the link gains", changes fast. In some cases, channel parameters become uncorrelated after a fraction of a millisecond [12]. These characteristics of mobile channels reduce the significance of the snapshot convergence property of the power control algorithms. The work in [100],[101] do not assume the snapshot analysis but the resultant power control is relatively difficult to implement in a very limited processing power handset. The target QoS is not usually strict but it has some margin which is the difference between the target QoS and the minimum allowed QoS as described in Section 2.1. We call any QoS level inside the margin by accepted

QoS level. *The preferred power control is that can achieve an accepted QoS level very fast at low power consumption.* The proposed power control algorithm fast achieves an accepted QoS level at very low power consumption. The distributed power control algorithms use the estimated SINR to update the power. The proposed algorithm in this work achieves two objectives by applying multi-objective optimization method. The first objective is minimizing the transmitted power and the second objective is achieving the target QoS which is represented here by the target CIR. In the next formulation, the power control problem has been represented by two objectives as follows: a) Minimizing the transmitted power. b) Keeping the SINR as close as possible to some target CIR value. In other words, the MO power control algorithm tracks the target CIR, while minimizing the transmitted power. The above statement could be interpreted mathematically for user *i*, *i*=1,…,*Q*, by the following error function

$$e_i(t) = \lambda_{1,i}\left|P_i(t) - P_{\min}\right| + \lambda_{2,i}\left|\Gamma_i(t) - \Gamma_i^T\right|, \quad \text{t=0,1,...} \tag{2.60}$$

where $0 \le \lambda_{1,i} \le 1$; $\lambda_{2,i} = 1 - \lambda_{1,i}$ are tradeoff factors of user *i*, Γ_i^T is the target CIR of user *i*, $\mathrm{P}_{\min}$ is the minimum transmitted power of the mobile station. The user's subscript *i* will be dropped from the tradeoff factors and the target CIR for simplicity. But generally each user can have different values of tradeoff factors as well as target CIR. Users with different values of target CIR (multi-level QoS) will be discussed in next Chapter.

The above error function (2.60) has been constructed from two objectives. The first objective is to keep the transmitted power $P_i(t)$ as close as possible to the minimum power $\mathrm{P}_{\min}$. The second objective is to keep the CIR $\Gamma_i(t)$ as close as possible to the target CIR. It is clear that (2.60) has the form of *Weighted Metrics* (2.59) method with *p*=1.

To generalize the optimization over all users and for time window of *N* slots we define the optimization problem as:

Find the minimum of the cost function

$$J(\mathbf{P}) = \left[\sum_{i=1}^{Q}\sum_{t=1}^{N}\varsigma^{N-t}e_i^2(t)\right], \tag{2.61}$$

with respect to the power vector **P**, where ς is an adaptation factor, and $\mathbf{P} = [\mathrm{P}_1, \mathrm{P}_2, .., \mathrm{P}_Q]'$.

Problem (2.60)-(2.61) is a non-smooth optimization problem because of the absolute function in (2.60). One of the advantages of using the cost function (2.60) is that it can be

used for different tasks, for example, it can be applied to reduce transmitted power, achieve some target QoS, increase the throughput, reduce the packet delay, and increase the fairness levels as will be shown in next Chapter.

The absolute function of the first term in (2.60) is not needed because the transmitted power can not be less than the minimum. The error function can be modified such as

$$e_i(t) = \lambda_1\left(P_i(t) - P_{\min}\right) + \hat{\lambda}_2(t)\left(\Gamma_i(t) - \Gamma^T\right), \quad t = 0,1,... \tag{2.62}$$

where $\hat{\lambda}_2(t) = sign\left(\Gamma_i(t) - \Gamma^T\right)\lambda_2$, the sign function is defined in (2.45).

Next we will show how to derive a new power control algorithm, by solving the minimization problem of (2.61). Suppose further that the power $P_i(t)$ is described by a linear autoregressive model as shown in Figure 2.6 [19]. The transmitted power is

$$P_i(t) = \sum_{k=1}^{n} w_i(k) P_i(t-k) = \mathbf{w}_i' \mathbf{X}_i(t), \quad t = 0,1,... \tag{2.63}$$

where $$\mathbf{w}_i = \left[w_i(1) \quad \cdots \quad w_i(n)\right]', \ \mathbf{X}_i(t) = \left[P_i(t-1) \quad \cdots \quad P_i(t-n)\right]' \tag{2.64}$$

$\mathbf{w}'$ means the transpose of $\mathbf{w}$. Observe that $\mathbf{X}_i(t)$ contains known, measured values of transmitted power.

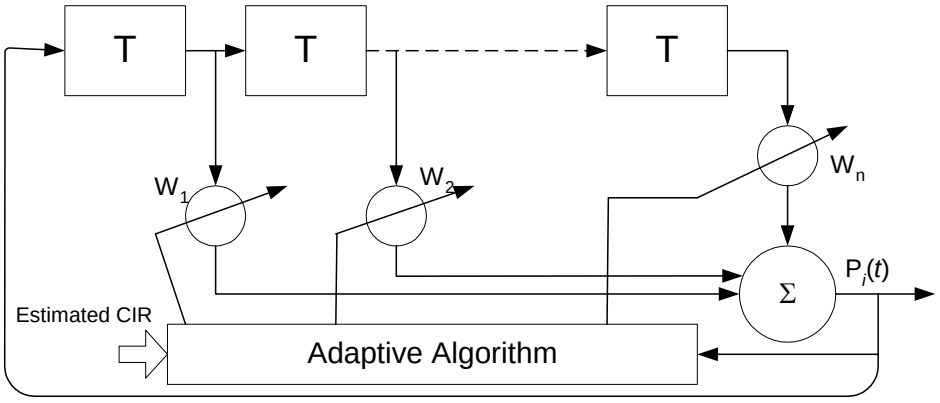

Figure 2.6. The autoregressive model of power control

Substitute (2.63) into (2.62) and (2.29). Then error $e_i(t)$ can be written as

$$e_i(t) = \lambda_1\left(\mathbf{w}_i' \mathbf{X}_i(t) - P_{\min}\right) + \hat{\lambda}_2(t)\left(\frac{G_{ki}(t)\mathbf{w}_i' \mathbf{X}_i(t)}{I_i(t)} - \Gamma^T\right) \tag{2.65}$$

Denote

$$\alpha_t := \left[\lambda_1 + \hat{\lambda}_2(t) \frac{G_{ii}(t)}{I_i(t)} \right] \tag{2.66}$$

and using this in (2.65), $e_i(t)$ becomes

$$e_i(t) = \alpha_t \mathbf{w}_i' \mathbf{X}_i(t) - \lambda_1 P_{\min} - \hat{\lambda}_2(t) \Gamma^T \tag{2.67}$$

Minimization of the cost function (2.61) with respect to P_i is now transformed into minimizing with respect to parameter vector **w.**

Necessary condition for minimum is for all i=1,…,Q:

$$2\sum_{t=1}^{N} \varsigma^{N-t} e_i(t) \frac{\partial e_i(t)}{\partial \mathbf{w}} = 0 \tag{2.68}$$

From (2.67)

$$\frac{\partial e_i(t)}{\partial \mathbf{w}} = \alpha_t \mathbf{X}_i'(t) \tag{2.69}$$

Substituting (2.67) and (2.69) into (2.68) we obtain

$$\sum_{t=1}^{N} \varsigma^{N-t} e_i(t) \frac{\partial e_i(t)}{\partial \mathbf{w}} = \sum_{t=1}^{N} \varsigma^{N-t} \left(\alpha_t \mathbf{w}_i' \mathbf{X}_i(t) - \lambda_1 P_{\min} - \hat{\lambda}_2 \Gamma^T \right) \alpha_t \mathbf{X}_i'(t) = 0 \tag{2.70}$$

Solving for $\mathbf{w}_i$

$$\left(\sum_{t=1}^{N} \left(\varsigma^{N-t} \alpha_t^2 \mathbf{X}_i(t) \mathbf{X}_i'(t) \right) \right) \mathbf{w}_i = \sum_{t=1}^{N} \varsigma^{N-t} \alpha_t \left(\lambda_1 P_{\min} + \hat{\lambda}_2 \Gamma^T \right) \mathbf{X}_i(t) \tag{2.71}$$

or

$$\mathbf{w}_i(N) = \mathbf{R}_{xx}^{-1}(N) \mathbf{R}_x(N), \; i = 1, ..., Q \tag{2.72}$$

where

$$\mathbf{R}_{xx}(N) := \sum_{t=1}^{N} \varsigma^{N-t} \alpha_t^2 \mathbf{X}_i(t) \mathbf{X}_i'(t) \tag{2.73}$$

$$\mathbf{R}_x(N) := \sum_{t=1}^{N} \varsigma^{N-t} \alpha_t \left(\lambda_1 P_{\min} + \hat{\lambda}_2 \Gamma^T \right) \mathbf{X}_i(t) \tag{2.74}$$

Formulae (2.72)-(2.74) are well-known from least squares techniques.

Equation (2.72) can be solved using the Recursive Least Square (RLS) method. To avoid the matrix inversion, $\mathbf{R}_{xx}(N)$ may be computed recursively as

$$\mathbf{R}_{xx}(N) = \varsigma \mathbf{R}_{xx}(N-1) + \alpha_N^2 \mathbf{X}_i(N)\mathbf{X}_i'(N) \tag{2.75}$$

Since the inverse of $\mathbf{R}_{xx}(N)$ is needed we can use the matrix inverse identity to obtain [24],

$$\mathbf{R}_{xx}^{-1}(N) = \frac{1}{\varsigma}\left[\mathbf{R}_{xx}^{-1}(N-1) - \frac{\mathbf{R}_{xx}^{-1}(N-1)\alpha_N^2 \mathbf{X}_i(N)\mathbf{X}_i^T(N)\mathbf{R}_{xx}^{-1}(N-1)}{\varsigma + \alpha_N^2 \mathbf{X}_i^T(N)\mathbf{R}_{xx}^{-1}(N-1)\mathbf{X}_i(N)}\right] \tag{2.76}$$

Also $\mathbf{R}_x(N)$ can be computed recursively as

$$\mathbf{R}_x(N) = \varsigma \mathbf{R}_x(N-1) + \alpha_N\left(\lambda_1 P_{\min} + \hat{\lambda}_2 \Gamma^T\right)\mathbf{X}_i(N) \tag{2.77}$$

The power control algorithm is easy to implement and is also computationally light to be applicable for existing wireless communication systems. Next the simplest case, where n=1 in (2.63) and N=1, is considered. Solving (2.72) we obtain:

$$w_i(t) = \frac{\lambda_1 P_{\min} + \hat{\lambda}_2(t)\Gamma^T}{\lambda_1 P_i(t-1) + \hat{\lambda}_2(t)\Gamma_i(t-1)},\ i = 1,...,Q;\ \text{t=1,2,...} \tag{2.78}$$

From (2.63), the transmitted power of user i at time t is given by

$$P_i(t) = \frac{\lambda_1 P_{\min} + \hat{\lambda}_2(t)\Gamma^T}{\lambda_1 P_i(t-1) + \hat{\lambda}_2(t)\Gamma_i(t-1)} P_i(t-1),\ \ i = 1,...,Q;\ t = 1,2,... \tag{2.79}$$

Due to the sharp changes in $\hat{\lambda}_2(t)$ sign, the transmitted power in (2.79) may take negative values as well as very large power values which are not part of the power feasible subspace. To overcome these problems only the positive values of $\hat{\lambda}_2(t)$ are considered, i.e. $\hat{\lambda}_2(t) = \lambda_2$. This simplification has considerably reduced the complexity of the MODPC algorithm at slight degradation in the convergence speed. The effect of this simplification is shown in Figure 2.37 in Section 2.6. The MODPC algorithm becomes

$$P_i(t) = \frac{\lambda_1 P_{\min} + \lambda_2 \Gamma^T}{\lambda_1 P_i(t-1) + \lambda_2 \Gamma_i(t-1)} P_i(t-1),\ \ i = 1,...,Q;\ t = 1,2,... \tag{2.80}$$

It is clear that setting $\lambda_1 = 0$ and $\lambda_2 = 1$ in (2.79), the DPC algorithm of (2.18) is obtained. This means that the DPC algorithm is special case of the MODPC algorithm. At the other extreme case where $\lambda_1 = 1$ and $\lambda_2 = 0$, the handset transmits at the minimum power regardless of SINR situation (no power control). The proper values of the tradeoff factors, which could be adaptive, can greatly enhance the performance of the algorithm

depending on the scenario. The adaptation of the tradeoff factors makes the system more cooperative in a distributed manner as will be shown in Section 2.4.8.2. In terms of MO optimization the proper values of the tradeoff factors for certain network condition is selected by a decision maker, which determines the optimum point from a Pareto optimal set. Simple but efficient decision maker is proposed in this thesis.

At steady state (i.e. $P_i(t+1) = P_i(t) = P_i^{ss}$), Equation (2.80) results in the steady state CIR of user i $\left(\Gamma_i^{ss}\right)$, which is given by

$$\Gamma_i^{ss} = \Gamma^T - \frac{\lambda_1}{\lambda_2}\left(P_i^{ss} - P_{\min}\right) \tag{2.81}$$

One of the key features of the MODPC algorithm can be observed in the steady state solution given in (2.81). It is clear that the steady state CIR equals the target CIR when the steady state power equals the minimum power. The penalty to be applied of using any excessive power is to reduce the steady state CIR. Decision maker should select the values of the tradeoff factors in order to guarantee that all users can achieve at least the minimum allowed CIR level. In the worst case situation the steady state power is the maximum allowed power$\left(\mathrm{P}_{\max}\right)$. The maximum allowed power is determined by the power amplifier of the handset. The MODPC algorithm with maximum power constraint is given by

$$P_i(t) = \min\left\{P_{\max}, \frac{\lambda_1 P_{\min} + \lambda_2 \Gamma_i^T}{\lambda_1 P_i(t-1) + \lambda_2 \Gamma_i(t-1)} P_i(t-1)\right\}, \quad i = 1,...,Q;\ t = 1,2,... \tag{2.82}$$

It is interesting to observe that the transmitted power of MODPC algorithm (2.80) is naturally upper bounded such as

$$P_i(t) \le P_{\min} + \frac{\lambda_2}{\lambda_1}\Gamma^T, \quad i = 1,...,Q \tag{2.83}$$

We assume that the maximum allowed power $\left(\mathrm{P}_{\max}\right)$ is less than the natural upper bound of the MODPC algorithm(2.83).

Solving for (λ_1 and λ_2) using (2.81) and the fact that $\lambda_1 + \lambda_2 = 1$(two equations in two unknowns) , the values of tradeoff factors are derived such as (assuming $\mathrm{P}_{\min} = 0$)

$$\lambda_2 = \frac{\mathrm{P}_{\max}}{\mathrm{P}_{\max} + \Gamma^{\mathrm{T}} - \Gamma_{\min}} \quad , \ \lambda_1 = \frac{\Gamma^{\mathrm{T}} - \Gamma_{\min}}{\mathrm{P}_{\max} + \Gamma^{\mathrm{T}} - \Gamma_{\min}} \tag{2.84}$$

The convergence properties of the MODPC algorithm are discussed in the next.

Proposition (2.9)

For any **P**(0)>0, the MODPC algorithm (2.80) with $\lambda_1 > 0$ will always converge to a unique fixed point $\hat{\mathbf{P}}$. At $\lambda_1 = 0$ the feasibility condition is necessary for convergence.

Proof:

We will prove that the MODPC algorithm is a standard power control algorithm. Then by Theorems 1 and 2 (in Section 2.4) the MODPC algorithm converges to a unique fixed point. The interference function $\Psi_i\left(\mathbf{P}(t)\right)$ of the MODPC algorithm for user *i* is given by

$$\Psi_i\left(\mathbf{P}(t)\right) = \frac{\lambda_1 P_{\min} + \lambda_2 \Gamma^T}{\lambda_1 P_i(t-1) + \lambda_2 \Gamma_i(t-1)} P_i(t-1), \quad i = 1,...,Q, \ \text{t=0,1,...} \tag{2.85}$$

Define the normalized total interference of user *i* as

$$\hat{I}_i(t,\mathbf{P}) = \sum_{\substack{j=1 \\ j\neq i}}^{Q} \frac{G_{kj}(t)}{G_{ki}(t)} P_j(t) + \frac{N_i}{G_{ki}(t)} \tag{2.86}$$

The CIR of user *i* can now be stated as

$$\Gamma_i(t) = \frac{P_i(t)}{\hat{I}_i(t,\mathbf{P})} \tag{2.87}$$

By dropping t (for simplicity), (2.85) can be represented as

$$\Psi_i(\mathbf{P}) = \frac{\hat{I}_i(\mathbf{P})\, a}{\lambda_1 \hat{I}_i(\mathbf{P}) + \lambda_2} \tag{2.88}$$

where $a = \lambda_1 P_{\min} + \lambda_2 \Gamma^T > 0$.

From (2.28), it is clear that, for any

$$\mathbf{P} \geq 0, \quad \mathrm{I}_i(\mathbf{P}) \geq 0 \tag{2.89}$$

And also if

$$\mathbf{P} \geq \mathbb{Q} \Rightarrow \ \hat{\mathrm{I}}_i(\mathbf{P}) \geq \hat{\mathrm{I}}_i(\mathbb{Q}), \ \text{where } \mathbb{Q} = \left[\mathrm{q}_1,...,\mathrm{q}_Q\right]'. \tag{2.90}$$

Since $0 \leq \lambda_1 \leq 1; \lambda_2 = 1 - \lambda_1$ and from (2.88), (2.89) then for any

$$\mathbf{P} \geq 0 \Rightarrow \Psi_i(\mathbf{P}) \geq 0, \quad \forall i = 1,...,Q \tag{2.91}$$

So the *positivity* condition has been proven.

The monotonicity condition will be proven by contradiction. Assume that for some $\mathbf{P} \geq \mathbb{Q} \quad \Psi_i(\mathbf{P}) < \Psi_i(\mathbb{Q}), \ i = 1,...,Q$. Then from (2.88)

$$\frac{\hat{I}_i(\mathbf{P})a}{\lambda_1 \hat{I}_i(\mathbf{P}) + \lambda_2} < \frac{\hat{I}_i(\mathbb{Q})a}{\lambda_1 \hat{I}_i(\mathbb{Q}) + \lambda_2}, \ \text{i=1,...,Q} \tag{2.92}$$

$$\hat{I}_i(\mathbf{P})a < \frac{\hat{I}_i(\mathbb{Q})a\left[\lambda_1 \hat{I}_i(\mathbf{P}) + \lambda_2\right]}{\lambda_1 \hat{I}_i(\mathbb{Q}) + \lambda_2}, \ \text{i=1,...,Q} \tag{2.93}$$

$$\hat{I}_i(\mathbf{P})a < \hat{I}_i(\mathbf{P})a\frac{\left[\lambda_1 \hat{I}_i(\mathbb{Q}) + \lambda_2 \dfrac{\hat{I}_i(\mathbb{Q})}{\hat{I}_i(\mathbf{P})}\right]}{\lambda_1 \hat{I}_i(\mathbb{Q}) + \lambda_2}, \ \text{i=1,...,Q} \tag{2.94}$$

But from (2.90)

$$0 < \frac{\left[\lambda_1 \hat{I}_i(\mathbb{Q}) + \lambda_2 \dfrac{\hat{I}_i(\mathbb{Q})}{\hat{I}_i(\mathbf{P})}\right]}{\lambda_1 \hat{I}_i(\mathbb{Q}) + \lambda_2} < 1, \ \text{i=1,...,Q} \tag{2.95}$$

and (2.94) does not hold. Thus the assumption (2.92) is not true. Therefore for any **P**

$$\mathbf{P} \geq \mathbb{Q} \ \Rightarrow \ \Psi_i(\mathbf{P}) \geq \Psi_i(\mathbb{Q}), \ \text{i=1,...,Q} \tag{2.96}$$

So the *monotonicity* condition has been proven.

Next we prove scalability.

From (2.86), for any

$$\alpha > 1 \Rightarrow \alpha \hat{I}_i(\mathbf{P}) \geq \hat{I}_i(\alpha\mathbf{P}), \quad i = 1,...,Q \tag{2.97}$$

The equality is achieved if the additive noise is zero. From (2.88) we get

$$\alpha\Psi(\mathbf{P}) = \alpha\frac{\hat{I}_i(\mathbf{P})a}{\lambda_1 \hat{I}_i(\mathbf{P}) + \lambda_2} \geq \frac{\hat{I}_i(\alpha\mathbf{P})a}{\lambda_1 \hat{I}_i(\mathbf{P}) + \lambda_2}, \quad i = 1,...,Q \tag{2.98}$$

From (2.86), it follows that for $\alpha > 1, \ \hat{I}_i(\alpha\mathbf{P}) > \hat{I}_i(\mathbf{P}), \quad \text{i=1,...,Q}$ thus

$$\alpha\Psi_i(\mathbf{P}) > \frac{\hat{I}_i(\alpha\mathbf{P})a}{\lambda_1 \hat{I}_i(\alpha\mathbf{P}) + \lambda_2} = \Psi_i(\alpha\mathbf{P}), \quad \text{i=1,...,Q} \tag{2.99}$$

Then the *scalability* condition has been proven.

From (2.91),(2.96) and (2.99) one can say that the MODPC algorithm is a standard interference function. This means that the MODPC algorithm converges to a unique fixed

point. If $\lambda_1 = 0$ the MODPC algorithm is reduced to DPC algorithm. The feasibility condition is necessary for DPC algorithm to converge [6].

Proposition (2.10)

In the noiseless case, for any $\mathbf{P}(0)>0$ and with proper selection of λ_1 and λ_2, the MODPC algorithm will converge to the CIR balance, i.e.

$$\begin{aligned} &\lim_{t\to\infty} \mathbf{P}(t) = \mathbf{P}^* \qquad t = 0,1,... \\ &\lim_{t\to\infty} \Gamma_i(t) = \gamma^* \qquad t = 0,1,...,\ i = 1,...,Q \end{aligned} \tag{2.100}$$

where γ^* is the maximum achievable CIR, and $\mathbf{P}^*$ is the corresponding eigenvector.

Proof:

From (2.88)

$$P_i(t+1) = \frac{a}{\lambda_1 + \lambda_2 / \hat{I}_i(t)} = \frac{a}{\lambda_1 \hat{I}_i(t) + \lambda_2} \hat{I}_i(t) = \beta_i(t) \hat{I}_i(t)\ ,\ \text{i=1,...,Q} \tag{2.101}$$

Now we have obtained the same form as the DPC algorithm [2]. The convergence proof of this algorithm is presented in [2]. For convergence, λ_1 and λ_2 are chosen so that

$$\lim_{k\to\infty} (\lambda^*)^k \prod_{k=0}^{k} \left(\frac{a}{\lambda_1 \hat{I}_i(t) + \lambda_2} \right) < \infty \tag{2.102}$$

where λ^* is the spectral radius of the non-negative matrix **H** (see Equation (2.6)).

As indicated in (2.60) and (2.81) there is a penalty to use the power. For this reason the MODPC algorithm goes through fewer numbers of iterations than other conventional algorithms to converge to the accepted solution. Figure 2.7 shows this property of MODPC algorithm. The power path trajectory of the MODPC algorithm and DPC algorithm for two users are shown in Figure 2.7. It is clear that the MODPC algorithm converges faster than the DPC algorithm to reach to the feasible region. It is indicated in Section 2.5 that the MODPC algorithm has less spectral radius than the DPC algorithm. This means that the MODPC algorithm is asymptotically faster than the DPC algorithm.

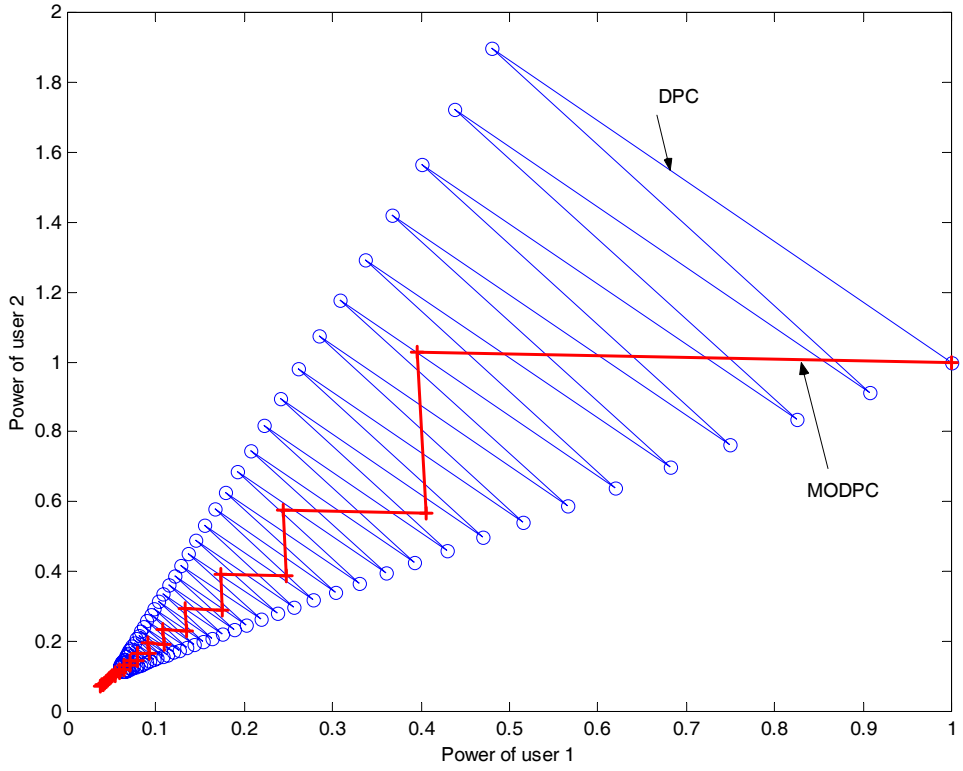

Figure 2.7. Comparison of convergence rates of DPC and MODPC.

2.4.8.1 Multi-Objective Totally Distributed Power Control (MOTDPC) algorithm

The MODPC algorithm, as other distributed algorithms, assumes the availability of the actual CIR at the MS. In this section we modify the MODPC algorithm to use an estimated CIR rather than the actual CIR. The estimation should be based on few quantization bits (worst case one bit) in the feedback channel. The same algorithm as in Section 2.4.7 has been applied to estimate the CIR.

From (2.47)-(2.49) and (2.56), the MOTDPC algorithm is given by

$$\tilde{\Gamma}_i(t) = \Gamma^T - \delta_i \left[\sum_{k=1}^{t-1} \nu_i(t-k) c_i(t,k) + \nu_i(t) \right], \quad \text{t=0,1,...,} \quad \text{i=1,...,Q} \tag{2.103}$$

$$P_i(t) = \frac{\lambda_1 P_{\min} + \lambda_2 \Gamma^T}{\lambda_1 P_i(t-1) + \lambda_2 \tilde{\Gamma}_i(t-1)} P_i(t-1), \quad i = 1,...,Q. \tag{2.104}$$

where $\tilde{\Gamma}_i(t)$ is the estimated CIR. Note that the target CIR is assumed to be known. This is one disadvantage of the MOTDPC algorithm because the target CIR is not fixed but adapted by the outer loop power control.

2.4.8.2 Soft Dropping Power Control

If the CIR target can not be achieved for every active user in the cell, i.e. the network is overloaded or congested, then the power control problem becomes infeasible. This means that no power vector in the allowed power subspace can achieve the required QoS for all users. If distributed power control techniques are applied for infeasible systems, then the transmitted power of some users will diverge to its maximum value without achieving the target CIR. This leads to a high interference in the cell and also in neighbor cells. This problem can be mitigated if some connections are dropped (transferred to another less-loaded cell or switched off). The main challenge here is how to find user terminals which have the worst impact on the system capacity. In other words, how to minimize the number of dropped connections. The optimal dropping algorithm is NP problem [1][102]. Some sub-optimal techniques for connection dropping have been proposed in [1], [25], [26],[102],[103]. Some removal algorithms assume a variable CIR target [25]. This is called soft dropping power control. In the soft dropping power control minimum and maximum target CIR is defined. In this work we have modified the MODPC algorithm (2.80) by using adaptive tradeoff parameters (λ_1 and λ_2) instead of fixed values. If the transmitted power of some users reaches the maximum value, then increasing the value of λ_1 (λ_2 =1-λ_1) of those users will decrease their targeted CIR. If the achieved CIR of a user is less than the minimum target CIR, then that connection will be dropped.

Define

$$\xi_i(t) := \lambda_{2,i}(t);\ \lambda_{1,i}(t) = 1 - \xi_i(t), \quad \text{t=0,1,...} \tag{2.105}$$

where $\xi_i(t)$ is the tradeoff parameter of user i.

The algorithm (2.80) could be rewritten as

$$P_i(t) = \frac{\left[1-\xi_i(t-1)\right]P_{\min} + \xi_i(t)\Gamma^T}{\left[1-\xi_i(t-1)\right]P_i(t-1) + \xi_i(t)\Gamma_i(t-1)} P_i(t-1), \quad \text{t=0,1,...,} \tag{2.106}$$

The parameter $\xi_i(t)$ can be updated with the following algorithm:

$$\xi_i(t) = \begin{cases} \alpha_1 \xi_i(t-1), & \text{if } \mathrm{P_i}(t-1) \le \rho_1 P_{\min}, \\ \alpha_2 \xi_i(t-1), & \text{if } \mathrm{P_i}(t-1) \ge \rho_2 P_{\max}, \\ \xi_i(t-1), & \text{else where,} \end{cases} \tag{2.107}$$

where α_1 is an increasing factor, α_2 is a decreasing factor, and ρ_1, ρ_2 are power factors.

If $\xi_i(t) < \xi_{min}$, the connection is dropped. Moreover, if $\xi_i(t) > \xi_{max}$, then choose $\xi_i(t) = \xi_{max}$.

Example

In this example we have simulated the operation of the soft dropping procedure represented by (2.106),(2.107). Four linear cells and 130 users uniformly distributed in 4 km^2 are assumed. The following typical values of the coefficients, α_1 =1.03, α_2 =0.99, ρ_1 =10, and ρ_2 =1 are assumed. The minimum allowed CIR is -16 dB and the target is -14 dB. The additive noise level is -130 dBm. The dropped connections of this simulation are shown in Figure 2.8. It is clear from the figure that the dropped connections are distributed around the cell border as expected.

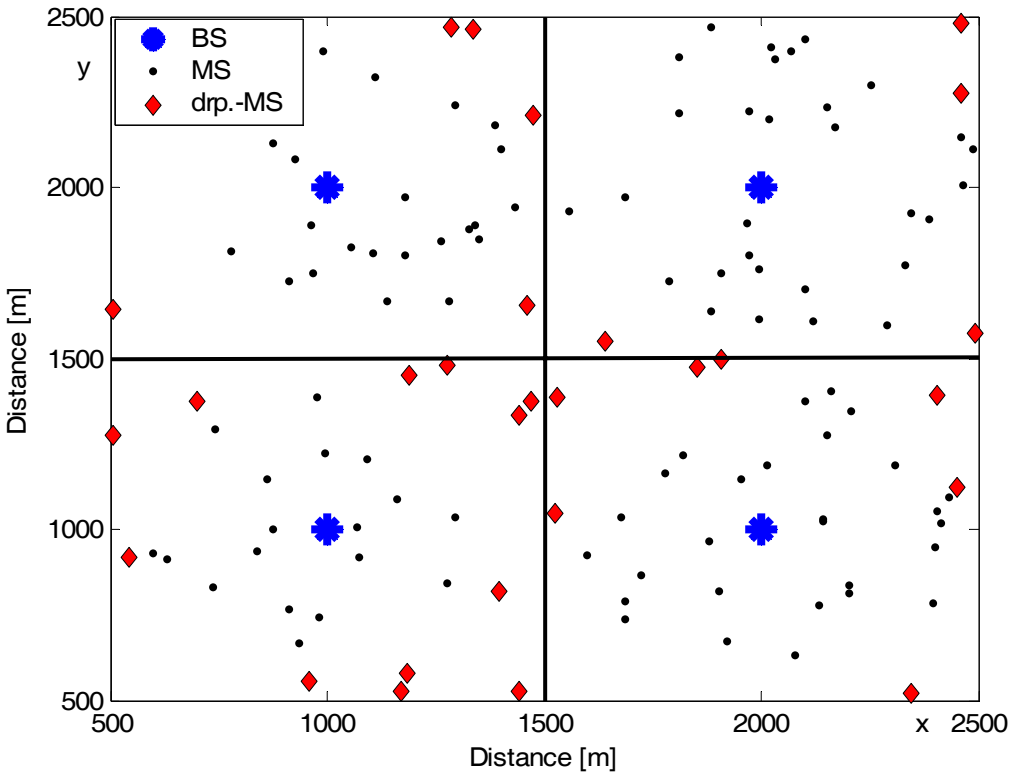

Figure 2.8. Dropped connections in highly congested network are marked with diamond.

2.4.9 Kalman Filter Distributed Power Control

In this Section we propose a novel distributed power control algorithm using Kalman filters. It is a well known fact that the Kalman filter is the optimum linear tracking device on the basis of second order statistics. This feature motivates us to apply the Kalman filter

in this type of applications. Kalman filter has been proposed in the literature recently in different applications related to the power control such as in interference estimation and prediction [105],[106]; power estimation [104]; and channel gain prediction for power control [106]. In this Section we use Kalman filter directly to estimate the best transmitted power in a distributed way.

Although the MODPC algorithm outperforms Kalman filter based power control in terms of convergence speed (as shown in Section 2.6), Kalman filter power control has a well-known linear behaviour which may make it preferred in some applications.

The power control is considered as linear time-variant first-order Markov model [19]. The transmitted power of user i at time slot t is given by

$$P_i(t) = w_i(t-1)P_i(t-1) \tag{2.108}$$

where the weight vector (states) $\mathbf{w}(t) = \left[w_1(t),...,w_Q(t)\right]'$ can be estimated by solving the following state-space equations

$$\mathbf{w}(t) = \mathbf{F}(t-1)\mathbf{w}(t-1) + \mathbf{q}(t-1), \tag{2.109}$$

$$\mathbf{y}(t) = \mathbf{G}(t)\mathbf{w}(t) + \mathbf{v}(t), \tag{2.110}$$

where $\mathbf{F}(t)$ is the transition matrix, the state vector $\mathbf{w}(t)$ represents the tap-weight vector at time slot t, $\mathbf{q}(t)$ is the process noise, $\mathbf{y}(t)$ is the desired QoS response, $\mathbf{G}(t)$ is the measurement matrix, and $\mathbf{v}(t)$ is the measurement noise. $\mathbf{q}(t)$ and $\mathbf{v}(t)$ are assumed to be zero-mean white noise with covariance matrices $\mathbf{Q}(t) = q_o\mathbf{I}$, and $\mathbf{R}(t) = \nu_o\mathbf{I}$ respectively.

To solve the problem in a distributed manner (i.e. each user updates its power based on local information), we have designed the matrices $\mathbf{F}$ and $\mathbf{G}$ in diagonal forms, such as

$$\mathbf{G}(t) = \begin{bmatrix} g_1(t) & 0 & \cdots & 0 \\ 0 & g_2(t) & 0 & \vdots \\ \vdots & 0 & \ddots & 0 \\ 0 & 0 & \cdots & g_Q(t) \end{bmatrix} \tag{2.111}$$

where $g_i(t)$ is the CIR of user i at time slot t, i.e. $g_i(t) = \dfrac{P_i(t)}{\hat{I}_i(t)}$.

The transition matrix $\mathbf{F}(t)$ is given by

$$\mathbf{F}(t)=\begin{bmatrix} f_1(t) & 0 & \cdots & 0 \\ 0 & f_2(t) & 0 & \vdots \\ \vdots & 0 & \ddots & 0 \\ 0 & 0 & \cdots & f_Q(t) \end{bmatrix} \tag{2.112}$$

where $f_i(t-1)=\dfrac{g_i(t-1)}{g_i(t)}$.

Assuming that all users have the same QoS, the desired system response is given by

$$\mathbf{y}(t)=\left[\Gamma^T,\Gamma^T,\cdots,\Gamma^T\right]' \tag{2.113}$$

To explain the proposed state space representation of the power control, assume the measurement noise and the process noise equal to zero. For one user *i* (scalar form), (2.109) and (2.110) are given by

$$w_i(t)=\frac{g_i(t-1)}{g_i(t)}w_i(t-1) \tag{2.114}$$

$$\Gamma^T=g_i(t)w_i(t) \tag{2.115}$$

In power control, the optimum transmitted power is determined to achieve the target CIR in the next time slot. From (2.108), the next time slot CIR can be predicted as

$$\tilde{g}_i(t+1)=g_i(t)w_i(t) \tag{2.116}$$

From (2.114)-(2.116), the adaptation weight is computed to achieve the target CIR in the next time slot. The modeling error (process noise) and the measurement noise should be taken into consideration to complete the state space modeling. Kalman filter is used to estimate the optimum adaptation weight $w_i(t)$ in order to make the next time slot CIR very close to the target CIR.

A. **Kalman filter algorithm**

Kalman filter algorithm is specified by the following equations [20]:

Let **C**(0) be the initial error covariance and **w**(0) the initial weight vector. Then for *t*=0,1,2,….

$$\hat{\mathbf{w}}^-(t)=\mathbf{F}(t-1)\hat{\mathbf{w}}^+(t-1)\ \ (\text{weight extrapolation}), \tag{2.117}$$

$$\mathbf{C}^-(t)=\mathbf{F}(t-1)\mathbf{C}^+(t-1)\mathbf{F}'(t-1)+\mathbf{Q}(t-1)\ \ (\text{error covariance extrapolation}), \tag{2.118}$$

$$\mathbf{K}(t)=\mathbf{C}^-(t)\mathbf{G}'(t)\left[\mathbf{G}(t)\mathbf{C}^-(t)\mathbf{G}'(t)+\mathbf{R}(t)\right]^{-1}\ \ (\text{Kalman gain}), \tag{2.119}$$

$$\hat{\mathbf{w}}^{+}(t)=\hat{\mathbf{w}}^{-}(t)+\mathbf{K}(t)\left[\mathbf{y}(t)-\mathbf{G}(t)\hat{\mathbf{w}}^{-}(t)\right] \quad (\text{weight update}), \tag{2.120}$$

$$\mathbf{C}^{+}(t)=\left[\mathbf{I}-\mathbf{K}(t)\mathbf{G}(t)\right]\mathbf{C}^{-}(t) \quad (\text{error covariance update}), \tag{2.121}$$

The algorithms in (2.117)-(2.121) can be solved in scalar form, since all the matrices are in diagonal form.

Proposition (2.11)

In feasible systems with snapshot assumption, using the proposed Kalman filter power control, all users will approach their CIR targets.

Proof.

From (2.117), (2.120) , the weight update equation for user i can be represented as

$$\begin{aligned}\hat{w}_i^{+}(t) &= f_i(t-1)\hat{w}_i^{+}(t-1)+K_i(t)\left[\Gamma^{T}-g_i(t)f_i(t-1)\hat{w}_i^{+}(t-1)\right]\\ &= f_i(t-1)\hat{w}_i^{+}(t-1)+K_i(t)\left[\Gamma^{T}-g_i(t-1)\hat{w}_i^{+}(t-1)\right].\end{aligned} \tag{2.122}$$

At steady state, let

$$\hat{w}_i^{+}(t)=\hat{w}_i^{s},\quad \mathrm{K_i}(t)=K_i^{s},\ \mathrm{g_i}(t)=g_i^{s},\ \text{and}\ \mathrm{f_i}(t)=f_i^{s} \quad . \tag{2.123}$$

Then

$$\hat{w}_i^{s}=f_i^{s}\hat{w}_i^{s}+K_i^{s}\left[\Gamma^{T}-g_i^{s}\hat{w}_i^{s}\right]=\frac{\mathrm{K_i^s}\Gamma^{T}}{1-f_i^{s}+\mathrm{K_i^s}g_i^{s}}. \tag{2.124}$$

Since at steady state, $f_i^{s}=1$, the steady-state weight becomes

$$\hat{w}_i^{s}=\frac{\Gamma^{T}}{g_i^{s}}. \tag{2.125}$$

For user *i*, the CIR becomes

$$\Gamma_i^{s}=\frac{\hat{w}_i^{s}P_i^{s}}{I_i^{s}}=\Gamma^{T}. \tag{2.126}$$

The convergence properties of the Kalman filter depend on the values of the covariance matrices. From (2.121) the error covariance equation can be represented as

$$C_i^{+}(t)=\left(1-K_i(t)g_i(t)\right)\left(f_i^{2}(t)C_i^{+}(t-1)+q_0\right), \tag{2.127}$$

where the Kalman gain (2.119) in scalar form is represented as

$$K_i(t)=\frac{\left(f_i^{2}(t-1)C_i^{+}(t-1)+q_o\right)g_i(t)}{g_i^{2}(t-1)C_i^{+}(t-1)+g_i^{2}(t)q_o+v_o} \tag{2.128}$$

By substituting (2.128) into (2.127), one obtains

$$C_i^+(t) = \frac{f_i^2(t-1)C_i^+(t-1)v_o + q_o v_o}{g_i^2(t-1)C_i^+(t-1) + g_i^2(t)q_o + v_o} \tag{2.129}$$

At steady state, one obtains

$$C_i^s = -\frac{q_o}{2} + \frac{q_o}{2}\sqrt{1 + 4\frac{v_o}{q_o\left(g_i^s\right)^2}} \tag{2.130}$$

We are interested in the nonnegative solution, because the variance $C_i^+(t)$ of uncertainty is, by definition, nonnegative [20]. From(2.130), if the factor v_o/q_o is small then faster convergence can be achieved [20].

B. **Convergence**

The convergence properties of the Kalman filter depend on the values of the covariance matrices. The convergence speed is important issue in power control due to the dynamical behavior of the mobile communication system. Unfortunately, it is rather difficult to find an analytical expression for the convergence speed of the Kalman filter because of the time varying nature of the system. The performance analysis of the Kalman filter depends on solving the Riccati equations. It is possible to simulate the Riccati equations without computing the state estimates themselves. This gives us a good indication of the convergence speed of the algorithm. The discrete-time Riccati equation is the solution of the following equation [20]

$$\mathbf{C}^-(t+1) = \mathbf{A}(t+1)\mathbf{B}^{-1}(t+1), \tag{2.131}$$

where

$$\begin{bmatrix}\mathbf{A}(t+1)\\ \mathbf{B}(t+1)\end{bmatrix} = \begin{bmatrix}\left(\mathbf{F}(t) + \mathbf{Q}(t)\left(\mathbf{F}^{-1}(t)\right)'\mathbf{G}'(t)\mathbf{R}^{-1}(t)\mathbf{G}(t)\right) & \mathbf{Q}(t)\left(\mathbf{F}^{-1}(t)\right)'\\ \left(\mathbf{F}^{-1}(t)\right)'\mathbf{G}'(t)\mathbf{R}^{-1}(t)\mathbf{G}(t) & \left(\mathbf{F}^{-1}(t)\right)'\end{bmatrix}\begin{bmatrix}\mathbf{A}(t)\\ \mathbf{B}(t)\end{bmatrix} \tag{2.132}$$

2.5 Convergence Speed Comparison of Power Control Algorithms

The convergence speed of a power control algorithm is an important factor in the selection of the optimum power control algorithm for a wireless communication system. In this section, the power control algorithm will be defined as a contraction mapping.

Equation (2.15) is in the form of contraction mapping. The convergence analysis of contraction mapping can be applied to (2.15). Suppose that, the power control algorithm

is feasible, i.e. $\mathbf{P}^* = \boldsymbol{\Psi}\left(\mathbf{P}^*\right)$ and $\Gamma_i = \Gamma^T \quad \forall \quad i = 1,\ldots,Q$, where $\mathbf{P}^* = \left[P_1^*,....,P_Q^*\right]'$ is the optimum power vector, and that the partial derivatives

$$\mathrm{d}_{ij}\left(\mathbf{P}\right) = \frac{\partial \Psi_i\left(\mathrm{P}_i,\Gamma_i\right)}{\partial \mathrm{P}_j} \qquad 1 \le \mathrm{i,j} \le \mathrm{Q} \tag{2.133}$$

exist for $\mathbf{P} \in \Re$ where $\Re = \left\{\mathbf{P} : \left\|\mathbf{P} - \mathbf{P}^*\right\| < \rho\right\}$ and ρ is a positive constant. Let **D**(**P**) be Q×Q matrix with elements $\mathrm{d}_{ij}\left(\mathbf{P}\right)$. A necessary condition for (2.15) to converge is that the spectral radius of **D**(**P***), $\left\{\rho\left[\mathrm{D}\left(\mathbf{P}^*\right)\right]\right\}$, is less than or equal to 1. Define a constant *m* >0 such that

$$\rho\left[\mathrm{D}\left(\mathbf{P}\right)\right] \le \mathrm{m} < 1 \qquad \mathbf{P} \in \Re \tag{2.134}$$

The rate of convergence depends linearly on *m*, and we have [87]

$$\left\|\mathbf{P}\left(t+1\right) - \mathbf{P}^*\right\| \le m\left\|\mathbf{P}\left(t\right) - \mathbf{P}^*\right\| \tag{2.135}$$

From (2.134) and (2.135), we may use the spectral radius of the matrix **D**(**P**) as an indication of the asymptotic average rate of convergence. Similar results with different methodology are presented in [56].

We will compare the convergence speeds of four different power control algorithms: DBA, DPC, FMA, and MODPC algorithms.

Starting with DBA algorithm, it is clear that (2.16) has the form of contraction mapping represented by (2.15). The elements of matrix **D**(**P**) are defined in (2.133). By taking partial derivatives of the right hand side of (2.16) we obtain

$$\mathrm{d}_{ij}^{\mathrm{DBA}}\left(\mathbf{P}\right) = \begin{cases} \beta & \mathrm{i=j} \\ \beta\dfrac{\mathrm{G_{kj}}}{\mathrm{G_{ki}}} & \mathrm{i} \ne \mathrm{j}\ ,\ \mathrm{k} \in \{1,2,..\mathrm{M}\} \end{cases} \tag{2.136}$$

In the case of DPC algorithm (2.18), The elements of matrix **D**(**P**) are

$$\mathrm{d}_{ij}^{\mathrm{DPC}}\left(\mathbf{P}\right) = \begin{cases} 0 & \mathrm{i=j} \\ \Gamma^{\mathrm{T}}\dfrac{\mathrm{G_{kj}}}{\mathrm{G_{ki}}} & \mathrm{i} \ne \mathrm{j}\ ,\ \mathrm{k} \in \{1,2,..\mathrm{M}\} \end{cases} \tag{2.137}$$

In the case of FMA algorithm (2.35), The elements of matrix **D**(**P**) are

$$d_{ij}^{FMA}(\mathbf{P}) = \begin{cases} (1-\hat{\beta}) & i=j \\ \hat{\beta}\Gamma^{T}\dfrac{G_{kj}}{G_{ki}} & i \neq j\ ,\ k \in \{1,2,..M\} \end{cases} \tag{2.138}$$

In the case of MODPC algorithm (2.80), The elements of matrix **D**(**P**) are

$$d_{ij}^{MODPC}(\mathbf{P}) = \begin{cases} 0 & i=j \\ \Gamma^{T}\dfrac{G_{kj}}{G_{ki}}\dfrac{1}{\left[\dfrac{\lambda_1}{\lambda_2}\hat{I}_i(t)+1\right]^2} & i \neq j\ ,\ k \in \{1,2,..M\} \end{cases} \tag{2.139}$$

Note that in (2.139) we have put P_{min}=0 for simplicity.

The spectral radius of a nonnegative matrix **A** is less than the spectral radius of a nonnegative matrix **B** if **A**<**B**. The convergence rates of the algorithms can be analyzed by comparing the matrix elements in (2.136), (2.137), (2.138) and (2.139). From (2.136) and (2.137), one can say that if $\beta = \dfrac{\Gamma^{T}}{1+\Gamma^{T}}$ then $\mathbf{D}^{DBA}(\mathbf{P}) > \mathbf{D}^{DPC}(\mathbf{P})$ which means that DPC algorithm is faster than DBA algorithm (different proof for this result is given in Appendix 2). From (2.138), if $\hat{\beta}$=1, we get the same convergence rate as DPC. For $\hat{\beta} \in (0,1)$, the DPC algorithm will be faster than FMA algorithm. The comparison between the convergence rates of DBA and FMA algorithms depends on the selection of the parameters $\hat{\beta}$ and β. Finally, from (2.139), it is clear that $d_{ij}^{MODPC}(\mathbf{P}) \leq d_{ij}^{DPC}(\mathbf{P})$ 1<i,j<Q with equality at $\lambda_1 = 0$. Thus we can conclude that MODPC algorithm is faster than the DPC algorithm.

To compare the convergence speed by simulation, consider 20 randomly distributed users in 1 Km^2 area with one base station. The average additive noise power is -90 dBm, the

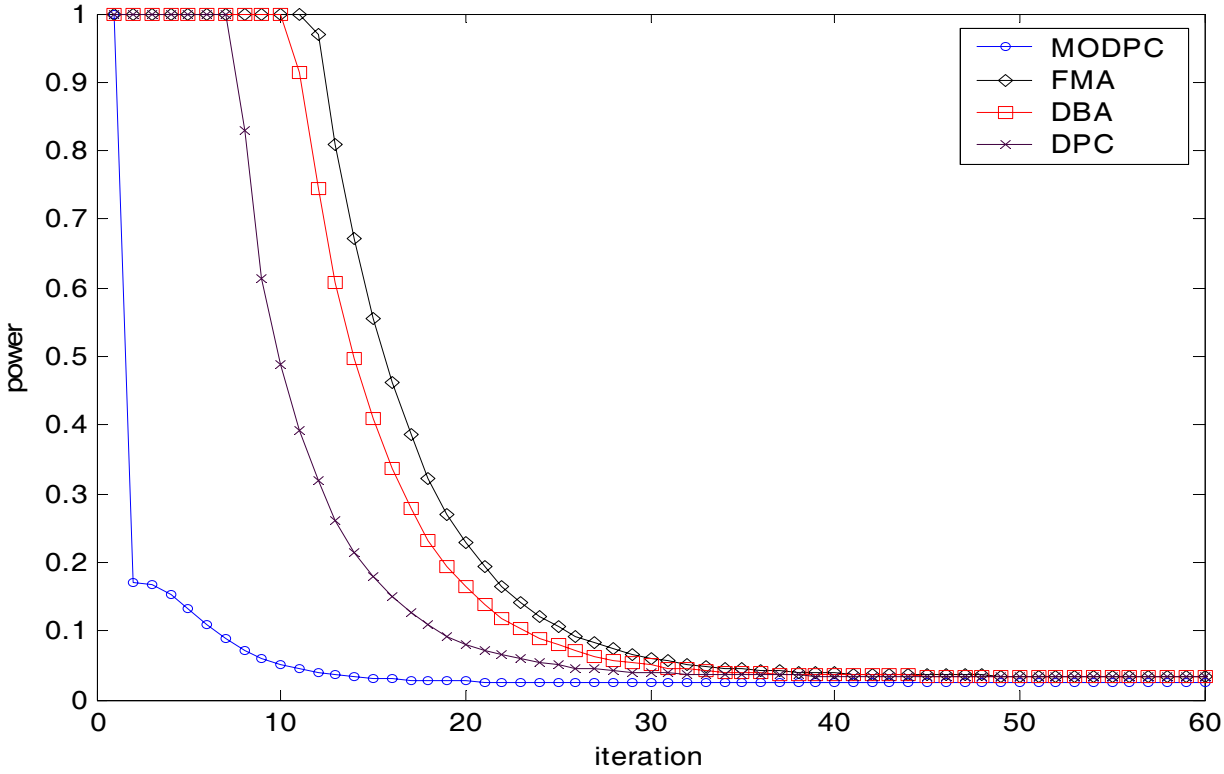

Figure 2.9. Convergence speed comparison of different power control algorithms

DBA parameter $\beta = \frac{\Gamma^T}{1+\Gamma^T}$ and the FMA parameter $\hat{\beta}$=0.9. The average transmitted power using the described algorithms is shown in Figure 2.9.

2.6 Simulation Results

To show the effectiveness of the proposed algorithms, we will compare our algorithms with different power control algorithms summarized in the beginning of this Chapter by simulation. Two scenarios have been performed by simulations. We assumed 120 users uniformly distributed in an area of 4 km^2 with four base stations. Perfect handover is assumed where each user is assigned to the base station with the least gain loss. An additive white Gaussian noise is assumed with zero mean and -120dBw variance. The channel is assumed static. In the second scenario, the same parameters as the first scenario are assumed with more realistic mobile channel including slow fading and the fast fading.

The first scenario shows the convergence behaviors of different power control algorithms. Since we will compare 10 different power control algorithms, it will be difficult to put the results together in the same Figure. The results of each power control algorithm will be given in a separate Figure. We will join more than one result in one Figure to clarify certain properties. The results of each algorithm have been represented by the norm of the error and the outage percentage. The error is defined as the difference between actual transmitted power vector of the power control algorithm and the optimum power vector. The optimum power vector is calculated using the centralized power control algorithm. The outage percentage is computed by counting the number of slots when the CIR of a user is less than the minimum allowed CIR (CIR threshold). The minimum allowed CIR has been set to 3 dB less than the target CIR. The target CIR is set to $\Gamma^T = -18dB$. Also the average transmitted power in dB is given for each power control algorithm in Tables 2.1 and 2.2. The power control algorithms that have been discussed are classified to distributed algorithms and totally distributed algorithms. The first group of results will be for the distributed algorithms and the second group is for the totally distributed algorithms.

Figure 2.10 shows a sample of the mobile-base stations distribution of the scenarios. Figure 2.11 displays the error norm and the outage of the system using distributed power control algorithm. It is clear that the power has converged to the optimum power at about time slot number 10. The outage is zero after time slot number 3. In this scenario, the distributed balancing algorithm and the fully distributed algorithm have very close characteristics of the DPC. Figure 2.14 presents the convergence behavior of the Foschini and Miljanic power control algorithm which is slower than the DPC. The coefficient β has been set to 0.75. Figure 2.15 shows the results of second order power control algorithm. The power of SOPC converges faster than the DPC but slower from outage point of view. Figure 2.16 displays the proposed multi-objective distributed power control algorithm. It is clear that the MODPC algorithm has faster convergence than the DPC in both power and outage. Figure 2.17 presents both DPC and MODPC algorithms for easier comparison. Figure 2.18 shows the second proposed Kalman power control algorithm. The KDPC has close characteristics to DPC algorithm. The simulation results of the totally distributed power control algorithms are (as expected) worse than the distributed power control algorithms. Figure 2.19 displays the convergence behavior of the

conventional fixed-step power control FSPC algorithm. Figure 2.20 displays the convergence behavior of the ESPC algorithm. The steady state adaptation size is 0.3. It is clear that the proposed Estimated Step Power Control ESPC algorithm outperforms the FSPC algorithm in both power and outage convergence characteristics. Figure 2.21 shows the convergence behavior of the fourth proposed algorithm which is an extension of the MODPC algorithm.

Table 2.1. Transmitted power comparisons for the first scenario

Power Control Algorithm	DPC	DBA	FDPC	FMA	SOPC	MODPC	KDPC	FSPC	ESPC	MOTDPC
Average transmitted power (dBw)	**-10.07**	**-9.89**	**-10.07**	**-7.95**	**-10.27**	**-13.81**	**-12.08**	**-2.33**	**-5.88**	**-11.46**

It is clear that the transmitted power converges in a very fast manner compared with other totally distributed algorithms. Table 1 indicates the average transmitted power of the different studied power control algorithms.

Table 2.1 indicates that the average consumption power of the proposed algorithms is less than the average consumption power of the other algorithms. In distributed algorithms the average consumption power of MODPC algorithm is -13.08 dBw whereas in DPC it is -10.07dBw. There is also tremendous power saving when we compare MOTDPC (-11.46 dBw) and FSPC (-2.33 dBw).

More realistic dynamic channel characteristics are assumed in the second scenario. To show the dynamics of transmitted power, we show the optimum power as well as the actual power of a randomly selected user. Figure 2.22 shows an error norm, a transmitted power and an outage using DPC algorithm. The fluctuations in the outage are due to the channel dynamics. Figure 2.23 displays the results of the DBA algorithm. As expected the results are close to the DPC algorithm results. The FDPC algorithm fails to converge to the optimum transmitted power in dynamically fluctuated channels as presented in Figure

2.24. It is clear that the outage approaches 90% in this case. Figures 2.25, 2.26 show the results of the SOPC and F&MPC algorithms respectively. Figure 2.27 displays the results of the MODPC algorithm. It is clear that the MODPC algorithm converges to the optimum solution. The Kalman distributed power control algorithm can converge to the optimum solution in a dynamic channel case suggested in Figure 2.28. In this scenario, the DPC algorithm has the fastest convergence rate of the conventional algorithms (Figures 2.22-2.26). Kalman distributed power control algorithm has almost the same convergence rate as the DPC algorithm. The MODPC algorithm converges considerably faster than the DPC algorithm in terms of Error norm and transmitted power. In terms of outage the MODPC performs as well as DPC. Figure 2.29 shows these comparison results. The results of the totally distributed algorithms are shown in Figures 2.30-2.32. From the results it is clear that both proposed totally distributed algorithms (MOTDPC and ESPC) converge faster than the conventional FSPC algorithm in terms of transmitted power and Error norm. Considering outage, the FSPC performs better than the proposed algorithms. Direct comparison is shown in Figure 2.33. Table 2.2 indicates another very important term of comparison which is the average consumption power. The MODPC has the least power consumption compared with all other power control algorithms. Also the proposed algorithms for the totally distributed power control consume considerably less average power than the conventional FSPC algorithm. From these results we can conclude that for distributed algorithms the MODPC algorithms outperform the other studied algorithms in terms of convergence speed and power consumption. The second advantage of the MODPC algorithm is that it needs no more resources than the conventional DPC algorithm. The MODPC is also simple to realize and to test. For the totally distributed systems, the MOTDPC algorithm outperforms the conventional FSPC algorithm in terms of convergence rate of power and power consumption. But it suffers from higher outage compared with the FSPC.

More simulations have been carried out on the ESPC algorithm. As described in Section 2.4.7 the ESPC tries to estimate the error signal from the ON-OFF power commands. Figures 2.34 and 2.35 show the cumulative distribution function (CDF) of E_b/N_o, at the receiver for three different power control algorithms. The algorithms are the FSPC, DCPC and the suggested ESPC. The target SNR is 6 dB. The maximum speed of users in Figures 2.34 is 5 km/h, and the adaptation factor $\delta = 0.1$. It is clear that the ESPC

algorithm performance is considerably better than that of the FSPC algorithm. The interesting feature of the ESPC algorithm is that it uses the same signaling information of the FSPC algorithm. In Figure 2.35, we present the situation in a fast fading environment where the maximum speed of users is 30 km/h. It is clear that the performance of the ESPC degrades (as expected) with fast fading environment. More detailed analysis can be found in [94]. The power control command errors impact on the totally distributed power control algorithms have not been considered in this Section. To see the impact of power control errors on the MOTDPC algorithm, one simulation example is shown in Figure 2.36. Different command error probabilities are used to investigate the MOTDPC algorithm robustness. It is clear that as the power control error probability increases the performance of the MOTDPC algorithm decreases, but still converges to the correct direction. The original MODPC algorithm (2.79) has been simplified to (2.80) by removing sharp changes in the sign of λ_2. Figure 2.37 shows a comparison between the original MODPC and the simplified version. It is interesting to see that the simplified MODPC performs generally better than the original one. The reason is that, in the original MODPC one may obtain a negative sign of the power or even very large values, these values are removed because the power values are limited between minimum and maximum values. This removing of the undesired power values reduces the performance of the original MODPC algorithm.

Table 2.2. Transmitted power comparisons for the second scenario

Power Control Algorithm	DPC	DBA	FDPC	FMA	SOPC	MODPC	KDPC	FSPC	ESPC	MOTDPC
Average transmitted power (dBw)	**-15.66**	**-15.56**	**-16.11**	**-14.00**	**-16.08**	**-19.82**	**-15.75**	**-8.40**	**-10.21**	**-11.15**

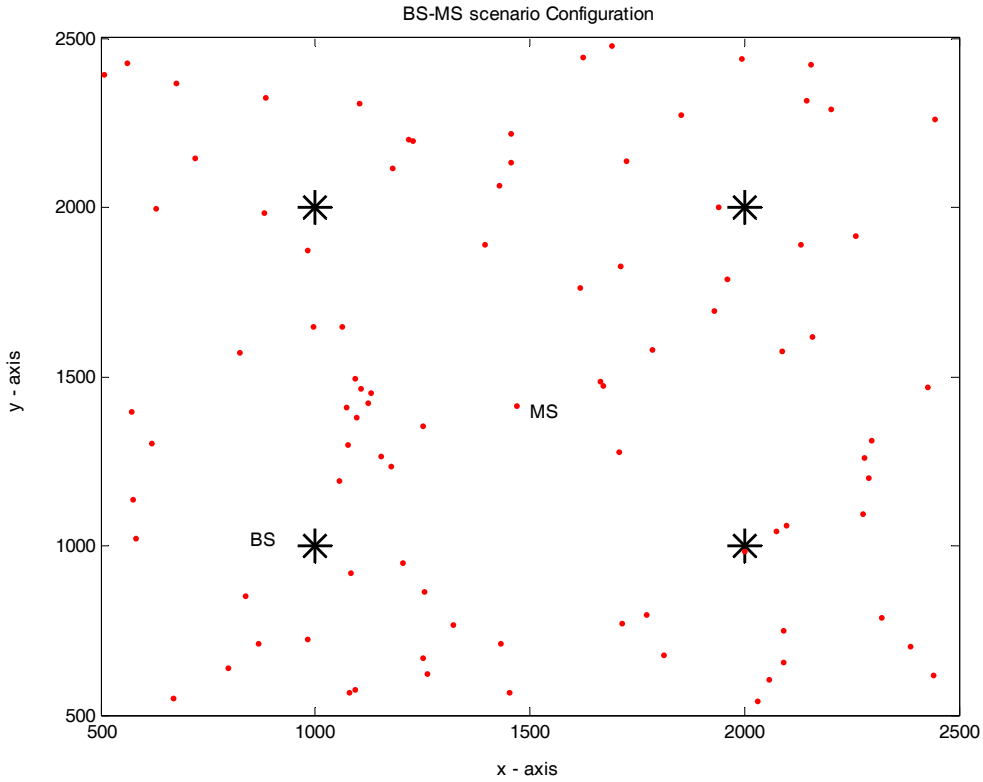

Figure 2.10. The MS-BS configuration.

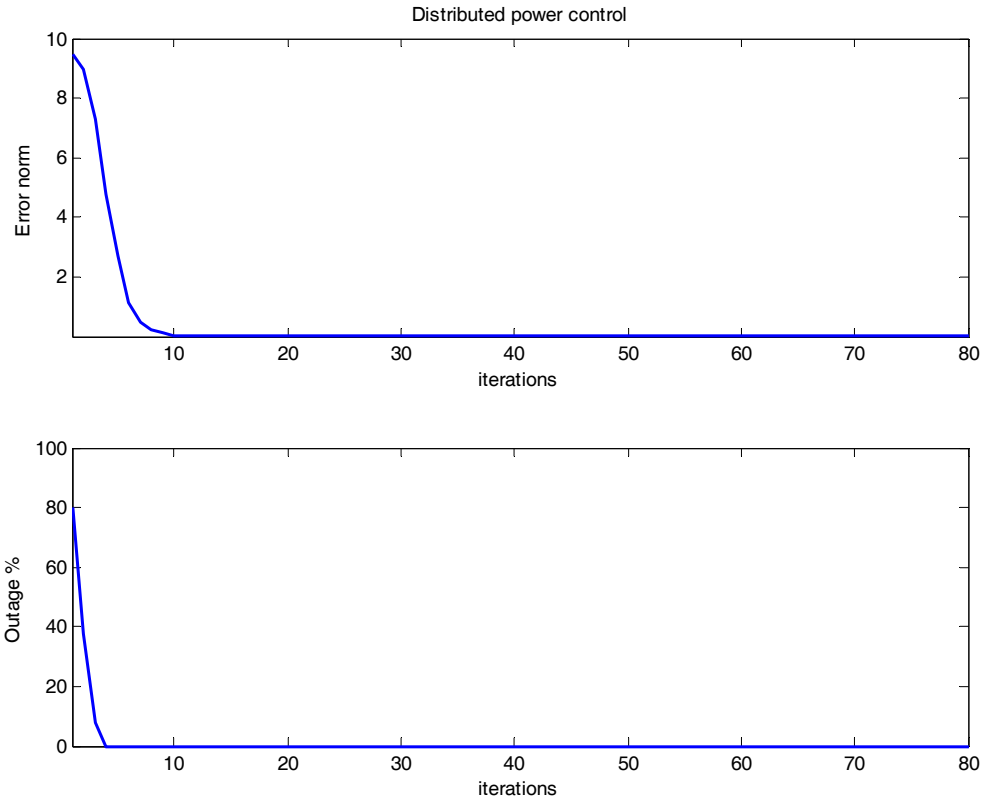

Figure 2.11. Error norm and the outage of DPC algorithm.

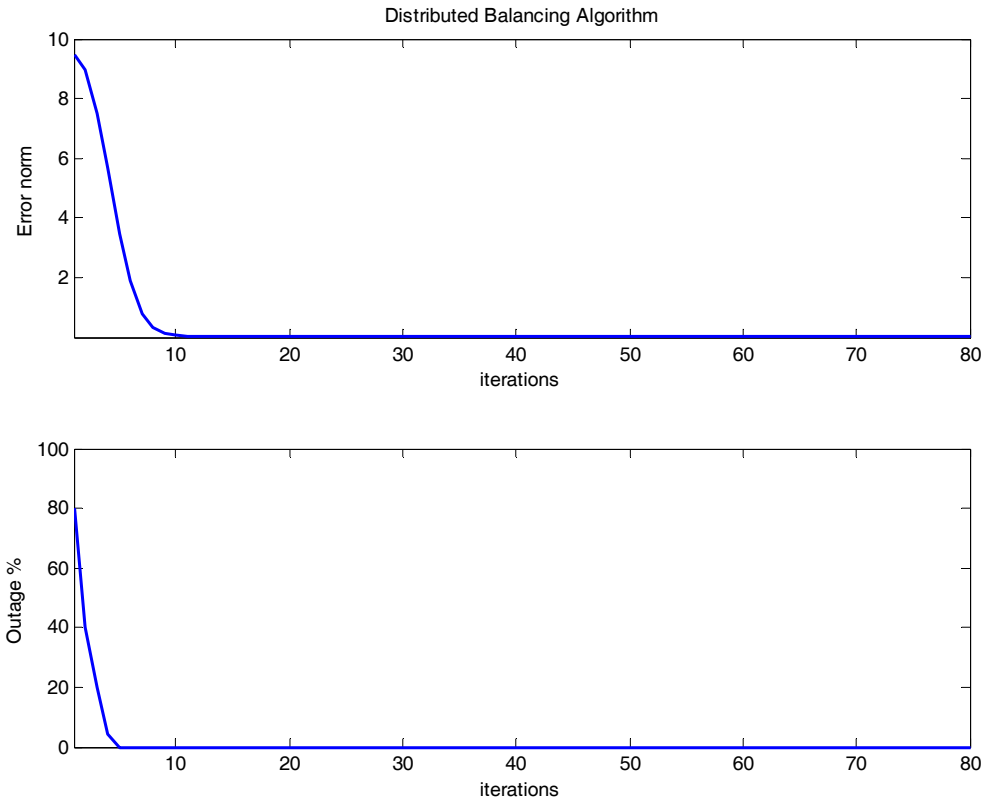

Figure 2.12. Error norm and outage of DBA algorithm.

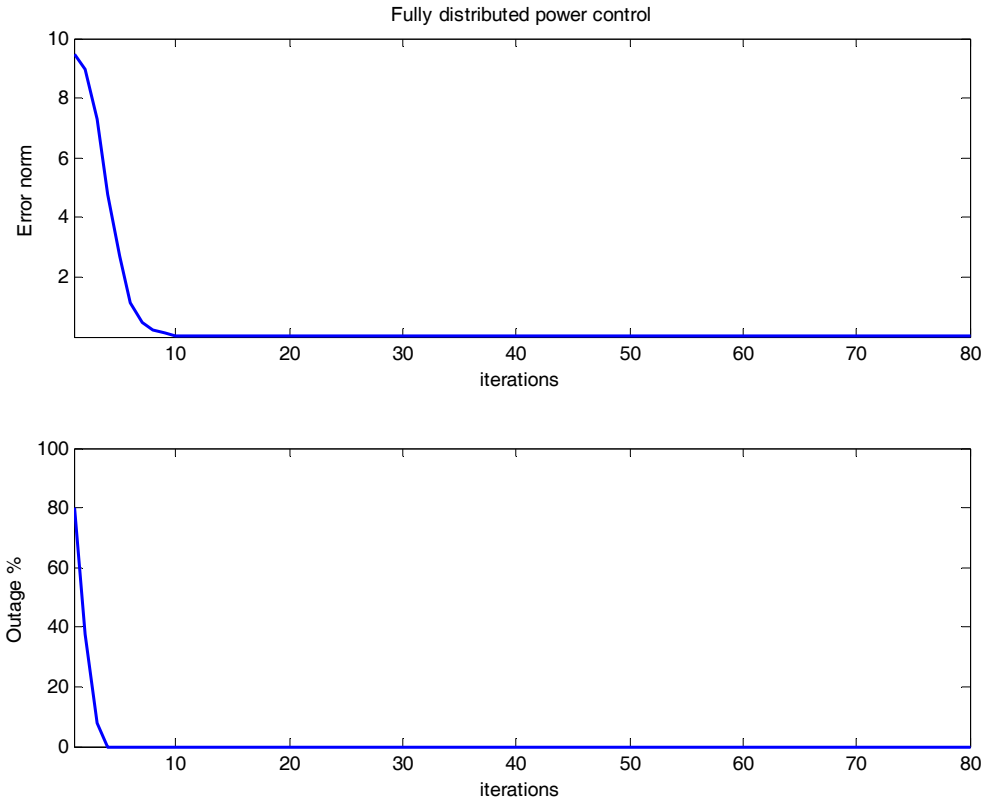

Figure 2.13. Error norm and outage of FDPC algorithm.

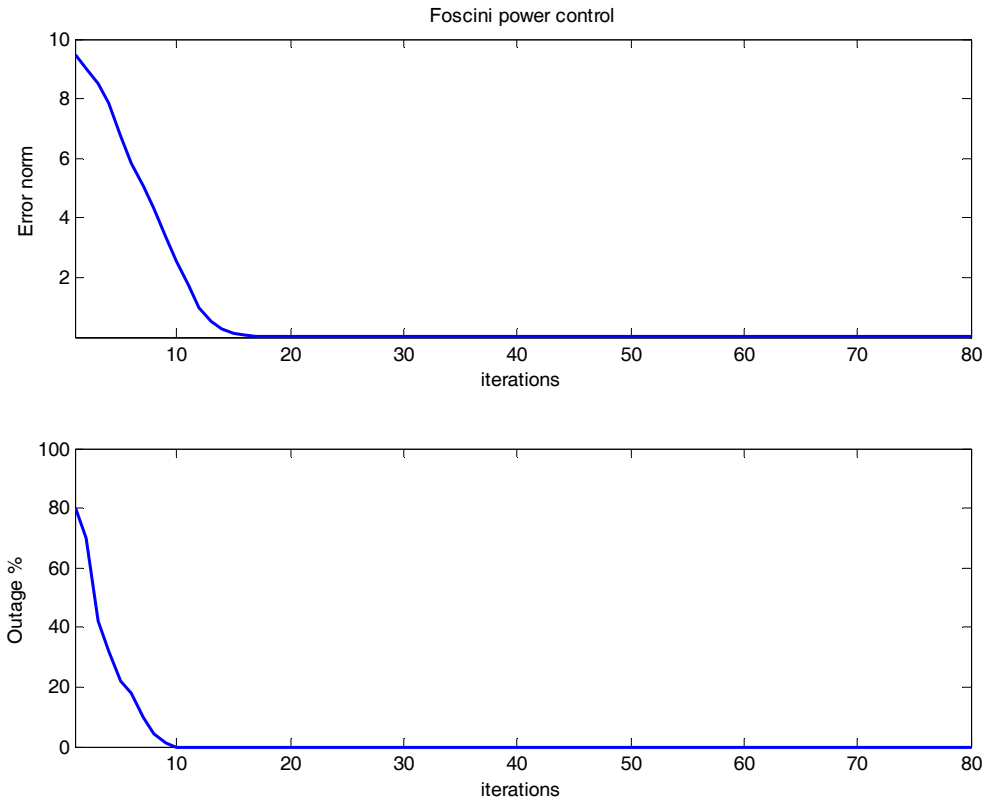

Figure 2.14. Error norm and the outage of FMA algorithm.

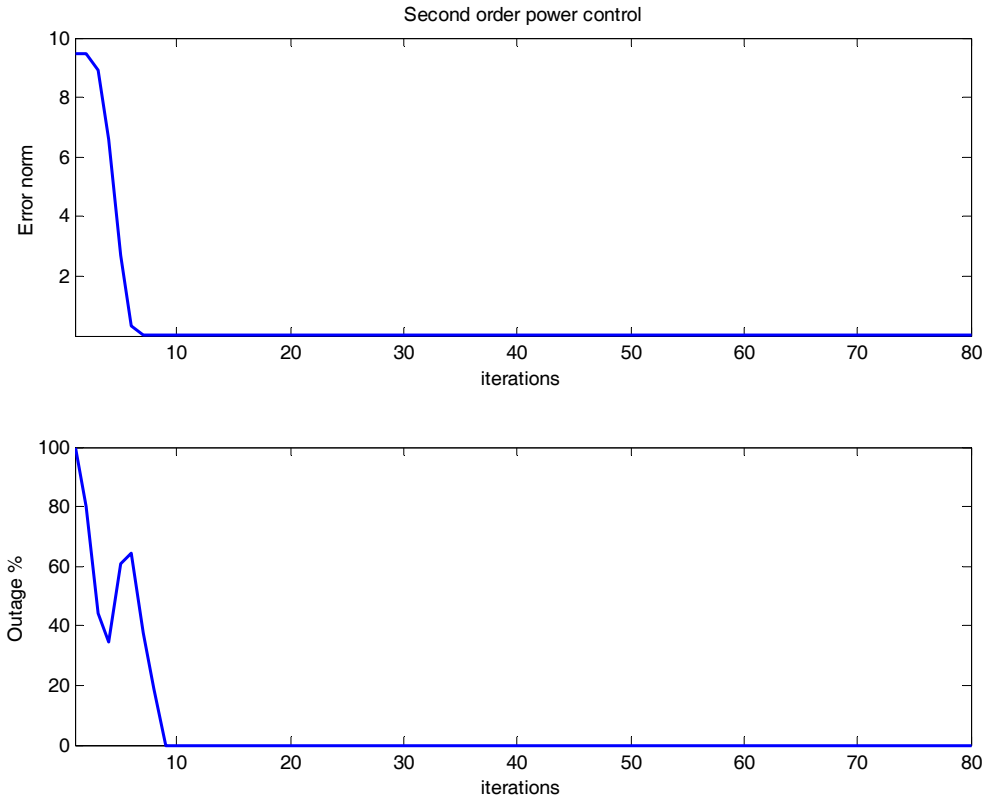

Figure 2.15. Error norm and the outage of SOPC algorithm.

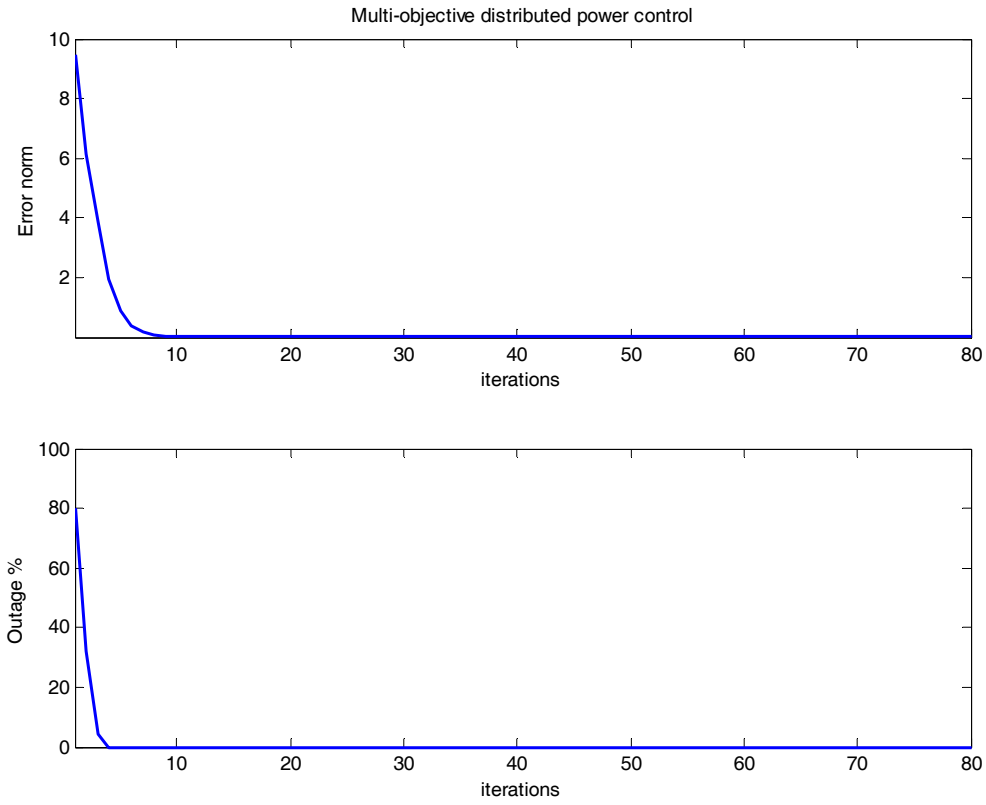

Figure 2.16. Error norm and the outage of MODPC algorithm.

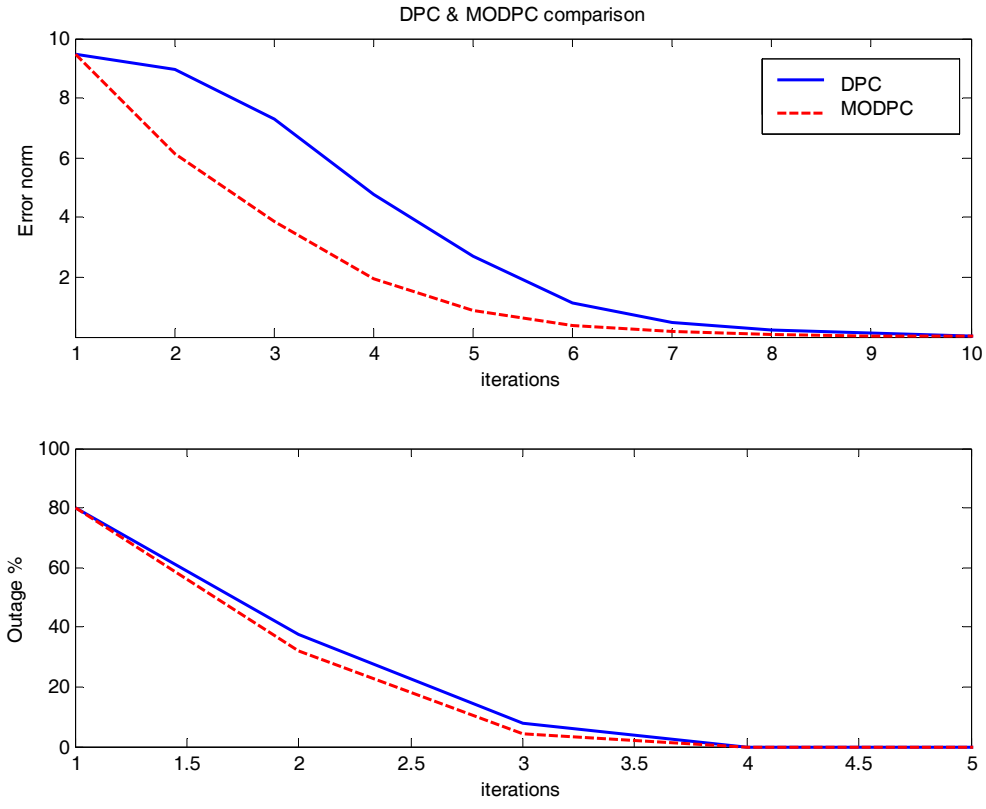

Figure 2.17. Error norm and the outage of DPC and MODPC algorithms.

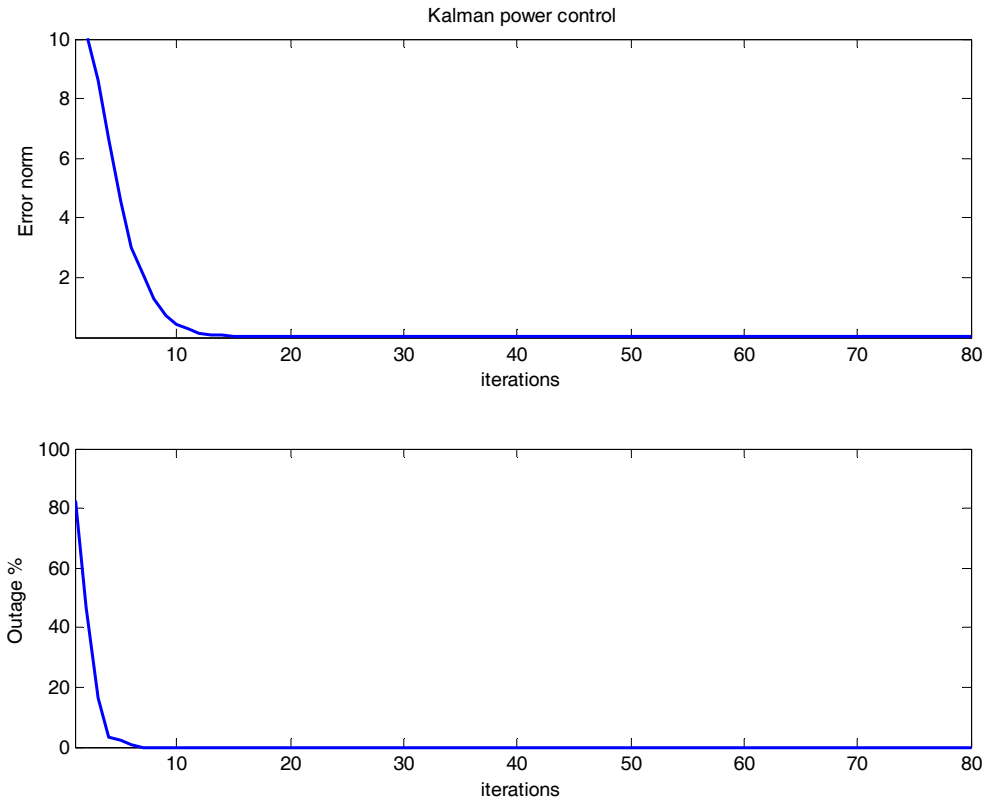

Figure 2.18. Error norm and the outage of KDPC algorithm.

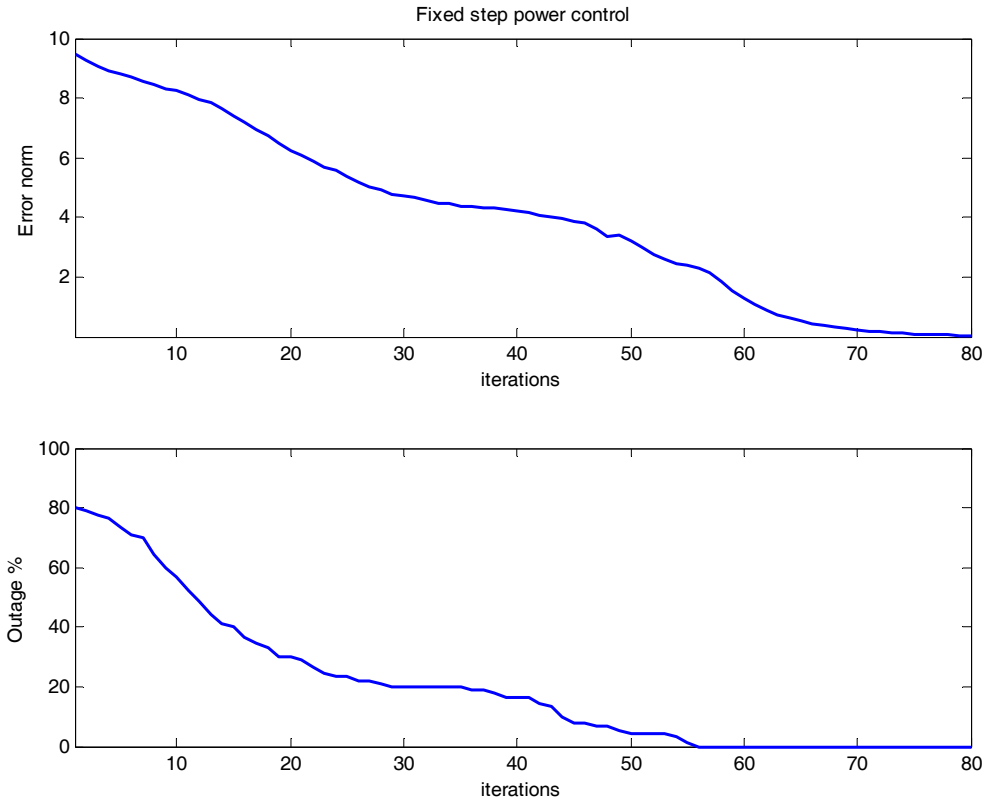

Figure 2.19. Error norm and outage of FSPC algorithm.

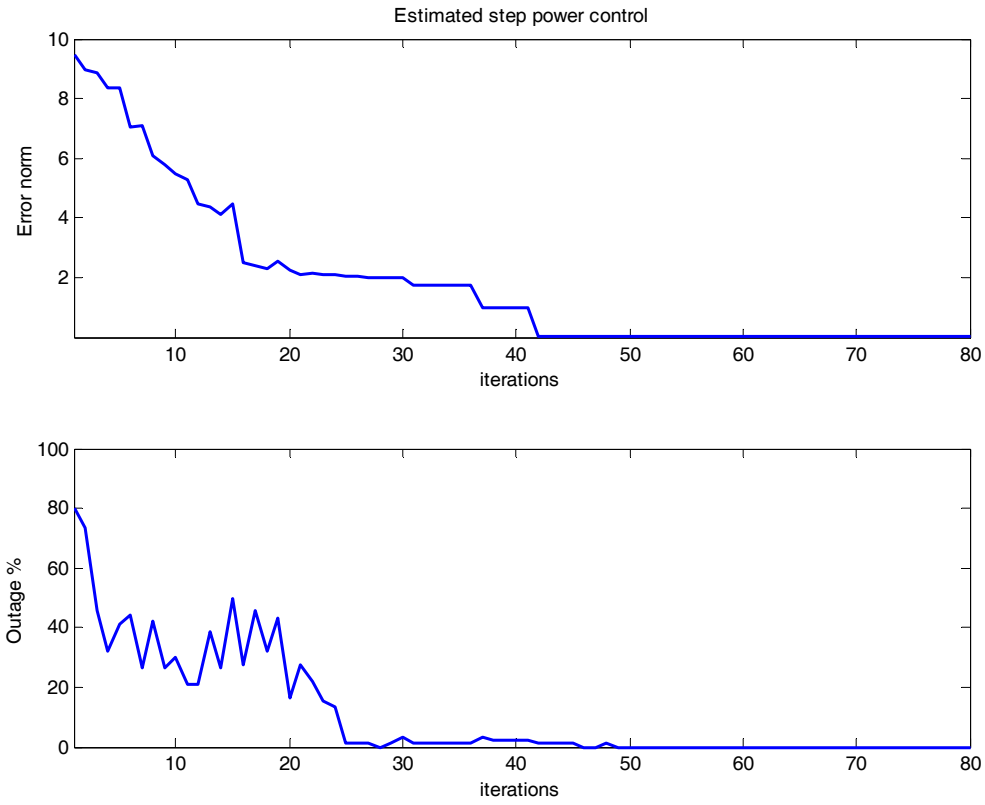

Figure 2.20. Error norm and outage of ESPC algorithm.

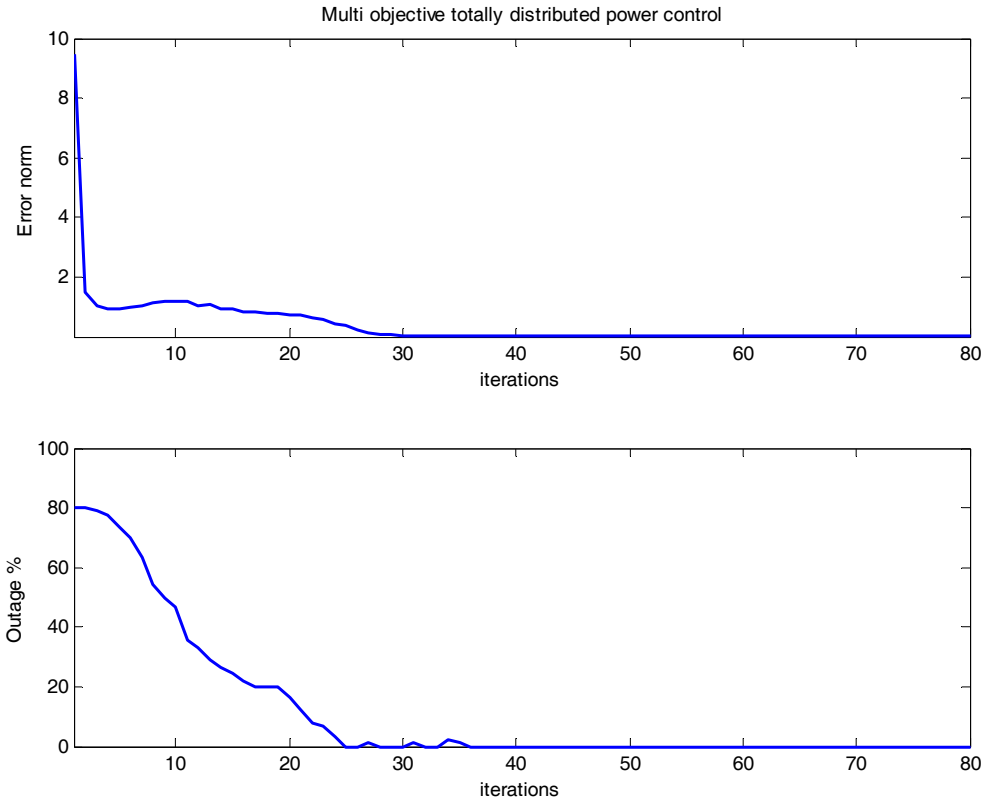

Figure 2.21. Error norm and outage of MOTDPC algorithm.

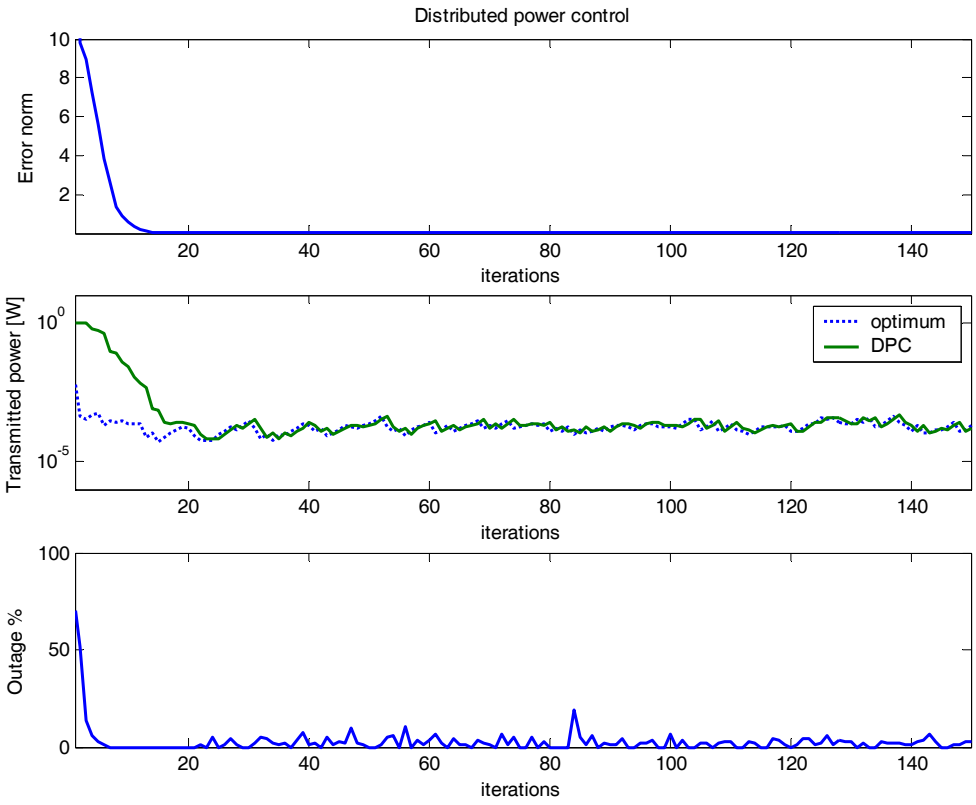

Figure 2.22. Error norm, transmitted power and outage of DPC algorithm.

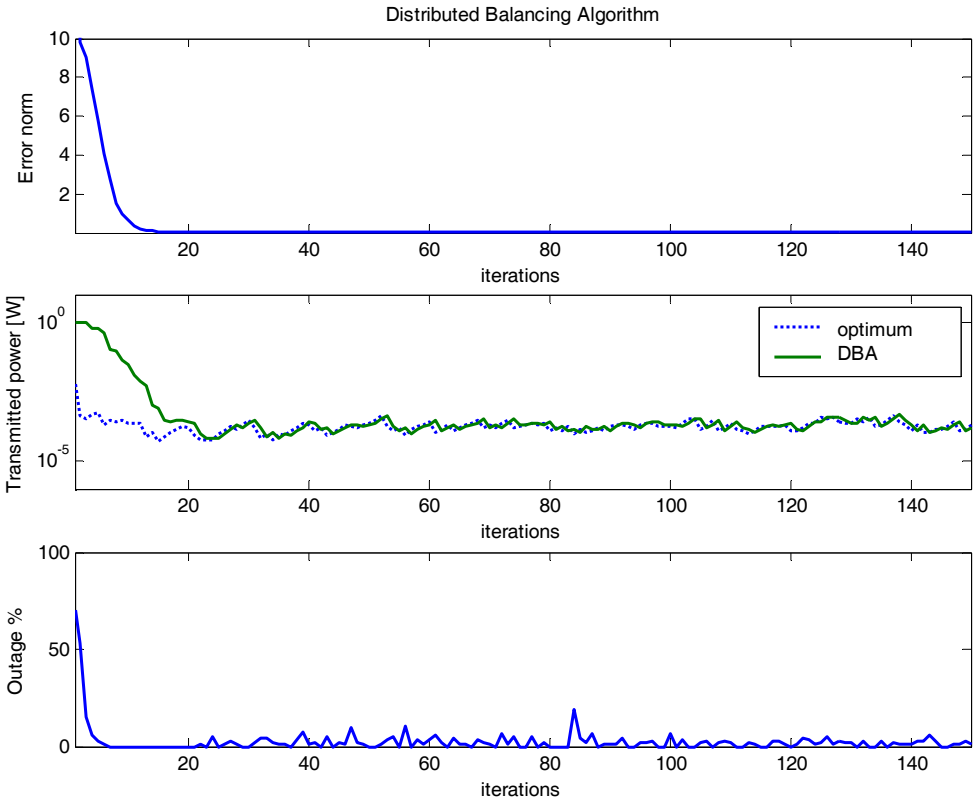

Figure 2.23. Error norm, transmitted power and outage of DBA algorithm.

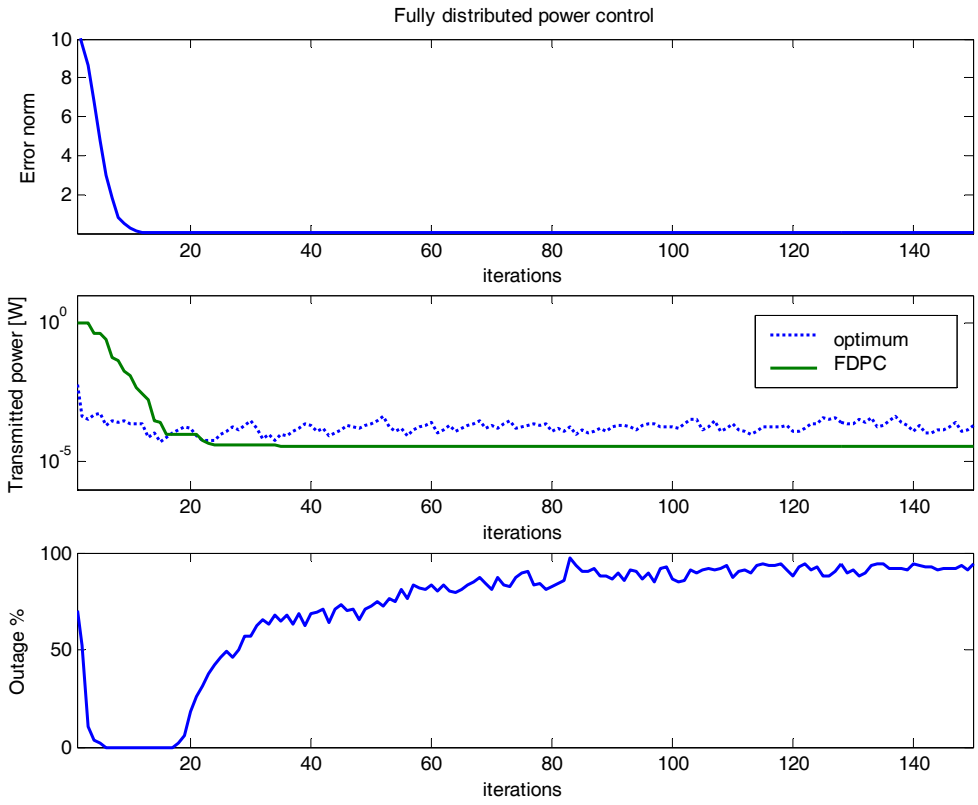

Figure 2.24. Error norm, transmitted power and outage of FDPC algorithm.

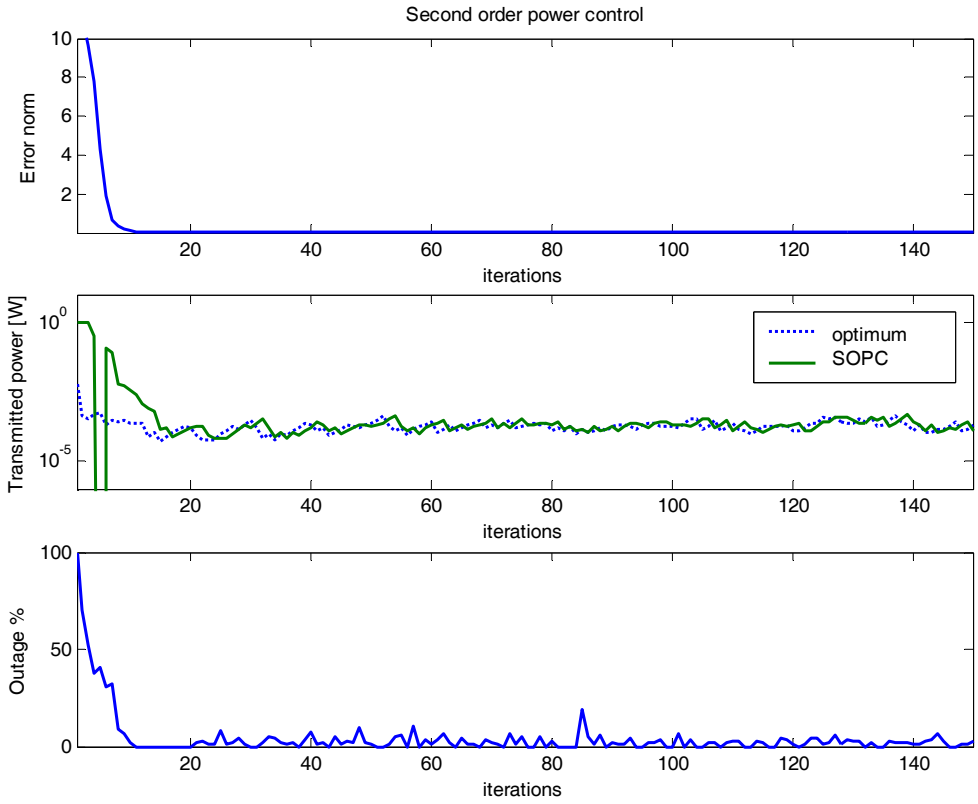

Figure 2.25. Error norm, transmitted power and outage of SOPC algorithm.

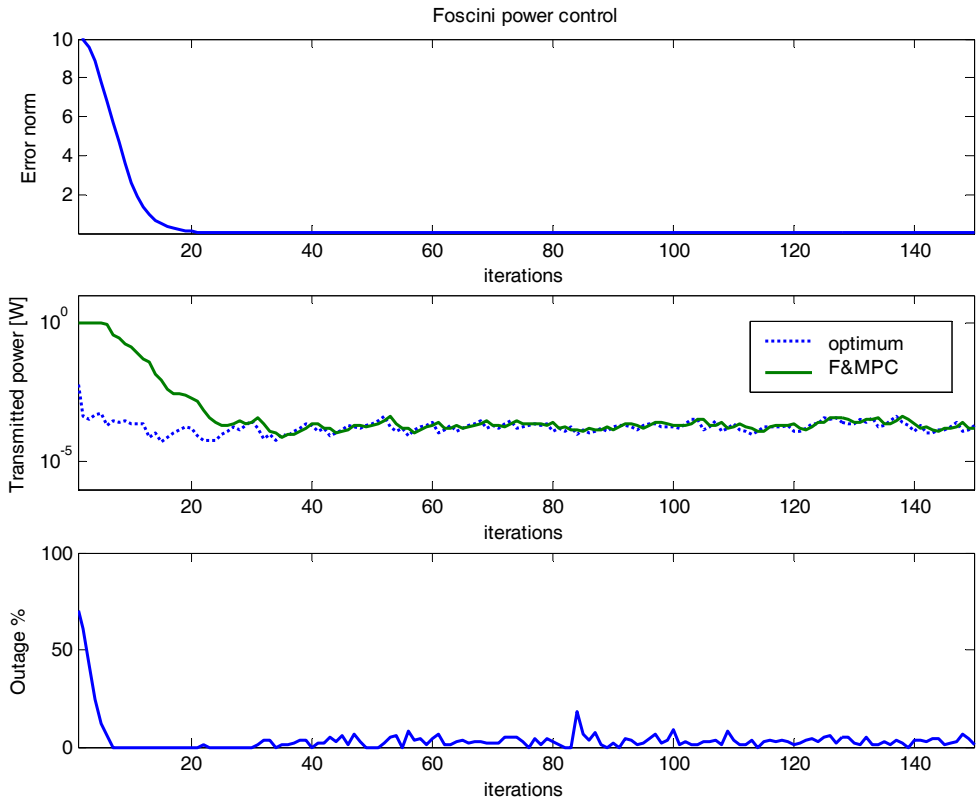

Figure 2.26. Error norm, transmitted power and outage of FMA algorithm.

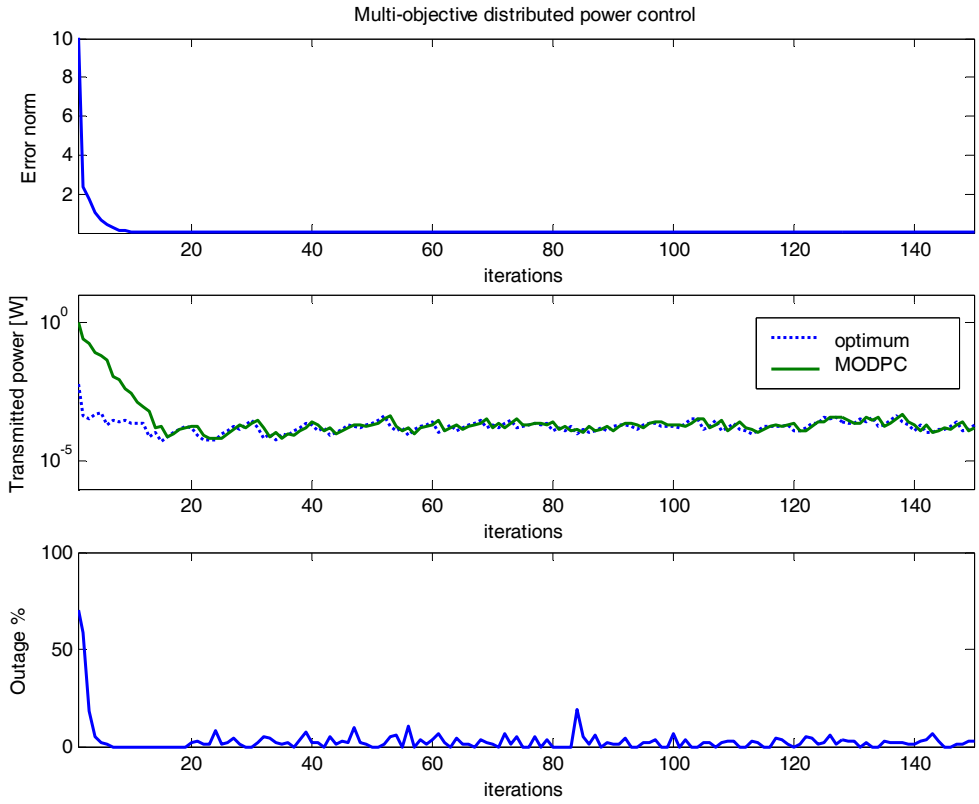

Figure 2.27. Error norm, transmitted power and outage of MODPC algorithm.

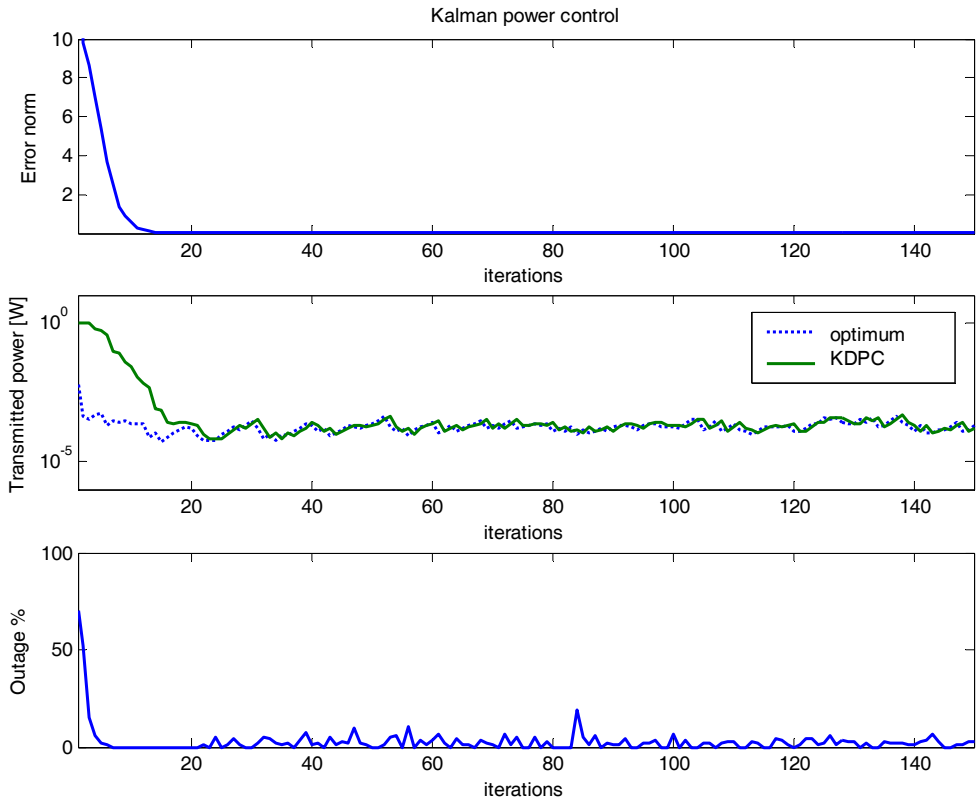

Figure 2.28. Error norm, transmitted power and outage of KDPC algorithm.

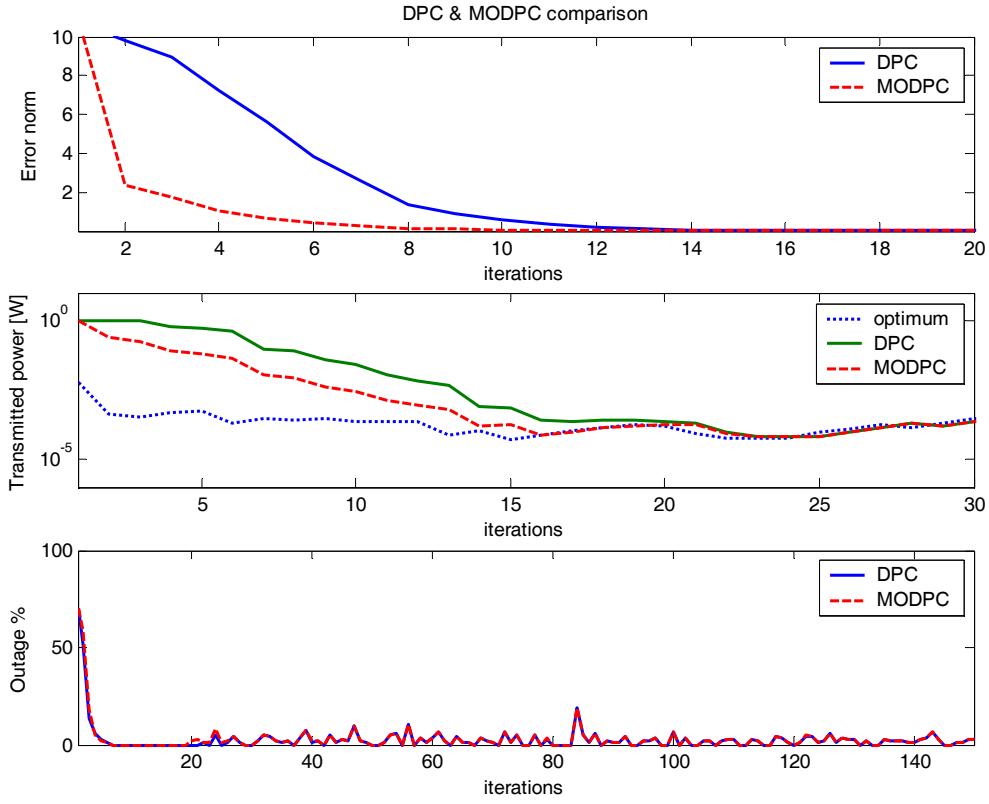

Figure 2.29. Error norm, transmitted power and outage comparison.

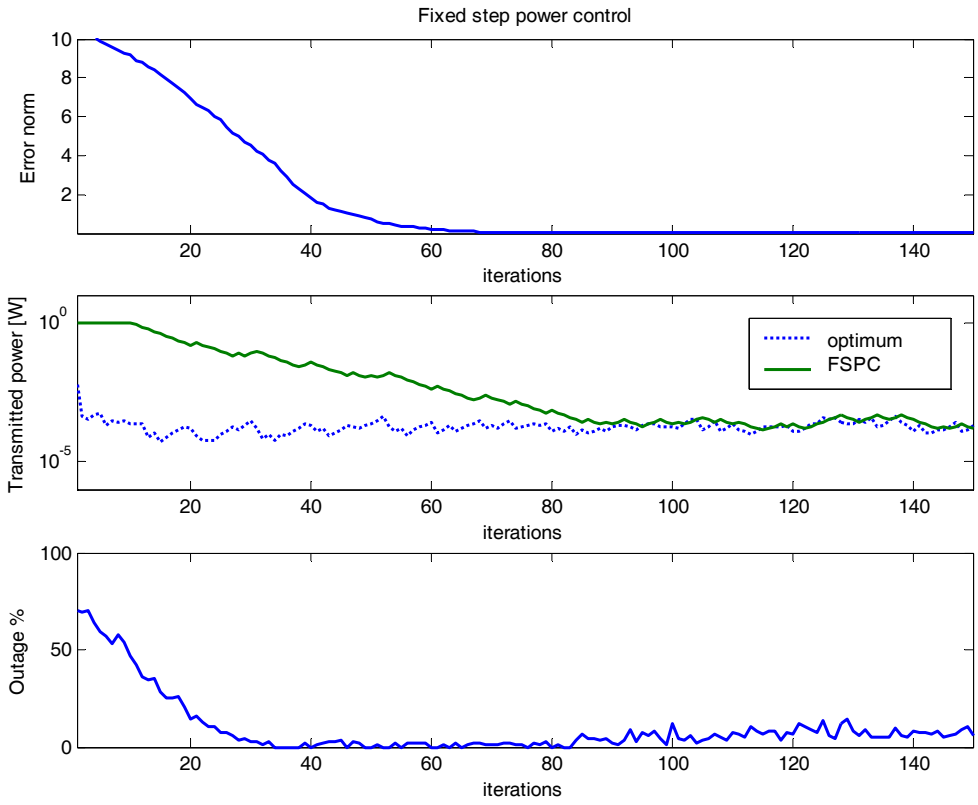

Figure 2.30. Error norm, transmitted power and outage of FSPC algorithm.

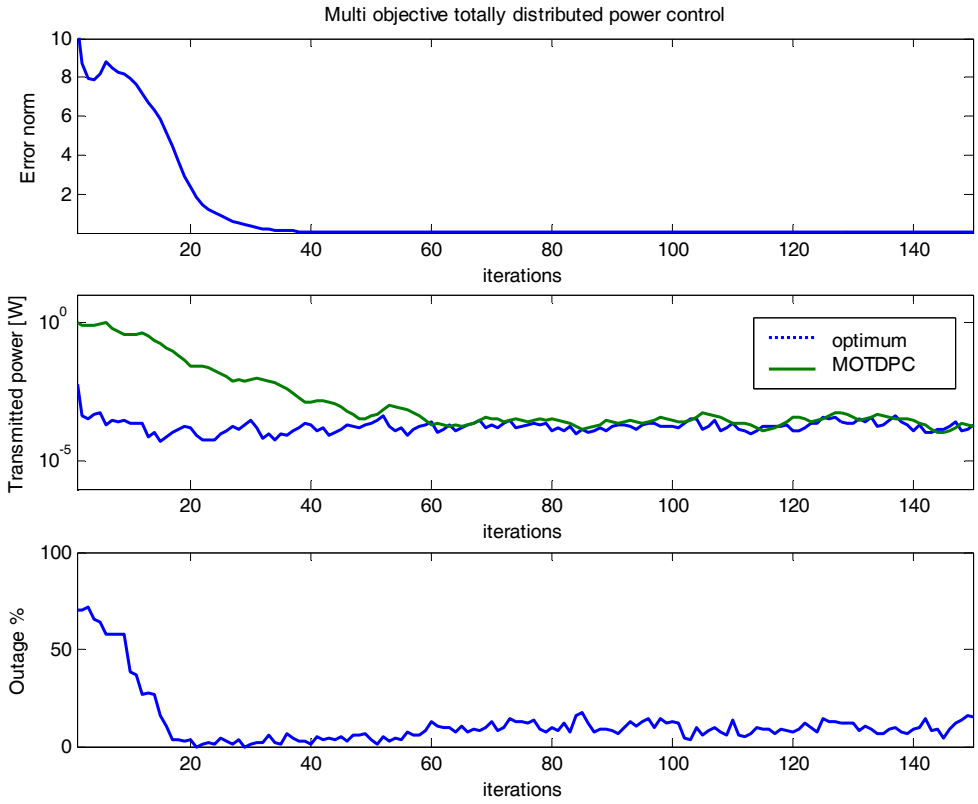

Figure 2.31. Error norm, transmitted power and outage of MOTDPC algorithm.

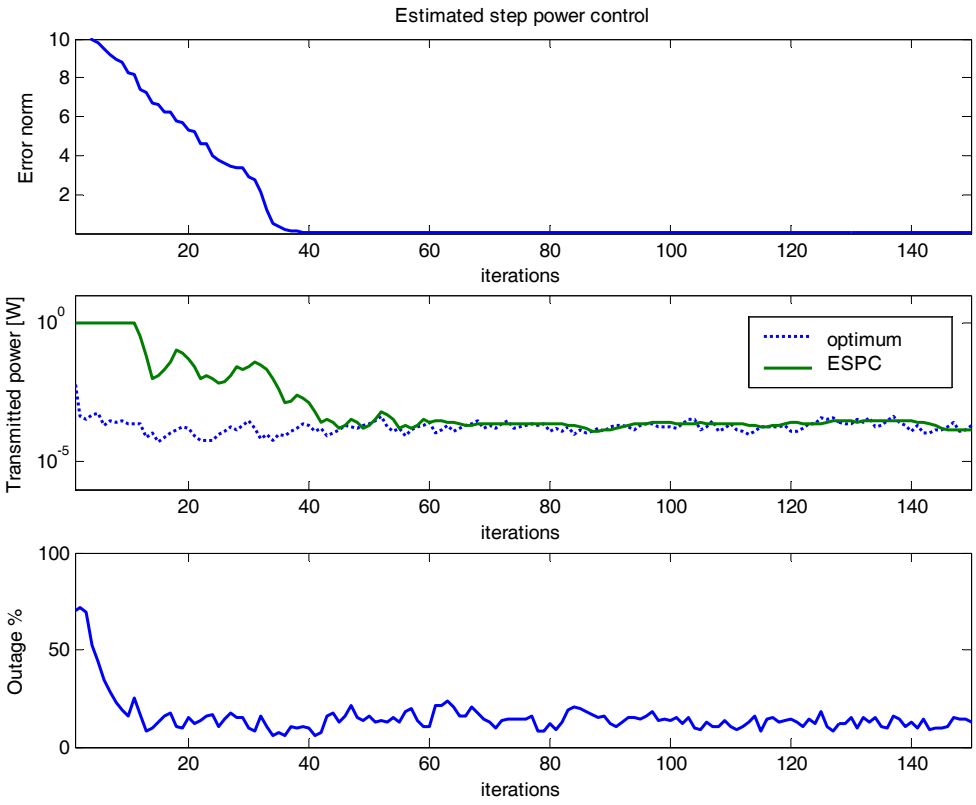

Figure 2.32. Error norm, transmitted power and outage of ESPC algorithm.

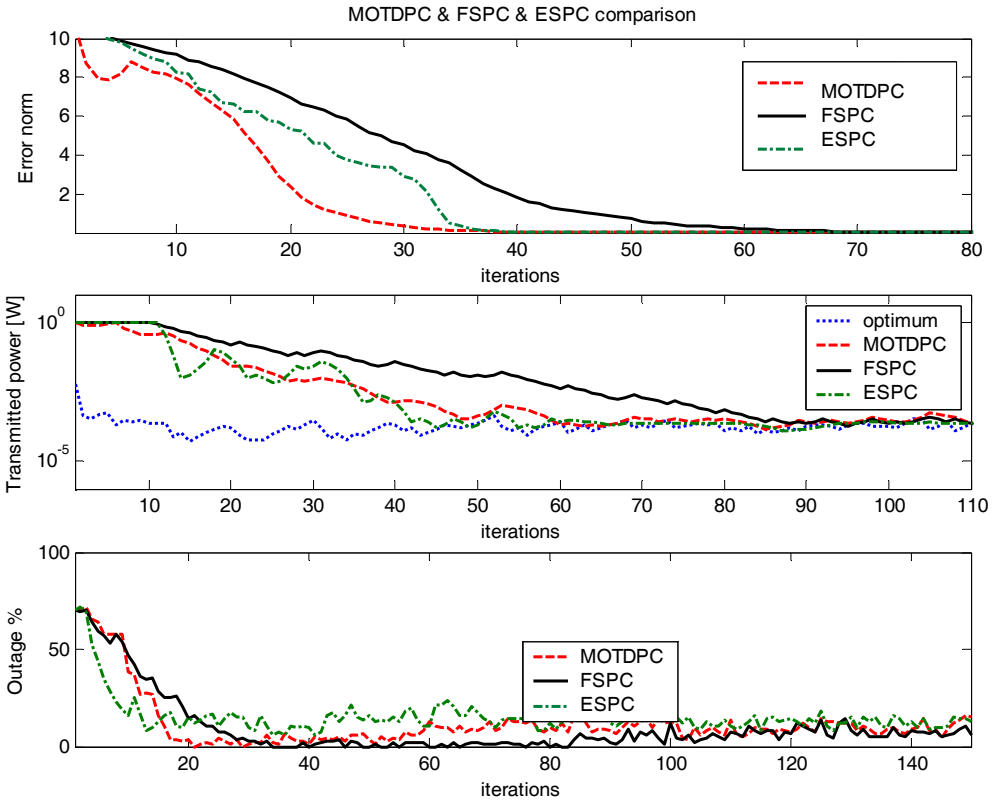

Figure 2.33. Error norm, transmitted power and outage comparison.

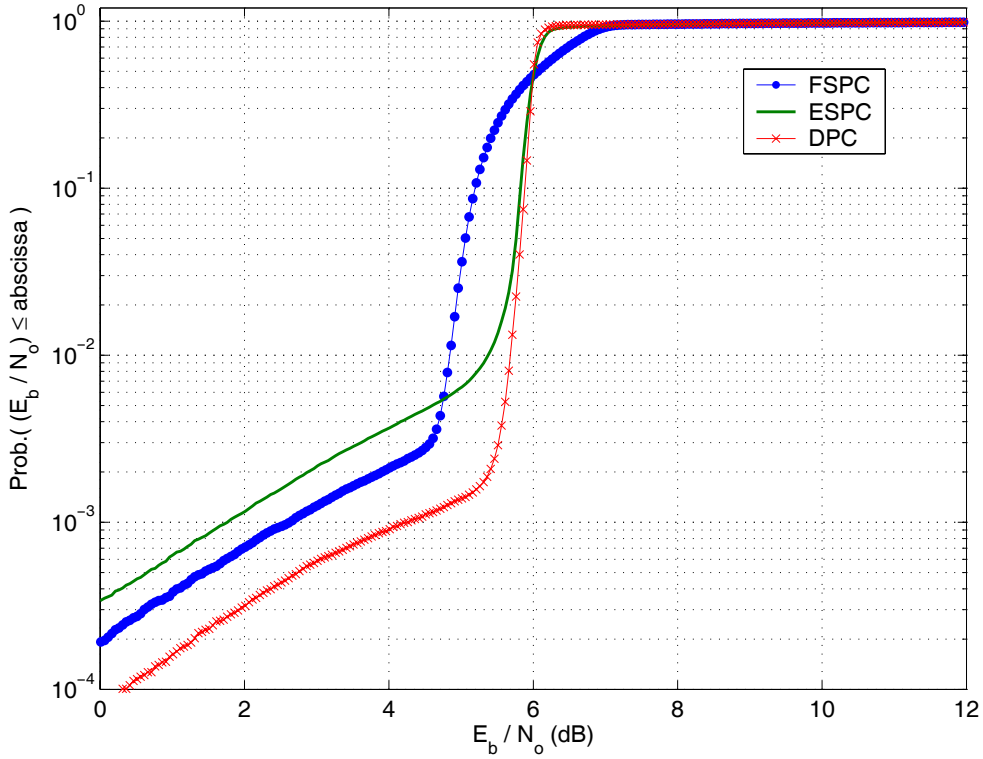

Figure 2.34. Cumulative distribution function (CDF) of the E_b/I_0 at the receiver, max. mobile speed is 5 km/h.

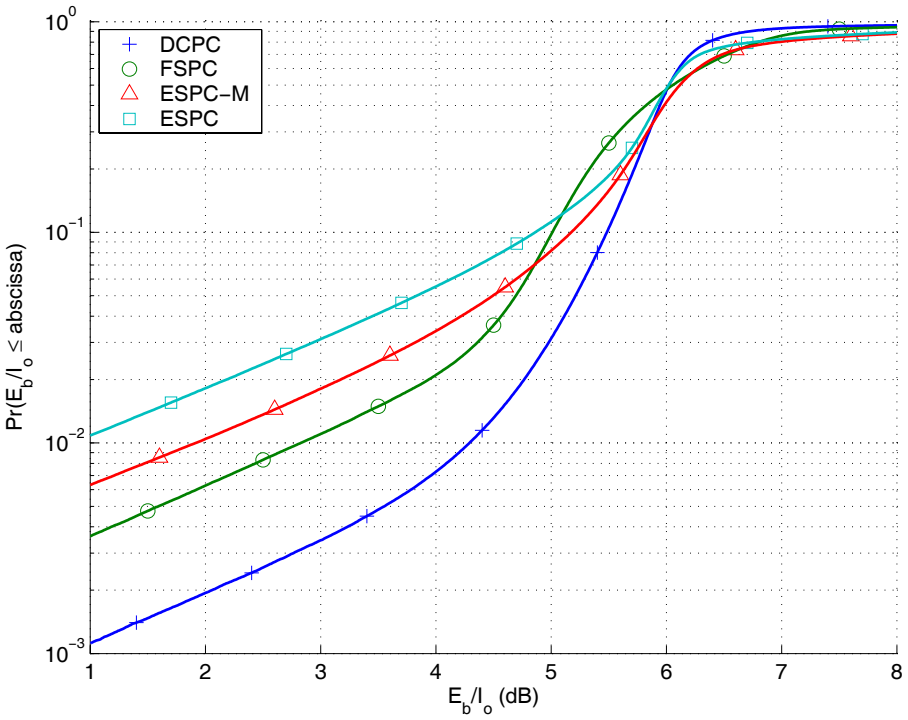

Figure 2.35. Cumulative distibution function (CDF) of the E_b/I_0 at the receiver, max. mobile speed is 30 km/h.

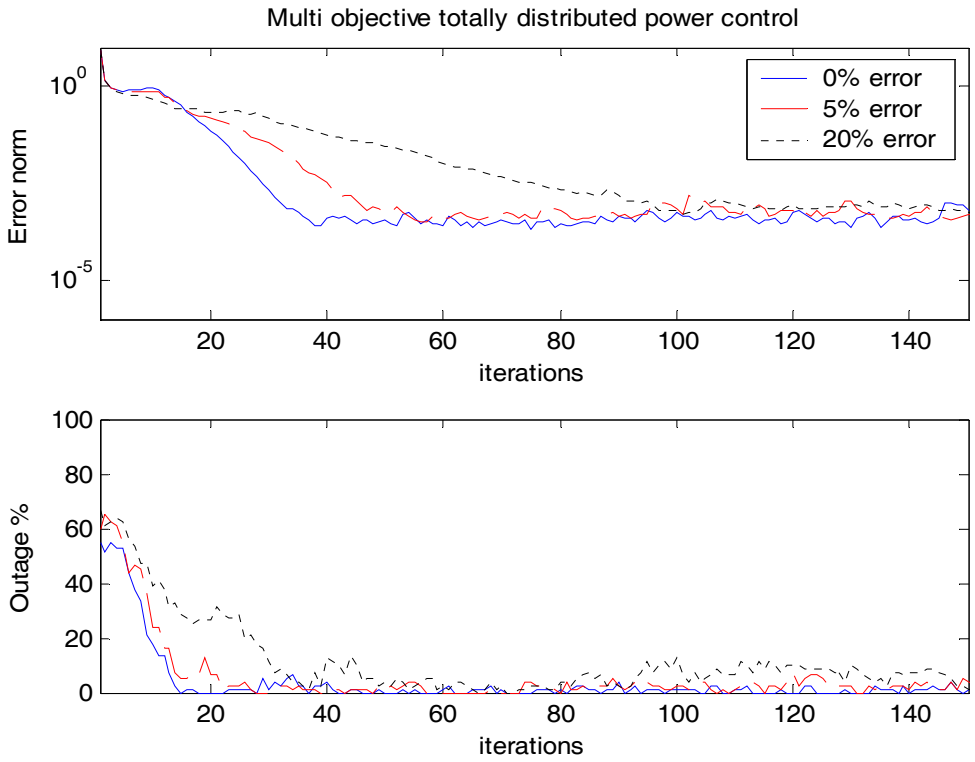

Figure 2.36. The MOTDPC algorithm with different PC error probabilities

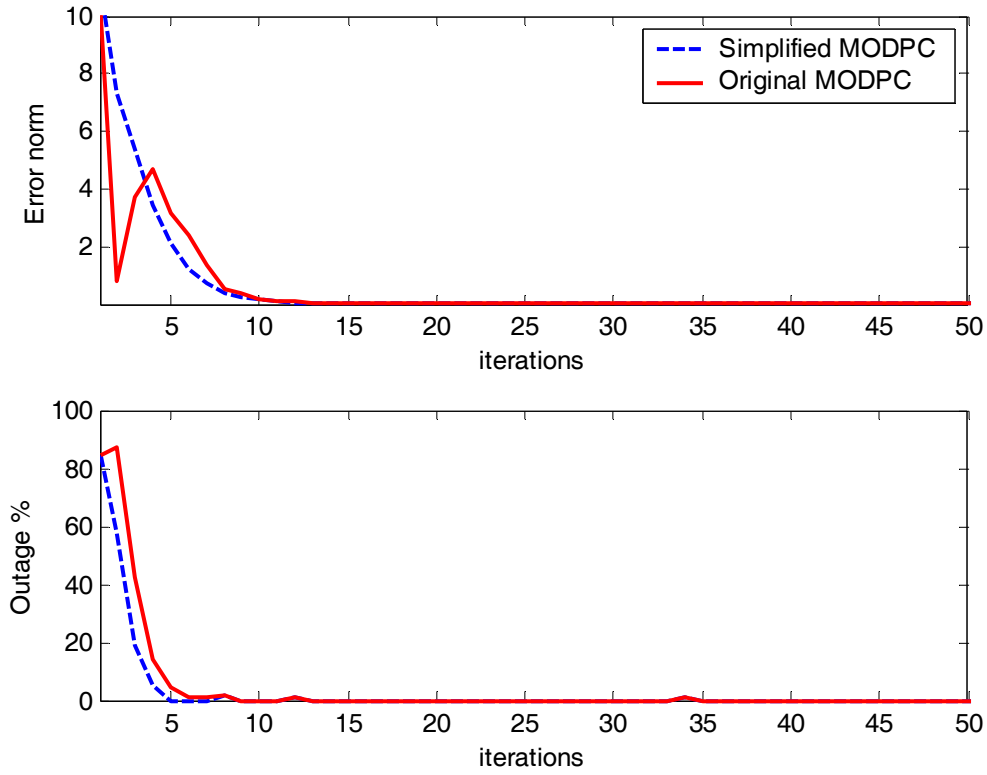

Figure 2.37. Comparison between the original and the simplified MODPC algorithms.

CHAPTER THREE

COMBINING POWER AND RATE CONTROL IN WIRELESS COMMUNICATION SYSTEMS

3.1 Introduction

The radio resource management (RRM) is a very essential component in wireless communication network. The RRM contains many sub-blocks like the connection admission controller, the traffic classifier, the radio resource scheduler, and the interference and noise measurements [82]. The main operation of the RRM is to manage the different available resources to achieve a list of target Quality of Services (QoS). The Radio Resource Scheduler (RRS) is an essential part of the RRM (see Section 1.2). The RRS has two important radio resources to control: mobile station (MS) transmitting power and transmitted data rate. The RRS uses those two resources to achieve different objectives like maximizing the number of simultaneous users, reducing the total transmitting power, and increasing the total throughput. The conventional way to achieve these objectives is to select one of them as a target to optimize and use other objectives as constraints. Novel algorithms based on Multi-Objective (MO) optimization and Kalman Filter techniques are proposed in this Chapter. Here we address the problem as how to combine both the power and the rate in an optimum way.

Shannon shows by his famous equation that the information rate is an increasing function in the signal to interference and noise ratio (see (4.89)). Increasing the information rate is generally very desirable in data communication systems but it is restricted by the SINR. Increasing the SINR can be achieved in two ways. The first way is by reducing the total interference and noise affected by that user. This depends on some characteristics of the noise and the interference. For example, if the structure of the interference from other users is known at the receiver then by applying one of the multi-user detection methods, that interference can be reduced. Also if the users are spatially distributed then the interference can be reduced by using a multi-antenna system (see Chapter 4). If the users concurrently use the channel (as in DS-CDMA) then the interference can be reduced by

using power control techniques. From previous studies we can see that some characteristics of the interference are assumed to be known or can be controlled. There are many sources of interference and noises that can not be reduced by the first way such as thermal noise, interference from other cells and many other sources of noise. The second way of increasing the SINR is simply by increasing the transmitted power. In a single user communication (point to point) or in broadcasting, this can be an acceptable solution and the main disadvantages are the cost and the nonlinearities in the power amplifiers. But in multi-user communication environment increasing the transmitted power means more co-channel and cross-channel interference problems.

Controlling the data rate as well as the transmitted power is an important topic in modern communication systems. The adaptive rate features are not needed for communication systems which are designed mainly for voice communication as in 1G and 2G cellular systems. In these systems the target SINR is specified, and the data rate is fixed and only the power is controlled as in IS-95. The modern communication systems (2.5G, 3G) are supporting the multi-rate data communication because they are designed not only for voice communication but also for data and multimedia communication. An efficient combining algorithm for the power control and the rate control is required for these systems. The term efficient here means how one can optimize between the transmitted power and data rate to meet the required specifications.

There are many proposed combining algorithms for the power and rate control in the literature. The specifications of those algorithms are quite varied. Some algorithms suggest maximizing the throughput; others minimizing the packet delay or minimizing the total power consumption.

Although our analysis in this Chapter can be applied for different communication schemes, we will concentrate mostly on the UMTS specifications.

The 3G mobile communication systems support the multi-rate transmission. There are mainly two methods to achieve the multi-rate transmission, the multi-code (MC) scheme and the variable-spreading length (VSL) scheme [73]. In UMTS the VSL scheme is called orthogonal variable spreading factor (OVSF) scheme. In MC-CDMA system, all the data signals over the radio channel are transmitted at a basic rate, R_b. Any connection can only transmit at rates mR_b, referred to as m-rate, where m is a positive integer. When a terminal needs to transmit at m-rate, it converts its data stream, serial-to-parallel, into m

basic-rate streams. Then each stream is spread by using different and orthogonal codes [72]. In VSL-CDMA system, the chip rate is fixed at a specified value (3.84 Mcps/s for UMTS) and the data rate can take different values. This means that the processing gain (PG) is variable. The processing gain can be defined as the number of chips per symbol. In UMTS, the processing gain (or the spreading factor) in the uplink can take one of the following values {4,8,16,32,64,128,256}[64]. The smallest spreading factor is equivalent to channel bit rate 960 Kb/s and the largest spreading factor is equivalent to channel bit rate 15Kb/s [64]. In many situations the performance of VLS-CDMA systems is preferred to MC-CDMA systems [73].

3.2 Optimal Centralized Power and Rate Control

In this Section, we will introduce an optimal methodology to find rate and the power values which achieve certain requirements. Since the computational cost of this method is very intensive, it is not possible to be implemented practically. In small dimensional problems it can be used for comparison purposes. Consider an uplink cellular cell with Q number of users. Each user has a set of m transmission rates $\mathbf{M} = \{r_1, r_2, ..., r_m\}$, $r_i \geq 0$, $i=1,2,\ldots,Q$, to choose from. The space of the achieved rates in the cell can be denoted as $\mathbf{N} = \{\mathbf{n}^1, \mathbf{n}^2, ..., \mathbf{n}^\kappa\}$, where $\mathbf{n}^j$ is the j^{th} vector of allocated rates of users, $\mathbf{n}^j = \{n_1^j, n_2^j, ..., n_Q^j\}$, $n_i^j \in \mathrm{M} \ \ \forall i \in \{1,...,Q\} \ and \ j \in \{1,...,\kappa\}$, where $\kappa \leq m^Q$. Each rate vector can be associated with power vector which contains the transmitted power values required to achieve the rates. By defining the objective we can select the optimum power and rate vector. For example, if the objective is to maximize the total transmission rates, then the optimum rate vector is the maximum sum vector in the space N. For 20 users and 8 data rates values, there are more than 10^{18} possible rate combinations that can be obtained in the set N (NP problem). This number is only for one time slot. One can see the complexity to find the optimal solution even when an efficient searching technique is used.

Example

To explain the optimal algorithm and how the solutions could be computed, assume a mobile communication system with two users. Each user can send at one of three available data rates. Assume snapshot assumption with channel gain of -80 dB and -95 dB, respectively. The data rates which each user can select from are {15,60,180}Kb/s.

The target SINR is fixed for both users at 7dB. The additive noise has zero mean value with -80 dB variance. The modulation type is assumed to be VLS-CDMA.

The space of the achieved rates of users contains $3^2 = 9$ pairs, namely **N**={(15,15),(15,60),(15,180),(60,15),(60,60),(60,180),(180,15),(180,60),(180,180)} kb/s. The required transmitting power of users to meet these rates can be easily computed using a modified version of equation of (2.12) with different target CIR values (see Section 3.4). The space of transmitted power pairs needed to achieve the data rate space N is Tp={(0.020,0.633),(0.021,2.529),(0.024,7.609),(0.080,0.669),(0.085,2.687),(0.098,8.161) ,(0.241,0.768),(0.258,3.115),(0.307,9.711)}. Now we can select the optimum solution based on the required objectives. If there are no power constraints and the objective is to get the highest data rate then the 9th solution is the optimum one. If the maximum transmitted power is 1 Watt, and the objective is to get the highest total data rate, then the 7th solution is the optimum one. If there is no power constraint but the objectives are the minimum total power and the data rate of second user should be greater than 20 Kb/s, then the 2nd solution is the optimum.

3.3 Maximum Throughput Power Control (MTPC) Algorithm

This algorithm has been suggested in [74]. The algorithm is based on the maximization of the total throughput in a cellular system. There is no need to generate all solutions in this method. Since the link gains and the interference of other users are required to calculate the transmitted power of each user, the MTPC algorithm is a centralized algorithm. The throughput of user *i* can be approximated when M-QAM modulation is used by

$$T_i = \Theta + \log_2\left(\Gamma_i\right) \tag{3.1}$$

where T_i is the throughput of user *i*, Θ is a constant, and Γ_i is the CIR of user *i*, which is given by (2.2).

The total throughput *T* is given by

$$T = \sum_{i=1}^{Q} T_i = Q\Theta + \log_2\left(\prod_{i=1}^{Q} \Gamma_i\right) \tag{3.2}$$

where *Q* is the number of users.

Now the problem can be defined as follows: *Given the link gains G_{ij} of the users, what is the power vector* $\mathbf{P}=\left[\mathrm{P}_1,\mathrm{P}_2,...,\mathrm{P}_Q\right]^{'}$ *which maximizes the total throughput* (3.2)? Since the first term in (3.2) is constant and the logarithmic function is an increasing function, then maximizing the multiplicative term ($\prod_{i=1}^{Q}\Gamma_i$) will lead to maximizing the total throughput *T*. The problem considered in [74] is

$$\max_{\mathbf{P}}\left[\prod_{i=1}^{Q}\Gamma_i\left(\mathbf{P}\right)\right] \text{ s.t. } \mathbf{P}\in\Omega \tag{3.3}$$

where $\Omega=\left\{\mathbf{P}\left|P_{\min}\le P_i\le P_{\max}, i=1,...,Q\right.\right\}\subset\Re^Q$.

The MTPC algorithm to solve (3.3) is given by

$$\begin{aligned} P_k\left(t+1\right)&=\frac{1}{\sum_{r\neq k}^{Q}\frac{G_{rk}}{\left(\sum_{j\neq r}^{Q}G_{rj}P_j\left(t\right)+N\right)}}, \quad t=0,1,..., \quad k=1,...,Q \\ P_{\min}&\le P_k\left(t+1\right)\le P_{\max} \end{aligned} \tag{3.4}$$

where G_{ij} is the channel gain between user *j* and base station *i* and *N* is an additive noise.. Without loss of generality user *i* is assumed to be assigned to base station *i*.

Proposition (3.1) [74]

Starting from any initial vector $\mathbf{P}\left(0\right)\in\Omega$, the iteration specified by (3.4) converges to a unique point $\mathbf{P}^*\in\Omega$, which achieves the global maximum.

3.4 Centralized Minimum Total Transmitted Power (CMTTP) Algorithm

This algorithm is the logical extension of the fixed rate centralized power control algorithm described in section (2.2). The mathematical formulation of the CMTTP problem is

Find the power vector $\mathbf{P}=\left[P_1,...,P_Q\right]^{'}$ *and the rate vector* $\mathbf{R}=\left[R_1,...,R_Q\right]^{'}$ *minimizing the cost function*

$$J\left(\mathbf{P}\right)=\mathbf{1}^{'}\mathbf{P}=\sum_{i=1}^{Q}P_i \tag{3.5}$$

subject to

$$\frac{R_s}{R_i}\frac{P_i G_{ki}}{\sum_{\substack{j=1 \\ j\neq i}}^{Q} P_j G_{kj} + N_i} \geq \delta_i^*, \qquad \forall i = 1,...,Q, \tag{3.6}$$

$$P_{\min} \leq P_i \leq P_{\max}\ ,\ \mathrm{R_i} \geq r_i\ , \quad \forall i = 1,...,Q \tag{3.7}$$

where δ_i^* is the minimum required SINR for user *i*, r_i is the minimum rate limit for *i*, and R_s is the chip rate. The problem presented in (3.5)-(3.7) can be reduced to a system of linear equations. If the constraints(3.6),(3.7) can not be achieved then the problem is called infeasible. In this case either some users have to be dropped from this link or some of the constraints have to be relaxed [78].

Proposition (3.2) [78]

1. At the optimal solution all QoS constraints are met with equality.
2. The optimal power vector is the one that achieves all rate constraints with equality.

From Proposition (3.2) the optimum rate vector is $\mathbf{R}^* = \left[r_1,...,r_Q\right]'$. The corresponding power vector can be obtained by solving the QoS equation. This is a system of linear equations in power. From (3.6) we have [78]

$$\frac{R_s}{r_i}\frac{P_i G_{ki}}{\sum_{\substack{j=1 \\ j\neq Q}}^{Q} P_j G_{kj} + N_i} = \delta_i^T, \qquad \forall i = 1,...,Q \tag{3.8}$$

where δ_i^T is the target SINR for user i.

Let $\tilde{r}_i = \frac{\delta_i^T r_i}{R_s}$ and substitute it into (3.8). We obtain

$$P_i = \tilde{r}_i\left[\sum_{\substack{j=1 \\ j\neq i}}^{Q} \frac{G_{kj}}{G_{ki}} P_j + \frac{N_i}{G_{ki}}\right] \tag{3.9}$$

In matrix form

$$\mathbf{P} = \mathbf{rHP} + \mathbf{ru} \tag{3.10}$$

where

$$\left(\mathbf{H}\right)_{ij} = \begin{cases} 0 & \mathrm{i} = \mathrm{j} \\ \dfrac{G_{kj}}{G_{ki}} > 0 & \mathrm{i} \neq \mathrm{j} \end{cases} \tag{3.11}$$

$$\left(\mathbf{u}\right)_i = \frac{N_i}{G_{ki}} \tag{3.12}$$

and

$$\mathbf{r} = \mathrm{diag}\left\{\tilde{\mathrm{r}}_1 \quad \cdots \quad \tilde{\mathrm{r}}_Q\right\} \tag{3.13}$$

Then the optimum power vector is

$$\mathbf{P}^* = \left[\mathbf{I} - \mathbf{rH}\right]^{-1} \mathbf{ru} \tag{3.14}$$

In order to obtain a non-negative solution of (3.14), the following condition should hold (see Section 2.2)

$$\rho\left(\mathbf{rH}\right) < 1 \tag{3.15}$$

where $\rho\left(\mathbf{A}\right)$ is the spectral radius of matrix **A** (see Chapter 2).

3.5 Statistical Distributed Multi-rate Power Control (SDMPC) Algorithm

A distributed solution of the optimization problem given by (3.5)-(3.7) is proposed for one cell case in [79]. It is assumed that every user has two states ON or OFF. The state ON refers to active state, i.e. the user sends data. The state OFF refers to idle state, where the transmitted power is zero. The transition probabilities of the *i*th user from idle to active state at any packet slot is υ_i, and from active to idle state is ζ_i. The durations of the active and idle periods are geometrically distributed with a mean of $1/\zeta_i$ and $1/\upsilon_i$ (in packet slots), respectively. The optimization problem (3.5)-(3.7) is slightly modified to Find

$$\min_{\mathbf{P}} \; J\left(\mathbf{P}\left(t\right)\right) = \sum_{i=1}^{Q} \beta_i\left(t\right) P_i\left(t\right) \tag{3.16}$$

subject to

$$\frac{R_s}{R_i}\frac{P_i G_{ki}}{\sum_{\substack{j=1 \\ j\neq Q}}^{Q} P_j \beta_j(t) G_{kj} + N_i} \geq \delta_i^*, \qquad \forall i = 1,...,Q, \tag{3.17}$$

$$P_{\min} \leq P_i \leq P_{\max}\ ,\ \mathrm{R_i} = r_i, \qquad \forall i = 1,...,Q, \tag{3.18}$$

One parameter has been added to the original optimization problem which is the indicator function $\beta_j(t)$. The indicator function is equal to one if the *j*th user is currently active, and zero otherwise. It is assumed in [79] that the random process $\hat{\beta}(t)$ has Markovian property since geometric distribution is memoryless over the duration of traffic.

The centralized solution (if the system is feasible) is given by

$$P_i(t) = \frac{\beta_i(t)\gamma_i}{G_{ki}} \times \frac{N_i}{1 - \sum_{j=1}^{Q} \beta_j(t)\gamma_j} \tag{3.19}$$

where

$$\gamma_i = \frac{\delta_i^T}{\delta_i^T + R_s / R_i} \tag{3.20}$$

The main idea behind the SDMPC algorithm is to estimate the other users' information part. Therefore the term $(\sum_{j=1}^{Q} \beta_j(t)\gamma_j)$ is estimated. The Markovian property of the random process $\beta_j(t)$ has been exploited to obtain a good estimate of the other users' information part.

The SDMPC algorithm is given by

$$P_i(t) = \frac{\beta_i(t)\gamma_i}{G_{ki}} \times \frac{N_i}{1 - \hat{\beta}(t)} \tag{3.21}$$

where $\hat{\beta}(t)$ is the estimation of $\sum_{j=1}^{Q} \beta_j(t)\gamma_j$.

The estimated parameter $\hat{\beta}(t)$ has been derived in [79] for two cases: (i) there is no "collision" at *t*, and (ii) a "collision" occurs at *t*. There are at least three drawbacks in this algorithm,

(1) In the cellular CDMA system there is a control channel always active (when the mobile phone is ON).

(2) In SDMPC algorithm, the channel gain and the average power of the additive noise are assumed to be known. But in reality they should be estimated as well. Good estimation of the channel gain and the noise variance is usually difficult. In practice it is easer to estimate CIR or SINR because they have direct impact on BER [82].

(3) They assume that the durations of active and idle periods are geometrically distributed. This assumption is oversimplified and far of the reality.

3.6 Lagrangian Multiplier Power Control (LRPC) Algorithm

As mentioned previously, the data rates which can be achieved belong to a set of integers. In the formulation of the optimization problem, to maximize the data rate we assume that the data rate is continuous. This assumption can be relaxed in the simulation by rounding the optimum data rate to the nearest floor of the data rate set. It can be proven that the solution of the optimization problem with continuity assumption is not necessarily the same as the solution of the actual discrete problem [95]. The advantage of the LRPC algorithm is that the optimization problem has been formulated without the continuity assumption of the data rates [80]. It has been assumed that each user has a set of *m* transmission rates $M = \{r_1, r_2, ..., r_m\}$ to choose from. Let the rates be ordered in ascent way, i.e. $r_1 < r_2 < .. < r_m$. To properly receive messages at transmission rate r_k, mobile *i* is expected to attain $\Gamma_i(\mathbf{P}) \geq \Gamma_{i,k}^T$.

Define $\mathbf{Y} = \left[y_i^k \right]$ to be a 0-1 matrix such that, for every mobile i and rate r_k

$$y_i^k = \begin{cases} 1, & \text{if mobile i is transmitting with rate } r_k \\ 0, & \text{otherwise} \end{cases} \tag{3.22}$$

The combined rate and power control is formulated as the following optimization problem [80]

$$\mathbf{R} \triangleq \max_{Y,P} \sum_{i=1}^{Q} \sum_{k=1}^{m} r_k y_i^k \tag{3.23}$$

subject to the following constraints

$$\sum_{k=1}^{m} y_i^k \le 1,\ y_i^k \in \{0,1\}, \text{and } 0 \le P_i \le P_{max} \tag{3.24}$$

$$P_i + \left(1 - y_i^k\right) B_i^k \ge \frac{P_i \Gamma_{i,k}^T}{\Gamma_i(\mathbf{P})} \tag{3.25}$$

where B_i^k is an arbitrary large number satisfying

$$B_i^k \ge \max_P \frac{P_i \Gamma_{i,k}^T}{\Gamma_i(\mathbf{P})} \tag{3.26}$$

The above optimization problem is solved using Lagrangian multiplier method. The main goal of LRPC algorithm is to maximize the total throughput of the system. Although the LRPC improves the system throughput, its power consumption for supported users as well as the outage probability are rather high. So it is not recommended to be used in the systems where the fairness is an important issue.

3.7 Selective Power Control (SPC) Algorithm

The SPC algorithm has been suggested in [80]. The SPC algorithm is a logical extension of the DCPC algorithm [6]. The main idea of the SPC algorithm is to adapt the target CIR of each user to utilize any available resources. The suggested SPC algorithm is given by

$$P_i(t+1) = \max_k \left\{ \frac{P_i(t)\Gamma_{i,k}^T}{\Gamma_i(\mathbf{P})} \times \chi\left(\frac{P_i(t)\Gamma_{i,k}^T}{\Gamma_i(\mathbf{P})} \le P_{max} \right) \right\}, \quad t = 0,1,..., \ \ i = 1,...,Q \tag{3.27}$$

where $\chi(E)$ is the indicator function of the event E. Although the SPC algorithm improves the outage probability compared with LRPC algorithm, its outage is still high. The convergence speed of the SPC algorithm is slow [83].

Jäntti in [81] proposed an improved version of the SPC algorithm. It is called Selective Power Control with Active Link Protection (SPC-ALP) Algorithm [81]. The SPC-ALP algorithm has less outage probability and better performance than the SPC algorithm. The main idea of the SPC-ALP algorithm is to admit the new users into the network with at least the minimum data rate and also if possible allow old users to choose higher data rates. This is done by defining three different modes of operation for each user,

- Standard mode, where the user updates its power using SPC algorithm. In this mode the rate can not be increased but it could be decreased if needed.

If there are more resources to be utilized by increasing the rate, the used mode is changed to the transition mode.

- Transition mode, where the user updates its power using ALP algorithm. Also the rate is adapted to the maximum rate that can be supported.
- Passive mode, where the user stops its transmission.

More details about the SPC-ALP algorithm can be found in [81].

3.8 Mathematical formulation of the RRM problem in MO framework

The application of MO optimization method in RRM is introduced in this section. As stated in the introduction of this Chapter, the QoS can be defined for a set of factors. In this Section we will consider only the Bit Error Rate (BER) and the user data rate in the uplink. The objectives of the RRS could be defined as

a) Minimize the total transmitting power.
b) Achieve the target SINR in order to achieve a certain BER level (depends on the application).
c) Maximize the fairness between the users. In our definition, the system is fair as long as each user is supported by at least its minimum required QoS. In this sense, minimizing the outage probability leads to maximizing the fairness.
d) Maximize the total transmitted data rate or at least achieve the minimum required data rate.

It is clear that objective (a) is totally conflicting with objective (d) and partially conflicting with objective (b). Objective (c) is totally incompatible with objective (d). Objective (b) is partially contradictory to the objective (d).

In the literature (e.g. Section 3.2-3.6), the RRM problem is usually formulated as a single objective (SO) optimization problem considering the others as constraints. Two very common formulations for solving the RRM problem in the literature are given. The first one is (e.g. MTPC and LRPC),

Find the rate vector $\mathbf{R} = \left[R_1, ..., R_Q \right]^{'}$ and the power vector $\mathbf{P} = \left[P_1, ..., P_Q \right]^{'}$ which maximize the following objective function

$$\max \sum_{i=1}^{Q} \Upsilon \left(R_i \right) \tag{3.28}$$

subject to the constraints

$$\delta_i \geq \delta_{i,\min} \tag{3.29}$$

$$P_{\min} \leq P_i \leq P_{\max} \text{ , } \mathrm{R}_{\mathrm{i,min}} \leq R_i \leq R_{i,\max},\ i = 1,..,Q, \tag{3.30}$$

where $\Upsilon(.)$ is a rate function, R_i is the data rate of user i, P_i is the transmitted power of user i, Q is the number of users, δ_i is the Signal to Interference and Noise Ratio (SINR) for user i, $\delta_{i,\min}$ is the minimum allowed SINR of user i, $P_{\min}$, $P_{\max}$ are the minimum and maximum transmitted power of the mobile terminal, respectively, and $R_{i,\min}$, $R_{i,\max}$ are the minimum and maximum transmitted data rate of user i, respectively. The rate function is generally an increasing function of the user data rate R_i. In the literature, the rate function has been defined as the throughput [74], [84]. In [85], it has also been defined as a utility function, which is used to achieve certain QoS requirements. The allowed BER for user i is determined by the value of $\delta_{i,\min}$.

There is another different SO optimization definition of the RRS problem in the literature. In this formulation, the total transmitted power is minimized (objective (a)) and the other objectives are defined as constraints. This formulation is widely used in the literature as e.g. in CMTTP and SDMPC, and see also [78]:

Find the rate vector $\mathbf{R} = \left[R_1,...,R_Q \right]'$ and the power vector $\mathbf{P} = \left[P_1,...,P_Q \right]'$ which solves the following optimization problem for all i = 1,…,Q

$$\min \sum_{i=1}^{Q} P_i \tag{3.31}$$

subject to the constraints

$$\delta_{\mathrm{i}} \geq \delta_{\mathrm{i,min}} \tag{3.32}$$

$$\mathrm{P}_{\min} \leq \mathrm{P}_{\mathrm{i}} \leq \mathrm{P}_{\max} \text{ , } \tag{3.33}$$

$$\mathrm{R}_{\mathrm{i,min}} \leq \mathrm{R}_{\mathrm{i}} \leq \mathrm{R}_{\mathrm{i,max}} \tag{3.34}$$

We can see from the above two formulations (3.28)-(3.30) and (3.31)-(3.34) that the objectives (a)-(d) are optimized by a single objective and number of constraints.

Solving the objectives (a)-(d) at the same time using MO optimization technique, leads to a more general solution than the conventional methods. In this Section we propose an MO optimization method to solve the RRM problem. In subsequent subsections we will suggest some new radio resource scheduler algorithms based on the MO optimization. The field is very wide and many different algorithms and methods can be derived based on the MO optimization. One formulation of the RRS optimization problem can be defined as:

$$\min_{P_i,R_i}\left\{\sum_{i=1}^{Q}P_i,-\sum_{i=1}^{Q}\Psi\left(R_i\right),O\_P\right\},\quad i=1,...,Q \tag{3.35}$$

subject to

$$P_{\min}\le P_i\le P_{\max}\ ,\ R_{i,\min}\le R_i\le R_{i,\max} \tag{3.36}$$

where O_P is the outage probability. The outage probability is defined as the probability that a user can not achieve at least the minimum required QoS. We can see that the O_P reflects the fairness situation in the communication system. The minus sign associated with the sum of the rate function in (3.35) refers to the maximization process of the total utility functions.

Defining the objectives and the constraints is the first step. Selecting the proper MO optimization method to solve the problem is the second step. Then the (weakly) Pareto optimal set of solutions is generated, where every solution is optimal in different sense (see the Appendix). Finally, the decision maker selects the optimum solution from the optimal set which best achieves the required specifications. In this Section we propose a framework to use the MO optimization techniques in RRM. Two new different algorithms based on the Multi-Objective optimization are introduced in the next subsections.

3.8.1 Multi-Objective Distributed Power and Rate Control (MODPRC) Algorithm

The MODPRC algorithm is a logical extension of the MODPC algorithm proposed in Chapter 2. The algorithm is based on minimizing a multi-objective definition of an error function. In this algorithm we defined three objectives. The objectives are 1) minimize the transmitted power, 2) achieve at least the minimum CIR, which is defined at the minimum data rate, and 3) achieve the maximum CIR, which is defined at maximum data rate. An optimized solution can be obtained by using an MO optimization. The

simulations indicated that our algorithm gives an optimistic performance in terms of data rate, outage probability, convergence speed and transmission power consumption.

The derivations of the algorithms are based on VSL-CDMA communication system. After the dispreading process at the receiver, the SINR is [24]

$$\delta_i(t) = \frac{R_s}{R_i(t)}\Gamma_i(t), \quad t=0,1,.. \tag{3.37}$$

where

$\delta_i(t)$ is the SINR of user *i* at *t*,

R_s is the fixed chip rate (=3.84 Mcps/s for UMTS),

$R_i(t)$ is the data rate for user *i* at *t*, and

$\Gamma_i(t)$ is the CIR of user *i* at *t*.

In wireless and digital communication, it is well known that the BER is a decreasing function in the SINR. In case of coherent binary PSK, the BER can be approximated by (when the interference assumed additive white Gaussian) [50]

$$\mathrm{BER}_{\mathrm{PSK}} = \frac{1}{2}\mathrm{erfc}\left(\sqrt{\delta}\right) \tag{3.38}$$

For example, if the BER should not be more than 10^{-4} then the target SINR would be obtained from (3.38) as $\delta^{\mathrm{T}} \geq 8.3$ dB. In case of fixed data rate power control there is one target CIR corresponding to the target SINR, because we have only one spreading factor value. In the case of multi-rate services there are different target CIR values corresponding to the target SINR. From (3.37) it is clear that, in case of constant target SINR maximizing CIR leads to maximizing data rate as follows:

$$R_i(t) = \frac{R_s}{\delta_i^T}\Gamma_i(t), \quad t=0,1,.. \tag{3.39}$$

Trying to achieve the maximum CIR for all users will end up in high outage probability. If there is a reasonable dropping algorithm then only one or a few number of users will be supported [103]. To reduce the outage probability, we define the target CIR at the minimum transmitted rate as

$$\Gamma_{i,\min} = \frac{R_{i,\min}}{R_s}\delta_i^T \tag{3.40}$$

Also we will define the maximum CIR which is defined at the maximum transmitted rate as

$$\Gamma_{i,\max} = \frac{R_{i,\max}}{R_s}\delta_i^T \tag{3.41}$$

The target SINR, the minimum/ maximum CIR, and the minimum/ maximum data rate are time dependent. We dropped the time symbol (t) for simplicity. In UMTS specifications the power is updated in slot by slot basis. The data rate is updated in frame by frame basis (see Chapter 4). To generalize the analysis we use the same time symbol for power and rate.

To increase the fairness, the users should achieve *at least* the minimum target CIR, which corresponds to the minimum transmitted rate (e.g. 15 Kb/s in UMTS).

The multi-rate power control problem is defined as:

Given the target SINR vector $\boldsymbol{\delta} = \left[\delta_1^T, \delta_2^T, ..., \delta_Q^T\right]'$, the minimum requested data rate vector $\mathbf{R}_{\min} = \left[R_{1,\min}, R_{2,\min}, ..., R_{Q,\min}\right]'$, and without loss of generality, assuming the maximum allowed data rate $R_{\max}$ to be the same for all users, find the optimum power vector $\mathbf{P} = \left[\mathrm{P}_1, \mathrm{P}_2, ..., \mathrm{P}_Q\right]'$ and the optimum rate vector $\mathbf{R} = \left[\mathrm{R}_1, \mathrm{R}_2, ..., \mathrm{R}_Q\right]'$ that minimize the following cost function

$$J(\mathbf{P}) = \left[\sum_{i=1}^{Q}\sum_{t=1}^{N}\gamma^{N-t}e_i^2(t)\right],\ t = 1, ..., N, \tag{3.42}$$

subject to

$$P_{\min} \le P_i \le P_{\max},\quad i = 1, ..., Q \tag{3.43}$$

N is the optimization time window, γ is a real-valued constant adaptation factor.

The error $e_i(t)$ has been defined according to the *weighted metrics method* (2.59) with p=1 as

$$\mathrm{e}_i(\mathrm{t}) = \lambda_{i,1}\left|\mathrm{P}_i(\mathrm{t}) - \mathrm{P}_{\min}\right| + \lambda_{i,2}\left|\Gamma_i(\mathrm{t}) - \Gamma_{i,\min}\right| + \lambda_{i,3}\left|\Gamma_i(\mathrm{t}) - \Gamma_{i,\max}\right| \tag{3.44}$$

where $0 \le \lambda_{i,1}, \lambda_{i,2}, \lambda_{i,3} \le 1$ are real-valued, constant tradeoff factors, $\sum_{k=1}^{3}\lambda_{i,k} = 1$. The

advantages of joining the weighting metrics method with the least squares formula of (3.42) are

- The least squares method is well known and its derivation is straightforward.
- General solution is obtained by using (3.42) minimizing over all users and for time window N.

The error function (3.44) is the mathematical interpretation of the RRM objectives given in (a)-(d) in Section (3.8). The first term of (3.44) is to keep the transmitted power $P_i(t)$ as close as possible to P_{min}, so we try to achieve objective (a). Objectives (b) and (c) will be achieved in the second part of the error function. In this part, the transmitted power is selected to obtain CIR very close to the minimum required CIR. Achieving the minimum required QoS for every user maximizes the fairness in the cell. The third term in (3.44) represents the objective (d), where the users will try to get the maximum allowed QoS if possible.

By solving (3.42) and (3.44) (using same procedure of MODPC algorithm in Section (2.4.8)) for one-dimensional (N=1) case we obtain for *i=1,…,Q*:

$$P_i(t+1) = \frac{\lambda_{i,1}P_{\min} + \lambda_{i,2}\Gamma_{i,\min} + \lambda_{i,3}\Gamma_{i,\max}}{\lambda_{i,1}P_i(t) + (\lambda_{i,2} + \lambda_{i,3})\Gamma_i(t)} P_i(t), \quad t = 0,1,\ldots, \tag{3.45}$$

and as before

$$R_i(t+1) = \frac{R_s}{\delta_i^T}\Gamma_i(t) \tag{3.46}$$

$$P_{\min} \le P_i(t) \le P_{\max} \;\; ; \;\; R_{i,\min} \le R_i(t) \le R_{\max}. \tag{3.47}$$

If the minimum solution places such demands to some users that they can not be achieved, then dropping or handoff process should be applied [103].

The multi-rate power control algorithm given by (3.45)-(3.47) has some interesting characteristics. By changing the values of the tradeoff factors λ_i, different solutions with different meanings are obtained. For example, when $\lambda_{i,1} = 1$, $\lambda_{i,2} = 0$, and $\lambda_{i,3} = 0$, it is clear that (3.45) will be reduced to a fixed level (no) power control and user i will send at minimum power. For $\lambda_{i,1} = 0$, $\lambda_{i,2} = 1$, and $\lambda_{i,3} = 0$, equation (3.45) becomes the distributed power control (DPC) algorithm of [6]. In this case, the fairness is maximized.

When $\lambda_{i,1}=0,\ \lambda_{i,2}=0,$ and $\lambda_{i,3}=1$, algorithm (3.45) will maximize the average transmitted rate (with using reasonable dropping algorithm for non-supported users). In this case one or few users will be supported, so the outage probability will be high. From previous extreme conditions, one can make a tradeoff between these objectives to get the best performance according to the required specifications. The selection of the tradeoff values should be based on the communication link condition as well as the network and the user requirements. Wide range of different solutions can be obtained by changing the values of tradeoff factors. The selection of one solution is a job of the decision maker. The decision maker rules are not considered here, but it would be an interesting topic for future research.

Proposition (3.3)

For any $\mathbf{P}(0)>\mathbf{0}$, the Multi-Objective Distributed Power and Rate Control (MODPRC) algorithm (3.45)- (3.47) will converge to a unique fixed point $\hat{\mathbf{P}}$.

Proof:

The proof is obtained by applying the same procedure as in proposition (2.10). The performance of the MODPRC algorithm is analyzed through intensive simulations in Section 3.10.

3.8.2 Multi-Objective Totally Distributed Power and Rate Control (MOTDPRC) Algorithm

In this section, we propose a slight modification of the MODPRC algorithm to be totally distributed algorithm. The MODPRC algorithm (3.45)- (3.47) assumes the availability of the actual CIR value. In the existing and near future cellular systems, only an up-down command of the power is available at the MS. The same procedure of the ESPC algorithm in Section 2.4.7 has been used to estimate the CIR. The estimated CIR is used with the MOTDPRC algorithm. The CIR (in dB) could be estimated as

$$\tilde{\Gamma}_i(t)_{dB}=\Gamma_i^T(t)_{dB}-\tilde{e}_i(t),\quad t=0,1,... \tag{3.48}$$

where $\tilde{e}_i(t)$ is estimated as in (2.50), $\Gamma_i^T(t)$ is the target CIR, and $\tilde{\Gamma}_i(t)$ is the estimated CIR. Using the estimated CIR in the MODPRC algorithm we obtain

$$P_i(t)=\frac{\lambda_{1,1}P_{\min}+\lambda_{1,2}\Gamma_{\min}+\lambda_{1,3}\Gamma_{\max}}{\lambda_{1,1}P_i(t-1)+(\lambda_{1,2}+\lambda_{1,3})\tilde{\Gamma}_i(t)}P_i(t-1),\quad t=0,1,... \tag{3.49}$$

$$R_i(t)=\frac{R_s}{\delta^T}\tilde{\Gamma}_i(t) \tag{3.50}$$

$$P_{\min}\le P_i(t)\le P_{\max}\ ;\ R_{i,\min}\le R_i(t)\le R_{\max} \tag{3.51}$$

Equations(3.49),(3.50) are functions in the estimated CIR. The MOTDPRC algorithm has some interesting properties as shown in Section 3.10.

3.8.3 Centralized Algorithm for the Tradeoff between Total Throughput Maximization and Total Power Minimization (MTMPC) Algorithm

Another application of the MO optimization in the RRM can be achieved by modifying the maximum throughput power control (MTPC) algorithm. A centralized power control algorithm for throughput maximization has been introduced in the Section (3.2). The algorithm is based on maximizing the throughput and ignoring the transmitted power levels. In practice reducing the transmitted power is very desirable. In this Section we will formulate the cost function with two objectives. The first objective is the maximization of the total throughput as in [74]. The second objective is to minimize the total transmitted power. The proposed approach is the first one in the literature treating the total throughput maximization and the total power minimization simultaneously using multi-objective optimization techniques.

The problem is defined as follows:

Given the link gains of the users find the power vector which increases the total throughput (as much as possible) and at the same time reduces the total transmitted power (as much as possible).

The problem can be represented mathematically as

$$\max\{O_1(\mathbf{P}),-O_2(\mathbf{P})\}\quad \text{s.t. } \mathbf{P}\in\Omega \tag{3.52}$$

where $\mathbf{P}=[P_1,P_2,...,P_Q]'$ is the power vector, the objective functions $O_1(\mathbf{P})=\prod_{i=1}^{Q}\Gamma_i$, and $O_2(\mathbf{P})=\sum_{i=1}^{Q}P_i$, and the admissible power set $\Omega=\{\mathbf{P}\,|\,P_{\min}\le P_i\le P_{\max}, i=1,...,Q\}$. The minus sign is used to minimize the second objective. We will use the weighting method

to solve the multi-objective optimization problem (see the Appendix). As mentioned in Chapter 2, the idea of the weighting method is to associate each objective function with a tradeoff factor (weighting coefficient) and maximize (or minimize) the weighted sum of the objectives [77]. Applying the weighting method in our problem we obtain,

$$\max_{\mathbf{P}} \{\mathbf{O}(\mathbf{P})\} \quad \text{s.t.} \quad \mathbf{P} \in \Omega, \tag{3.53}$$

where

$$\mathbf{O}(\mathbf{P}) = \lambda_1 \prod_{i=1}^{Q} \Gamma_i(\mathbf{P}) - \lambda_2 \mathbf{1}'\mathbf{P} \tag{3.54}$$

is the multi-objective function, $\mathbf{1} = [1,1,..,1]'$, and the tradeoff factors real numbers, $0 \le \lambda_1 \le 1,$ and $\lambda_2 = 1 - \lambda_1$.

Necessary conditions for solving problem (3.53) are

$$\nabla \mathbf{O}(\mathbf{P}) = \mathbf{0}, \tag{3.55}$$

where $\nabla \mathbf{O}(\mathbf{P}) = \left[\partial \mathbf{O}/\partial P_1, \partial \mathbf{O}/\partial P_2, \cdots, \partial \mathbf{O}/\partial P_Q\right]'$ is the gradient of **O.**

Substituting the CIR equation (2.2) into (3.54) we obtain

$$\mathbf{O}(\mathbf{P}(t)) = \lambda_1 \prod_{i=1}^{Q} \frac{P_i(t) G_{ii}}{\sum_{\substack{j=1 \\ j \ne i}}^{Q} P_j(t) G_{ij} + n} - \lambda_2 \sum_{i=1}^{Q} P_i(t) \tag{3.56}$$

To maximize the reward function (3.56), we find the power vector **P** which satisfies (3.55). Since the obtained equations are nonlinear, it will be very complicated to get an analytical solution. An iterative solution for *k=1,…,Q* will be formulated (we will drop the iteration argument *t* for simplicity)

$$\frac{\partial O}{\partial P_k} = \lambda_1 \frac{\left(G_{kk} \prod_{i \ne k}^{Q} G_{ii} P_i\right) \prod_{i=1}^{Q} \left(\sum_{j \ne i}^{Q} G_{ij} P_j + n\right) - \left(\prod_{i=1}^{Q} G_{ii} P_i\right) \left(\sum_{r \ne k}^{Q} G_{rk} \prod_{i \ne r}^{Q} \left(\sum_{j \ne i}^{Q} G_{ij} P_j + n\right)\right)}{\left(\prod_{i=1}^{Q} \left(\sum_{j \ne i}^{Q} G_{ij} P_j + n\right)\right)^2} - \lambda_2 = 0 \tag{3.57}$$

After simplification

$$\lambda_1 \frac{\left(G_{kk}\prod_{i\neq k}^{Q}G_{ii}P_i\right)-\left(\prod_{i=1}^{Q}G_{ii}P_i\right)\sum_{r\neq k}^{Q}\frac{G_{rk}}{\left(\sum_{j\neq r}^{Q}G_{rj}P_j+n\right)}}{\prod_{i=1}^{Q}\left(\sum_{j\neq i}^{Q}G_{ij}P_j+n\right)}-\lambda_2=0, \tag{3.58}$$

which can be rewritten as

$$\lambda_1 G_{kk}\prod_{i\neq k}^{Q}G_{ii}P_i-\lambda_1\left(\prod_{i=1}^{Q}G_{ii}P_i\right)\sum_{r\neq k}^{Q}\frac{G_{rk}}{\left(\sum_{j\neq r}^{Q}G_{rj}P_j+n\right)}=\lambda_2\prod_{i=1}^{Q}\left(\sum_{j\neq i}^{Q}G_{ij}P_j+n\right) \tag{3.59}$$

or

$$\lambda_1 G_{kk}-\lambda_1 G_{kk}P_k\sum_{r\neq k}^{Q}\frac{G_{rk}}{\left(\sum_{j\neq r}^{Q}G_{rj}P_j+n\right)}=\frac{\lambda_2}{\prod_{i\neq k}^{Q}G_{ii}P_i}\prod_{i=1}^{Q}\left(\sum_{j\neq i}^{Q}G_{ij}P_j+n\right) \tag{3.60}$$

Solving for P_k leads to

$$P_k=\left[\lambda_1 G_{kk}-\frac{\lambda_2}{\prod_{i\neq k}^{Q}G_{ii}P_i}\prod_{i=1}^{Q}\left(\sum_{j\neq i}^{Q}G_{ij}P_j+n\right)\right]\frac{1}{\lambda_1 G_{kk}\sum_{r\neq k}^{Q}\frac{G_{rk}}{\left(\sum_{j\neq r}^{Q}G_{rj}P_j+n\right)}} \tag{3.61}$$

and further to

$$P_k(t+1)=\frac{1}{\sum_{r\neq k}^{Q}\frac{G_{rk}}{\left(\sum_{j\neq r}^{Q}G_{rj}P_j(t)+n\right)}}-\frac{\lambda_2}{\lambda_1 G_{kk}\prod_{i\neq k}^{Q}G_{ii}P_i(t)}\frac{\prod_{i=1}^{Q}\left(\sum_{j\neq i}^{Q}G_{ij}P_j(t)+n\right)}{\sum_{r\neq k}^{Q}\frac{G_{kr}}{\left(\sum_{j\neq r}^{Q}G_{rj}P_j(t)+n\right)}} \tag{3.62}$$

Consider $\lambda_2=0$, then from (3.54) the problem is reduced to maximizing the throughput, and from (3.62) we obtain MTPC algorithm (3.4) after constraining the transmitted power. Without power constraints (3.4) is rewritten as:

$$\hat{P}_k(t+1) = \frac{1}{\sum_{r\neq k}^{Q} \frac{G_{rk}}{\left(\sum_{j\neq r}^{Q} G_{rj}P_j(t) + n\right)}} \tag{3.63}$$

After some mathematical manipulations (3.62) can be rewritten in a more compact form as

$$P_k(t+1) = \frac{\hat{P}_k(t+1)}{\left[1 + \frac{\lambda_2}{\lambda_1}\frac{\hat{P}_k(t+1)}{\prod_{i=1}^{Q}\Gamma_i(t)}\right]}, \quad t = 0,1,.... \tag{3.64}$$

where $P_k \in [P_{min}, P_{max}]$, *k=1,…,Q*. From (3.64), the new transmitted power is a scaled value of the transmitted power in case of maximum throughput algorithm.

Example

To compare our algorithm with the maximum throughput algorithm presented in Section 3.3, we will use the same numerical example as given in [74]. Consider the noiseless system with Q=5 users and the path gain matrix, **G**, shown below.

$$\mathbf{G}(\text{dB}) = \begin{bmatrix} -5.8 & -18.2 & -55.3 & -20.3 & -33.6 \\ -36.0 & -9.7 & -43.5 & -22.2 & -15.9 \\ -41.6 & -30.9 & -9.3 & -38.6 & -36.5 \\ -14.2 & -20.6 & -38.5 & -6.8 & -36.6 \\ -22.6 & -23.9 & -20.1 & -16.4 & -10.8 \end{bmatrix} \tag{3.65}$$

The tradeoff factors have been set to $\{\lambda_1, \lambda_2\} = \{0.9999, 0.0001\}$. In this case we penalize power usage. From Table 3.1, we can see that the summation of the SINR (dB) of the users (which is related to the total throughput as in (3.3)) has not changed very much in both schemes (only 0.04%) but the power has been reduced by more than 98% in the case of MTMPC method.

Table 3.1 Comparison between MTMPC and MTPC algorithms

	MTMPC algorithm $\lambda_1 = 0.0001$ and $\lambda_2 = 0.9999$		MTPC algorithm $\lambda_1 = 1$ and $\lambda_2 = 0$	
User	P (dBw)	SINR (dB)	$\hat{P}$ (dBw)	SINR (dB)
1	-13.9789	16.8345	-0.5580	16.9295
2	-16.8918	-0.8548	-6.6072	-0.9234
3	-4.6187	36.0956	13.4264	36.8300
4	-12.8725	8.6383	1.2111	8.5561
5	-14.3460	-5.9278	-1.5289	-6.5922
	Average Power (W)= **0.1**	Sum(SINR(dB))=**54.78**	Average Power (W)= **5** w	Sum(SINR(dB))=**54.8**

3.9 Multi-rate Distributed Power Control using Kalman Filter

In this Section we propose a new combining algorithm of the power control and rate control by using Kalman filters. The algorithm is a direct extension of the distributed Kalman power control algorithm proposed in Section 2.4.9. We will try to avoid the repetition of unnecessary equations and proofs (which have been given in Section 2.4.9). There are at least two methods to assign the data rate for each user. One method is based on competition where each user tries to get the maximum possible data rate based on the channel and interference conditions (as in MODPRC algorithm). If the user can not get at least his minimum required data rate, he will be assumed in outage. The second method is softer where each user requests certain data rate based on his application and the network checks the feasibility to assign the requested data rate to the user. If it is OK, the network gives the permission for the mobile to send at the requested data rate, otherwise another round of negotiation between the mobile and the networks starts. The algorithm proposed in this Section belongs to the second type. As indicated in Section 2.4.9, we can formulate the RRM problem in state-space form.

The transmitted power of user i at time slot t is defined

$$P_i(t+1) = w_i(t) P_i(t), \quad i = 1,...,Q, \tag{3.66}$$

where the optimum weight vector $\mathbf{w}(t) = \left[w_1(t),..., w_Q(t) \right]^{'}$ can be estimated by solving the following state-space equations

$$\mathbf{w}(t+1) = \mathbf{F}(t)\mathbf{w}(t) + \mathbf{q}(t) \tag{3.67}$$

$$\mathbf{y}(t+1) = \mathbf{G}(t+1)\mathbf{w}(t+1) + \mathbf{v}(t+1) \tag{3.68}$$

Here **F**, **G**, **q**, and **v** are given in Section 2.4.9. The main difference between the algorithm presented in this Section and the KDPC algorithm proposed in Section 2.4.9 is the contents of the desired QoS vector **y**(t) in (3.68). In KDPC algorithm **y**(*t*) is vector of the

target CIR, where all the components of $\mathbf{y}(t)$ were assumed to be identical. This assumption can be relaxed. Now each component of the desired response vector $\mathbf{y}(t)$ can represent different target QoS. If we assume that each user requested a certain (feasible) data rate, then the desired response at time slot t is given by

$$\mathbf{y}(t) = \left[\Gamma_1^T(t), \Gamma_2^T(t), \cdots, \Gamma_Q^T(t)\right]', \quad t = 0,1,... \tag{3.69}$$

where the target CIR of user i (for DS-CDMA systems) is given by

$$\Gamma_i^T(t) = \frac{R_i^T(t)}{R_s}\delta_i^T(t), \quad t = 0,1,... \tag{3.70}$$

and $R_i^T(t)$ is the target data rate of user i at time slot t.

The optimum power vector can be estimated by applying Kalman filter algorithm of (2.117)-(2.121) to (3.66)-(3.70).

3.9.1 Minimum Variance Distributed Power and Rate Control

In the previous Section we assumed that the target data rate of each user is given. In this subsection we propose an algorithm to estimate the best transmitted power as well as data rate to achieve the target SINR. Different formulation is used to construct the state space formulation of the problem.

Rewriting Eq. (3.6) as

$$\frac{R_s}{R_i(t)}\frac{P_i(t)G_{ki}(t)}{\sum_{\substack{j=1\\ j\neq i}}^{Q} P_j(t)G_{kj}(t) + N_i(t)} = \delta_i^T(t) \qquad t=0,1,... \tag{3.71}$$

Now only the SINR parameter has been predefined.

Define

$$\alpha_i(t) \triangleq \frac{R_s G_{ki}(t)}{\sum_{\substack{j=1\\ j\neq i}}^{Q} P_j(t)G_{kj}(t) + N_i(t)} \qquad t=0,1,... \tag{3.72}$$

From (3.71) and (3.72) we obtain

$$\alpha_i(t)P_i(t) - \delta_i^T(t)R_i(t) = 0 \tag{3.73}$$

Now the problem is, how to find the optimum power and rate value which achieve (3.73) by using Kalman filter. The measurement model can be expressed as

$$\tilde{\mathbf{y}}(t+1) = \mathbf{Z}(t+1)\tilde{\mathbf{w}}(t+1) + \tilde{\mathbf{v}}(t+1), \quad t = 0,1,... \tag{3.74}$$

where

$$\tilde{\mathbf{y}}(t) = [0,0,...,0]^{'} \tag{3.75}$$

$$\mathbf{Z}(t) = \begin{bmatrix} \alpha_1(t) & 0 & \cdots & -\delta_1^T(t) & 0 & \cdots & 0 \\ 0 & \alpha_2(t) & 0 & 0 & -\delta_2^T(t) & 0 & 0 \\ \vdots & & & & & & \\ 0 & \cdots & \alpha_Q(t) & 0 & \cdots & 0 & -\delta_Q^T(t) \end{bmatrix}, \tag{3.76}$$

$$\tilde{\mathbf{w}}(t) = \left[P_1(t)\cdots P_Q(t), R_1(t), \cdots R_Q(t)\right]^{'}, \tag{3.77}$$

$\tilde{\mathbf{v}} \sim N(0, \Re_{nn})$, where $\Re_{nn}$ is the measurement error covariance matrix. The parameters can be modeled as constants with uncertainty $\tilde{\mathbf{q}}(t)$; i.e. the state-space model used in this formulation takes the form

$$\tilde{\mathbf{w}}(t+1) = \tilde{\mathbf{w}}(t) + \tilde{\mathbf{q}}(t), \quad t = 0,1,... \tag{3.78}$$

where $\mathbf{q} \sim N(0, \Re_{vv})$,where $\Re_{vv}$ is the uncertainty covariance matrix.

The Kalman filter provides the minimum-variance estimates of the RRS parameters (transmitted power and data rates).

3.10 Simulation Results

The simulation part will be divided to different scenarios to make an extensive comparison between the proposed algorithms and the existing algorithms, and also to evaluate the performance of our proposed algorithms.

In the first part of simulations, we will compare the proposed MODPRC algorithm with the optimum power-rate algorithm (Section 3.2) and the maximum throughput power control (MTPC) algorithm. Because of the huge computational complexity of the optimum power-rate control, this simulation will be carried out on only five users. In this part, the snapshot assumption is assumed in the simulation. A white Gaussian noise is added with zero mean and -63 dBm mean power. The set of allowed rates is {15,30,60,120,240,480,960}Kb/s. The maximum power is assumed to be 1 W. The data rate has been assumed to be continuous for the MODPRC algorithm and the MTPC algorithm. The user is assumed to be in outage, if at least one of the QoS requirements (the minimum data rate or the target SINR) can not been achieved. Figure 3.1 shows a

comparison between the optimum power-rate control, the MODPRC and the MTPC algorithms. The objective of the optimum power-rate control is to achieve the maximum rate sum with zero outage and power constraints. In the Figure we can see that MODPRC algorithm has achieved the same total rate with the following tradeoff factors $\lambda_1 = 0.001,\ \lambda_2 = 0.830,$ and $\lambda_3 = 0.169$. The MTPC algorithm fails to achieve the same total data rates as shown in the same Figure. The average power profile is shown in Figure 3.2. It is clear that the optimum average power is less than the required power in the other cases (MTPC and MODPRC). The average power needed by the MTPC algorithm is less than the MODPRC algorithm. The outage probability was 0.20 for both MODPRC and MTPC algorithms.

In CDMA systems the maximization of the total CIR products (3.3) can be directly mapped to the maximization of the total data rate products. One can say that the MTPC algorithm maximizes the total data rate products in the cell. Figure 3.3 shows that the total data rates product of the MTPC algorithm converges to the optimum value. The interesting result here is that the MODPRC algorithm can converge (with less fluctuations) to the same optimum solution if the tradeoff factors are selected as $\lambda_1 = 0.001,\ \lambda_2 = 0.895,$ and $\lambda_3 = 0.104$. Another interesting result in this simulation is that the average power of the MODPRC algorithm is slightly less than the MTPC algorithm as indicated in Figure 3.4. The outage probability was 0.20 for both MODPRC and MTPC algorithms. This simulation part shows that the MODPRC algorithm was able to solve the power rate optimization problem for two different criteria, which are the maximization of the total sum of users' data rates and the maximization of the total product of users' data rates. The key point is to find the correct tradeoff factors to achieve the required objective. To clarify this point more, we will show the behavior of the MODPRC algorithm with the extreme tradeoff factors values. For the same previous scenario, we test the MODPRC algorithm performance at the following extreme values of tradeoff factors $(\lambda_1, \lambda_2, \lambda_3) \in \{(1,0,0),(0,1,0),(0,0,1)\}$. The average power, the total rate sum and the outage probability are shown in Figures 3.5, 3.6, and 3.7 respectively. Figure 3.5 shows the average power in the three studied situations. In the first case $(\lambda_1, \lambda_2, \lambda_3) = (1,0,0)$ the objective is only minimizing the total power. For this reason the power is very small compared with other two situations. At the same time the sum of data

rate is (almost) zero and the outage is very high (100%) as shown in Figures 3.6, and 3.7 respectively. In the second case $(\lambda_1, \lambda_2, \lambda_3) = (0,1,0)$ where the objective is to minimize the outage, the average power is fair. The sum of data rates is fair as well and the outage converges to zero as shown in Figures 3.5, 3.6, and 3.7 respectively. In the third case $(\lambda_1, \lambda_2, \lambda_3) = (0,0,1)$ where the objective is to maximize the total data rates, the average power is the highest. The total data rate is the highest as well and the outage is considerably high as shown in Figures 3.5, 3.6, and 3.7 respectively. One can see that the performance of the MODPRC algorithm has a wide range of behavior depending on the tradeoff factor values.

Now a more sophisticated simulation scenario will be considered. In this part of simulation consider 16 base stations distributed in an area of 16 km^2 containing 100 users uniformly distributed. A white Gaussian noise is added with zero mean and 1 pW average power. Perfect handover is assumed, i.e., each user is assigned to the base station which has the best conditions. Uncorrelated log-normal shadowing is considered. The user is assumed to be in outage if his SINR is less than the target SINR (δ^T) or if the achieved data rate is less than the minimum required data rate. The target SINR is assumed to be δ^T=6 dB for all users. The minimum required data rate is 15 Kb/s for all users. The variable data rate is realized by using a variable processing gain that is defined as the ratio of chip rate to the user information bit rate. The achieved data rate is assumed to continue without upper bound. All the simulations will be carried out for the uplink case.

We will compare our proposed algorithms with different algorithms discussed in this Chapter. The performance comparison will be based on the achieved average data rate, power consumption and outage probability.

Figures 3.8-3.10 show the performance comparison between the MODPRC algorithm and the MOTDPRC algorithm. In this simulation the tradeoff factors have been tuned at $\lambda_1 = 0.001,\ \lambda_2 = 0.980,$ and $\lambda_3 = 0.019$ for both algorithms. The power consumption and the outage of the MOTDPRC are worse than the MODPRC algorithm. The average data rate of the MOTDPRC is very close to the MODPRC algorithm. It is clear that the MOTDPRC algorithm does not perform as well as that of MODPRC algorithm. This result is logical since the MOTDPRC algorithm uses an estimated CIR rather than the actual CIR.

Figures 3.11-3.13 indicate the performance comparison between the MODPRC algorithm and the MTPC algorithm. The tradeoff factors of the MODPRC algorithm have been tuned to get as close to the average data rate as the MTPC algorithm. The tradeoff factors have been tuned to $\lambda_1 = 0.002,\ \lambda_2 = 0.893,$ and $\lambda_3 = 0.105$. The average data rate of the MTPC algorithm has been achieved using the MODPRC algorithm but at a higher average power and outage. This is due to the fact that the MTPC algorithm is a centralized algorithm and the MODPRC algorithm is a distributed one. One can note from Figure 3.12 that the MODPRC algorithm has a faster convergence than the MTPC algorithm.

As explained in Subsection 3.8.3 the MTMPC algorithm is an extension of the MTPC algorithm to achieve a similar (or close) data rate at less transmitted power. Figures 3.14-3.16 show the performance comparison between the MTMPC algorithm and the MTPC algorithm. It is clear from the Figures that with a small degradation on the average rate, the MTMPC algorithm can greatly reduce the average transmitted power. In this simulation scenario the average rate of the MTMPC algorithm degraded by about 30%, but the average saved power was about 98%. The performance of the MTMPC algorithm is degraded as the additive white noise increases. The logarithmic scale has been used in Figure 3.14 because of the large difference in the average transmitted power of MTPC and MTMPC algorithms. From Figure 3.16, we see that the outage probability of the MTMPC is slightly worse than the MTPC algorithm. This is an expected result because the MTMPC algorithm reduces the transmitted power to be close to the minimum.

The MODPRC algorithm gives us two degrees of freedom in the determination of the power-rate specifications. In this simulation we will compare the behavior of the MODPRC algorithm with the SPC algorithm at three different tradeoff factor values. Figures 3.17-3.19 show the performance comparison between the SPC algorithm and the MODPRC algorithm at $\lambda_1 = 0.005,\ \lambda_2 = 0.940,$ and $\lambda_3 = 0.055$. It is clear that the MODPRC algorithm achieves less outage and less power consumption. But the SPC achieves a higher average rate. By increasing the weight of the data rate and reducing the weight of the fairness of the MODPRC algorithm, using values such as $\lambda_1 = 0.000,\ \lambda_2 = 0.500,$ and $\lambda_3 = 0.500$, we obtain the same average data rate as obtained by using SPC algorithm as shown in Figures 3.20-3.22. The outage probabilities are also comparable, but the MODPRC algorithm needs higher transmitted power. The reason is

that in the SPC algorithm, if one of the QoS requirements of a user can not be achieved, this user is dropped out and his transmitted power becomes zero. But in the MODPRC algorithm all users are transmitting whether their QoS requirements are achieved or not. This is more realistic, because in UMTS systems, even when the throughput is temporarily reduced to zero for some users, their control channel power will not be zero!

The previous algorithms are based on the competition between users to divide the radio resources between them. The assignment of the radio resources of the multi-rate power control using Kalman filter is based on the negotiations between the users and the network. A different simulation scenario has been used to evaluate the performance of Kalman filter applications as multi rate power control.

In the next simulation we consider again the uplink of a CDMA system that has a chip rate of 3.84 Mb/s. The transmitted data rate should be one in the following set {15, 30, 60, 120, 240, 480, 960} Kb/s. We have assumed 120 users uniformly distributed in an area of 4 Km^2 with four base stations. Uncorrelated log-normal shadowing is assumed. The channel noise is assumed to be Gaussian and white with zero mean and 10^{-13} w variance. The users are moving with a maximum speed of 30 Km/h. A user is assumed to be in outage, if his SNR is less than the target SINR (δ^T). The target SNR is assumed to be the same for all users and also equal to δ^T=6 dB. Figure 3.23 shows the actual CIR of one of the users when his transmitted data rate changed at time slot 15 from 15Kb/s to 240Kb/s. The new data rate has changed again at time slot 45 to 15Kb/s. The target CIR is shown in Figure 3.23 as well. Figure 3.24 shows the transmitted power of the corresponding user and the optimum power. The optimum power is computed using centralized power control (Section 3.3). It is clear from the Figures 3.23-3.24 that Kalman filter converges to the optimum solution. The fluctuations in the results are caused by the dynamical behavior of the wireless mobile channels.

Finally, we will simulate the case of minimum variance power and rate control. As described in Section 3.9.1 there is no pre-requested data rate or data rate objectives needed to be achieved. The algorithm specifies the optimum power and rate values to achieve the target SINR. A simple scenario will be used for simulation. Assume 5 users randomly distributed in a cell with one base station. The additive white noise has zero mean and -80dBw variance. The maximum power and rate are assumed to be 10 W and 256 Kb/s respectively. During the simulation we start with zero initial power and with the

maximum initial data rate. Snapshot assumption is assumed. The power values and the rate values of the users are shown in Figures 3.25 and 3.26 respectively. Each color represents a different user. It is clear from Figure 3.26 that all users achieved the highest data rate (256 Kb/s) except the user with red dashed line where his achieved data rate is small. Also his power is rather high as shown in Figure 3.25. The same scenario but with uncorrelated slow and fast fading have been applied. The power values and the rate values of the users are shown in Figures 3.27 and 3.28 respectively. The practical significance of the minimum variance power and rate control algorithm is rather limited because it does not guarantee all QoS specifications.

From the simulations one can conclude that the MODPRC algorithm can achieve different performance criteria by changing only the tradeoff factors values. If the QoS requirements of a user have changed within the same call (e.g. from voice call to video conferencing), then the user modifies only the tradeoff factors to optimize the power for the new situation. The problem is how to find the optimum tradeoff factors to achieve the required specifications. This problem is one of the biggest problems in the multi-objective optimization field. The decision maker takes the responsibility to select the optimum solution. This point is very interesting for future research. During the simulations the following tradeoff factors $\lambda_1, \lambda_2, \lambda_3 = 0.01, 0.97, 0.02$ gave good results in many situations.

The MTMPC algorithm reduces considerably the total power consumption with comparably slight degradation in the data rate, when compared to MTPC. The MTMPC algorithm is reasonable for systems with energy constraints like sensor networks. Kalman filter application in multi-rate power shows fast convergence speed to the required power. Kalman filters have very wide applications in different scientific fields. The behavior of Kalman filters is well understood. Our proposed algorithms introduce good bases for further research in this field.

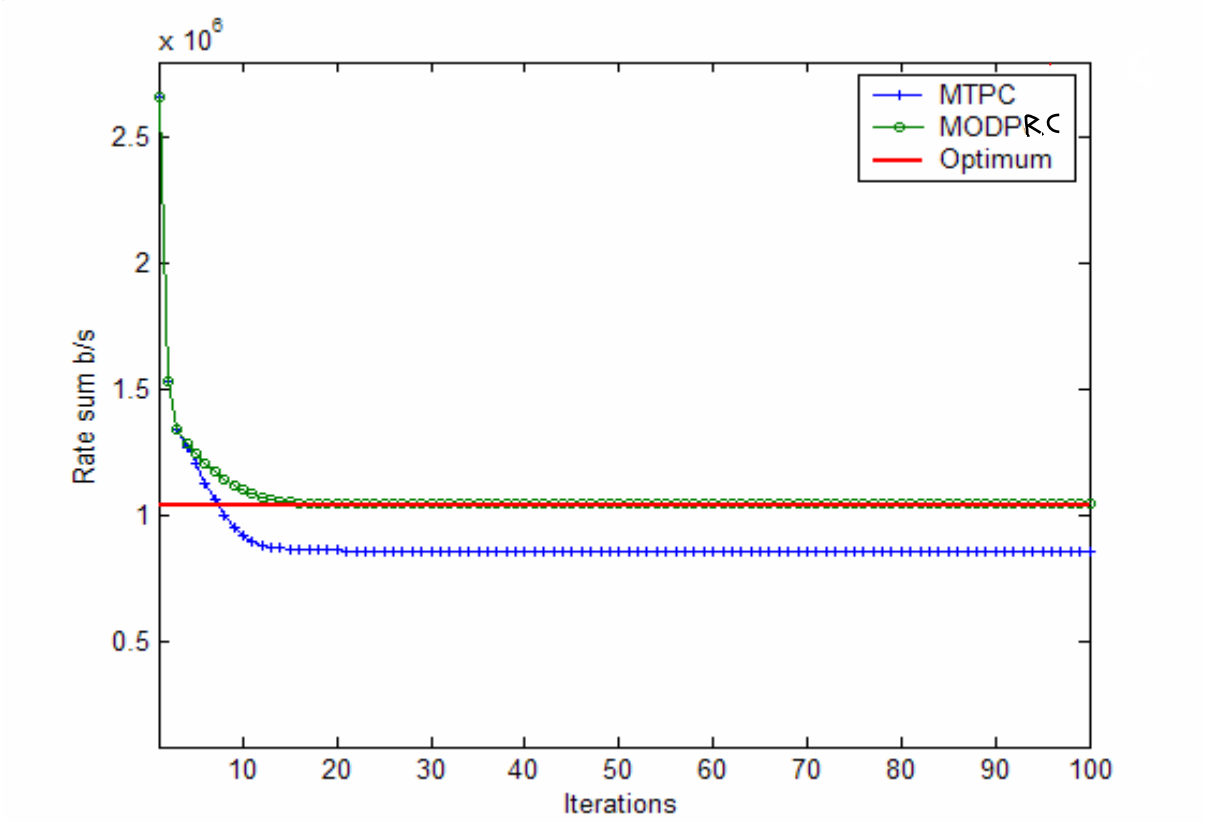

Figure 3.1. Total rate comparisons between optimum algorithm, MTPC algorithm and MODPRC algorithm.

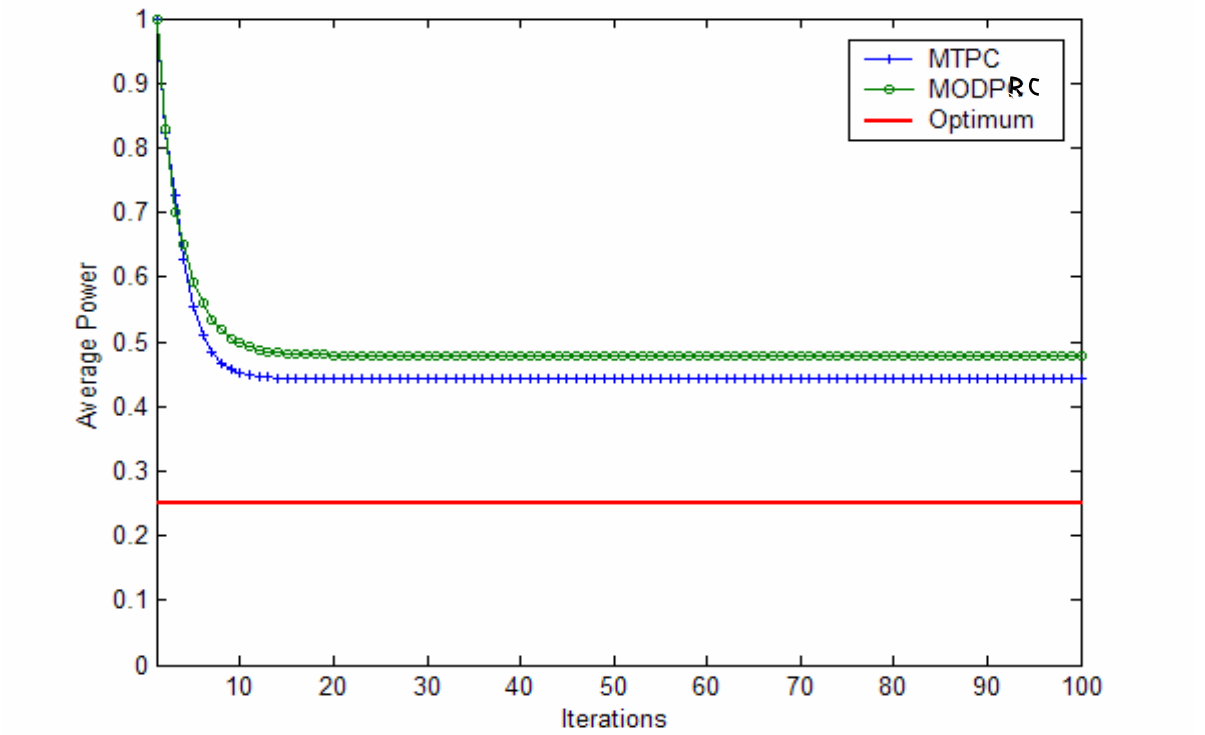

Figure 3.2. Average power comparisons between optimum algorithm, MTPC algorithm and MODPRC algorithm.

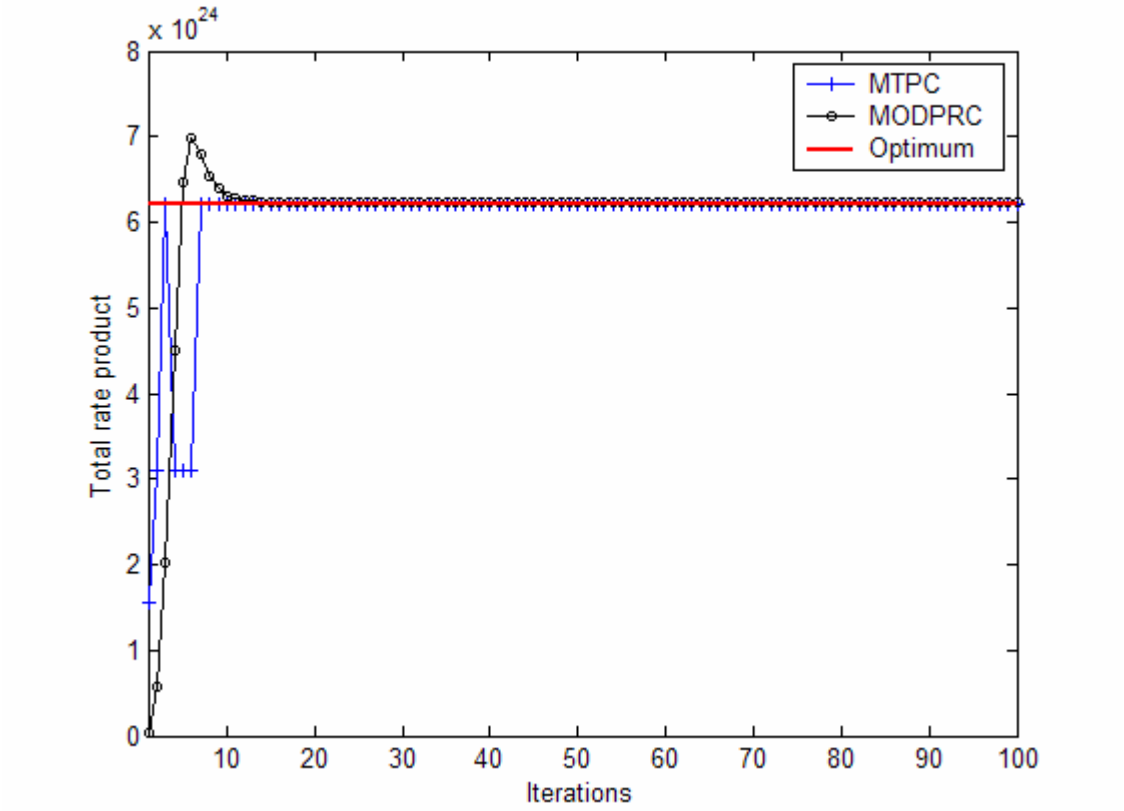

Figure 3.3. Rate product comparisons between optimum algorithm, MTPC algorithm and MODPRC algorithm.

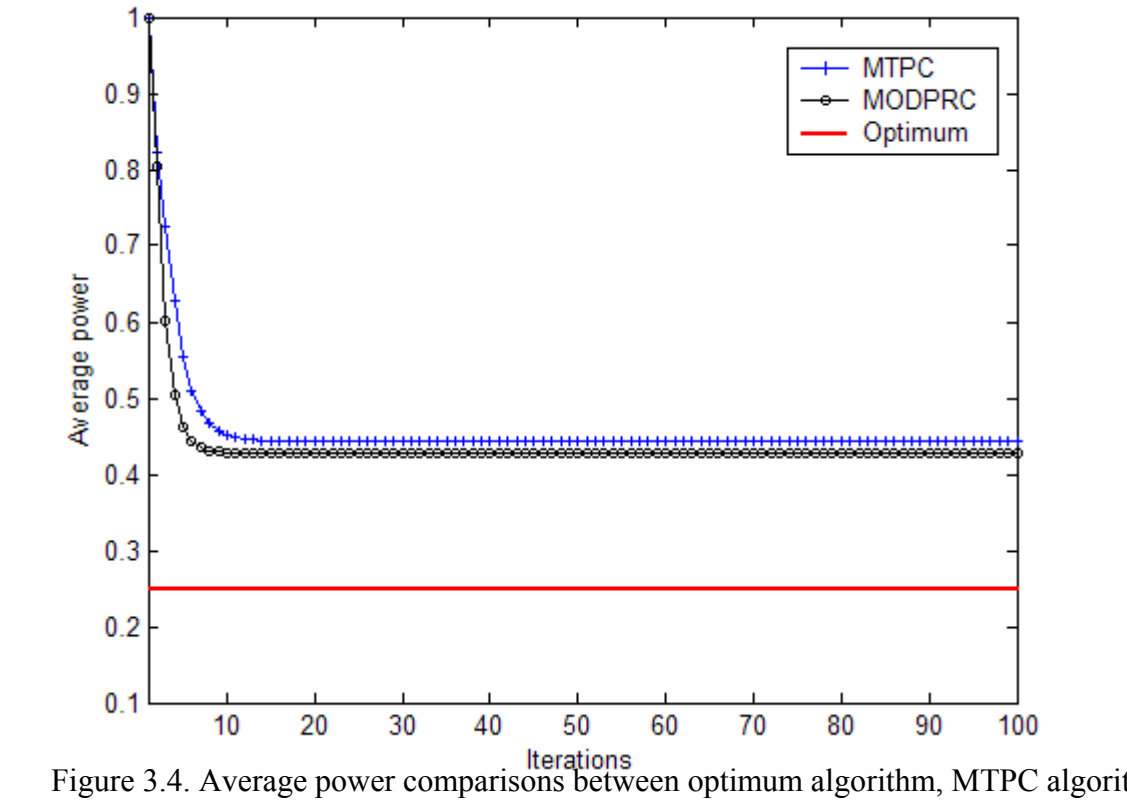

Figure 3.4. Average power comparisons between optimum algorithm, MTPC algorithm and MODPRC algorithm.

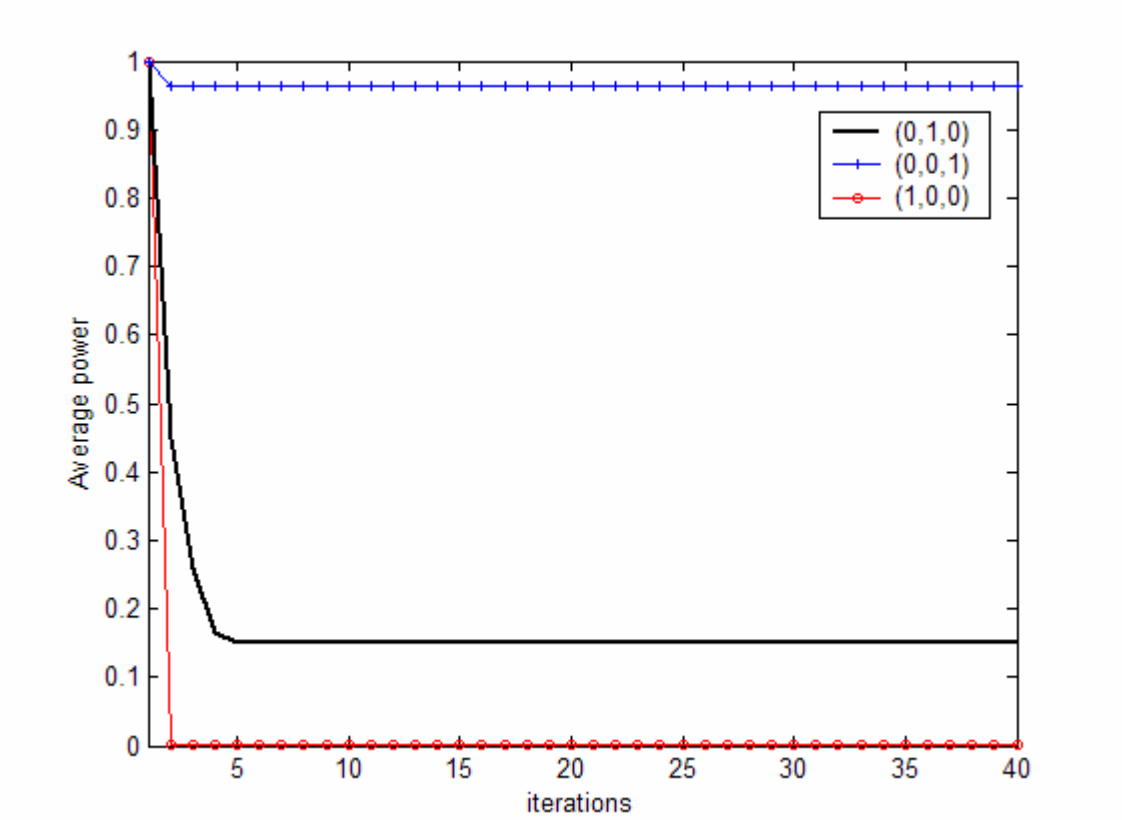

Figure 3.5. Average power comparisons of MODPRC algorithm at extreme tradeoff factors.

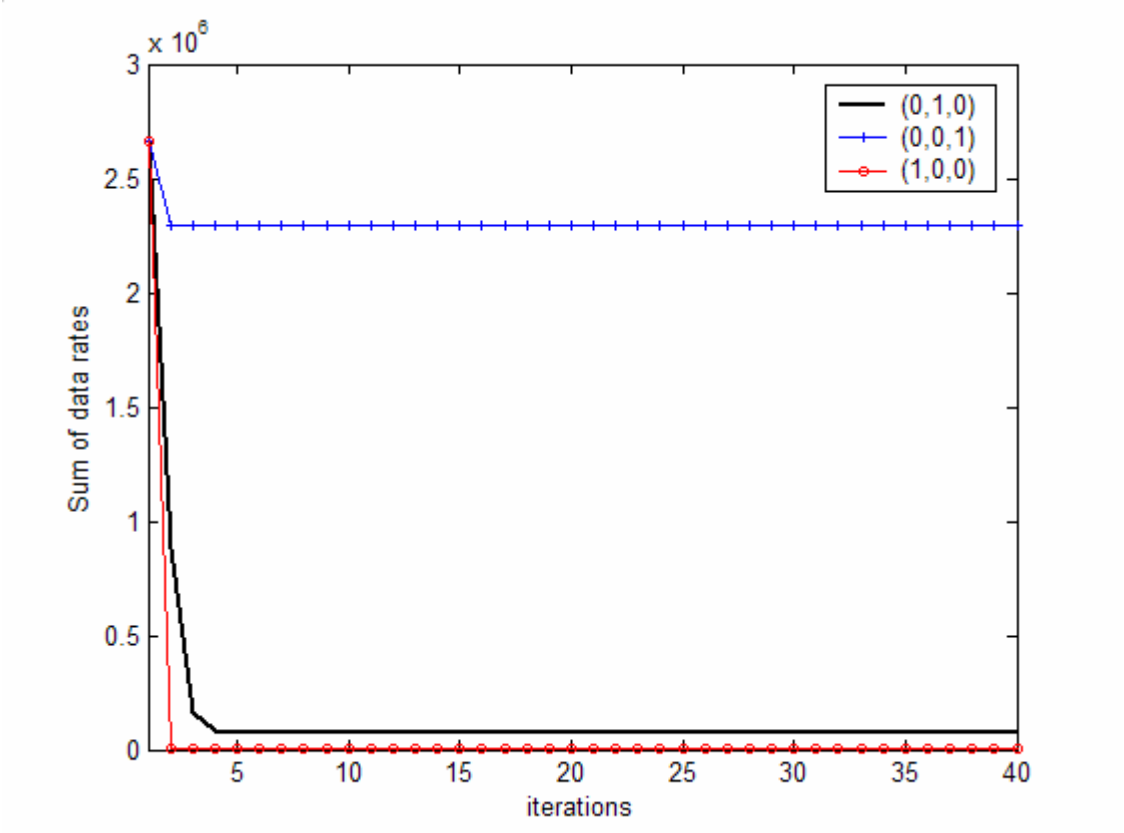

Figure 3.6. Data rate comparisons of MODPRC algorithm at extreme tradeoff factors.

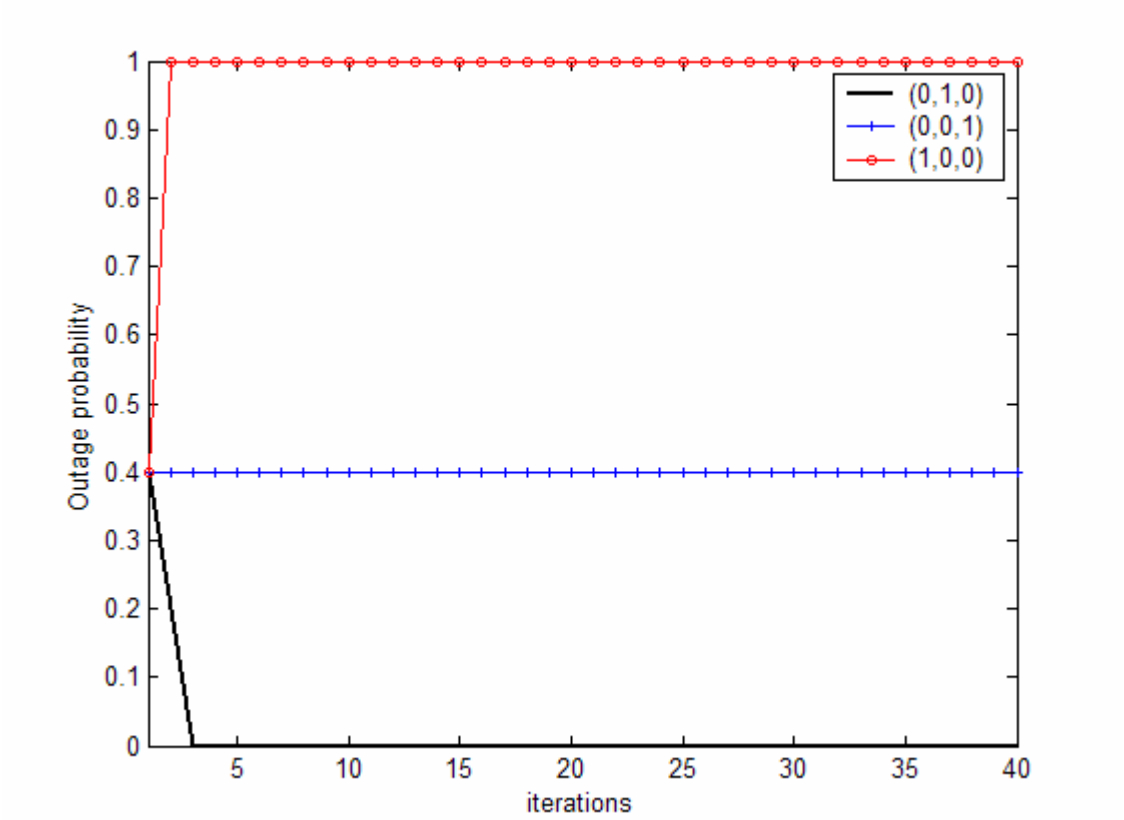

Figure 3.7. Outage comparisons of MODPRC algorithm at extreme tradeoff factors.

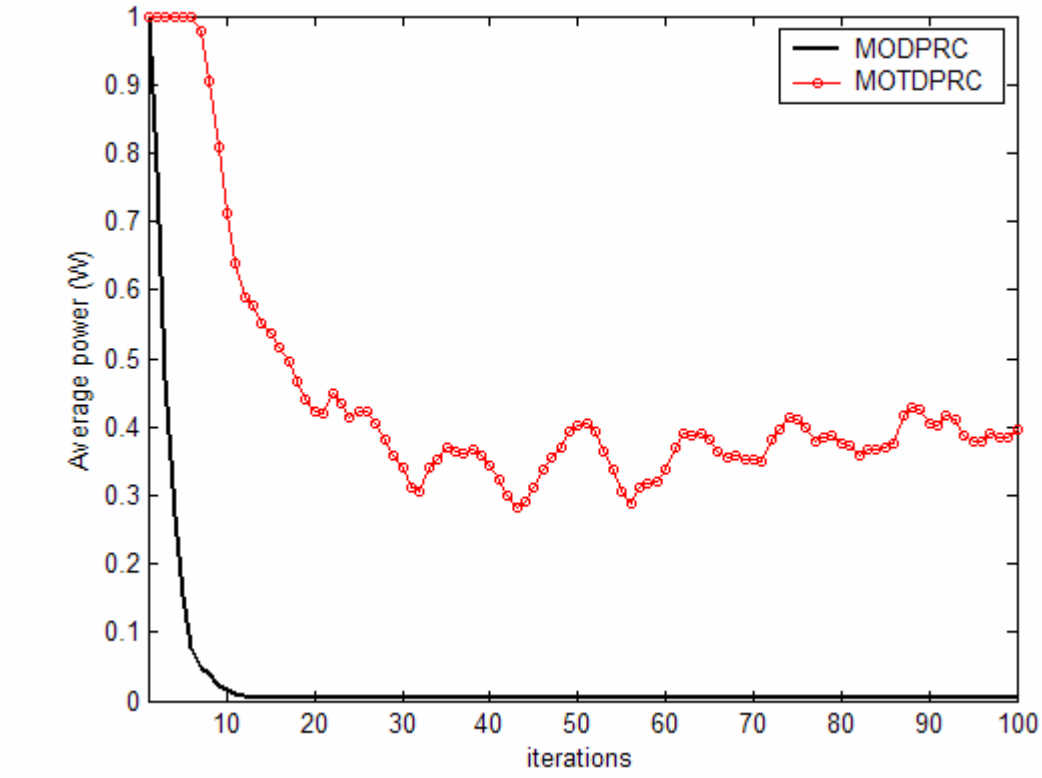

Figure 3.8. Average power comparisons of MODPRC and MOTDPRC algorithms.

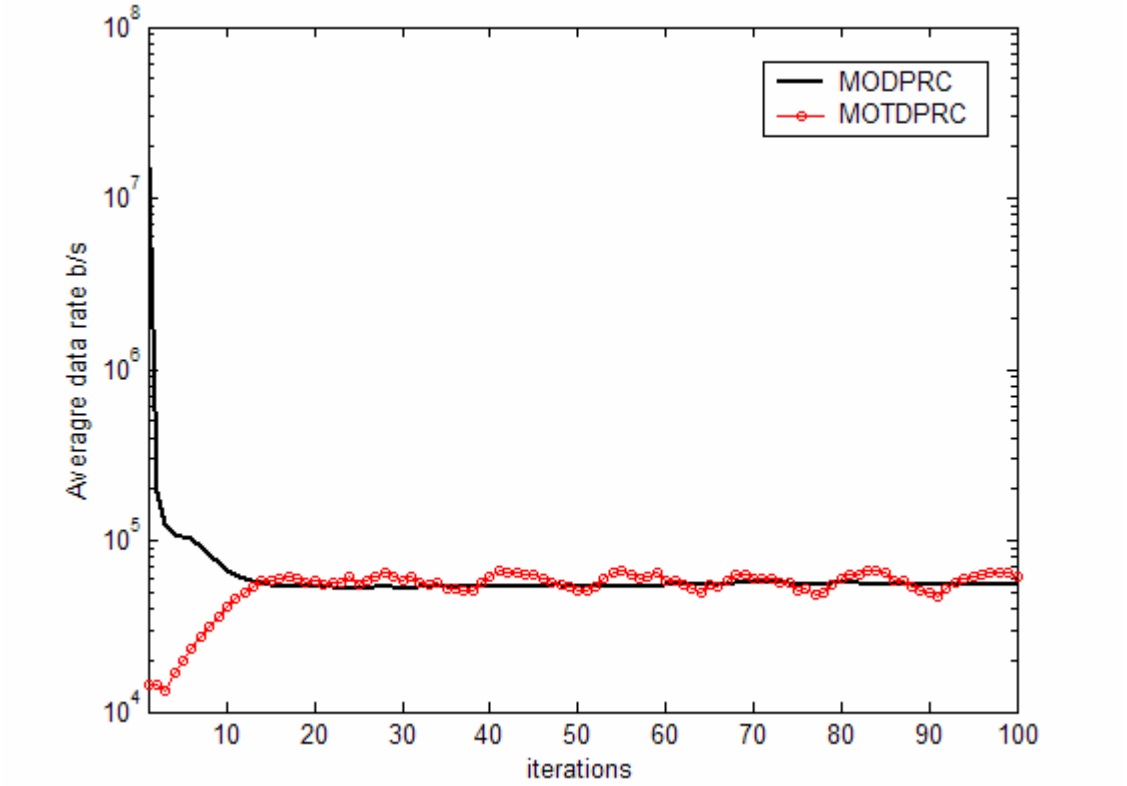

Figure 3.9. Average data rate comparisons of MODPRC and MOTDPRC algorithms.

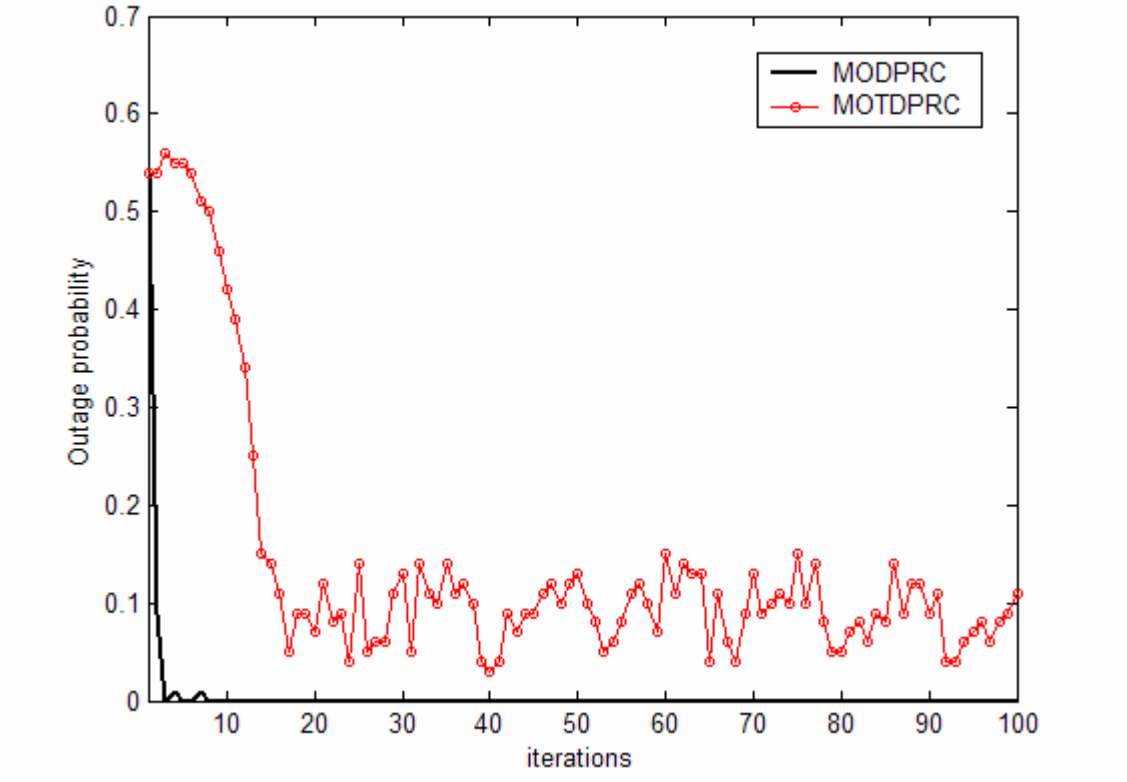

Figure 3.10. Outage comparisons of MODPRC and MOTDPRC algorithms.

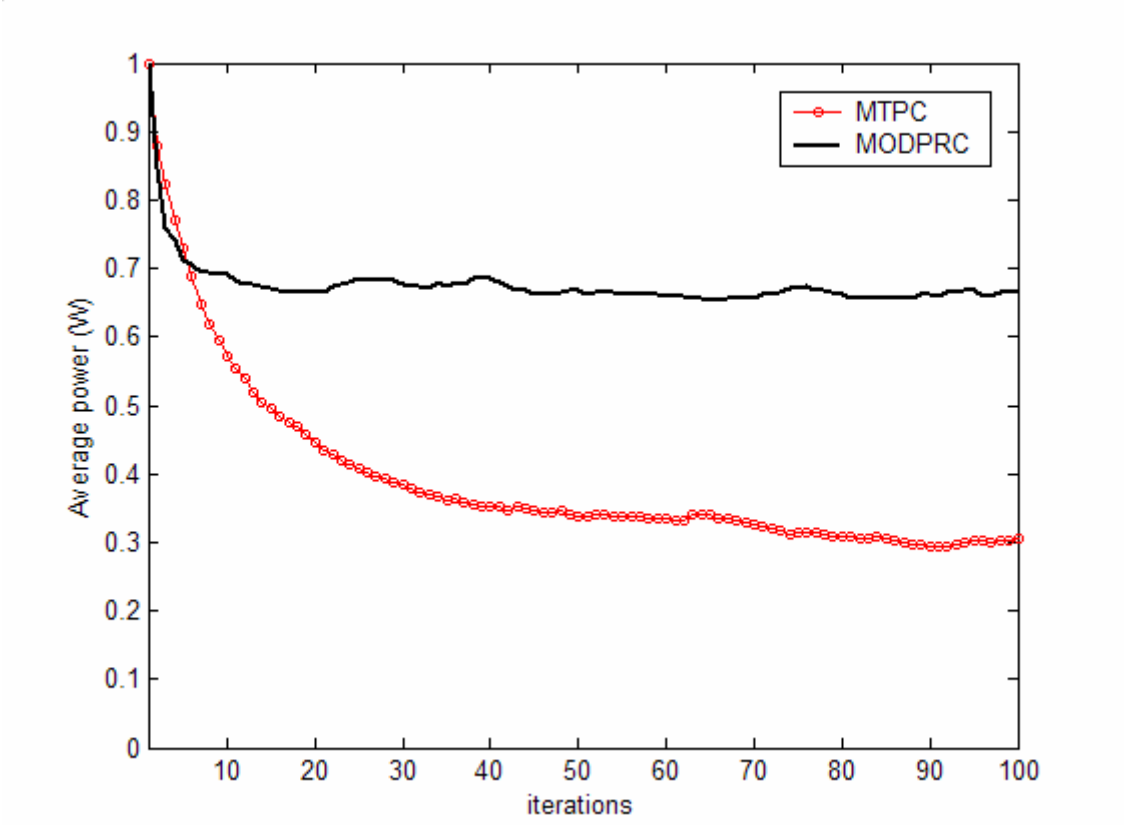

Figure 3.11. Average power comparisons of MODPRC and MTPC algorithms.

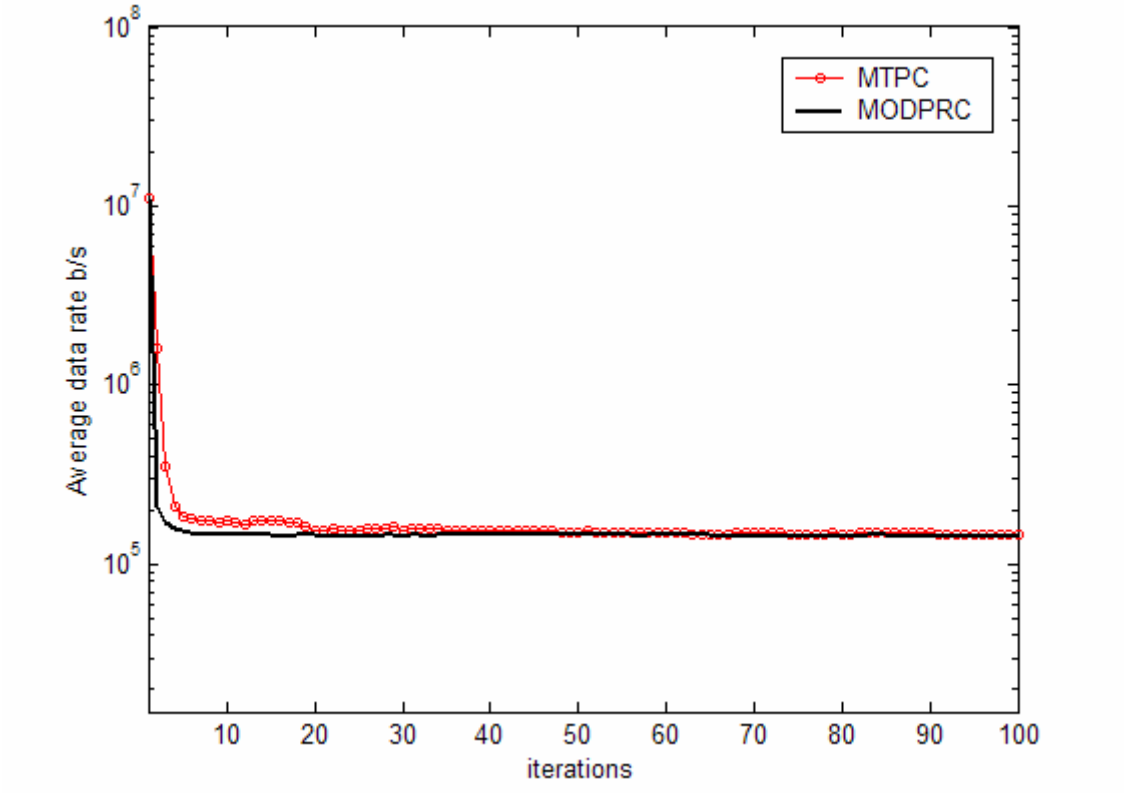

Figure 3.12. Average data rate comparisons of MODPRC and MTPC algorithms.

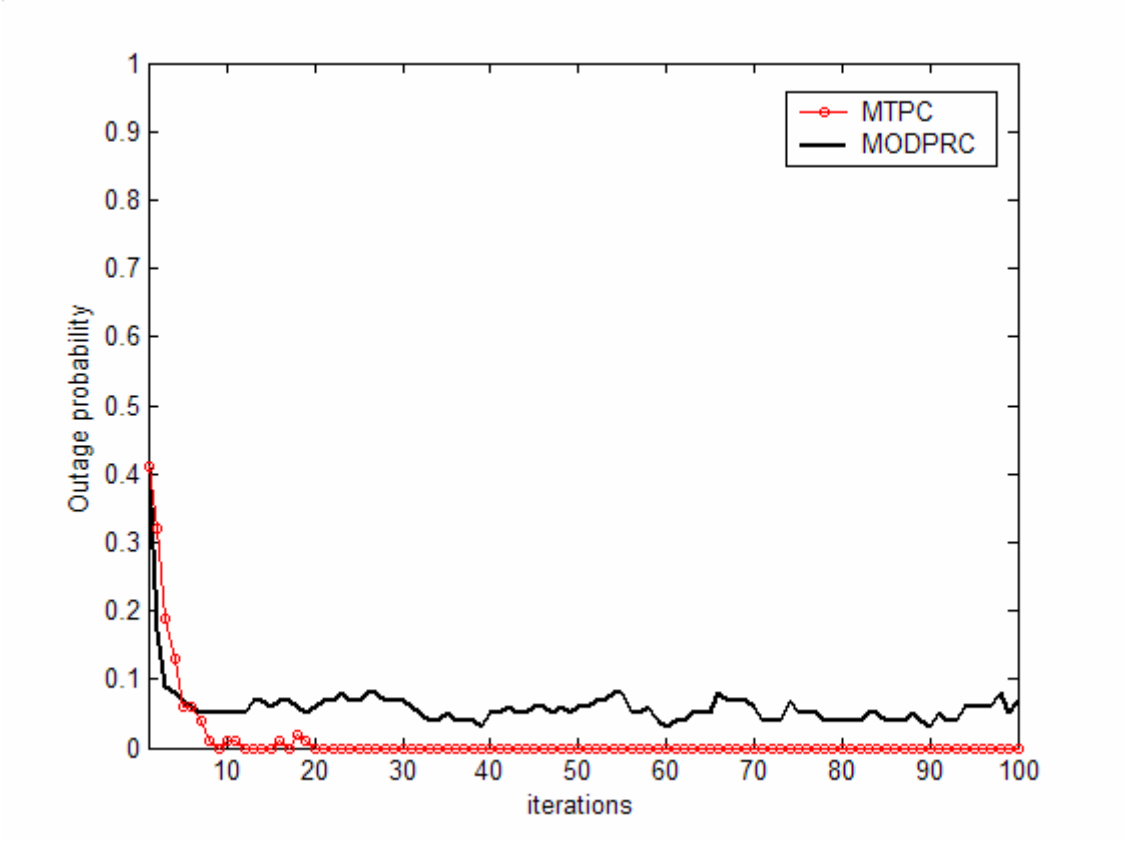

Figure 3.13. Outage comparisons of MODPRC and MTPC algorithms.

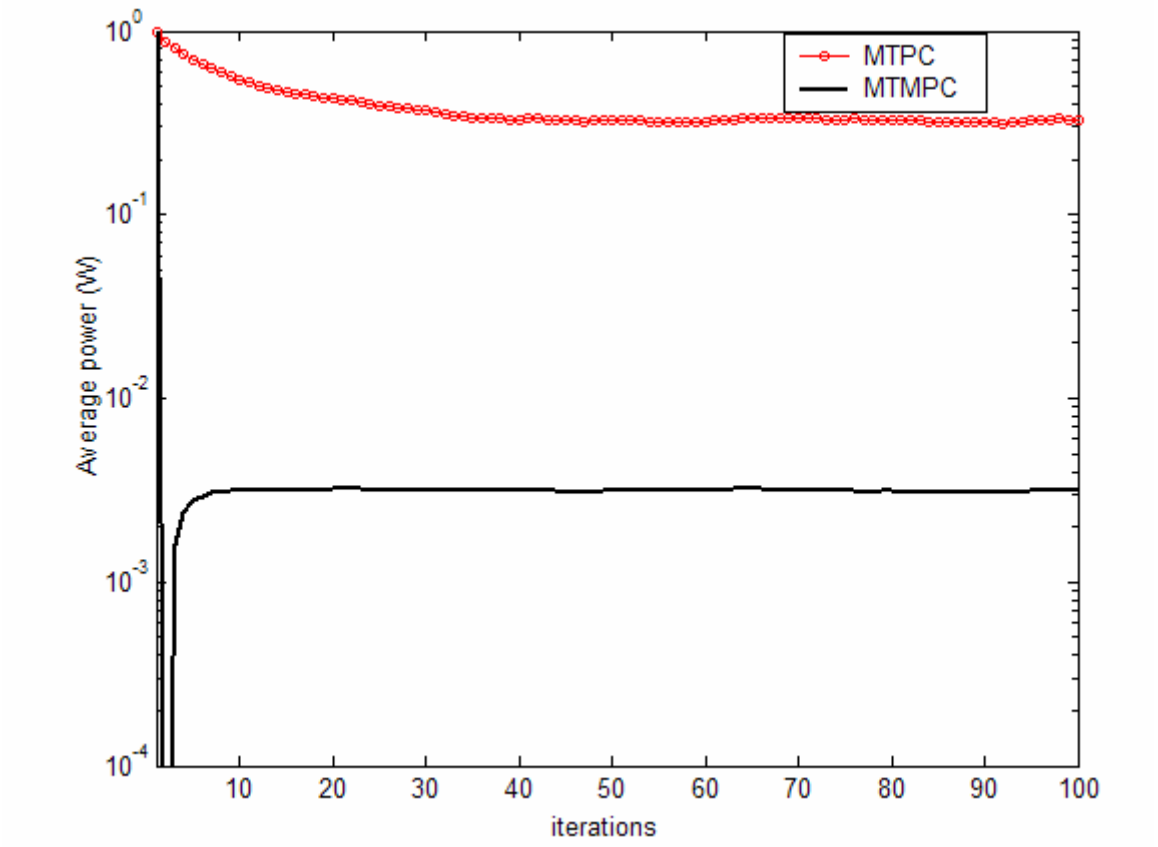

Figure 3.14. Average power comparisons of MTPC and MTMPC algorithms.

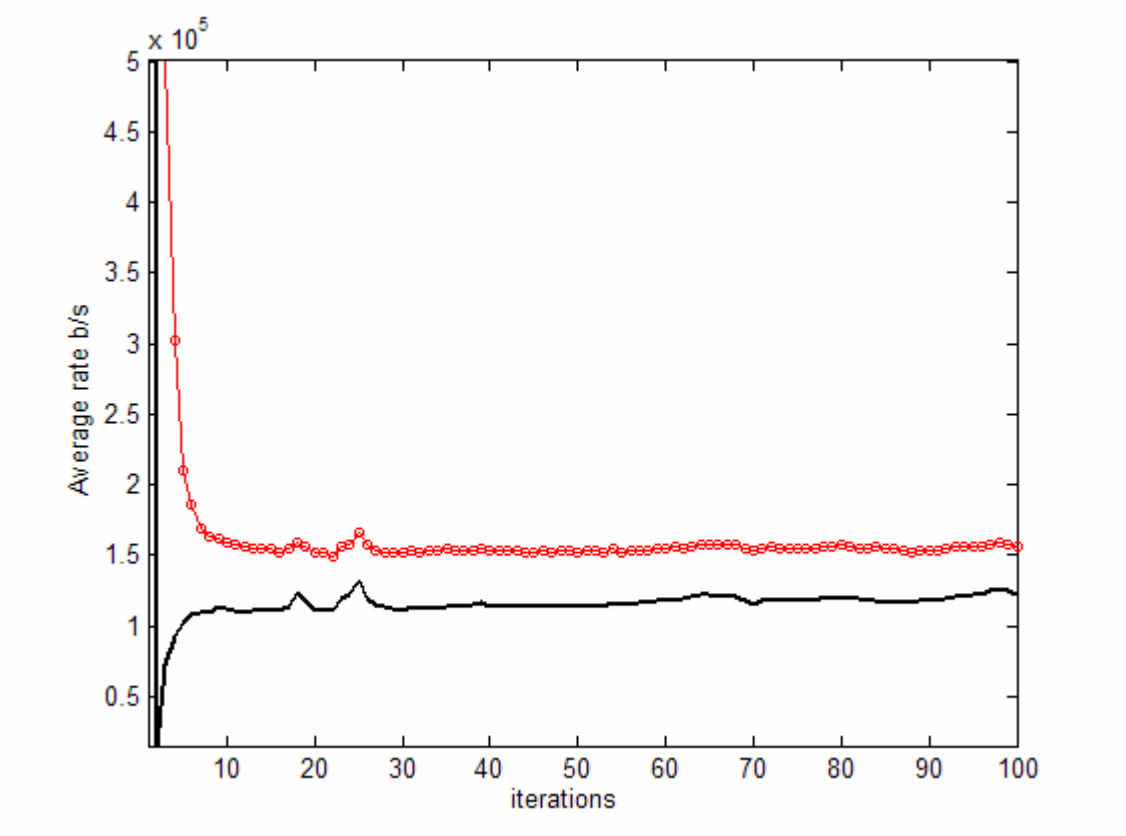

Figure 3.15. Average data rate comparisons of MTPC and MTMPC algorithms.

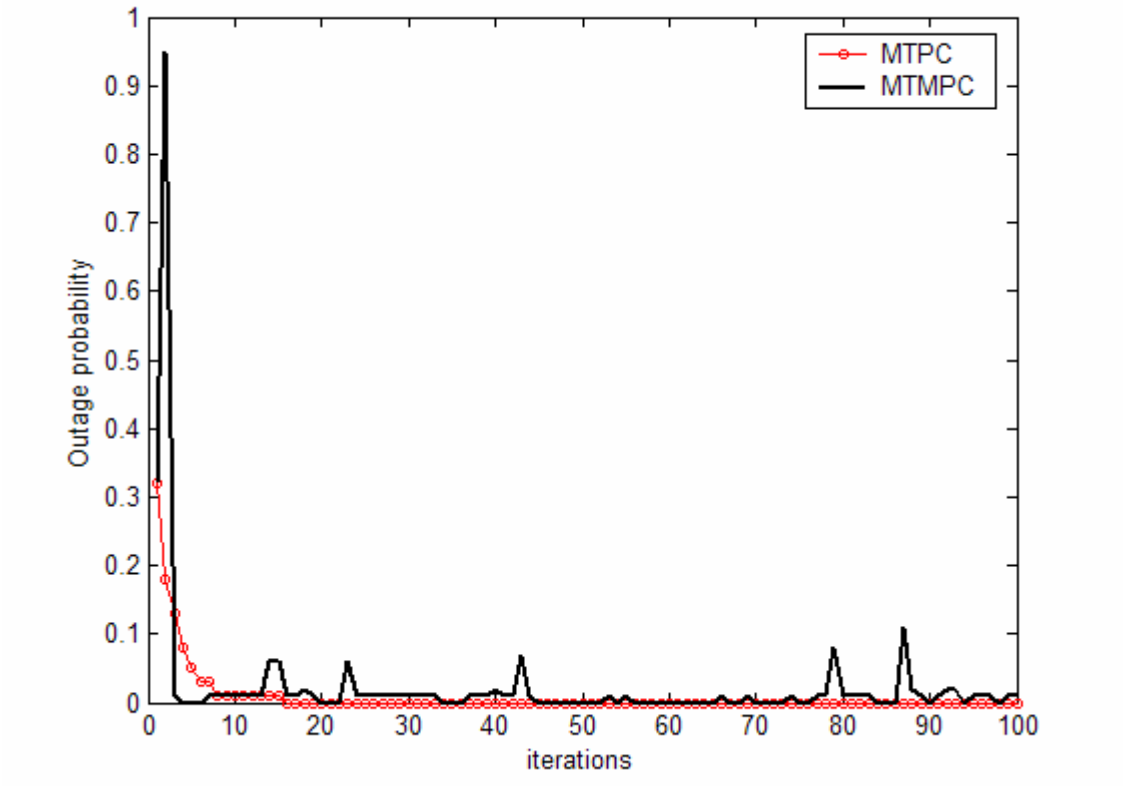

Figure 3.16. Outage comparisons of MTPC and MTMPC algorithms.

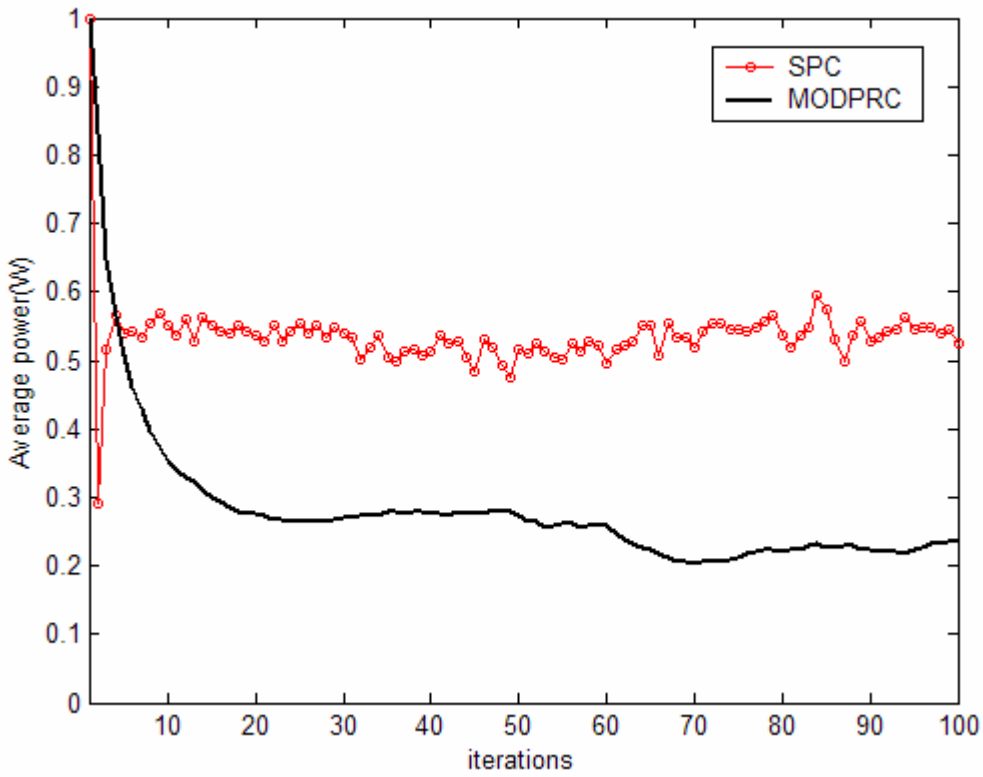

Figure 3.17. Average power comparisons of MODPRC and SPC algorithms.

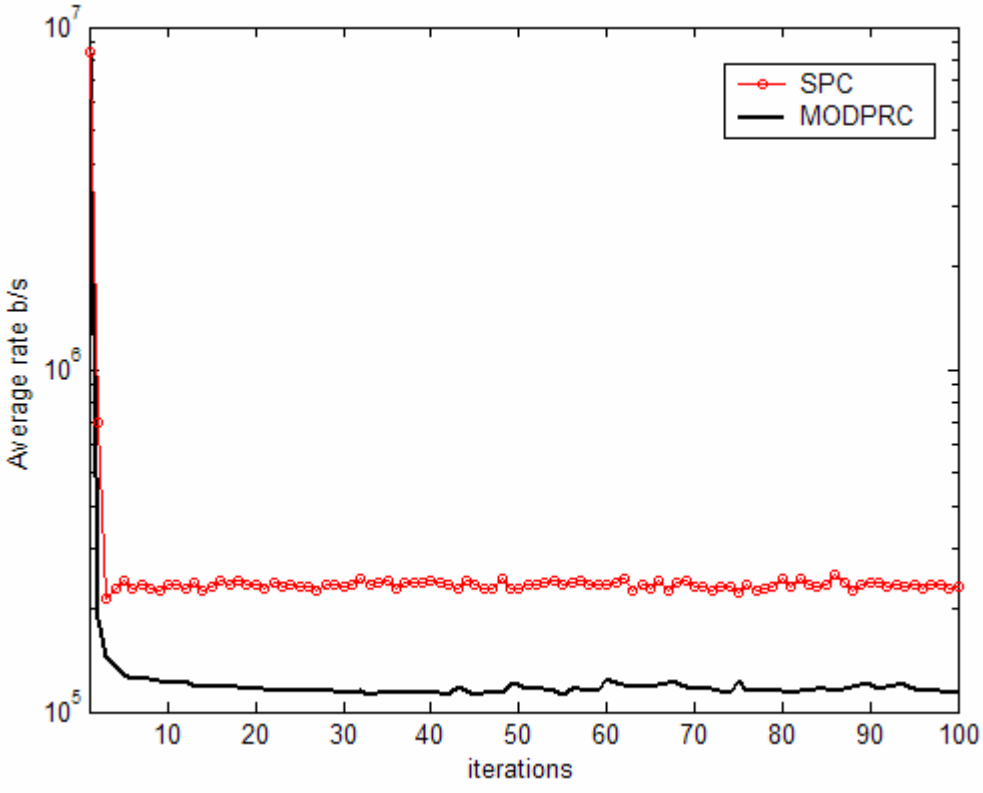

Figure 3.18. Average data rate comparisons of MODPRC and SPC algorithms.

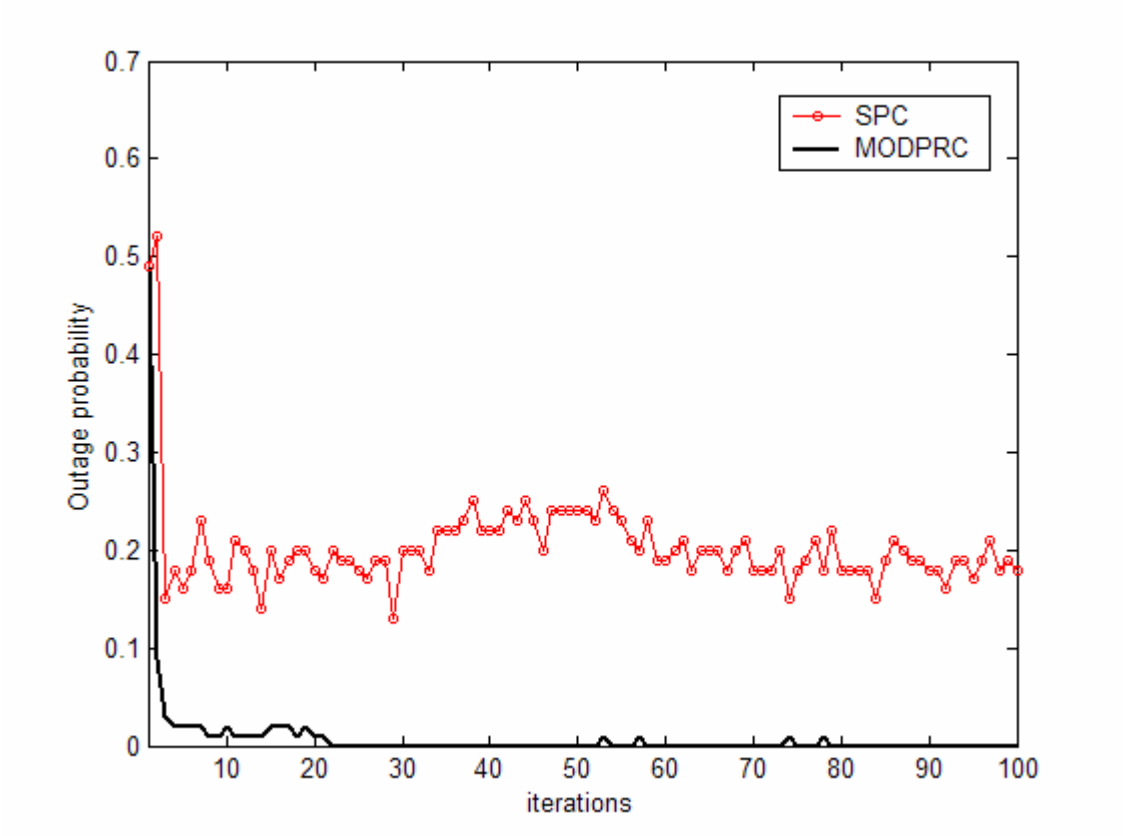

Figure 3.19. Outage comparisons of MODPRC and SPC algorithms.

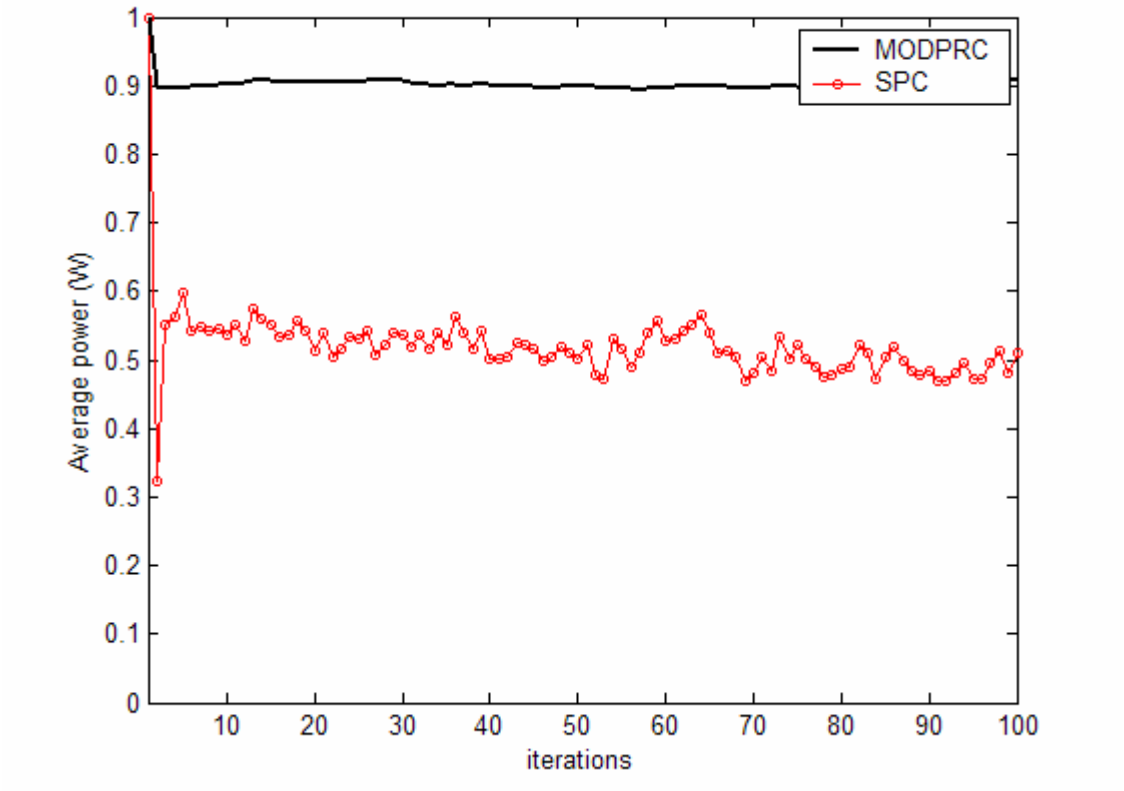

Figure 3.20. Average power comparisons of MODPRC and SPC algorithms.

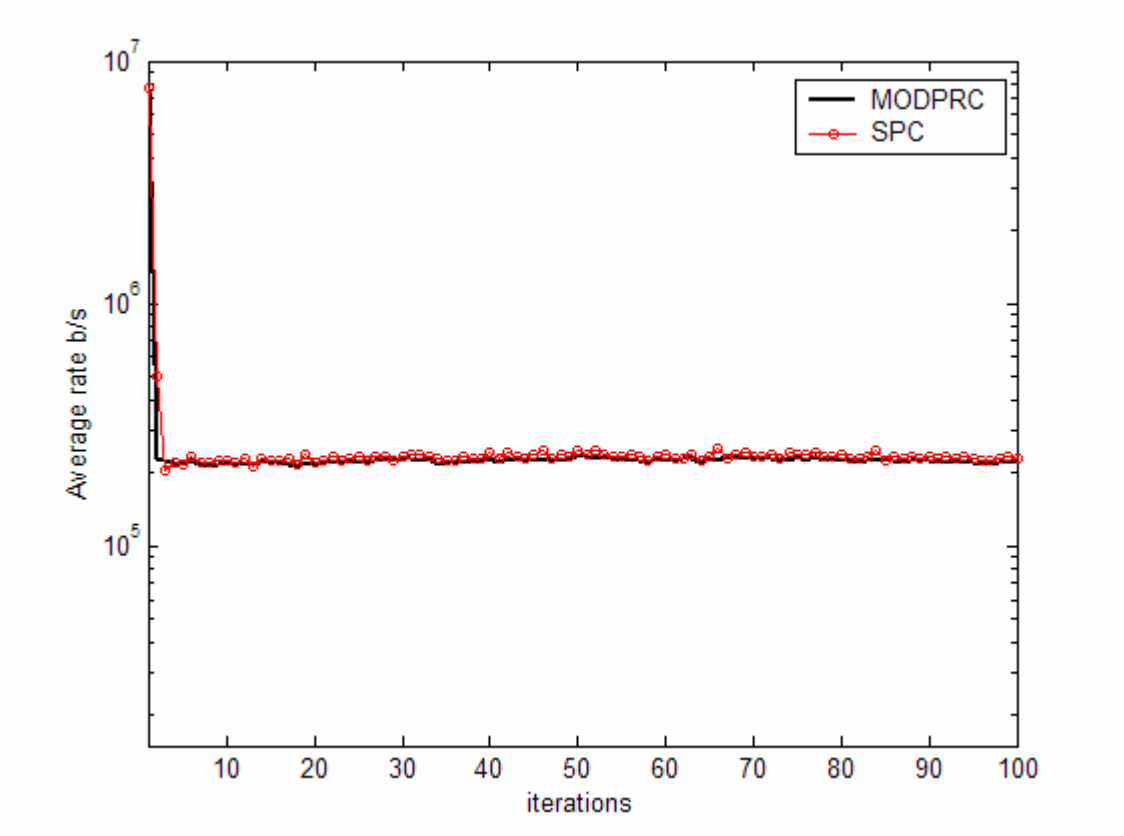

Figure 3.21. Average data rate comparisons of MODPRC and SPC algorithms.

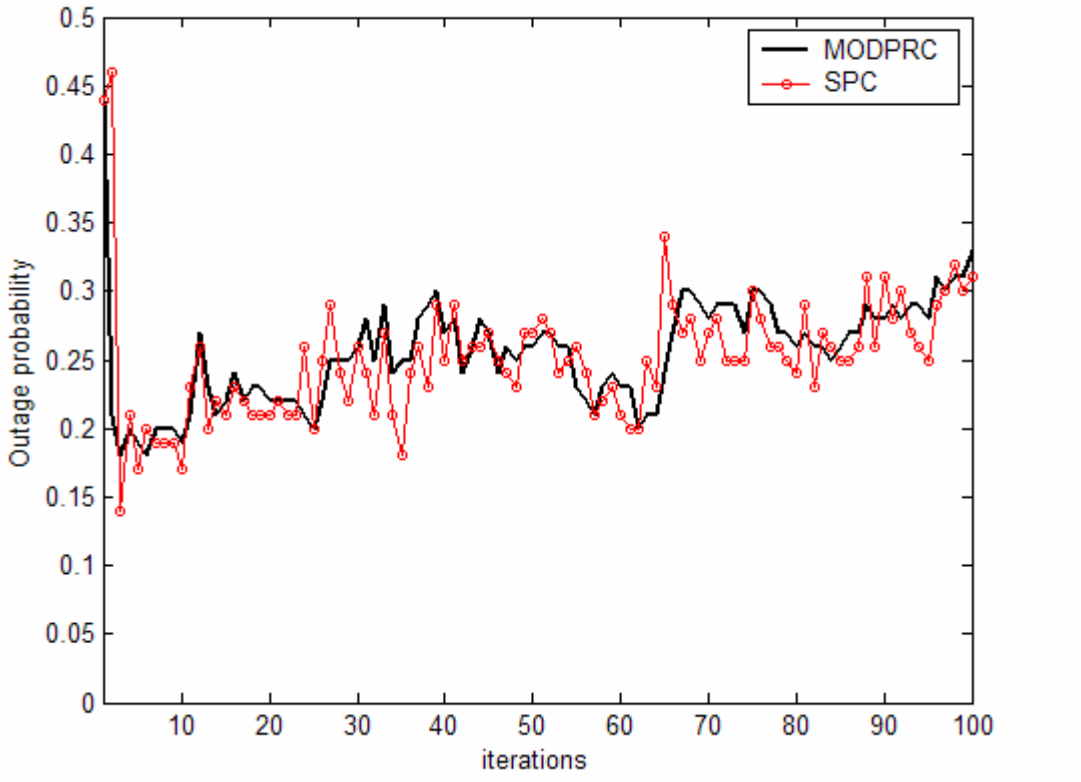

Figure 3.22. Outage comparisons of MODPRC and SPC algorithms.

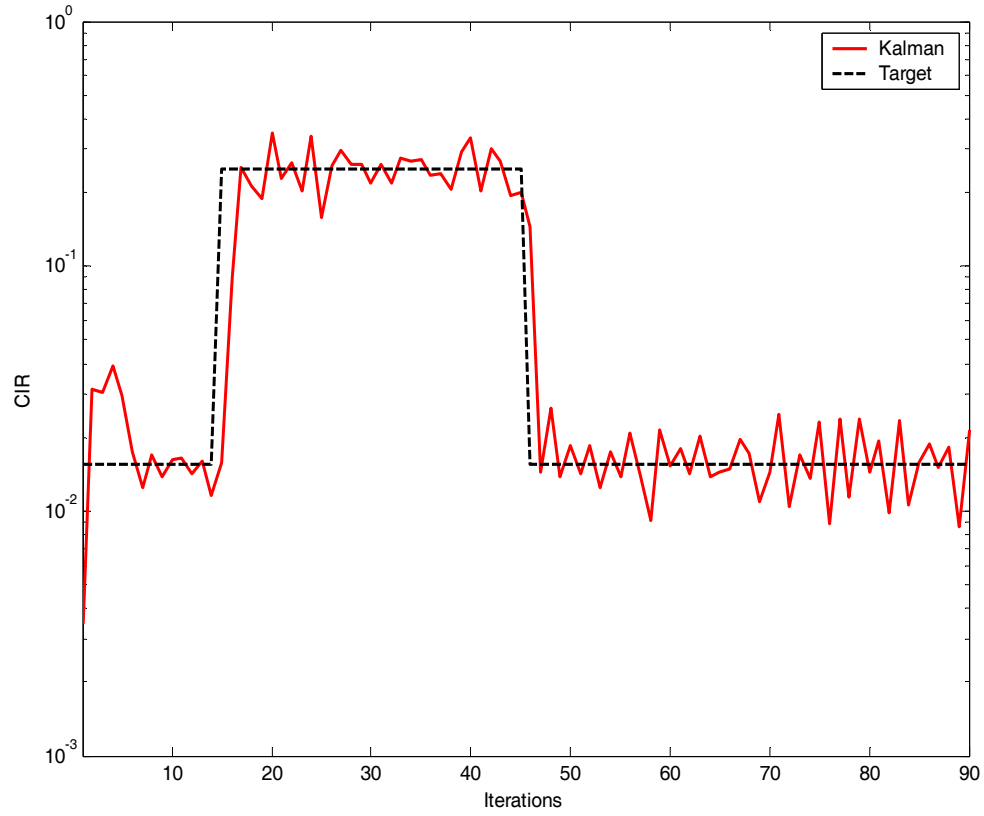

Figure 3.23. The actual CIR with the target using Kalman filters.

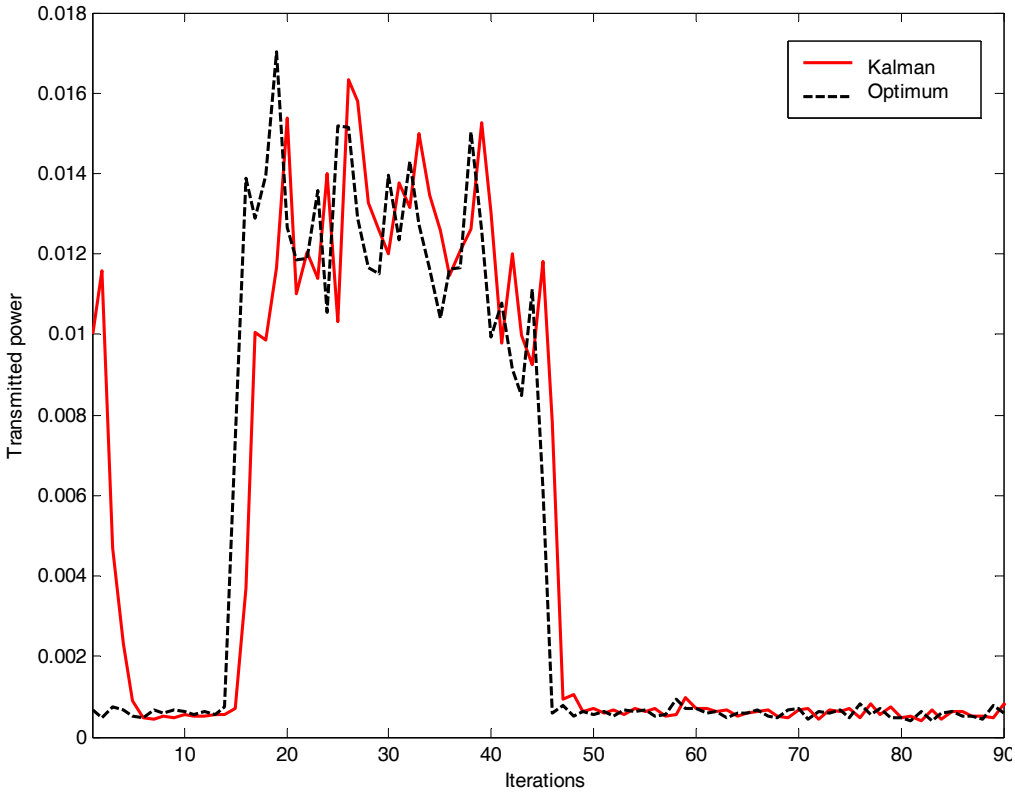

Figure 3.24. The transmitted power of one user using Kalman filters compared with the optimum power.

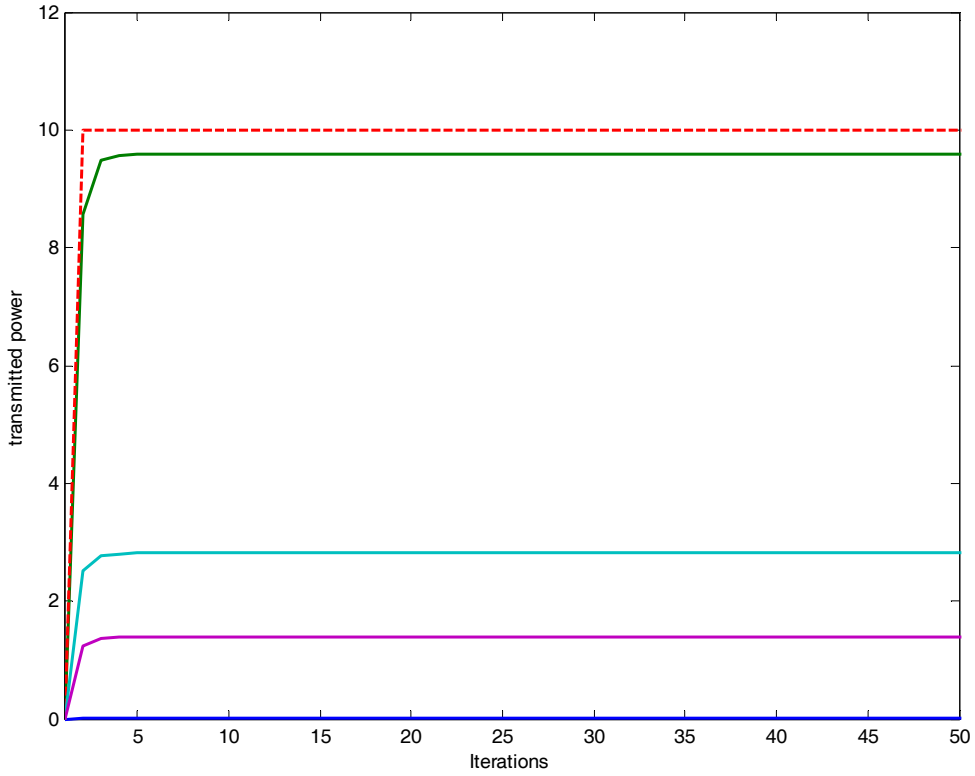

Figure 3.25. The transmitted power of five users using minimum variance power and rate control algorithm.

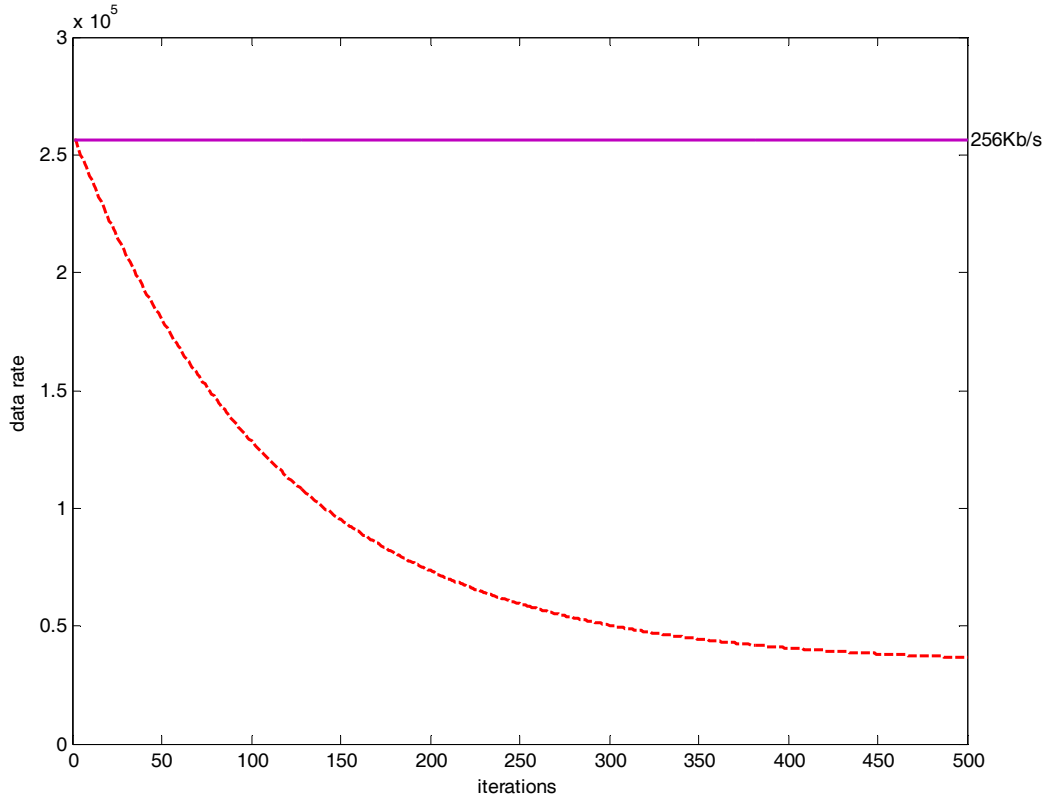

Figure 3.26. The data rate using minimum variance power and rate control algorithm.

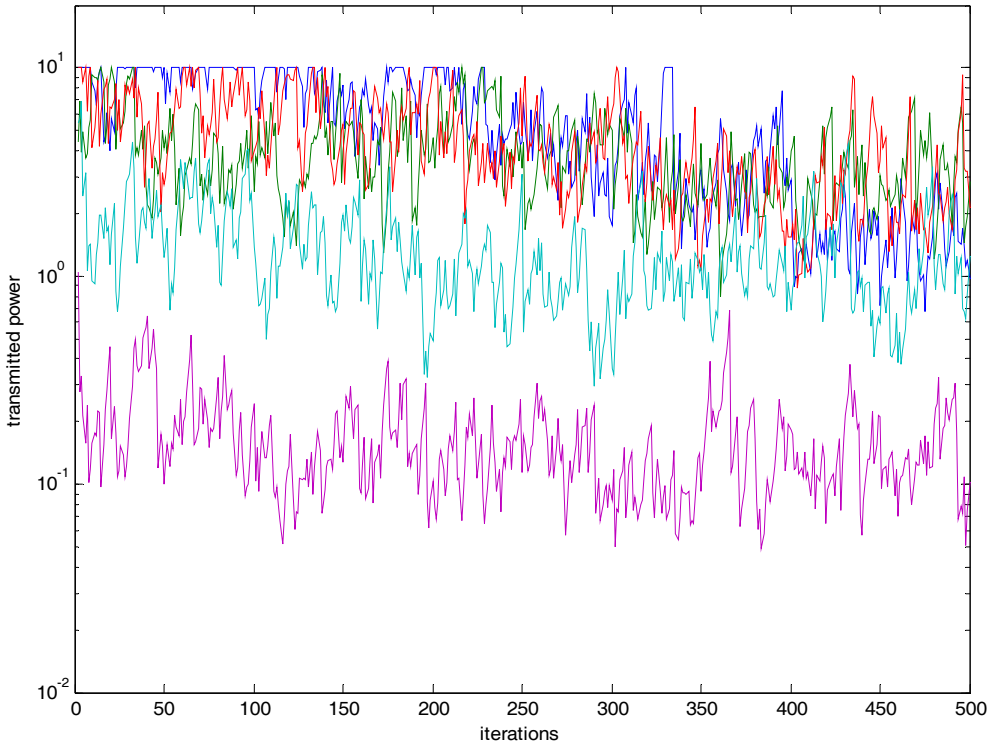

Figure 3.27. The power of five users (with different colors) using minimum variance power and rate control algorithm with dynamical channel.

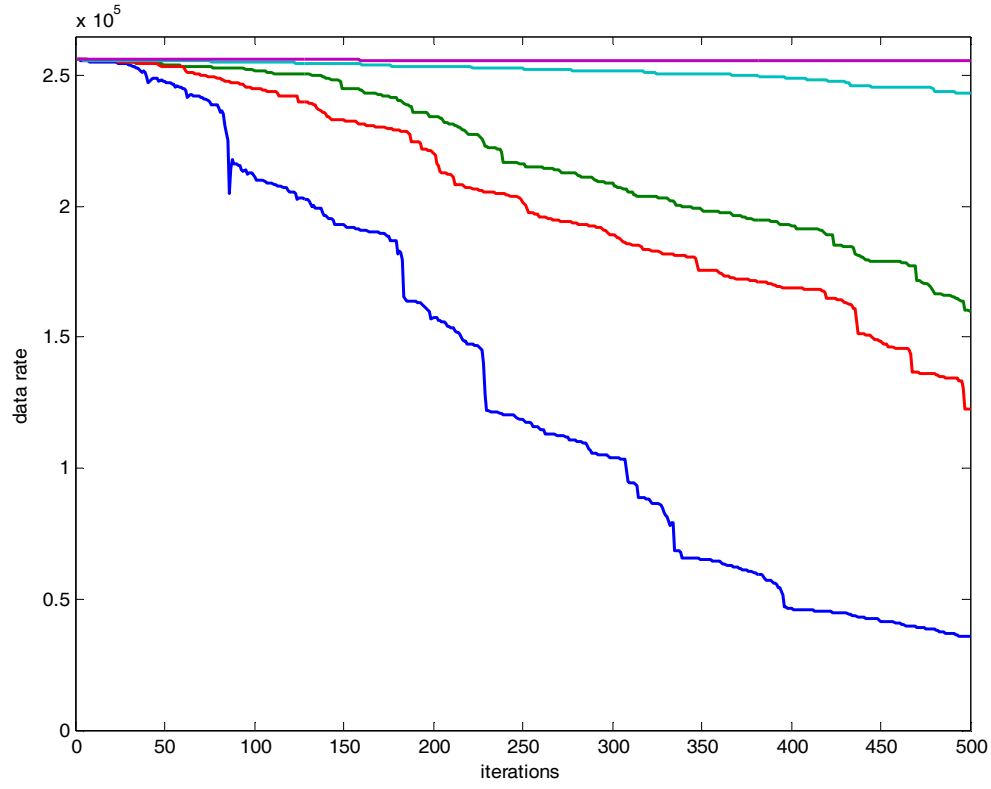

Figure 3.28. The data rates of five users (with different colors) using minimum variance power and rate control algorithm with dynamical channel.

CHAPTER FOUR

SMART ANTENNA SYSTEMS

4.1 Introduction

The receiver and transmitter antennas are one of the most critical components in the design of wireless communication systems. A good design of the antenna can relax system requirements, improve overall system performance and greatly reduce the infrastructure costs [27]. It has been demonstrated that using a beamforming antenna instead of an omni-directional antenna in the mobile communication systems can increase the system capacity and improve the overall system performance [10],[14], and [28]. This performance enhancement is due to the reduction in the interference by attenuating the interference signals which have different directions of arrivals than the desired signal direction of arrival at the receiver antenna site. This is called spatial processing because the direction of arrival is related to the mobile location. The system performance can be further improved by exploiting the delay spread of the received signals. The signal of each mobile arrives to the base station antenna in multi-path form. Each path usually has its own delay and direction of arrival. Using the smart antenna alone means that we receive (ideally) only one path and ignore the others. Joining temporal processing and spatial processing can considerably enhance the overall system performance. In the next section, an introduction of smart antennas and some adaptation techniques are given. General overview of the spatial/temporal processing is presented in Section 4.3. A new algorithm for antenna weight computation for frequency selective channels is proposed in Section 4.3. The capacity improvement from information theory point of view is presented in Section 4.4.

4.2 Smart antennas and adaptation

The joining of smart antenna and radio resource management is one of the results in this thesis. For this reason, special attention is given to the smart antenna analysis. The beamforming antenna system can be classified as a Fixed Beamforming Network, a Switched Beam Systems, and an Adaptive Antenna Systems [12]. By using an adaptive

antenna system, it is possible to achieve greater performance improvements than are attainable using a switched beam system or a fixed beamforming network [12].

A smart antenna system consists of a set of antenna elements distributed in a certain configuration. Each antenna terminal is connected through a complex weight as shown in Figure 4.1. By the smart adaptation of these weights the radiation pattern of the antenna array can be adjusted in a proper way to minimize a certain error function or to maximize a certain reward function. This adaptation is performed using an adaptive algorithm. Many adaptive algorithms have been published in the literature [11], [12], [15], [16] and [17].

The distance between the antenna elements is very small compared with the distance between the array and the transmitter antenna. Therefore it is convenient to ignore the differences in the amplitude between the received signals at each antenna terminal, but the differences in the phase can not be ignored. The reason is that even for a very small time delay difference between the antenna elements, the phase differences are considerable due to the multiplication of the time delay and the carrier frequency. Next, a brief summary of smart antenna models is given. The presentation follows [12].

The phase difference $\Delta\Psi_m$ between the antenna element *m* and the reference element at the origin is given by

$$\Delta\Psi_m = \beta\Delta d_m = \beta\left(x_m\cos(\phi)\sin(\theta) + y_m\sin(\phi)\sin(\theta) + z_m\cos(\theta)\right),\ m = 1,...,M, \qquad (4.1)$$

where (θ,ϕ) are the elevation angle and the azimuth angle, respectively, β is the phase propagation factor, and (x_m, y_m, z_m) is the Cartesian position of the antenna element *m* with respect to a reference element (assumed to be at the origin).

The output signal *z*(*t*) can be represented as

$$z(t) = \sum_{k=1}^{M} w_k u_k(t), \qquad (4.2)$$

or in a more compact form as

$$z(t) = \mathbf{w}^H\mathbf{u}(t), \qquad (4.3)$$

where $\mathbf{w} = [w_1 \ \cdots \ w_M]^H$ is the weight vector, the superscript H represents the Hermitian transpose, and $\mathbf{u}(t) = [u_1(t)\cdots u_M(t)]^T$ is the received signal vector. The phase differences between the signals at each antenna terminal depend on the direction of arrival

(DoA) of each signal. It is convenient to take the first element as a reference element so that $\Delta\Psi_1 = 0$. The input signal at each antenna terminal is the convolution between the transmitted signal and the channel impulse response

$$u_{ij}(\tau,t) = s_i(t) * h_{ij}(\tau,t), \quad i = 1,..., Q, \quad j = 1, ..., M, \tag{4.4}$$

where the star indicates the convolution operation, $s_i(t)$ is the transmitted signal from user i, and h_{ij} is the impulse response of the channel between user (mobile station) i and antenna element j at the base station, Q is the number of MS, and u_{ij} is the received signal from user i at antenna terminal j of the BS .

The channel between the mobile station and the base station can be modeled using the Vector Channel Impulse Response (VCIP) as

$$\mathbf{h}_i(\tau,t) = \sum_{l=1}^{B_i} \mathbf{a}_i(\theta_l,\phi_l)\alpha_{il}(t)\delta(t-\tau_l), \quad i = 1,..., Q \tag{4.5}$$

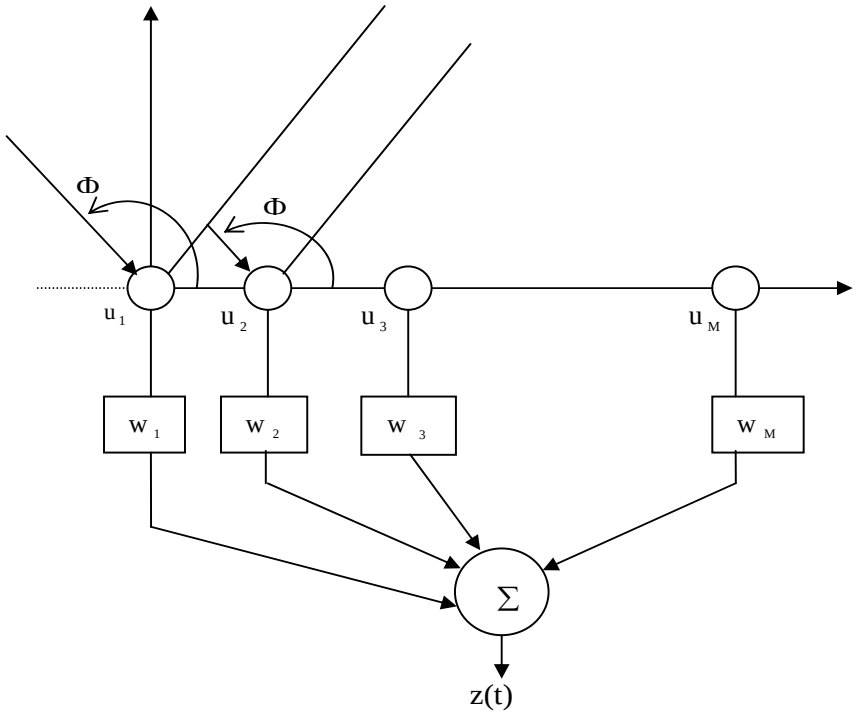

Figure 4.1

where $\mathbf{a}_i(\theta_1, \phi_1)$ is the steering vector of the MS *i*, and it is given by

$$\mathbf{a}_i(\theta_l, \phi_l) = \left[1 \;\; \exp\left(-\Delta\Psi_2(\theta_l, \phi_l)\right) \cdots \exp\left(-\Delta\Psi_M(\theta_l, \phi_l)\right)\right]', \quad i = 1, \ldots, Q, \tag{4.6}$$

$\Delta\Psi_m$ is given by (4.1), the subscript l represents the number of path, $\mathbf{h}_i$ is the channel impulse response vector and τ_1 is the time delay of the signal of user i to the base station through path l. It is assumed also that there are B_i paths for the signal of user i . $\alpha_{il}(t)$ is the complex channel gain and it is given by

$$\alpha_{il}(t) = \sqrt{\rho_{il}} \exp\left(j\left(2\pi f_{il} t + \varphi_{il}\right)\right), \quad i = 1, \ldots, Q, \tag{4.7}$$

where ρ_{il} is the absolute channel gain given by

$$\rho_{il} \approx \frac{A_{il}}{d_{il}^{\eta_{il}}}, \quad i = 1, \ldots, Q, \tag{4.8}$$

Here A_{il} is the log-normal shadowing effect for path *l* of user *i* , d_{il} is the distance between the base station and user *i* through path *l*, η_{il} is the path loss exponent for user *i* through path *l*, f_{il} is the Doppler shift, and φ_{il} is the phase offset.

The received signal of user *i* at antenna terminal *j* can be described as

$$\begin{aligned} u_{ij}(t) &= s_i(t) * \sum_{l=1}^{B_i} \exp(-j\Delta\Psi_{jl}) \sqrt{\rho_{il}} \exp\left(j\left(2\pi f_{il} t + \varphi_{il}\right)\right) \delta(t - \tau_l) + n_j(t) \\ &= \sum_{l=1}^{B_i} \exp(-j\Delta\Psi_{jl}) \sqrt{\rho_{il}} \exp\left(j\left(2\pi f_{il} t + \varphi_{il}\right)\right) s_i(t - \tau_l) + n_j(t) \end{aligned} \tag{4.9}$$

where $n_j(t)$ is an additive noise at antenna terminal *j*.

Equation (4.9) can be rewritten in a more compact form:

$$\mathbf{u}_i(t) = \mathbf{a}_i \boldsymbol{\alpha}_i(t) \mathbf{s}_i(t) + \mathbf{n}(t), \quad i = 1, \ldots, Q \tag{4.10}$$

where

$$\mathbf{a}_i = \begin{bmatrix} \exp\left(-j\Delta\Psi_{11}\right) & \cdots & \exp\left(-j\Delta\Psi_{1B_i}\right) \\ \vdots & \cdots & \vdots \\ \exp\left(-j\Delta\Psi_{M1}\right) & \cdots & \exp\left(-j\Delta\Psi_{MB_i}\right) \end{bmatrix}, \qquad i = 1, \ldots, Q \tag{4.11}$$

is the steering matrix,

$$\boldsymbol{\alpha}_i(t) = diag\left(\sqrt{\rho_{il}}\exp\left(j\left(2\pi f_{il}t + \varphi_{il}\right)\right)\right)$$

$$= \begin{bmatrix} \sqrt{\rho_{i1}}\exp\left(j\left(2\pi f_{i1}t + \varphi_{1l}\right)\right) & 0 & 0 \\ \vdots & \ddots & \vdots \\ 0 & 0 & \sqrt{\rho_{iB_i}}\exp\left(j\left(2\pi f_{iB_i}t + \varphi_{iB_i}\right)\right) \end{bmatrix} \tag{4.12}$$

and the transmitted signal vector $\mathbf{s}_i(t) = \left[s_i(t-\tau_1) \quad \cdots \quad s_i\left(t-\tau_{B_i}\right)\right]'$, $i = 1,..., Q$.

The total received signal then becomes from (4.10)

$$\mathbf{u} = \sum_{i=1}^{Q}\mathbf{u}_i = \sum_{i=1}^{Q}\mathbf{a}_i\boldsymbol{\alpha}_i\mathbf{s}_i + \mathbf{n} \tag{4.13}$$

The output signal of receiver i (which is used to receive the signal from transmitter i) is

$$z_i(t) = \mathbf{w}_i^H\mathbf{a}_i\boldsymbol{\alpha}_i(t)\mathbf{s}_i(t) + \mathbf{w}_i^H\sum_{\substack{k=1 \\ k\neq i}}^{Q}\mathbf{a}_k\boldsymbol{\alpha}_k(t)\mathbf{s}_k(t) + \mathbf{w}_i^H\mathbf{n}(t), \tag{4.14}$$

Now the problem can be stated as follows: What is the optimum weight vector $\mathbf{w}_i$ to enhance the performance of user i? Note that the additive white noise $\mathbf{n}(t)$ can not be considerably affected by adapting the antenna weights because it is not directive. The second term of (4.14) represents the interference from other users. This term can be minimized by the proper selection of the weight vector.

Generally the weights should be adjusted to minimize (or reduce) the interference from other users, or equivalently to maximize the SINR for the user. Next we will present different commonly used algorithms for the weight computation.

4.2.1 Conventional Beamformer

In the conventional beamformer the weights are selected to be the complex conjugates of the steering vector, i.e., for one path case the weight vector is selected as

$$\mathbf{w}_i^H\mathbf{a}_i = c, \qquad i = 1,..., Q, \tag{4.15}$$

where c is a positive, and real number. This method does not take into consideration the interference of other users. The SINR at the array output can be derived by substituting (4.15) into (4.14) and setting the second term equal to zero. The average signal to noise power (the noise is assumed to be uncorrelated) becomes

$$SINR_i = \frac{c^2 \alpha_i^2 P_i}{\delta_N^2}, \qquad i = 1,...,Q \tag{4.16}$$

where P_i is the average signal power, δ_N^2 is the noise variance. Using the conventional beamformer gives some gain for SINR depending on the number of antenna elements. The main advantage of this method is its simplicity. It provides the maximum output SINR, if the noise is uncorrelated and there is no directional jammer. However, it is not wise to use this method in mobile communication systems, where there are many users sharing the same frequency (for WCDMA) and therefore many unintentional jammers.

4.2.2 Null-Steering Beamformer

This technique is more effective than the conventional beamformer in minimizing the signals of strong directional jammers. If we know the DoA of all users in the cell, the problem can be solved by finding the weights deterministically. If there are *Q* users in the cell, and the weights are calculated for user i, then the desired weight vector is the solution of the following system of linear equations (see (4.14))

$$\begin{aligned} &\mathbf{w}_i^H \mathbf{a}_i = 1, \text{ and} \\ &\mathbf{w}_i^H \mathbf{a}_k = 0, \quad \forall k \in \{1,2,..,Q\} \text{ and } k \neq i, i = 1,...,Q \end{aligned} \tag{4.17}$$

The above system of linear equations can be solved exactly, if the number of users *Q* is less than or equal to the number of antenna elements M. Generally the problem can be solved as

$$\mathbf{w}_i^H = D'\left(\mathbf{A}^H \mathbf{A}\right)^{-1} \mathbf{A}^H, \qquad i = 1,..., Q, \tag{4.18}$$

where $D = \begin{bmatrix} 0 & \cdots & 1 & 0 & \cdots & 0 \end{bmatrix}'$; 1 *is at the* i^{th} *element, and* $\mathbf{A} = \begin{bmatrix} \mathbf{a}_1 & \cdots & \mathbf{a}_Q \end{bmatrix}$

The main advantage of the null-steering beamformer is its ability to null even strong directed interferences. The disadvantages are: a) DoA of all users should be known at the receiver, b) The number of antenna elements should be comparable with the number of users. If the number of users is much more than the number of antenna elements, then the method becomes less effective and the weights approach zero.

4.2.3 Minimum Variance Distortionless Response (MVDR) Beamformer

The MVDR beamformer overcomes the disadvantages of the null steering beamformer. In this method only the steering vector of the desired user is needed. The concept of MVDR

beamformer is based on minimizing the average output array power while maintaining unity response in the looking-direction. The problem can be described mathematically as follows:

$$\hat{\mathbf{w}}_i = \arg\min E[|z(t)|^2], \qquad i = 1,...,Q \tag{4.19}$$

subject to

$$\mathbf{w}_i^H \mathbf{a}_i = 1, \tag{4.20}$$

where z(t) is given by (4.3) and E[.] is the expectation operator. The weights obtained by solving the optimization problem given in (4.19)-(4.20) will minimize the total noise, including interferences and uncorrelated noise. So MVDR beamformer maximizes the output SINR [11].

Substituting (4.3) into (4.19) the problem can be stated as follows:

Find the minimum of

$$\mathbf{w}_i \mathbf{R}_{uu} \mathbf{w}_i^H , \qquad i = 1,..., Q \tag{4.21}$$

subject to

$$\mathbf{w}_i^H \mathbf{a}_i = 1. \tag{4.22}$$

The autocovariance of the received signal **u** can be computed by

$$\mathbf{R}_{uu} = E[\mathbf{u}\mathbf{u}^H]. \tag{4.23}$$

The MVDR problem can be solved using Lagrange multiplier method to obtain

$$\hat{\mathbf{w}}_i = \frac{\mathbf{R}_{uu}^{-1}\mathbf{a}_i}{\mathbf{a}_i^H \mathbf{R}_{uu}^{-1}\mathbf{a}_i}, \qquad i = 1,..., Q \tag{4.24}$$

To find the optimum weights using the MVDR method, the DoA of the desired user is needed. Since in mobile communication systems, the users are moving, and the characteristics of the channel are time varying, an adaptive algorithm is needed to update the weights for the varying conditions. The sample matrix inversion (SMI) method can be used in adaptive beamforming algorithms. The weights are updated at every k^{th} iteration using the K-sample covariance matrix:

$$\hat{\mathbf{R}}_K = \frac{1}{K}\sum_{j=1}^{K} \mathbf{u}(t_j)\mathbf{u}(t_j)^H \tag{4.25}$$

where $\hat{\mathbf{R}}_K$ is the unstructured maximum likelihood estimate of $\mathbf{R}_{uu}$. It converges to

$\mathbf{R}_{uu}$ as K$\to\infty$ under the ergodic assumption. The SMI based adaptive MVDR weights are given by [29]:

$$\hat{\mathbf{w}}_i = \frac{\hat{\mathbf{R}}_K^{-1}\mathbf{a}_i}{\mathbf{a}_i^H\hat{\mathbf{R}}_K^{-1}\mathbf{a}_i}, \quad i = 1,..., Q, \tag{4.26}$$

which has the same form as in (4.24).

4.2.4 Minimum Mean Square Error (MMSE) Beamformer

If the transmitter sends a reference signal known to the receiver (like pilot signal), then this signal could be used to calculate the optimum weights even if there is no information about the DoA or about the channel characteristics. One of the methods which use a reference signal is the MMSE beamformer. The MMSE is based on finding the optimum weights which minimize the mean square error

$$\hat{\mathbf{w}}_i = \arg\min E\left[\left|\mathbf{w}_i^H\mathbf{u}(t) - d_i(t)\right|^2\right], \qquad i = 1,..., Q, \tag{4.27}$$

where $d_i(t)$ is the training sequence for user i at time t. The optimum weights can be obtained by setting the gradient of the cost function with respect to $\mathbf{w}_i$ equal to zero; thus one obtains the Wiener-Hopf equation for the optimum weights [19]:

$$\hat{\mathbf{w}}_i = \mathbf{R}_{uu}^{-1}\mathbf{P}, \qquad i = 1,..., Q \tag{4.28}$$

where $\mathbf{R}$ is computed as indicated in (4.23) and

$$\mathbf{P} = E\left[\mathbf{u}d_i^*\right], \qquad i = 1,..., Q \tag{4.29}$$

A recursive form of (4.28) is given in [11], [19] as:

$$\mathbf{w}_i(t+1) = \mathbf{w}_i(t) - \mu\left(E[\mathbf{u}(t)\mathbf{u}^H(t)]\mathbf{w}_i(t) - E[\mathbf{u}(t)d_i^*(t)]\right) \tag{4.30}$$

where constant μ is a positive scalar (gradient step size) that controls the convergence characteristic of the algorithm, that is, how fast and how close the estimated weights approach the optimal weights.

If we assume that the signals are ergodic, then the adaptive algorithm can be approximated as

$$\mathbf{w}_i(t+1) = \mathbf{w}_i(t) - \mu\mathbf{u}(t)e_i(t), \qquad t = 0,1,..., \qquad i = 1,..., Q \tag{4.31}$$

$$e_i(t) = \mathbf{w}_i^H(t)\mathbf{u}(t) - d_i^*(t). \tag{4.32}$$

Here $e_i(t)$ is the instantaneous error between the array output and the desired response. The main disadvantage of the adaptive LMS algorithm and its different versions is its slow convergence speed [19]. This is an essential problem in mobile communication due to the nature of fast varying channel characteristics. The convergence of the LMS algorithm depends on the eigenvalue distribution of the correlation matrix [19], [24].

4.2.5 Recursive Least Square (RLS) Algorithm

The RLS algorithm is more efficient (in many situations) than the LMS algorithm. In [29], the RLS algorithm has been proposed for weight adaptation in the uplink of CDMA mobile communication system.

The RLS algorithm minimizes the cumulative square error [11]

$$\mathbf{w}_n = \arg \quad \min \left\{ \sum_{t=0}^{n} \mu_t \left| e(t) \right|^2 \right\}, \tag{4.33}$$

where the error $e(t)$ is the difference between the reference signal and the actual array output. The weight updating algorithm is [19]:

$$\mathbf{w}(t) = \mathbf{w}(t-1) + \mathbf{K}(t) e(t). \tag{4.34}$$

Here $\mathbf{K}(t)$ is the gain update and it is given by

$$\mathbf{K}(t) = \frac{\mathbf{P}(t-1)\mathbf{u}(t)}{\frac{1}{\mu_t} + \mathbf{u}^H(t)\mathbf{P}(t-1)\mathbf{u}(t)}, \tag{4.35}$$

where $\mathbf{P}(t) = \mathbf{R}^{-1}(t)$ is solved recursively as

$$\mathbf{P}(t) = \mathbf{P}(t-1) - \frac{\mathbf{P}(t-1)\mathbf{u}(t)\mathbf{u}^H(t)\mathbf{P}(t-1)}{\frac{1}{\mu_t} + \mathbf{u}^H(t)\mathbf{P}(t-1)\mathbf{u}(t)}. \tag{4.36}$$

μ_t is a real scalar, it is called forgetting factor. There are different updating algorithms for the forgetting factor such as:

$$\mu_t = \alpha \mu_{t-1} + (1-\alpha) \qquad 0 < \alpha < 1 \tag{4.37}$$

so that the old samples are deemphasized.

4.2.6 Subspace Methods for Beamforming

In the subspace technique the structure of the signals at the array input is exploited for beamforming applications [17], [31], [32] and [34]. If there are Q users in the cell then the sum of received signals at an M antenna element array (see (4.13)) is

$$\mathbf{u} = \sum_{i=1}^{Q} \mathbf{u}_i = \sum_{i=1}^{Q} \mathbf{a}_i \boldsymbol{\alpha}_i \mathbf{s}_i + \mathbf{n} \,. \tag{4.38}$$

Since each user i has B_i different paths which are assumed to come from different directions of arrivals (DoA), (4.38) can be written in a more compact form using matrix vector notation:

$$\mathbf{u} = \mathbf{AS} + \mathbf{n} \,, \tag{4.39}$$

where $\mathbf{A} = [\mathbf{a}_1\boldsymbol{\alpha}_1 \;\vdots\; \mathbf{a}_2\boldsymbol{\alpha}_2 \;\vdots\; \cdots \;\vdots\; \mathbf{a}_Q\boldsymbol{\alpha}_Q]$ is an MxD dimensional matrix, $\mathbf{a}_i$ an MxB_i matrix, $\mathbf{S} = \left[\mathbf{s}_1 \vdots \mathbf{s}_2 \vdots \cdots \vdots \mathbf{s}_Q\right]'$ an B_ixT matrix, $D = \sum_{i=1}^{Q} B_i$ and T = number of samples.

If there is only one single path for each user, then the dimension of matrix **A** will be $M \times Q$ and the dimension of matrix S will be $Q \times T$, where Q in this case is the number of users or in a more general terms, the number of uncorrelated signals.

Using the data model of (4.39), the input covariance matrix $\mathbf{R}_{uu}$ can be expressed as

$$\mathbf{R}_{uu} = E[\mathbf{u}\mathbf{u}^H] = \mathbf{A}E[\mathbf{S}\mathbf{S}^H]\mathbf{A}^H + E[\mathbf{n}\mathbf{n}^H] \tag{4.40}$$

or

$$\mathbf{R}_{uu} = \mathbf{A}\mathbf{R}_{ss}\mathbf{A}^H + \delta_n^2\mathbf{I}, \tag{4.41}$$

where $\mathbf{R}_{ss} = E[\mathbf{S}\mathbf{S}^H]$ is the signal correlation matrix.

The matrix $\mathbf{R}_{uu}$ can be decomposed, for example by singular value decomposition, to obtain

$$\mathbf{R}_{uu} = \mathbf{W}\boldsymbol{\Sigma}V' \tag{4.42}$$

where **W** and **V** are M×M orthogonal matrices, and $\boldsymbol{\Sigma} = diag\left(\sigma_1, \sigma_2, \cdots, \sigma_M\right)$ is a diagonal matrix with $\sigma_i \geq 0$. The nonnegative numbers $\{\sigma_i\}$ are called the singular values of $\mathbf{R}_{uu}$ and $\sigma_1 \geq \sigma_2 \geq \cdots \geq \sigma_M$. If $\mathbf{R}_{uu}$ has rank r then $\mathbf{R}_{uu}$ has exactly r strictly positive singular values so that $\sigma_r > 0$ and $\sigma_{r+1} = \sigma_{r+2} = \cdots = \sigma_M = 0$.

Assume that all incident signals are not highly correlated and their number is less than the number of antenna elements, i.e., $M>D$. Then by examining the singular values of $\mathbf{R}_{uu}$ we will find D singular values with considerable values. The other (M-D) singular values have very small values. These small values represent the variance of the background noise.

The received signal space can be decomposed into two subspaces. The first subspace that is spanned by the eigenvectors associated with the first D eigenvalues is called the *signal subspace*. The second subspace that is spanned by the eigenvectors associated with the last (M-D) eigenvalues is called the *noise subspace*. It has been proven that the noise subspace is orthogonal to the steering vectors [12]. This fact can be exploited in the estimation of the DoA of the signals. When the DoA of the interference signals is estimated it can be cancelled out by making the weight vector orthogonal to the interference subspace [34].

Many different algorithms exploit the eigenstructure of the covariance matrix of the received signal [17], [11] and [34]. The main disadvantage of the beamformers that are based on the Eigen Decomposition (ED) methods is that the number of users is limited by the number of antenna elements. Therefore, they are not suitable to commercial CDMA applications, which must support a large number of users [35]. There are some techniques used to overcome this limitation. In [17] the fact that in CDMA systems the desired user power is much larger than that of each interference power due to the processing gain of the CDMA demodulation has been exploited. They have used the eigenvector corresponding to the largest eigenvalue as the optimum weight of the array. The main advantage of this method is that it can be used with any number of users, if the SINR of the desired user is very high [17].

4.2.7 Adaptive Beamforming using Kalman Filter

The constrained optimization problem presented in equations (4.21)-(4.22) can be solved using Kalman filtering approach [22]. Equation (4.19) can be rewritten as follows:

$$\min \mathrm{E}[\left|0\text{-}z(t)\right|^2] \tag{4.43}$$

subject to

$$\mathbf{w}_i^H \mathbf{a}_i = 1 \tag{4.44}$$

To incorporate Kalman filtering, the measurement equation can be written as

$$\begin{bmatrix} 0 \\ 1 \end{bmatrix} = \begin{bmatrix} \mathbf{u}^H(t) \\ \mathbf{a}_i^H \end{bmatrix} \mathbf{w}_i(t) + \begin{bmatrix} v_1(t) \\ v_2(t) \end{bmatrix}. \tag{4.45}$$

Here $v_1(t)$ is the residual error and $v_2(t)$ is the constraint error. These errors are assumed to be zero mean Gaussian and independent random variables. In matrix form Equation (4.45) becomes

$$\mathbf{Y} = \mathbf{B}^H(t)\mathbf{w}_i(t) + \mathbf{V}(t), \tag{4.46}$$

where $\mathbf{Y} = \begin{bmatrix} 0 \\ 1 \end{bmatrix}$, $\mathbf{B}^H(t) = \begin{bmatrix} \mathbf{u}^H(t) \\ \mathbf{a}_i^H \end{bmatrix}$ and $\mathbf{V}(t) = \begin{bmatrix} v_1(t) \\ v_2(t) \end{bmatrix}$.

Further, the correlation matrix of **V**(t) is

$$\mathbf{Q} = \begin{bmatrix} \delta_{v_1}^2 & 0 \\ 0 & \delta_{v_2}^2 \end{bmatrix} \tag{4.47}$$

The state space model of the constrained Kalman algorithm may be written as

$$\mathbf{w}_i(t) = \mathbf{w}_i(t-1) \tag{4.48}$$

Now, we may use Kalman filter to solve equations (4.46) and (4.48) to minimize the residual error in the mean-square sense while maintaining a distortionless response along the looking direction. The discrete Kalman filter can be written as [20]:

$$\hat{\mathbf{w}}_i(t) = \hat{\mathbf{w}}_i(t-1) + \bar{\mathbf{K}}(t-1)[\mathbf{Y} - \mathbf{B}^H(t-1)\hat{\mathbf{w}}_i(t-1)]. \tag{4.49}$$

The Kalman gain $\bar{\mathbf{K}}(t)$ is given by

$$\bar{\mathbf{K}}(t) = \mathbf{G}(t-1)\mathbf{B}(t)[\mathbf{B}^H(t)\mathbf{G}(t-1)\mathbf{B}(t) + \mathbf{Q}], \tag{4.50}$$

where the filtered weight-error correlation matrix **G**(t) is

$$\mathbf{G}(t) = [\mathbf{I} - \bar{\mathbf{K}}(t)\mathbf{B}^H(t)]\mathbf{G}(t-1). \tag{4.51}$$

It has been proven that the constrained Kalman-type array processor can converge to the minimum-variance distortionless-response (MVDR) beamformer [22].

4.2.8 Least Square Despread Respread Multitarget Array (LS-DRMTA)

The algorithm proposed in [36] and [12] is based on re-spreading of the received data bits. The re-spread signal is compared with the received signal (before the despreading), and the difference is used as an error signal. This error is minimized by adjusting the antenna weights. Figure 4.2 shows the block diagram of the LS-DRMTA for user *i*.

The re-spread signal is given by

$$r_i(t) = b_{in} C_i(t - \tau_i) \qquad (\text{n-1})T_b \le t < nT_b, \quad i = 1, ..., Q, \tag{4.52}$$

where $C_i(t)$ is the spreading code for user *i* and b_{in} is the n^{th} received data for user *i*.

The LS-DRMTA is used to minimize an error function by adjusting the weight vector $\mathbf{w}_i$. The cost function is given by

$$F(\mathbf{W}_i) = \sum_{k=1}^{K} \left| y_i(t) - r_i(t) \right|^2 = \sum_{k=1}^{K} \left| \mathbf{w}_i^H \mathbf{x}(t) - r_i(t) \right|^2, \tag{4.53}$$

where K is the data block size and is set equal to the number of samples in one bit period in LS-DRMTA.

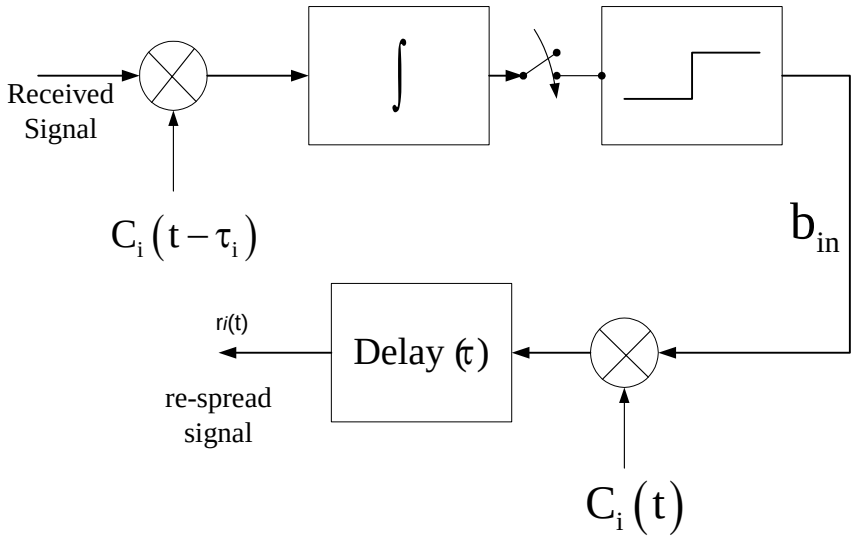

Figure 4.2. LS-DRMTA block diagram for user *i*.

4.3 Spatial-Temporal Processing

The capacity as well as the performance of the cellular communication systems can be greatly enhanced by exploiting any known characteristics of the communication link. The natural spatial distribution of the users and the access delay distribution of the signal paths are two important characteristics which can be exploited. Using the adaptive antenna array one can enhance the reception from certain direction of arrivals (DoA) and attenuate the others as has been shown in the previous section. Usually the Signal of Interest (SoI) arrives at the receiver's antennas as multi-path components, where each component has its own DoA as well as access delay. For wideband signals those multi-paths could be uncorrelated. The adaptive antenna system will attenuate the other uncorrelated paths of the SoI. This time spreading of the SoI can be exploited as well by using two different methods. The first is to use a general wideband array as shown in Figure 4.3 [12]. If the length of each tapped delay line is long enough to capture the delayed multi-path components, then the wideband array can capture power in components which arrive with different delays and recombine them [12]. The other method is to use a Rake receiver with the adaptive antenna array. The Rake receiver is capable of receiving multiple signal paths and adding them coherently using multiple fingers. Each Rake finger is time locked to a different delay to capture the multi-path components arriving with different path delays.

Combining the Rake receiver with adaptive antenna array one can exploit spatial as well as time distributions of the signals. Figure 4.4 shows the conventional way to combine a Rake receiver with adaptive antenna [12]. Any adaptive algorithm can be used to compute the optimum weight vector for each significant path which is captured by the rake fingers. The main problem of the spatial/temporal processing is the high computational cost.

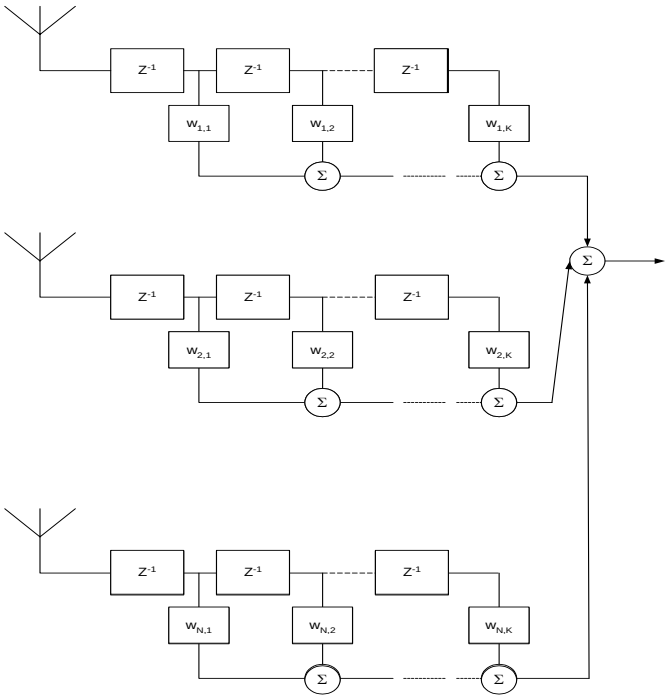

Figure 4.3. Wideband adaptive antenna system

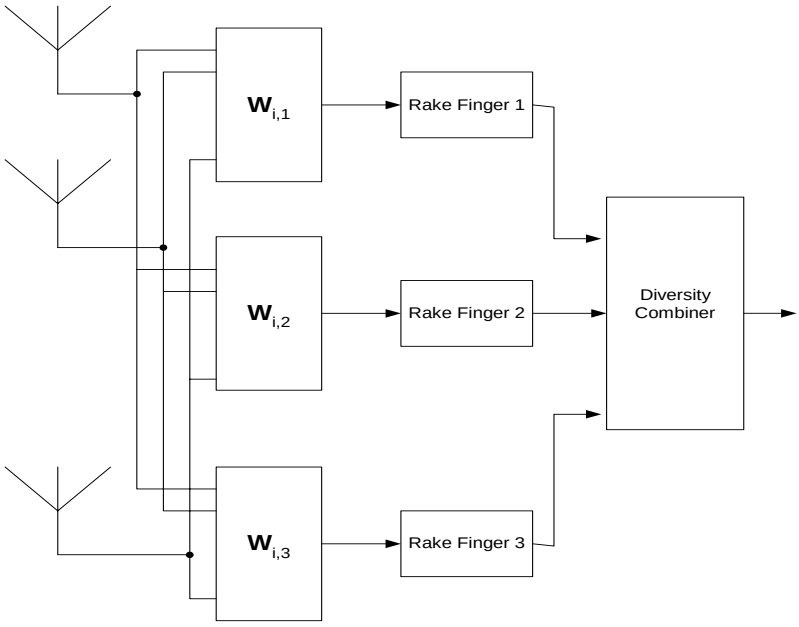

Figure 4.4. Adaptive antenna system and Rake Receiver

For example if the number of antennas is 6 and the number of rake fingers is 6, this means that 36 weights should be adapted each time. A new method is proposed next to reduce

the computational cost. There are some other techniques to reduce the computational complexities of the receivers [90].

4.3.1 General MVDR (GMVDR) Algorithm for Frequency Selective Channels

The main idea of the MVDR algorithm is to find the weight vector which minimizes the total received power except the power coming from directions of interest (4.2.3). In the MVDR techniques we need to know the DoA of the desired user's paths. There are several techniques to estimate the DoAs of users, such as MUSIC and ESPRIT methods [12]. The main idea of the GMVDR algorithm is that we compute the optimum weight vector which minimizes the total received power except the power of signals coming from all the significant paths of the SoI.

The problem can be described mathematically as follows:

Find

$$\min \ \mathrm{E}\left[\left|\mathrm{z_i}\right|^2\right], \qquad i=1,2,..,Q, \tag{4.54}$$

subject to

$$\begin{aligned} &\mathbf{w}_i^H \mathbf{a}_{i,1} = 1 \\ &\mathbf{w}_i^H \mathbf{a}_{i,2} = 1 \\ &\vdots \\ &\mathbf{w}_i^H \mathbf{a}_{i,M_i} = 1 \end{aligned} \tag{4.55}$$

where $\mathbf{a}_{i,k}$ is the steering vector of path k for user i. If we assume that the first element is the reference element then the steering vector can be defined as

$$\mathbf{a}_{i,k} = \left[1 \quad \exp(-j\Delta\Psi_{2ik}) \quad \cdots \quad \exp(-j\Delta\Psi_{Nik})\right]', \qquad i=1,...,Q \tag{4.56}$$

In the normal MVDR algorithm, we have only one equality constraint to represent the user's DoA.

Using Lagrange multiplier method, the total cost function becomes

$$C_i = E\left[\mathbf{w}_i^H \mathbf{u}\mathbf{u}^H \mathbf{w}_i\right] + \sum_{k=1}^{M_i} \gamma_k \left(\mathbf{w}_i^H \mathbf{a}_{i,k} - 1\right) \tag{4.57}$$

where γ_k is the k^{th} Lagrange multiplier factor.

Necessary conditions for minimization are

$$\frac{\partial C_i}{\partial \mathbf{w}_i} = 2\mathbf{w}_i^H \mathbf{R}_{uu} + \sum_{k=1}^{M_i} \gamma_k \mathbf{a}_{i,k}^H = 0, \qquad i = 1,...,Q\,, \tag{4.58}$$

$$\frac{\partial C_i}{\partial \gamma_j} = \mathbf{w}_i^H \mathbf{a}_{i,j}^H - 1 = 0, \qquad j = 1,2,..,M_i\,, \tag{4.59}$$

where $\mathbf{R}_{uu} = E\left[\mathbf{u}\mathbf{u}^H\right]$.

From (4.58) the optimum weight vector is obtained as

$$\mathbf{w}_i^H = -\frac{1}{2}\sum_{k=1}^{M_i} \gamma_k \mathbf{a}_{i,k}^H \mathbf{R}_{uu}^{-1}, \qquad i = 1,...,Q \tag{4.60}$$

Now substituting (4.60) in (4.59) for all *j* results in

$$\begin{aligned}
&\mathbf{a}_{i,1}^H \mathbf{R}_{uu}^{-1}\mathbf{a}_{i,1}\gamma_1 + \mathbf{a}_{i,2}^H \mathbf{R}_{uu}^{-1}\mathbf{a}_{i,1}\gamma_2 + \cdots + \mathbf{a}_{i,M_i}^H \mathbf{R}_{uu}^{-1}\mathbf{a}_{i,1}\gamma_{M_i} = -2,\\
&\mathbf{a}_{i,1}^H \mathbf{R}_{uu}^{-1}\mathbf{a}_{i,2}\gamma_1 + \mathbf{a}_{i,2}^H \mathbf{R}_{uu}^{-1}\mathbf{a}_{i,2}\gamma_2 + \cdots + \mathbf{a}_{i,M_i}^H \mathbf{R}_{uu}^{-1}\mathbf{a}_{i,2}\gamma_{M_i} = -2,\\
&\vdots\\
&\mathbf{a}_{i,1}^H \mathbf{R}_{uu}^{-1}\mathbf{a}_{i,M_i}\gamma_1 + \mathbf{a}_{i,2}^H \mathbf{R}_{uu}^{-1}\mathbf{a}_{i,M_i}\gamma_2 + \cdots + \mathbf{a}_{i,M_i}^H \mathbf{R}_{uu}^{-1}\mathbf{a}_{i,M_i}\gamma_{M_i} = -2.
\end{aligned} \tag{4.61}$$

The optimum Lagrange multiplier factors can be obtained by solving the system of linear equations given in (4.61)

In the matrix form, (4.61) can be represented as

$$\mathbf{A}_i \mathbf{\Gamma}_i = -2\mathbf{1}, \qquad i = 1,...,Q \tag{4.62}$$

where

$$\mathbf{A}_i = \begin{bmatrix}
\mathbf{a}_{i,1}^H \mathbf{R}_{uu}^{-1}\mathbf{a}_{i,1} & \mathbf{a}_{i,2}^H \mathbf{R}_{uu}^{-1}\mathbf{a}_{i,1} & \cdots & \mathbf{a}_{i,M_i}^H \mathbf{R}_{uu}^{-1}\mathbf{a}_{i,1}\\
\mathbf{a}_{i,1}^H \mathbf{R}_{uu}^{-1}\mathbf{a}_{i,2} & \mathbf{a}_{i,2}^H \mathbf{R}_{uu}^{-1}\mathbf{a}_{i,2} & \cdots & \mathbf{a}_{i,M_i}^H \mathbf{R}_{uu}^{-1}\mathbf{a}_{i,2}\\
\vdots & & & \vdots\\
\mathbf{a}_{i,1}^H \mathbf{R}_{uu}^{-1}\mathbf{a}_{i,M_i} & \cdots & \cdots & \mathbf{a}_{i,M_i}^H \mathbf{R}_{uu}^{-1}\mathbf{a}_{i,M_i}
\end{bmatrix} \tag{4.63}$$

$$\mathbf{\Gamma}_i = \left[\gamma_1 \gamma_2 \cdots \gamma_{M_i}\right]' \tag{4.64}$$

$\mathbf{1} = \left[11\cdots 1\right]'$ is M×1 vector of ones

From (4.62), the optimum Lagrange factors become

$$\mathbf{\Gamma}_i = -2\mathbf{A}_i^{-1}\mathbf{1} \tag{4.65}$$

Equation (4.60) can be rewritten as

$$\mathbf{w}_i^H = -\frac{1}{2}\mathbf{\Gamma}'\hat{\mathbf{a}}_i \mathbf{R}_{uu}^{-1}, \qquad i = 1,...,Q \tag{4.66}$$

where

$$\hat{\mathbf{a}}_i = \begin{bmatrix} \mathbf{a}_{i,1}^H \\ \vdots \\ \mathbf{a}_{i,M_i}^H \end{bmatrix} \tag{4.67}$$

Substituting (4.65) into (4.66) gives

$$\mathbf{w}_i^H = \mathbf{1}'\mathbf{A}_i^{-1}\hat{\mathbf{a}}_i\mathbf{R}_{uu}^{-1}, \qquad i = 1,...,Q \tag{4.68}$$

This result could be compared with the conventional (single path) MVDR algorithm given by (4.24)

$$\hat{\mathbf{w}}_i^H = \frac{\mathbf{a}_i^H\mathbf{R}_{uu}^{-1}}{\mathbf{a}_i^H\mathbf{R}_{uu}^{-1}\mathbf{a}_i}, \qquad i = 1,...,Q. \tag{4.69}$$

It is clear that algorithm (4.69) is a special case (one path) of (4.68).

From (4.63) it is clear that $\mathbf{A}_i$ can be decomposed as

$$\mathbf{A}_i = \hat{\mathbf{a}}_i\mathbf{R}_{uu}^{-1}\hat{\mathbf{a}}_i^H, \qquad i = 1,...,Q \tag{4.70}$$

so that in order to get a non-singular matrix, the number of antenna elements should be greater than or equal to the number of Rake fingers. It should be noted that the GMVDR algorithm is effective only in the frequency selective channels.

4.4 Information-Theoretic analysis of Uplink Beamforming

The concepts of smart antennas and weight adaptation techniques are presented in the previous sections. In this section, the effect of using multiple antennas on the communication systems will be analyzed from the information-theoretic point of view. An upper bound of the system capacity for reliable communication will be determined using information theory. Certain concepts of information theory will be covered next

4.4.1 Some information theory concepts [24], [47], [50] and [51]

- The information content in a discrete event s_k is defined as

$$I(s_k) = \log_2\left(\frac{1}{P_k}\right), \tag{4.71}$$

  where P_k is the probability of occurrence.

- The Entropy is the mean of the information content over all the possible outcomes K as

$$H(\varphi) = E[I(s_k)] = \sum_{k=0}^{K-1} P_k \log_2\left(\frac{1}{P_k}\right), \tag{4.72}$$

where φ is the set of all possible outcomes. The entropy is a measure of the average information per source symbol.

- A simple communication system is represented as

$$Y=X+N, \tag{4.73}$$

where X is a discrete channel input, Y is the measured channel output, and N is additive noise to the channel. We can define the conditional entropy H(X\Y) as the amount of uncertainty remaining about the channel input after the channel output has been observed:

$$H(X \setminus Y) = \sum_{k=0}^{K-1} H(X \setminus Y = y_k) P(y_k) = \sum_{k=0}^{K-1}\sum_{j=0}^{J-1} P(x_j \setminus y_k) P(y_k) \log_2\left(\frac{1}{P(x_j \setminus y_k)}\right). \tag{4.74}$$

where $P(x_j \setminus y_k)$ is the probability of x_j conditioned on y_k.

- The mutual information I(X;Y) represents the uncertainty about the channel input that is resolved by observing the channel output. It is defined as

$$I(X;Y) = H(X) - H(X \setminus Y). \tag{4.75}$$

Substituting (4.72) and (4.74) into (4.75) gives

$$I(X;Y) = \sum_{j=0}^{J-1} P(x_j) \log_2\left(\frac{1}{P(x_j)}\right) - \sum_{k=0}^{K-1}\sum_{j=0}^{J-1} P(x_j \setminus y_k) P(y_k) \log_2\left(\frac{1}{P(x_j \setminus y_k)}\right). \tag{4.76}$$

It is clear that I(X;Y) =0 if and only if the input and output symbols of the channel are statistically independent (i.e. $P(x_j\setminus y_k)=P(x_j)$).

- The channel capacity has been defined as the maximum mutual information I(X;Y) as

$$C = \max_{\{P(x_j)\}} I(X;Y) \tag{4.77}$$

- The differential entropy of a continuous random variable X with a probability density function (pdf) $f_X(x)$ is

$$h(x) = \int_{-\infty}^{\infty} f_X(x) \log_2\left(\frac{1}{f_X(x)}\right) dx. \tag{4.78}$$

Recall that pdf of a Gaussian distributed random variable, $x \sim N(\mu_x, \delta^2_x)$, is

$$f_X(x)=\frac{1}{\sqrt{2\pi}\delta_x}\exp\left(\frac{-(x-\mu_x)^2}{2\delta_x^2}\right). \tag{4.79}$$

By substituting equation (4.79) into (4.78) we get

$$h(x)=\log_2\left(\sqrt{2\pi}\delta_x\right)+\frac{1}{2}\log_2(e)=\frac{1}{2}\log_2\left(2\pi\delta_x^2 e\right). \tag{4.80}$$

It is not difficult to prove that for any arbitrary *pdf* $f_y(y)$ with the same mean and variance, i.e., $\mu_y=\mu_x;\delta_y^2=\delta_x^2$, one has

$$h(y)\le\frac{1}{2}\log_2\left(2\pi e\delta_x^2\right). \tag{4.81}$$

The equality holds, when x=y. Equation (4.81) implies that for a finite variance δ_x^2, the Gaussian random variable has the largest differential entropy.

- The pdf of a multivariate Gaussian distribution is defined as

$$f_{\mathbf{X}}(\mathbf{x})=\frac{1}{(2\pi)^{n/2}|\mathbf{M}|}\exp\left(-\frac{1}{2}(\mathbf{x}-\mathbf{m}_x)'\mathbf{M}^{-1}(\mathbf{x}-\mathbf{m}_x)\right) \tag{4.82}$$

where $\mathbf{x}=[x_1,\ldots,x_n]'$, $\mathbf{M}$ is an n×n covariance matrix with elements $\{\rho_{ij}\}$ with $\rho_{ij}=E[(x_i-m_i)(x_j-m_j)]$, and $\mathbf{m}_x=[\mu_{x1},\mu_{x2,..},\mu_{xn}]'$ is the column vector of mean values.

- The differential entropy of a multivariate Gaussian distribution is

$$h(\mathbf{x})=-\int_{x_1}\int_{x_2}\cdots\int_{x_n}\frac{1}{(2\pi)^{n/2}|\mathbf{M}|^{1/2}}\exp\left(-\frac{1}{2}(\mathbf{x}-\mathbf{m}_x)'\mathbf{M}^{-1}(\mathbf{x}-\mathbf{m}_x)\right)\left[-\log_2\left((2\pi)^{n/2}|\mathbf{M}|^{1/2}\right)-\frac{1}{2}(\mathbf{x}-\mathbf{m}_x)'\mathbf{M}^{-1}(\mathbf{x}-\mathbf{m}_x)\log_2(e)\right]dx_1\cdots dx_n \tag{4.83}$$

Analogously to (4.80)

$$h(\mathbf{x})=\frac{1}{2}\log_2\left((2\pi e)^n|\mathbf{M}|\right). \tag{4.84}$$

- The information capacity of a channel is defined as the maximum of the mutual information I(X,Y) that satisfies the power constraints, i.e.,

$$C=\max_{f_{X_k}(x)}[I(X_k;Y_k):E[X_k^2]=P_x], \tag{4.85}$$

$$I(X_k;Y_k)=h(Y_k)-h(N_k),\qquad k=1,\ldots,K \quad . \tag{4.86}$$

As we have seen the maximum of I(X;Y) over the input pdfs f(x) is obtained when {Xi} are statistically independent zero-mean Gaussian random variables [24], i.e.,

$$f_x(x_k) = \frac{1}{\sqrt{2\pi}P_{x_i}} \exp\left(-\frac{x_k^2}{2P_{x_i}}\right), \tag{4.87}$$

where P_{x_i} is the average power of signal x_i.

From equations (4.72), (4.77) and (4.78), the channel capacity can be obtained as

$$C = \frac{1}{2}\log_2\left(2\pi\left(P_x + \delta_N^2\right)e\right) - \frac{1}{2}\log_2\left(2\pi\delta_N^2 e\right) = \frac{1}{2}\log_2\left(1 + \frac{P_x}{\delta_N^2}\right), \tag{4.88}$$

where δ_N^2 is the average noise power.

In other terms we may rewrite (4.88) as

$$C = \tfrac{1}{2}\log_2\left(1 + SINR\right) \tag{4.89}$$

where SINR is the signal to interference and noise ratio.

4.4.2 Capacity of a channel with a single user and multi-receivers [51]

Studying the capacity of a channel with a single user and multi-receivers will lead to a general formulation for the capacity of more complicated scenarios. Assume a single user transmitting his signal, which is received by multi-receivers (or multi-antennas). Suppose the received signal is presented as the vector $\mathbf{x}=[x_1,x_2,\ldots,x_K]$. An additive white zero mean Gaussian noise is added at each antenna terminal to the signal. This noise is represented as $\mathbf{N}=[n_1,n_2,\ldots,n_K]$ with $n_i \sim N(0,\delta^2_i)$. The covariance matrix of the noise is $\boldsymbol{\Sigma}=\text{diag}(\delta^2_{1,},\delta^2_{2,\ldots},\delta^2_K)$. Since the received signal is given by Y=X+N, the capacity can be determined directly as

$$C = \frac{1}{2}\log_2\left((2\pi e)^K\left|\mathbf{R}_{xx} + \boldsymbol{\Sigma}\right|\right) - \frac{1}{2}\log_2\left((2\pi e)^K\left|\boldsymbol{\Sigma}\right|\right) = \frac{1}{2}\log_2\left(\left|\mathbf{I} + \mathbf{R}_{xx}\boldsymbol{\Sigma}^{-1}\right|\right), \tag{4.90}$$

where $\mathbf{R}_{xx}$ is the covariance matrix of the received signal.

Since the received signal is for one user, the covariance matrix for a correlated received signal can be represented as

$$\mathbf{R}_{xx}=\begin{bmatrix} P_1 & \sqrt{P_1P_2} & \cdots & \sqrt{P_1P_K} \\ \sqrt{P_1P_2} & P_2 & \cdots & \sqrt{P_2P_K} \\ \vdots & \vdots & \ddots & \\ \sqrt{P_1P_K} & \cdots & \cdots & P_K \end{bmatrix}, \tag{4.91}$$

where P_i, i=1,…,K is the received power at antenna terminal i. It can be proven that the channel capacity is given by [51]

$$C=\frac{1}{2}\log_2\left(1+\sum_{i=1}^{K}\frac{P_i}{\delta_i^2}\right). \tag{4.92}$$

From equation (4.92), it is clear that the capacity is increasing in log scale with users.

4.4.3 Capacity of a channel with multi-users and multi-receivers

The analysis of a channel capacity with multi-users and multi-receivers is more difficult than the case of a single user and multi-receivers. This difficulty comes from the interference effect of each user on the other users. The analysis of the channel capacity in this case depends on the decoding process. There are two ways for decoding. The first is the simplest one. “The least cost” is to decode every user separately and deal with other interference signals as a background noise. The other method is the joint decoding. In the joint decoding all users’ signals are decoded simultaneously to minimize the interference between them. The joint decoding is more sophisticated than the independent decoding method, however, it is expensive to implement. Some suboptimal methods have been used to reduce the complexity, and still provide some gain over the independent decoding method.

From (4.39) for multi-user wireless communication system and single receiver with antenna array the received signal is

$$\mathbf{u}=\mathbf{A}\mathbf{s}+\mathbf{n} \tag{4.93}$$

For simplicity, the study here will be restricted to narrowband systems. By assuming that the signals and noises are uncorrelated, one can write:

$$\begin{aligned} \mathbf{R}_{ss}&=E\left\{\mathbf{s}(t)\mathbf{s}^H(t)\right\}=diag\left\{P_1,\cdots,P_Q\right\}, \\ \mathbf{R}_N&=E\left\{\mathbf{n}\mathbf{n}^H\right\}=\delta_n^2\mathbf{I}, \\ \mathbf{R}_{uu}&=\mathbf{A}\mathbf{R}_{ss}\mathbf{A}^H+\delta_n^2\mathbf{I}. \end{aligned} \tag{4.94}$$

The variables are defined in Section 4.2.6. To find the capacity in this case, we have to

assume multivariate Gaussian distribution for both the transmitted signals and for the added noise. We will assume independent decoding for the received signals.

To find the capacity for user k, the total interference and noise covariance matrix of user k is defined as

$$\mathbf{R}_{uk} = \mathbf{R}_{uu} - \mathrm{P_k}\mathbf{a}_k\mathbf{a}_k^{\mathrm{H}} \tag{4.95}$$

The capacity is given by

$$\mathrm{C_k} = \max \mathrm{I}[\mathbf{u}; \mathrm{s_k}(\mathrm{t})] = \mathrm{h}(\mathbf{u}) - \mathrm{h}[\mathbf{u} \setminus \mathrm{s_k}(\mathrm{t})] \tag{4.96}$$

$$\Rightarrow C_k = \frac{1}{2}\log_2\left(\frac{\left|\mathbf{R}_{uk} + P_k\mathbf{a}_k\mathbf{a}_k^H\right|}{\left|\mathbf{R}_{uk}\right|}\right) = \frac{1}{2}\log_2\left|\mathbf{I} + P_k\mathbf{a}_k\mathbf{a}_k^H\mathbf{R}_{uk}^{-1}\right| \tag{4.97}$$

Since $|\mathbf{I}+\mathbf{AB}|=|\mathbf{I}+\mathbf{BA}|$ the achievable rate of user k is [59]

$$\mathrm{R_k} \le \frac{1}{2}\log_2\left(1 + \mathrm{P_k}\mathbf{a}_k^{\mathrm{H}}\mathbf{R}_{uk}^{-1}\mathbf{a}_k\right). \tag{4.98}$$

In this thesis we have studied the beamforming, where the antenna array vector is optimally combined to a single output through a weight vector. The optimality is achieved by a proper selection of the weight vector. Now we will see that the optimal combining of the antenna outputs will not change the users' achievable rates.

As shown in Section 4.2, the output signal of user k is

$$\mathrm{z_k}(\mathrm{t}) = \mathbf{w}_k^{\mathrm{H}}\mathbf{u}(\mathrm{t}) = \mathbf{w}_k^{\mathrm{H}}\mathbf{a}_k\mathrm{s_k}(\mathrm{t}) + \mathbf{w}_k^{\mathrm{H}}\left(\mathbf{n}(\mathrm{t}) + \sum_{\substack{\mathrm{j}=1 \\ \mathrm{j}\neq\mathrm{k}}}^{\mathrm{Q}}\mathbf{a}_\mathrm{j}\mathrm{s_j}(\mathrm{t})\right). \tag{4.99}$$

The covariance of the output signal is

$$E\left[z_k(t)z_k^*(t)\right] = P_k\left|\mathbf{w}_k^H\mathbf{a}_k\right|^2 + \mathbf{w}_k^H\mathbf{R}_{uk}\mathbf{w}_k\,. \tag{4.100}$$

The optimum weight vector, which maximizes the CIR, is given by the MVDR [11] as

$$\mathbf{w}_k = \frac{\mathbf{R}_{uk}^{-1}\mathbf{a}_k}{\mathbf{a}_k^H\mathbf{R}_{uk}^{-1}\mathbf{a}_k}. \tag{4.101}$$

Then the CIR for user k from equation (4.100) is given by

$$\mathrm{CIR_k} = \mathrm{P_k}\mathbf{a}_k^{\mathrm{H}}\mathbf{R}_{uk}^{-1}\mathbf{a}_k\,. \tag{4.102}$$

By substituting equation (4.102) into the original Shannon capacity formula we obtain

$$\mathrm{R_k} \le \frac{1}{2}\log_2\left(1+\mathrm{CIR_k}\right) = \frac{1}{2}\log_2\left(1+\mathrm{P_k}\mathbf{a}_{\mathrm{k}}^{\mathrm{H}}\mathbf{R}_{\mathrm{uk}}^{-1}\mathbf{a}_{\mathrm{k}}\right), \tag{4.103}$$

which is identical to (4.98). This indicates that the optimal combining of the antennas outputs will not change the users' achievable rates

4.4.4 Capacity of a channel with multi-users, multi-receivers, and multi-paths

Single path is assumed in the previous section. Now we will show the impact of multi-path environment on the channel upper capacity. The output signal of the antenna array in multi-path case is given by

$$z_k(t) = \mathbf{w}_k^H\mathbf{u}(t) = \mathbf{w}_k^H\sum_{l=1}^{B_k}\mathbf{a}_{kl}s_k\left(t-\tau_{kl}\right) + \mathbf{w}_k^H\left(\mathbf{n}(t) + \sum_{\substack{j=1\\ j\neq k}}^{Q}\sum_{l=1}^{B_j}\mathbf{a}_{jl}s_j\left(t-\tau_{jl}\right)\right) \tag{4.104}$$

If the weight vector is computed for one path (ex. the strongest path) then the other paths which have different delays and DoA will be added to the interference part of the received signal. Without any loss of generality assume the strongest path is the first, then (4.104) can be rewritten as

$$z_k(t) = \mathbf{w}_k^H\mathbf{u}(t) = \mathbf{w}_k^H\mathbf{a}_{k1}s_k\left(t-\tau_{k1}\right) + \mathbf{w}_k^H\left(\mathbf{n}(t) + \sum_{\substack{j=1\\ j\neq k}}^{Q}\sum_{l=1}^{B_j}\mathbf{a}_{jl}s_j\left(t-\tau_{jl}\right) + \sum_{l=2}^{B_j}\mathbf{a}_{kl}s_k\left(t-\tau_{kl}\right)\right), \tag{4.105}$$

where B_k is the number of signal paths of user k. It is clear that the interference part becomes larger now which means less capacity. In this case the MVDR algorithm (alone) is not the optimum. One method is to find the optimum weight vector of each signal path then using Rake receiver to equalize the different signal delays. Using the GMVDR algorithm (4.68) one can compute the optimum weight vector for all paths. In this case all signal paths can be exploited. Equation (4.104) can be rewritten in more compact form as

$$z_k(t) = \mathbf{w}_k^H\hat{\mathbf{a}}_k^H\mathbf{s}_k + \mathbf{w}_k^H\left(\mathbf{n}(t) + \sum_{\substack{j=1\\ j\neq k}}^{Q}\hat{\mathbf{a}}_j^H\mathbf{s}_j\right) \tag{4.106}$$

where

$$\hat{\mathbf{a}}_k^H = \left[\mathbf{a}_{k1}, \mathbf{a}_{k2}, .., \mathbf{a}_{kB_k}\right] \tag{4.107}$$

$$\mathbf{s}_k = \left[s_k^*\left(t-\tau_1\right), s_k^*\left(t-\tau_2\right), ..., s_k^*\left(t-\tau_{B_k}\right)\right]^H \tag{4.108}$$

The covariance of the output signal is

$$E\left[z_k(t)z_k^*(t)\right] = \mathbf{w}_k^H \hat{\mathbf{a}}_k^H \mathbf{R}_{kk} \hat{\mathbf{a}}_k \mathbf{w}_k + \mathbf{w}_k^H \mathbf{R}_{uk} \mathbf{w}_k \tag{4.109}$$

where $\mathbf{R}_{kk} = E\left[s_k s_k^H\right]$.

If the covariance matrix of the interference can be estimated (usually difficult to obtain) then (4.68) can be rewritten as

$$\mathbf{w}_k^H = \mathbf{1}^T \mathbf{A}_k^{-1} \hat{\mathbf{a}}_k \mathbf{R}_{uk}^{-1} \tag{4.110}$$

Substitute (4.110) into (4.109) to obtain

$$E\left[z_k(t)z_k^*(t)\right] = \mathbf{1}'\mathbf{A}_k^{-1}\hat{\mathbf{a}}_k\mathbf{R}_{uk}^{-1}\hat{\mathbf{a}}_k^H\mathbf{R}_{kk}\hat{\mathbf{a}}_k\mathbf{R}_{uk}^{-1}\hat{\mathbf{a}}_k^H\mathbf{A}_k^{-1}\mathbf{1} + \mathbf{1}'\mathbf{A}_k^{-1}\hat{\mathbf{a}}_k\mathbf{R}_{uk}^{-1}\mathbf{R}_{uk}\mathbf{R}_{uk}^{-1}\hat{\mathbf{a}}_k^H\mathbf{A}_k^{-1}\mathbf{1} \tag{4.111}$$

From (4.70)

$$\mathbf{A}_k = \hat{\mathbf{a}}_k \mathbf{R}_{uk}^{-1} \hat{\mathbf{a}}_k^H \tag{4.112}$$

Then (4.111) can be reduced to

$$E\left[z_k(t)z_k^*(t)\right] = \mathbf{1}'\mathbf{R}_{kk}\mathbf{1} + \mathbf{1}'\mathbf{A}_k^{-1}\mathbf{1} \tag{4.113}$$

The first part represents the received signal of interest which is the sum of the signal covariance matrix.

The capacity in this case is

$$R_k \le \frac{1}{2}\log_2\left(1 + CIR_k\right) = \frac{1}{2}\log_2\left(1 + \frac{\mathbf{1}'\mathbf{R}_{kk}\mathbf{1}}{\mathbf{1}'\mathbf{A}_k^{-1}\mathbf{1}}\right) \tag{4.114}$$

Observe that in case of single path, (4.114) is reduced to (4.103).

4.5 Simulation Results

The first part of simulations is performed to compare different adaptive antenna algorithms. We have assumed 50 users uniformly distributed within an area containing four base stations as shown in Figure 4.5. In the simulations the following parameters are used. Additive white noise with zero mean and -100dBw variance is assumed. Further, DS/CDMA system is assumed with processing gain (PG) of 128. The path loss exponent is 4 and the shadowing factor is assumed to be 2 dB. In the simulations, centralized power control algorithm is employed to adjust the transmitted power of each user. In Figure 4.6 we can see the CIR in dB with respect to the number of users.

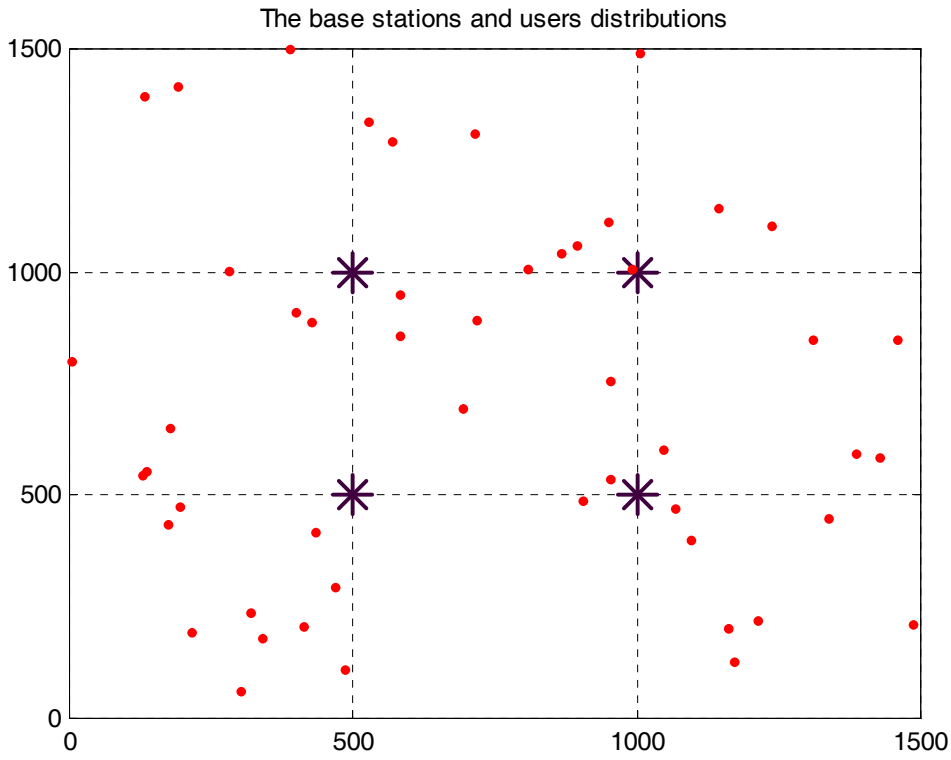

Figure 4.5 The base stations and users' distributions.

Figure 4.6 shows that the null steering beamformer behaves worst in a multi-cell environment with additive white noise; also it needs good estimation for the DoAs for all users. The MVDR gives relatively good results; its problem is that it needs an estimation for the DoA for the desired user, and good estimation for the inverse of the correlation matrix. The GMVDR is exactly the same as MVDR in single path case. The adaptive version of the MVDR method has slow convergence. The RLS was as expected faster than the LMS algorithm. The subspace method gives good results for small number of users, i.e. when the number of users is comparable with the number of antenna elements. For this reason it has not been shown in Figure 4.6. The GMVDR algorithm has been tested in the second part of simulations. Ten users uniformly distributed in an area of 1 km^2 with one base station have been assumed. Frequency selective channel with an additive white noise is assumed. Four antenna terminals are assumed at the base station. Three paths are assumed for each user. The paths have random DoAs. The antenna beamforming of one user is shown in Figure 4.7. It is clear that the antenna beam enhances the reception in the directions of the significant paths of the desired user's signal.

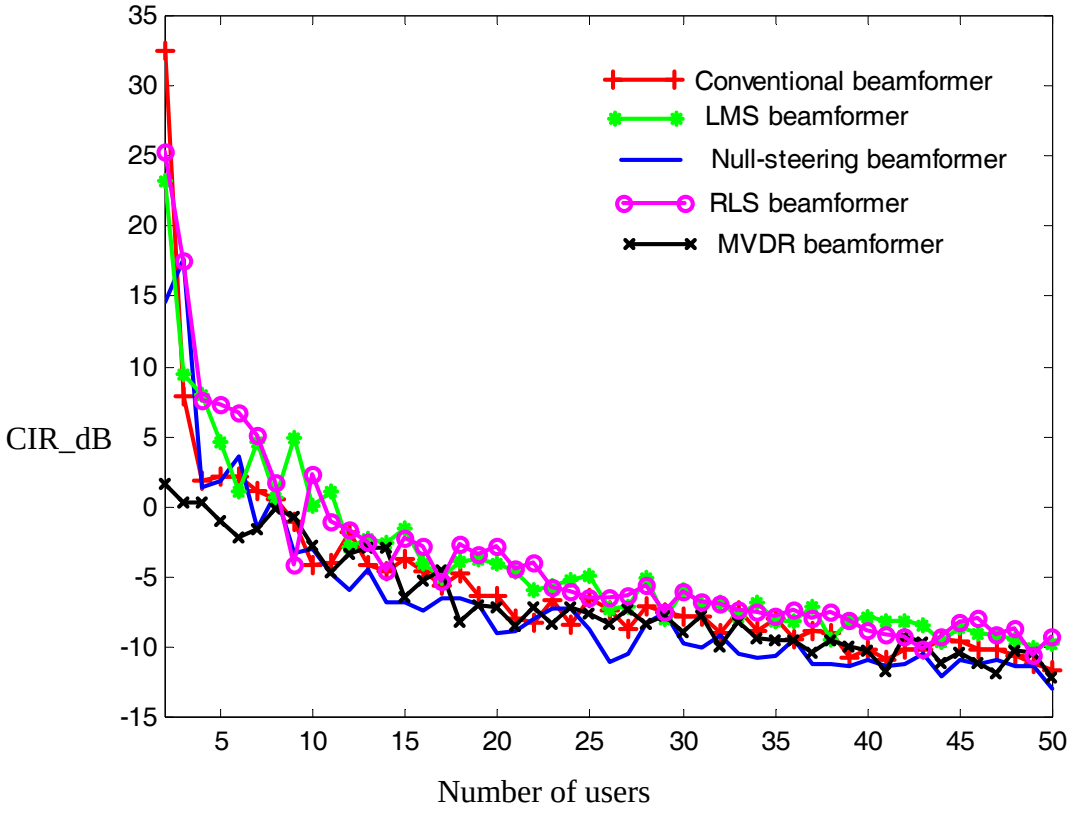

Figure 4.6. CIR (dB) versus the number of users.

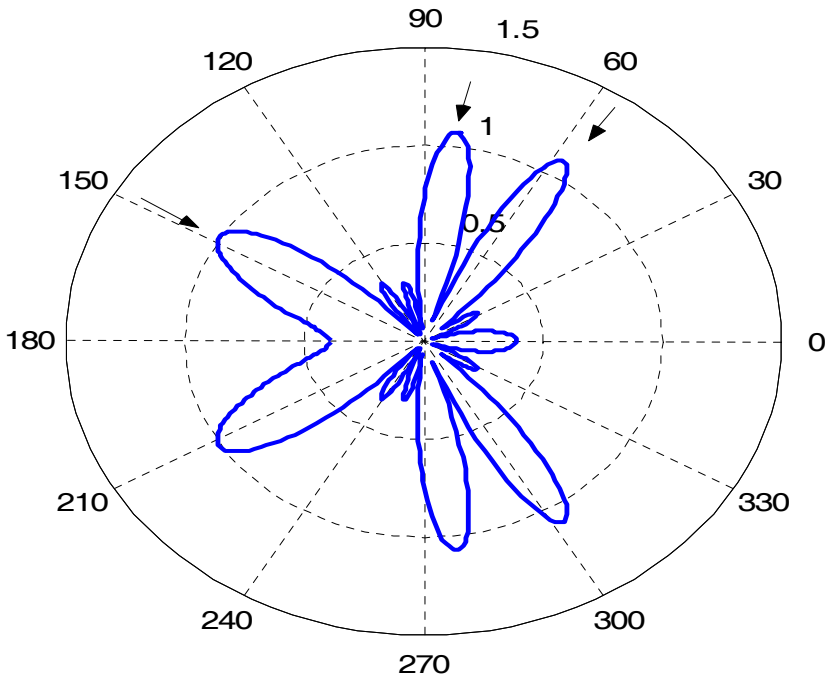

Figure 4.7. The beamforming characteristic of the multi-path GMVDR algorithm

CHAPTER FIVE

JOINING RADIO RESOURCE MANAGEMENT AND SMART ANTENNAS

5.1 Introduction

It has been shown in previous chapters that the SINR is the backbone of the system performance. At low SINR, duplicating the SINR means duplicating the upper bound capacity, which means less infrastructures, less cost, better performance,…and so on. For this reason many researchers work to exploit any available or discovered phenomena to increase the SINR of the communication system. In Chapter 3 we discussed the optimum sharing way of the available resources between users, in other words, the optimum SINR value to be assigned for each user to achieve the required network and user objectives. It has been indicated in Chapter 4 that the SINR can be enhanced by reducing the interference through spatial and temporal processing. The performance can be further enhanced by using (Multi-Input Multi-Output) MIMO smart antenna system. That means using smart antenna system at the receiver as well as at the transmitter. MIMO antenna system usually means in the literature exploiting of uncorrelated multi-paths of the transmitted signal to obtain different channels at the same time, bandwidth, and code. We use the term MIMO here for MIMO beamforming. Equation (4.103) indicates that the same upper capacity can be achieved in both cases. In this chapter we will show how to join the MIMO smart antenna and the radio resource scheduler.

The joining algorithm of radio resource scheduler and smart antenna should considerably reduce the transmission power while achieving the target QoS performance. The convergence to an acceptable performance should be fast enough to handle the dynamical behavior of the mobile communication systems.

A smart antenna can minimize the interference between users with different DoA signals, while the RRS optimizes the transmitted power and rate to maximize the capacity and to achieve the required QoS at the same time.

It has been shown in Chapter 4 that the smart antenna weights are dependent on the received signal power “to construct the covariance matrix”. Chapter 3 shows that the

transmitted power and rate are dependent on the CIR. The CIR is dependent on the smart antenna weights, as is shown in Section 5.2. So we can see the direct effect of the RRS and beamforming to each other. By optimal or even sub-optimal joining of the two-interference management approaches, one can greatly improve the capacity and the QoS of the mobile communication system.

5.2 Influence of MIMO beamforming on communication system performance

A general configuration of a cellular system with a smart antenna system at base station as well as mobile stations is shown in Figure 5.1. Suppose there are Q users uniformly distributed in an area with radius R, which contains V BSs. Assume that each BS has M antenna elements, and there are N antenna elements at each MS. There are some limitations of using the smart antenna at the MS such as the limited space, processing power, and the dynamic nature of the local environment near MSs [12]. But in general, the optimum adaptation of the antenna weights of the BS and MS will further enhance the performance of the cell [46],[48],[53]. Moreover using a MIMO smart antenna has important applications in the Wireless Local Loop systems [12]. In our model, we assumed that array beamforming is used in the receiving part of the BS and also in the transmission part of the MS (Uplink beamforming).

The main advantages of using beamforming in the transmitter of the MS are

a) Steering the radiation pattern in certain directions to increase the CIR and reduce the transmitted power.
b) Reducing the angle spread at the BS.
c) In the case of multi-cells, using the antenna array at the MS will enhance the performance of the system by reducing the transmitted power in the direction of the other BSs.

Another interesting point is that the calculated weights at the BS can be used to calculate the weights at the MS in TDD systems [60].

Without loss of generality, it is assumed that the MS *i* communicates with BS *i*.

The output signal of user *i* at BS *i* can be described as

$$Z_{ii} = \sum_{j=1}^{M} u_{iji} w_{iji}, \qquad i = 1,...,Q \tag{5.1}$$

where u_{iji} is the signal of user *i* received at antenna terminal of element j in the BS *i*, w_{iji} is the j^{th} weight adjusted for user *i* in BS *i*.

From (5.1) the received signal power from user *i* at BS *i* is

$$P_{ii} = |Z_{ii}|^2 = \left| \sum_{j=1}^{M} u_{iji} w_{iji} \right|^2 \tag{5.2}$$

and the interference signal power for user i is

$$N_{ii} = \sum_{\substack{k=1 \\ k \neq i}}^{Q} \left| \sum_{j=1}^{M} u_{kji} w_{iji} \right|^2 + \sigma_n^2 \tag{5.3}$$

where σ_n^2 is the variance of the additive noise.

The additive noise at the antenna terminals is assumed to be identically distributed, uncorrelated, and to have zero mean. The input signal at each antenna terminal is the convolution between the transmitted signal and the channel impulse response as

$$u_{iji} = S_{ii}(t) * \mathbf{h}_{ii}(\tau, t) \tag{5.4}$$

where $S_{ii}(t)$ is the transmitted signal from user *i* (assigned to BS *i*), and $\mathbf{h}_{ii}$ is the impulse response vector of the channel between MS *i* and BS *i*.

We assume the transmitted baseband signal for user *i* to be

$$r_i(t) = \sqrt{P_{ti}}\, \tilde{B}_i(t) C_i(t) \tag{5.5}$$

where P_{ti} is the transmitted signal power and $\tilde{B}_i(t)$ is the binary data signal for user *i.* The binary data signal has been assumed to be ± 1 with equal probability. $C_i(t)$ is the spreading code for user *i* with ± 1 chips.

The channel between MS *i* and BS *i* has been modeled using Vector Channel Impulse Response (VCIP)

$$\mathbf{h}_{ii}(\tau, t) = \sum_{l=0}^{B_i} \mathbf{a}_{ii}(\theta_l, \phi_l) \alpha_{iil}(t) \delta(t - \tau_{iil}) \tag{5.6}$$

where $\mathbf{a}_{ii}$ is the steering vector, $B_i + 1$ is the number of signal paths of user *i*, and $\alpha_{iil}(t)$ is the complex channel gain (see chapter 4 for more details).

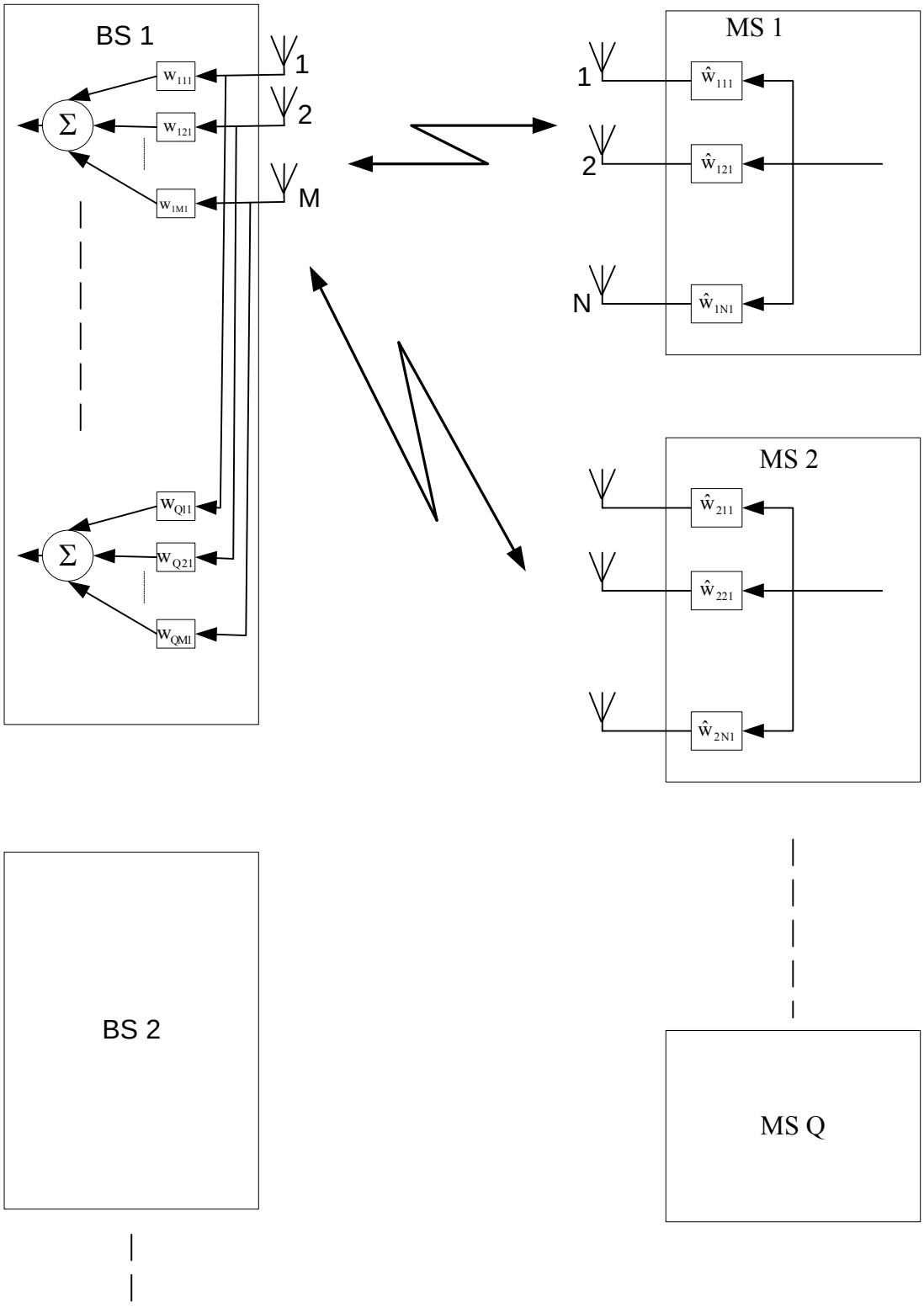

Figure 5.1. Simplified System Model

From equation (4.9) , the received signal at terminal j is

$$\begin{aligned} u_{iji} &= S_{ii}(t) * \sum_{l=0}^{B_i} \exp\left(-j\beta\ \Delta\Psi_{ijil}\ \right)\sqrt{\rho_{iil}}\ \exp\left(\ j\left(2\pi\, f_{iil}t+\varphi_{iil}\right)\right)\delta\left(t-\tau_{iil}\right) \\ &= \sum_{l=0}^{B_i} \exp\left(-j\beta\ \Delta\Psi_{ijil}\ \right)\sqrt{\rho_{iil}}\ \exp\left(\ j\left(2\pi\, f_{iil}t+\varphi_{iil}\right)\right)S_{ii}\left(t-\tau_{iil}\right), \quad i=1,...,Q \end{aligned} \tag{5.7}$$

The variables are defined in Section 4.2. According to our model we have defined an antenna array at the MS. Then the transmitted signal from each MS can be defined as

$$S_{ii}(t) = \sum_{j=1}^{N} \hat{w}_{iji}.\exp\left(-j\beta\Delta\hat{\Psi}_{iji}\right) r_i(t), \qquad i=1,...,Q \tag{5.8}$$

where $\Delta\hat{\Psi}_{iji} = x_j\cos\left(\hat{\phi}_{ii}\right)\sin\left(\hat{\theta}_{ii}\right) + y_j\sin\left(\hat{\phi}_{ii}\right)\sin\left(\hat{\theta}_{ii}\right) + z_j\cos\left(\hat{\theta}_{ii}\right)$, and $\hat{\phi}_{ii}, \hat{\theta}_{ii}$ are the azimuth and the elevation angles of the BS *i* relative to the MS *i* respectively, and $\hat{w}_{iji}$ is the weight of MS *i* at antenna terminal *j*.

Using a smart antenna in the communication system has a direct effect on the CIR in the system. Most RRS algorithms are based on the estimation of the CIR for each user. The RRS and smart antenna can be joined together mathematically based on the CIR as a common factor. In distributed RRS algorithms, only local information is needed to be known to transmit the optimum power and data rate.

The distributed feasible updating algorithms can be represented as

$$P_i(t+1) = f_i\left(\mathbf{P}(t), \mathbf{R}(t), \boldsymbol{\theta}_i^T(t), \Gamma_i(t)\right), \quad i=1,...,Q, \quad t=0,1,... \tag{5.9}$$

$$R_i(t+1) = g_i\left(\mathbf{P}(t), \mathbf{R}(t), \boldsymbol{\theta}_i^T(t), \Gamma_i(t)\right) \tag{5.10}$$

where f_i and g_i are the power and rate updating functions of terminal i respectively (these functions depend on the modulation type, and the optimization criteria), $\mathbf{P}(t)$, $\mathbf{R}(t)$ are the power and rate vectors at time slot t respectively, $\boldsymbol{\theta}_i^T(t)$ is a vector of target parameters (such as target SINR, maximum packet delay,…etc) of user i at time slot t. Note that the data rate itself has been represented in many applications as one item of the target QoS vector $\boldsymbol{\theta}_i^T(t)$, but here we assumed it to be a free parameter, which can be determined by the RRS, and $\Gamma_i(t)$ is the CIR of user *i* at time slot *t* [7].

There are different types of interference functions in the literature (see Chapters 2 and 3).

The CIR can be derived from (5.2) ,(5.3) and (5.7) as

$$\Gamma_{ii}(t)=\frac{\left|\sum_{j=1}^{M}\left[\sum_{l=0}^{B_i}\exp\left(-j\beta\Delta\Psi_{ijil}\right)\sqrt{\rho_{iil}}\exp\left(j\left(2\pi f_{iil}t+\varphi_{iil}\right)\right)S_{iv}\left(t-\tau_{iil}\right)\right]w_{iji}\right|^2}{\sum_{\substack{k=1\\k\neq i}}^{Q}\left|\sum_{j=1}^{M}\left[\sum_{l=0}^{B_k}\exp\left(-j\beta\Delta\Psi_{kjil}\right)\sqrt{\rho_{kil}}\exp\left(j\left(2\pi f_{kil}t+\varphi_{kil}\right)\right)S_{kv}\left(t-\tau_{kil}\right)\right]w_{iji}\right|^2+\sigma_n^2}. \tag{5.11}$$

To simplify (5.11) a narrowband (flat fading) channel is assumed. The following expression is then obtained:

$$\Gamma_{ii}(t)=\frac{\left|S_{ii}\left(t-\tau_0\right)\right|^2\left|\sum_{j=1}^{M}\left[\sum_{l=0}^{B_i}\exp\left(-j\beta\Delta\Psi_{ijil}\right)\sqrt{\rho_{iil}}\exp\left(j\left(2\pi f_{iil}t+\varphi_{iil}\right)\right)\right]w_{iji}\right|^2}{\sum_{\substack{k=1\\k\neq i}}^{Q}\left|S_{ki}\left(t-\tau_0\right)\right|^2\left|\sum_{j=1}^{M}\left[\sum_{l=0}^{B_k}\exp\left(-j\beta\Delta\Psi_{kjil}\right)\sqrt{\rho_{kil}}\exp\left(j\left(2\pi f_{kil}t+\varphi_{kil}\right)\right)\right]w_{iji}\right|^2+\sigma_n^2} \tag{5.12}$$

From (5.8) and (5.12) the following expression can be derived:

$$\Gamma_{ii}(t)=\frac{\left|r_i(t)\right|^2\left|\hat{\mathbf{w}}_{ii}^H\hat{\mathbf{a}}_{ii}\right|^2\left|\mathbf{w}_{ii}^H\mathbf{a}_{ii}\boldsymbol{\alpha}_{ii}\right|^2}{\sum_{\substack{k=1\\k\neq i}}^{Q}\left|r_k(t)\right|^2\left|\hat{\mathbf{w}}_{kk}^H\hat{\mathbf{a}}_{ik}\right|^2\left|\mathbf{w}_{ii}^H\mathbf{a}_{ki}\boldsymbol{\alpha}_{ki}\right|^2+\sigma_n^2},\qquad i=1,\ldots,Q \tag{5.13}$$

where $\mathbf{w}_{ii}=\left[w_{i1i}\ w_{i2i}\cdots w_{iMi}\right]^H$ is the weight vector, and the superscript H represents the Hermitian transpose,

$$\boldsymbol{\alpha}_{ii}=\left[\sqrt{\rho_{ii1}}\exp\left(j\left(2\pi f_{ii1}t+\varphi_{iv1}\right)\right)\ \cdots\ \sqrt{\rho_{iiB_i}}\exp\left(j\left(2\pi f_{iiB_i}t+\varphi_{iiB_i}\right)\right)\right] \tag{5.14}$$

$$\mathbf{a}_{ii}=\begin{bmatrix}\exp\left(-j\beta\Delta\Psi_{i1i1}\right) & \exp\left(-j\beta\Delta\Psi_{i1i2}\right) & \cdots & \exp\left(-j\beta\Delta\Psi_{i1iB_i}\right)\\ \exp\left(-j\beta\Delta\Psi_{i2i1}\right) & \exp\left(-j\beta\Delta\Psi_{i2i2}\right) & \cdots & \exp\left(-j\beta\Delta\Psi_{i2iB_i}\right)\\ \vdots & & & \vdots\\ \exp\left(-j\beta\Delta\Psi_{iMi1}\right) & \exp\left(-j\beta\Delta\Psi_{iMi2}\right) & \cdots & \exp\left(-j\beta\Delta\Psi_{iMiB_i}\right)\end{bmatrix} \tag{5.15}$$

$$\hat{\mathbf{w}}_{ii}=\left[\hat{w}_{i1i}\quad \hat{w}_{i2i}\quad \cdots\quad \hat{w}_{iNi}\right]^H \tag{5.16}$$

and

$$\hat{\mathbf{a}}_{ii}=\left[\exp\left(-j\beta\Delta\hat{\Psi}_{i1i}\right)\ \cdots\ \exp\left(-j\beta\Delta\hat{\Psi}_{iNi}\right)\right]^T \tag{5.17}$$

From (5.11) we see the direct influence of the MIMO antenna weights on the CIR. To

clarify the influence of the MIMO antenna weights on the system capacity we derive the maximum achievable CIR in flat fading channel case. As stated in Chapter 2 the channel matrix **H** determines the link performance. It can be used to determine the maximum achievable CIR in the case of noiseless channels. The **H** matrix can be redefined in the case of uplink MIMO smart antenna as

$$\mathbf{H}=\begin{bmatrix} 0 & \dfrac{\left|\hat{\mathbf{w}}_{22}^{H}\hat{\mathbf{a}}_{12}\right|^2\left|\mathbf{w}_{11}^{H}\mathbf{a}_{21}\boldsymbol{\alpha}_{21}\right|^2}{\left|\hat{\mathbf{w}}_{11}^{H}\hat{\mathbf{a}}_{11}\right|^2\left|\mathbf{w}_{11}^{H}\mathbf{a}_{11}\boldsymbol{\alpha}_{11}\right|^2} & \cdots & \dfrac{\left|\hat{\mathbf{w}}_{QQ}^{H}\hat{\mathbf{a}}_{1Q}\right|^2\left|\mathbf{w}_{11}^{H}\mathbf{a}_{Q1}\boldsymbol{\alpha}_{Q1}\right|^2}{\left|\hat{\mathbf{w}}_{11}^{H}\hat{\mathbf{a}}_{11}\right|^2\left|\mathbf{w}_{11}^{H}\mathbf{a}_{11}\boldsymbol{\alpha}_{11}\right|^2} \\ \dfrac{\left|\hat{\mathbf{w}}_{11}^{H}\hat{\mathbf{a}}_{21}\right|^2\left|\mathbf{w}_{22}^{H}\mathbf{a}_{12}\boldsymbol{\alpha}_{12}\right|^2}{\left|\hat{\mathbf{w}}_{22}^{H}\hat{\mathbf{a}}_{22}\right|^2\left|\mathbf{w}_{22}^{H}\mathbf{a}_{22}\boldsymbol{\alpha}_{22}\right|^2} & 0 & \cdots & \dfrac{\left|\hat{\mathbf{w}}_{QQ}^{H}\hat{\mathbf{a}}_{2Q}\right|^2\left|\mathbf{w}_{22}^{H}\mathbf{a}_{Q2}\boldsymbol{\alpha}_{Q2}\right|^2}{\left|\hat{\mathbf{w}}_{22}^{H}\hat{\mathbf{a}}_{22}\right|^2\left|\mathbf{w}_{22}^{H}\mathbf{a}_{22}\boldsymbol{\alpha}_{22}\right|^2} \\ \vdots & & & \vdots \\ \dfrac{\left|\hat{\mathbf{w}}_{11}^{H}\hat{\mathbf{a}}_{Q1}\right|^2\left|\mathbf{w}_{QQ}^{H}\mathbf{a}_{1Q}\boldsymbol{\alpha}_{1Q}\right|^2}{\left|\hat{\mathbf{w}}_{QQ}^{H}\hat{\mathbf{a}}_{QQ}\right|^2\left|\mathbf{w}_{QQ}^{H}\mathbf{a}_{QQ}\boldsymbol{\alpha}_{QQ}\right|^2} & \dfrac{\left|\hat{\mathbf{w}}_{22}^{H}\hat{\mathbf{a}}_{Q2}\right|^2\left|\mathbf{w}_{QQ}^{H}\mathbf{a}_{2Q}\boldsymbol{\alpha}_{2Q}\right|^2}{\left|\hat{\mathbf{w}}_{QQ}^{H}\hat{\mathbf{a}}_{QQ}\right|^2\left|\mathbf{w}_{QQ}^{H}\mathbf{a}_{QQ}\boldsymbol{\alpha}_{QQ}\right|^2} & \cdots & 0 \end{bmatrix} \tag{5.18}$$

To compare the results of (5.18) with those given by Section 2.2, a single path channel with zero Doppler shift and zero phase offset will be assumed. The CIR for user *i* can be defined as

$$\Gamma_{ii}(t)=\frac{\left|r_i(t)\right|^2\left|\hat{\mathbf{w}}_{ii}^{H}\hat{\mathbf{a}}_{ii}\right|^2\left|\mathbf{w}_{ii}^{H}\mathbf{a}_{ii}\right|^2 G_{ii}}{\sum_{\substack{k=1\\k\neq i}}^{Q}\left|r_k(t)\right|^2\left|\hat{\mathbf{w}}_{kk}^{H}\hat{\mathbf{a}}_{ik}\right|^2\left|\mathbf{w}_{ii}^{H}\mathbf{a}_{ki}\right|^2 G_{ki}+\sigma_n^2}=\frac{\left|r_i(t)\right|^2\xi_{ii}G_{ii}}{\sum_{\substack{k=1\\k\neq i}}^{Q}\left|r_k(t)\right|^2\xi_{ki}G_{ki}+\sigma_n^2} \tag{5.19}$$

where all the beamforming algorithms try to adjust the antenna array weights to minimize the factor $\frac{\xi_{ki}}{\xi_{ii}}$. The minimization of this factor leads to minimization of the interferences at user *i*.

Now the matrix **H** in (5.18) becomes

$$\mathbf{H}=\begin{bmatrix} 0 & \dfrac{G_{21}}{G_{11}}\left(\dfrac{\xi_{21}}{\xi_{11}}\right) & \cdots & \dfrac{G_{Q1}}{G_{11}}\left(\dfrac{\xi_{Q1}}{\xi_{11}}\right) \\ \dfrac{G_{12}}{G_{22}}\left(\dfrac{\xi_{12}}{\xi_{22}}\right) & 0 & \cdots & \dfrac{G_{Q2}}{G_{22}}\left(\dfrac{\xi_{Q2}}{\xi_{22}}\right) \\ \vdots & & & \vdots \\ \dfrac{G_{1Q}}{G_{QQ}}\left(\dfrac{\xi_{1Q}}{\xi_{QQ}}\right) & \dfrac{G_{2Q}}{G_{QQ}}\left(\dfrac{\xi_{2Q}}{\xi_{QQ}}\right) & \cdots & 0 \end{bmatrix}. \tag{5.20}$$

Comparing (5.20) with (2.6) in Chapter 2 we can see that the spectral radius of the matrix defined by (5.20) is smaller than the spectral radius of the other matrix. The reason is that, using proper adaptation techniques leads to

$$\xi_{ii} \geq \xi_{ik} \quad , \qquad \forall \ i, \ k \ = 1,..,Q \tag{5.21}$$

The smaller spectral radius means the larger maximum achievable CIR, which means higher capacity and better performance.

Example 1

An improvement in the maximum achievable CIR will be demonstrated next when a MIMO antenna system is used. In this simulation, four BSs distributed in an area of 4 km^2 are assumed. The conventional beamforming for weight calculation is used. Figure 5.2 shows the maximum achievable CIR with respect to the number of users in two different cases. In the first case, an omni-directional antenna at the BS as well as the MS is assumed. In the second case, 4 antenna elements at each BS and 2 antenna elements at each mobile station are employed.

Example 2

In this example we demonstrate the reduction in the transmitted power when using a MIMO antenna system. The QoS is assumed to be the same for all users. Here 200 users uniformly distributed within an area of 4 km^2 with 4 BSs are assumed. The target CIR is assumed to be –18 dB. The average power of the additive white noise is 1 nW. Figure 5.3 shows the results of this example. In the case of omni-directional antenna at the BS as well as the MS "beamforming (1,1)" the average transmitted power should be 8.3 dBw to achieve the target CIR. In the case of using 4 antenna elements at the MS and an omni-directional antenna at the BS "beamforming (1,4)", the average power has been reduced to –5.7 dBw. In the case of omni-directional antenna at the MS and 4 antenna elements at the BS "beamforming (4,1)", the average power has been reduced to –13 dBw. Finally in MIMO case where 4 antenna elements are used at the BS as well as MS the average transmitted power dropped to –25 dBw.

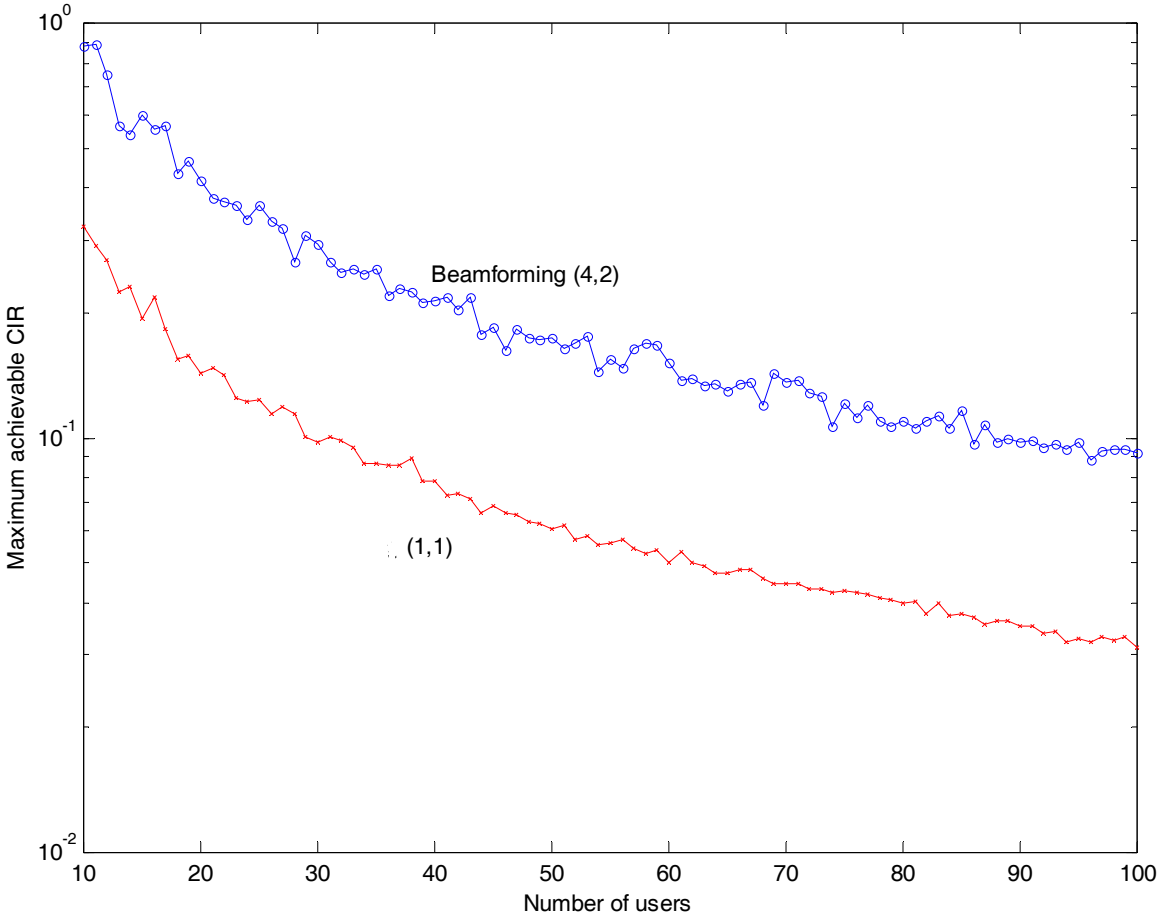

Figure 5.2. Maximum achievable CIR in MIMO beamforming

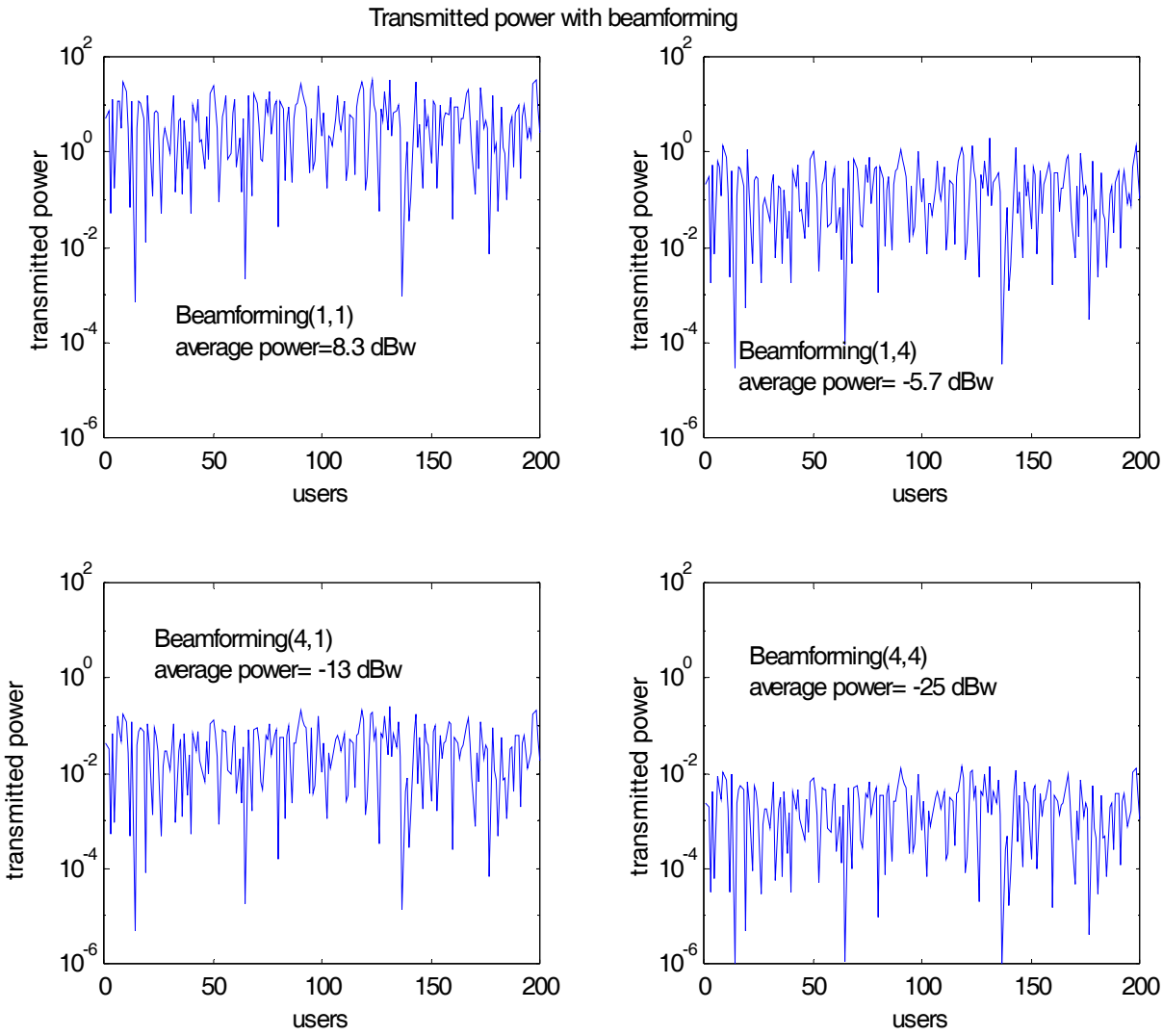

Figure 5.3. Average power reduction of MIMO beamforming

5.3 Joining Algorithms for Smart Antenna and RRS

The radio resources scheduler optimization problem in the presence of MIMO beamforming antenna weights is usually a complex, multi-dimensional, non-linear, and non-convex problem. Generally, all the RRS optimization problems (Chapter 3) can be reformulated to find the optimum antenna weights as well. By taking the MTMPC algorithm (Section 3.8.3) as an example, the RRS optimization problem becomes

$$(\mathbf{P},\mathbf{W}) = \arg\max\left\{O_1(\mathbf{P}), -O_2(\mathbf{P})\right\} \quad \text{s.t. } \mathbf{P} \in \Omega \tag{5.22}$$

where

$$\mathbf{P} = \left[P_1, P_2, ..., P_Q \right]' \tag{5.23}$$

$$O_1(\mathbf{P}) = \prod_{i=1}^{Q} \frac{\left| r_i(t) \right|^2 \left| \hat{\mathbf{w}}_{ii}^H \hat{\mathbf{a}}_{ii} \right|^2 \left| \mathbf{w}_{ii}^H \mathbf{a}_{ii} \boldsymbol{\alpha}_{ii} \right|^2}{\sum_{\substack{k=1 \\ k \neq i}}^{Q} \left| r_k(t) \right|^2 \left| \hat{\mathbf{w}}_{kk}^H \hat{\mathbf{a}}_{ik} \right|^2 \left| \mathbf{w}_{ii}^H \mathbf{a}_{ki} \boldsymbol{\alpha}_{ki} \right|^2 + \sigma_n^2}, \tag{5.24}$$

$$O_2(\mathbf{P}) = \sum_{i=1}^{Q} P_i \ , \tag{5.25}$$

and $\Omega = \left\{ \mathbf{P} \middle| P_{\min} \le P_i \le P_{\max}, i = 1, ..., Q \right\}$, and $\mathbf{W}$ is a vector of all antennas weights in the system. In next Section we show how to join the smart antenna and RRS using Kalman filters.

5.3.1 Joining Smart Antenna and RRS using Kalman Filters

In this part, the smart antenna array is assumed only at the base station. The two problems (RRS and antenna weights adaptation) are solved separately using Kalman filters. As was mentioned in Chapter 4, [22] has proposed to use Kalman filter to adjust the antenna weights. In chapter 3, Kalman filter was proposed to solve the radio resource scheduling problem. In this section, both methods will be combined.

The system equation is (for $i=1,\ldots,Q$)

$$\begin{bmatrix} \hat{w}_i(t) \\ \mathbf{w}_i(t) \end{bmatrix} = \begin{bmatrix} f_i(t-1) & 0 & 0 & \cdots & 0 \\ 0 & 1 & 0 & \cdots & 0 \\ 0 & 0 & 1 & & 0 \\ 0 & 0 & 0 & \ddots & \vdots \\ 0 & 0 & 0 & \cdots & 1 \end{bmatrix} \begin{bmatrix} \hat{w}_i(t-1) \\ \mathbf{w}_i(t-1) \end{bmatrix} + \begin{bmatrix} q_o(t-1) \\ 0 \\ \vdots \\ 0 \end{bmatrix} \tag{5.26}$$

and the measurement equation is

$$\begin{bmatrix} \Gamma_i^T \\ 0 \\ 1 \end{bmatrix} = \begin{bmatrix} g_i(t) & 0 & \cdots & 0 \\ 0 & u_1^* & \cdots & u_M^* \\ 0 & a_1^* & \cdots & a_M^* \end{bmatrix} \begin{bmatrix} \hat{w}_i(t) \\ \mathbf{w}_i(t) \end{bmatrix} + \begin{bmatrix} v_o(t) \\ v_1(t) \\ v_2(t) \end{bmatrix} \tag{5.27}$$

Equations (5.26) and (5.27) can be rewritten as

$$\begin{aligned}\hat{\mathbf{W}}_i(t) &= \mathbf{F}(t-1)\hat{\mathbf{W}}_i(t-1)+\mathbf{q}(t-1), \qquad t=1,2,...\\ \mathbf{Y}(t) &= \mathbf{G}(t)\hat{\mathbf{W}}_i(t)+\mathbf{V}(t)\end{aligned} \tag{5.28}$$

where $\mathbf{q}(t)$ and $\mathbf{V}(t)$ are assumed to be zero mean white Gaussian noise with covariance matrices $\mathbf{Q}=\begin{bmatrix}\xi & 0 & \cdots & 0\\ 0 & 0 & \cdots & 0\\ \vdots & \vdots & \cdots & \vdots\\ 0 & 0 & \cdots & 0\end{bmatrix}$ and $\mathbf{R}=\begin{bmatrix}\delta^2_{v_o} & 0 & 0\\ 0 & \delta^2_{v_1} & 0\\ 0 & 0 & \delta^2_{v_2}\end{bmatrix}$ respectively.

The other variables are defined in Chapters 3 and 4.

Kalman filter for the system (5.28) is [20]:

Let C(0) be the initial error covariance and W(0) the initial weight.

weight extrapolation

$$\bar{\mathbf{W}}^-(t)=\mathbf{F}(t-1)\bar{\mathbf{W}}^+(t-1)$$

error covariance extrapolation

$$\mathbf{C}^-(t)=\mathbf{F}(t-1)\mathbf{C}^+(t-1)\mathbf{F}^T(t-1)+\mathbf{Q}(t-1)$$

Kalman gain

$$\mathbf{K}(t)=\mathbf{C}^-(t)\mathbf{G}^T(t)\left[\mathbf{G}(t)\mathbf{C}^-(t)\mathbf{G}^H(t)+\mathbf{R}(t)\right]^{-1} \tag{5.29}$$

weight update

$$\bar{\mathbf{W}}^+(t)=\bar{\mathbf{W}}^-(t)+\mathbf{K}(t)\left[\mathbf{Y}(t)-\mathbf{G}(t)\bar{\mathbf{W}}^-(t)\right]$$

error covariance update

$$\mathbf{C}^+(t)=\left[\mathbf{I}-\mathbf{K}(t)\mathbf{G}(t)\right]\mathbf{C}^-(t)$$

Example 3

Here 20 users uniformly distributed within one cell are assumed. The beamforming is assumed in the uplink at the BS with 4 antenna elements. Figure 5.4 shows the transmitted power for a randomly selected user. In the first case, Kalman filter for the power control and beamforming is utilized. In the second case, Kalman filter is used for only power control and an omni-directional antenna has been assumed at the BS. The simulation demonstrates (Figure 5.4) that in the case of joining the power control and beamforming the algorithm becomes considerably faster with much less power. Figure 5.5 shows the CIR for a randomly selected user in three different scenarios. It indicates that in CDMA systems using power control alone is better than using spatial processing without power control. Joining both power control and spatial processing can

considerably enhance the capacity and the available resources by increasing the achieved CIR.

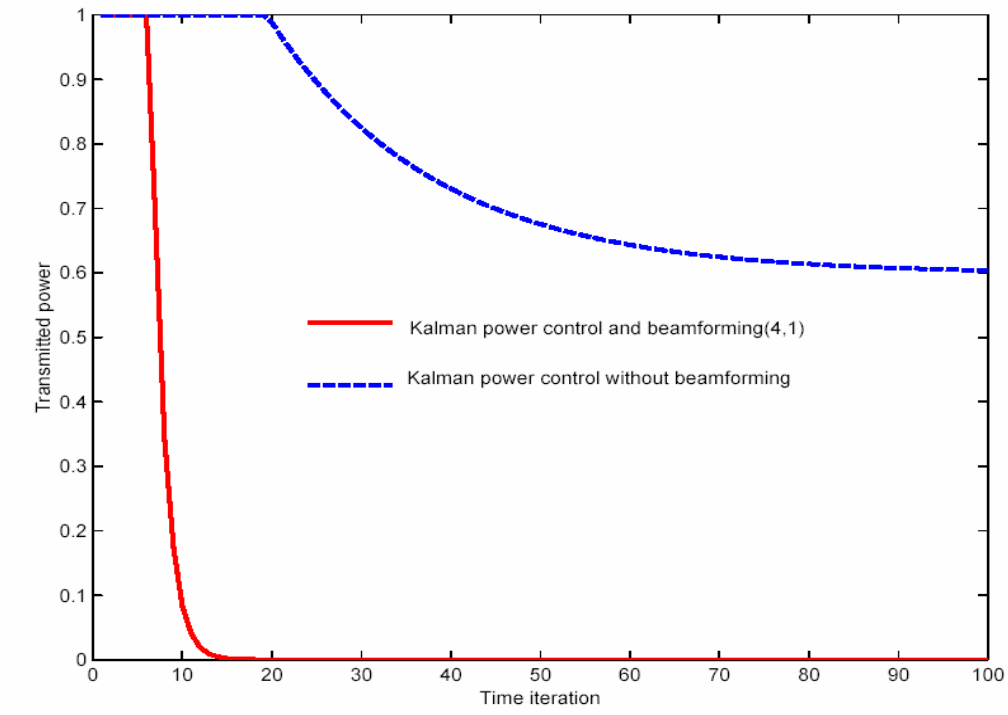

Figure 5.4. Transmitted power of Kalman power control and beamforming

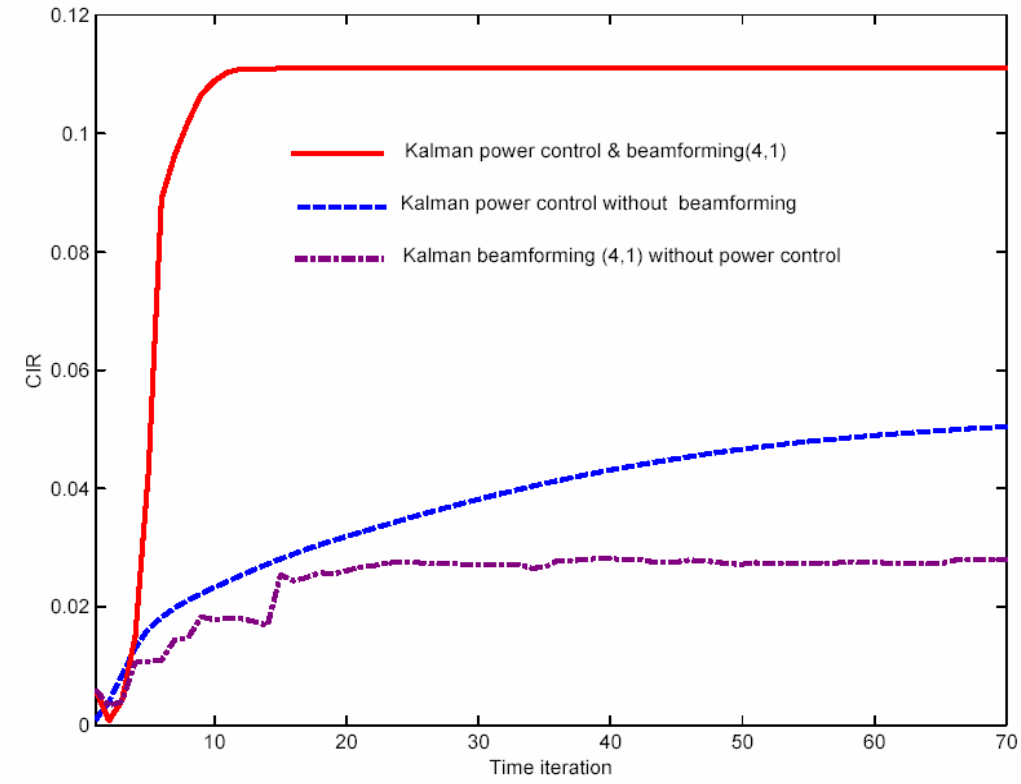

Figure 5.5. CIR of Kalman power control and beamforming

5.3.2 Influence of Smart Antenna Systems on the Performance of Radio Resource Scheduling in CDMA Cellular Systems

In this Section we are going to propose a pseudo code to join the smart antenna (at the BS) and the RRS of the uplink in cellular communication system. Some of the UMTS standards will be followed. A chip level cellular CDMA simulator has been written to examine the system performance. Including more realistic channel models into the simulation indicates that many results in the literature about the smart antenna performance are very optimistic [115]-[116]. The reason for obtaining these dramatic enhancements is due to the simple channel models which have been used. When we assume more realistic channel parameters in our simulator like the multi-path, Doppler, phase offset, different mobile speeds, and time varying environment, a fair improvement in the RRS performance is obtained.

The uplink dedicated channel structure is shown in Figure 5.6 [64]. The Dedicated Physical Data Channel (DPDCH) and the Dedicated Physical Control Channel (DPCCH) are I/Q multiplexed. The power is updated in slot by slot basis. Since the time width of the slot is 0.6667 ms, then the power adaptation rate is 1500 Hz. The information of the used Processing Gain (PG) is distributed through 15 slots which form the frame. The PG is defined as the chip rate to the data rate. The time width of the frame is 15×0.6667ms=10 ms which means that the data rate can be updated every 10 ms. The rate information is sent with Transport Format Combination Indicator (TFCI). If the TFCI is not decoded correctly, the whole data frame is lost [64]. The DPCCH consists of 4 fields as Pilot bits, TFCI, Transmission Power Control (TPC) bits, and FeedBack Information (FBI) bits. More detailed explanation can be found in [64]. Without loss of generality we propose the GMVDR algorithm to compute the optimum weights of antennas. Generally speaking any other algorithm can be used with minor modifications. As shown in Figure 5.7, the antenna weights are adapted by taking samples from the base band signal at each antenna element. These samples are used to construct the covariance matrix which is used to solve the GMVDR problem. Briefly, in UMTS systems, the data symbols are spread using orthogonal spreading codes. The chip rate is 3.84 Mb/s. The processing gain is variable and depending on the required data rate and the link condition. In the UMTS the uplink PG can take any value in the following set {4,8,16,32,64,128,256}. The highest data rate is achieved at the minimum PG as 3.84/4

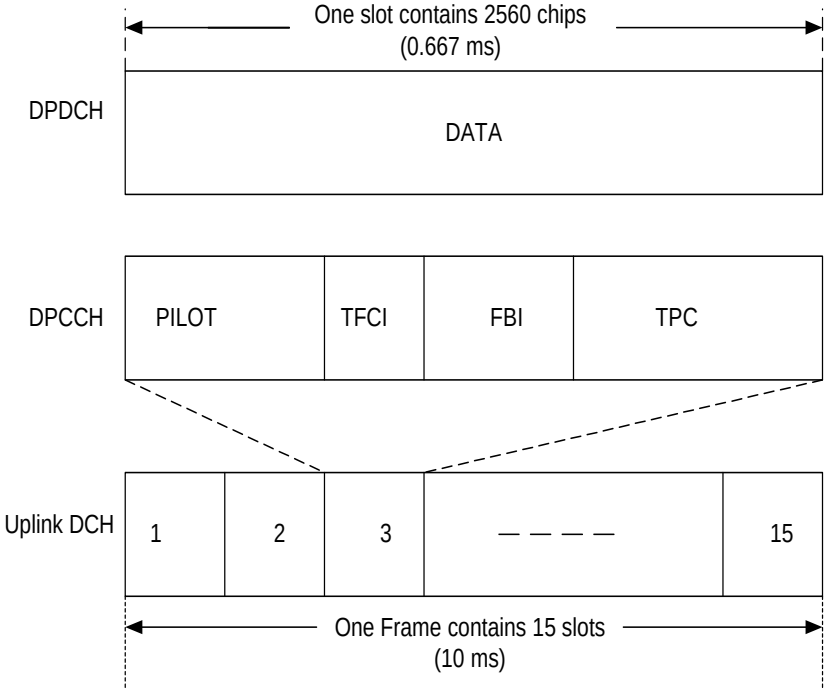

Figure 5.6. Uplink dedicated channel structure

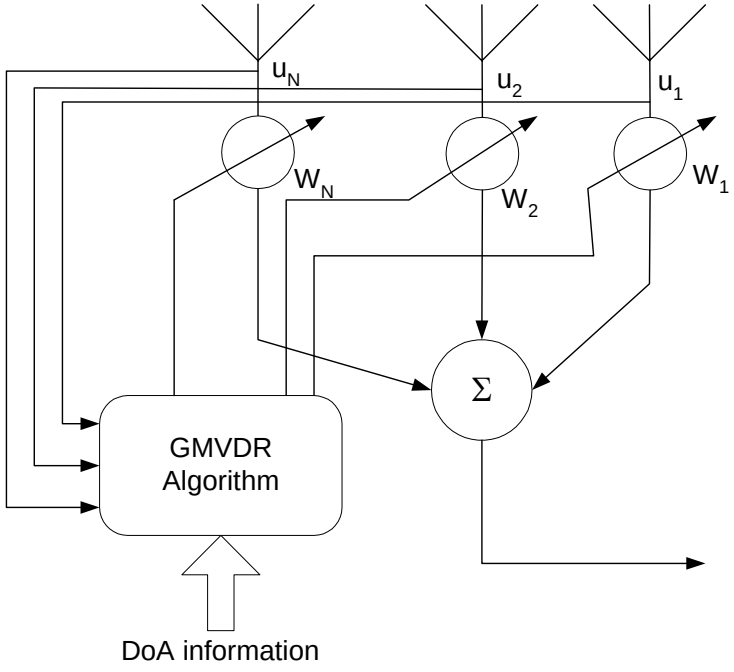

Figure 5.7. The antenna configuration

Mb/s=960 Kb/s. The slowest data rate is obtained at the maximum PG as 3.84/256 Mb/s=15 Kb/s. Reducing the PG will enhance the transmitted data rate but will reduce the received signal to interference ratio (SINR) as well. The relation between the SINR and the PG can be described as

$$\delta_i(t) = PG_i(t) \times \Gamma_i(t), \qquad t = 0,1,... \tag{5.30}$$

where $\delta_i(t)$ is the signal to interference ratio of user i at iteration t, and the $\Gamma_i(t)$ is the CIR.

Next we introduce the pseudo-code for joining the RRS and smart antenna. We assumed in this procedure that all users try to send at the highest possible rate.

1) *Start with random initial power P(0)=Po , and with maximum PG=256.*
2) *Estimate the CIR from the feedback information in the time slot, then update the transmitted power according to one of power control algorithms such as (3.45) (with maximum power constraints).*
3) *Construct the auto-covariance matrix according to (4.25) for one time slot.*
4) *Estimate the DoA of the desired user then update the antenna weights using one of the adaptation algorithms such as (4.66).*
5) *At the end of each 15 time slots (time frame) average previous frame CIR (with some weighting in order to make higher weights for recent time slots CIR) then update the transmitted rate according to one of rate adaptation algorithms such as (3.46) and (3.47).*
6) *Goto step 2.*

The previous steps concentrate on the adaptation process of three main parameters. The parameters are the transmitting power, the transmitting data rate, and the antenna weights.

Example 4

Two scenarios are examined in this example. In all simulated scenarios multi-path frequency selective channel is assumed. A zero mean additive white noise with variance 10^{-10} is assumed. The processing gain is selected according to the UMTS standard. The maximum access delay is taken to be 350 ns. The maximum number of paths is 3, and the maximum user speed is 5 Km/h. The maximum transmitted power of users is 1 W. In the first scenario we assume one cell with 10 users. The MODPRC algorithm is used as the

RRS. The tradeoff factors have been selected as $\lambda_1 = 0.01,\ \lambda_2 = 0.9,$ and $\lambda_3 = 0.09$. The antenna at MS is omni-directional antenna. The configuration of the users and the BS is shown in Figure 5.8. From Figure 5.8 it is clear that user 1 is very close to the BS. The number of antenna elements at the base station is 2. The simulation has been run for 350 slots which is equivalent to 0.23 second. Figure 5.9 shows the transmitted power of the best user (user 1) and worst user (user 5) and the average transmitted power of all users. The average transmitted power is 0.87 W. Figure 5.10 shows the transmitted data rate of the best user (user 1) and worst user (user 5) and the average data rates of all users. The average transmitted data rate in this scenario is 59.25 Kbps.

In the second scenario we have assumed 4 antennas at the base station. The users' configuration is the same as in the first scenario to have fair comparison. The same tradeoff factors are used as well. The transmitted power is shown in Figure 5.11. It is clear that the transmitted power of user 1 as well as the average transmitted power has been reduced when compared with omni-directional case. The transmitted power of user 5 is still at the maximum power (1 W), but his data rate has increased 4 times as shown by Figure 5.12. The average transmitted power in this scenario is 0.59 W. The average transmitted data rate in this scenario is 103.23 Kbps. Comparing the first and second scenario we can see that the average transmitted power of the second scenario has been reduced by more than 30 % and the average data rate is increased by more than 74%. Fewer fluctuations in the data rate are observed when using multi-antenna system than omni-directional antenna.

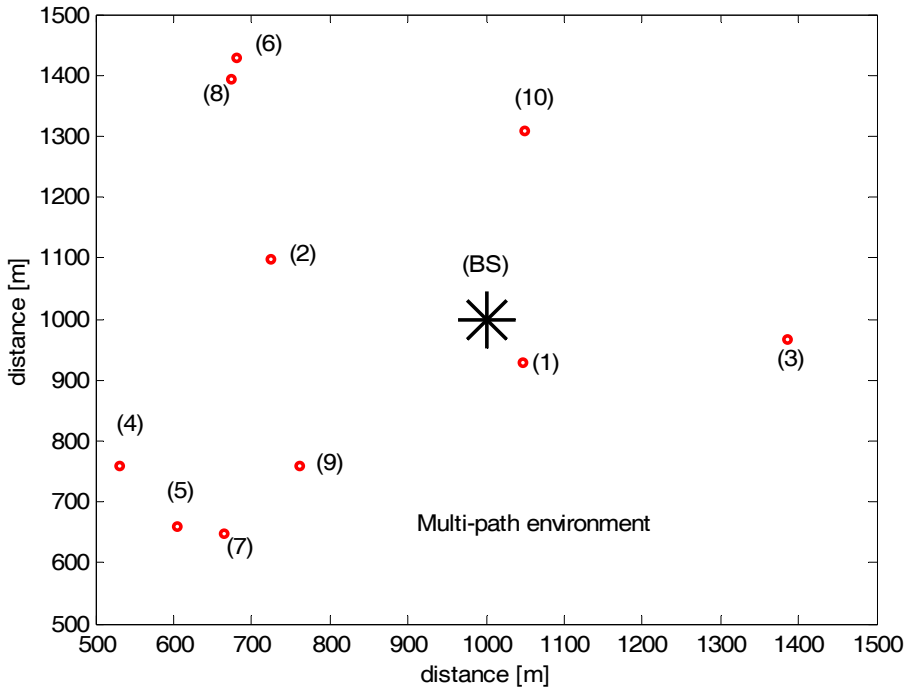

Figure 5.8. The configuration of the users in the cell.

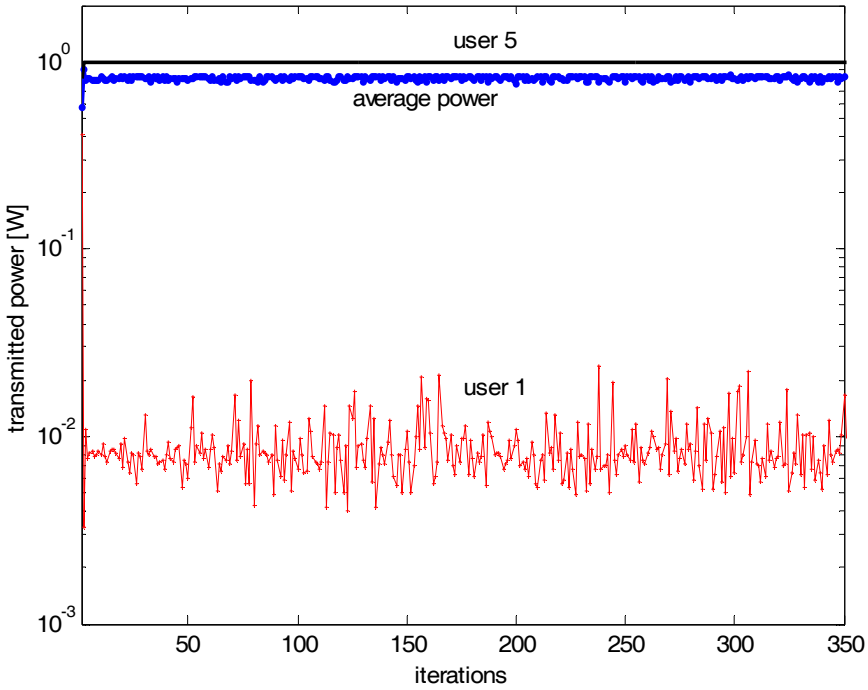

Figure 5.9. The transmitted power of first scenario

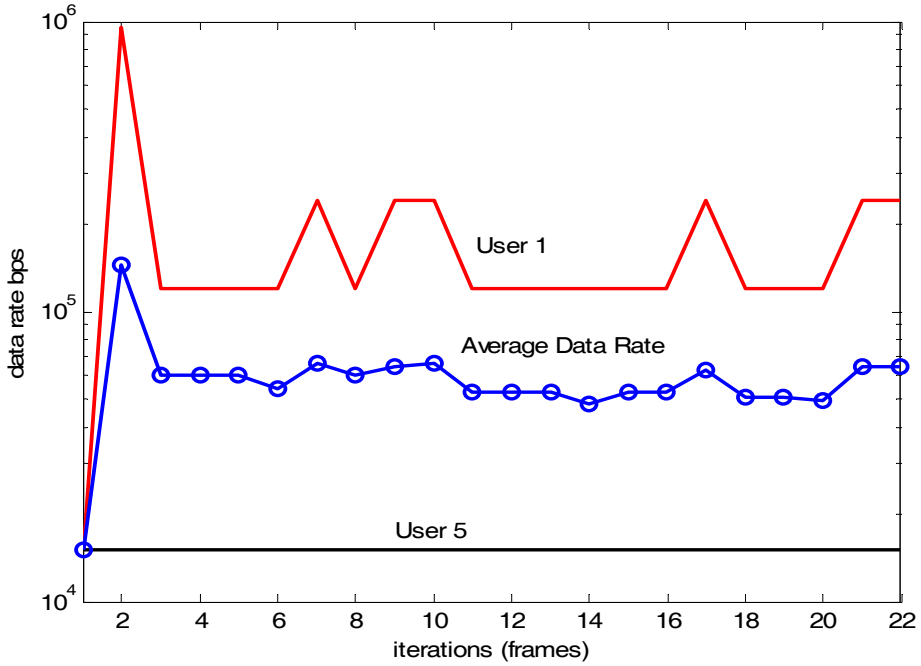

Figure 5.10. The data rate of first scenario.

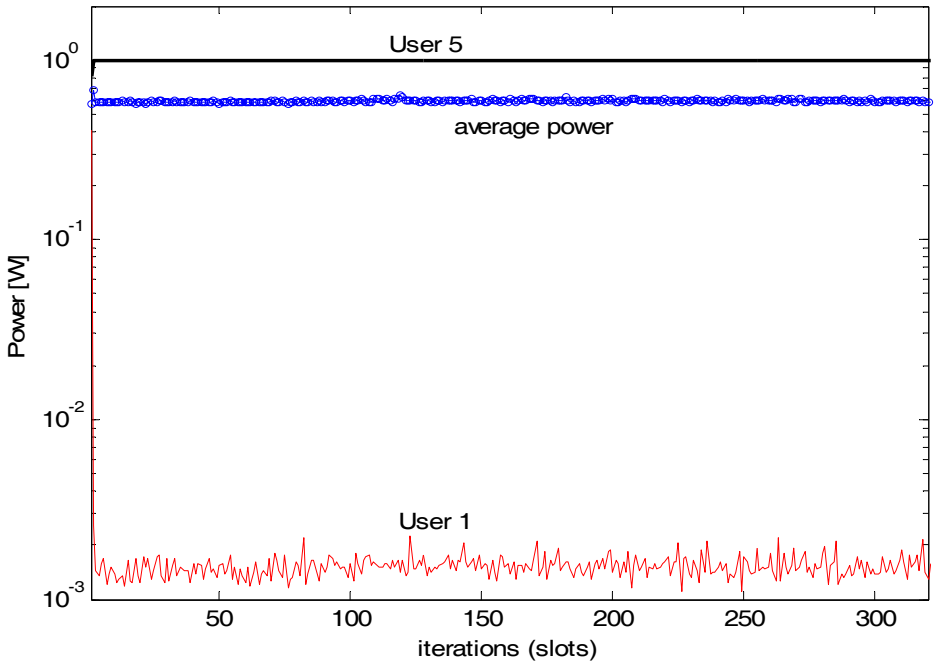

Figure 5.11. The transmitted power of second scenario.

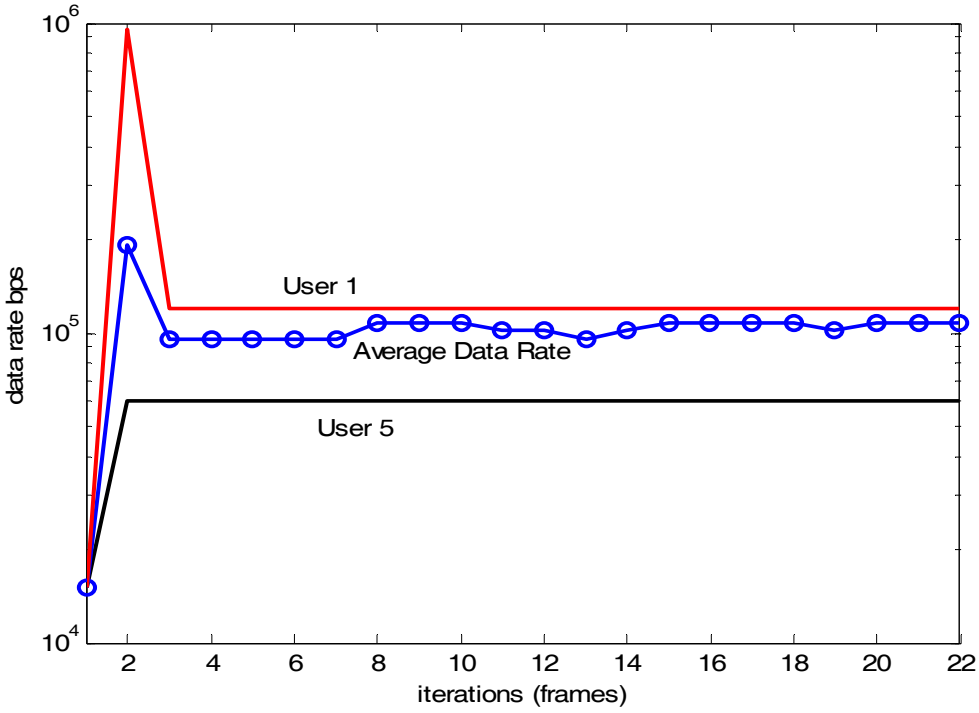

Figure 5.12. The data rate of second scenario.

CHAPTER SIX

CONCLUSIONS

Two different subjects have been studied in this thesis. The first subject is the radio resource scheduler, and the second is smart antennas. Both are very important subjects in multi-user wireless communication systems. Novel algorithms have been proposed in both subjects and also in joining them.

The mobile communication channel is shared by many users at the same time. To maximize the capacity as well as the performance, the radio resources should be wisely divided between users. The radio resource scheduler takes the responsibility to address the optimum transmitted power and data rate of each radio terminal. The network situation and the QoS requirements of each user should be taken into consideration during the optimization process. The RRS problem has been treated in two different situations. In the first situation the data rate is assumed to be fixed, so the RRS problem is reduced to power control. In the second situation the RRS problem is the combined power and rate control. The first contribution area of this thesis is the application of Multi-Objective optimization methods in RRS (fixed and variable rate). The Multi-Objective optimization is a very strong tool in optimizing different and conflicted objectives, which makes it powerful method for RRS. Our work is the first in the literature to suggest using analytical multi-objective optimization to solve these types of problems. Three new algorithms have been proposed based on MO optimization. The first one is the Multi-Objective Distributed Power Control (MODPC) algorithm, which is presented in Section (2.7). The MODPC algorithm has been derived by minimizing an error function of two objectives. The first objective is to minimize the transmitted power and the second objective is to minimize the outage. One of the benefits of the MODPC algorithm is that the snapshot assumption is not necessary during the problem formulation. The MODPC algorithm is easy to implement and the simulations show that it is faster than all other studied conventional algorithms. The analytical analysis shows its superiority in convergence speed compared with other algorithms presented in the literature. Simple but

efficient tuning method of the tradeoff factors is introduced. The MODPC algorithm has been extended to include the data rate in the objectives. A new algorithm has been obtained which is called Multi-Objective Distributed Power and Rate Control (MODPRC) algorithm. This algorithm has also the same benefits as the MODPC algorithm (Section 3.8.1). In MODPRC algorithm, the MO optimization is formulated to achieve the following objectives:

1. Minimize the total transmitting power.
2. Achieve the target SNR in order to get certain BER level (depends on the application).
3. Maximize the fairness between users. In our definition, the system is fair as long as each user is supported by at least his minimum required QoS. In this sense, minimizing the outage probability leads to maximizing the fairness.
4. Maximize the transmitted data rate or at least achieve the minimum required data rate.

The tradeoff between objectives can be carried out by choosing the values of the tradeoff factors. Intensive simulations have been performed to compare the performance of the MODPRC algorithm with other algorithms. The third algorithm is the Maximum Throughput and Minimum Power Control (MTMPC) algorithm. In this part we have constructed a centralized power control algorithm based on the tradeoff between the maximization of the total throughput of the users and the minimization of their total transmitted power in cellular systems. Power control algorithm for total throughput maximization has been proposed in [74]. In our algorithm, we use the same throughput maximization objective, but another objective for power minimization has been added. The Multi-objective optimization problem is solved using *weighting method*. A centralized power control algorithm is obtained. The simulations show that at low additive white noise levels the total transmitted power can be reduced up to 95% compared with the algorithm given in [74] while the total throughput is reduced only by less than 3%. This subject is treated in Section 3.8.3. One of the main disadvantages of using MO optimization method is the tuning of the tradeoff factors. The optimum tradeoff factors depend on the required solution. The MODPC algorithm and the MODPRC algorithm like other conventional algorithms assume perfect estimation of the CIR. This is not feasible in existing and near future systems. Only few bits are sent in feedback

channel from BS to MS to represent the CIR. A new algorithm to estimate the actual CIR from the power control ON-OFF commands has been proposed. The MO algorithms are modified to be used with this estimated CIR rather than the perfect one. Two modified algorithms have been obtained, which are the Multi-Objective Totally Distributed Power Control (MOTDPC) algorithm and the Multi-Objective Totally Distributed Power and Rate Control (MOTDPRC) algorithm. The CIR estimation algorithm has been combined with the distributed power control algorithm to obtain a new algorithm called Estimated Step Power Control (ESPC) algorithm. This algorithm has been compared with the Fixed Step Power Control (FSPC) algorithm which is used in existing cellular systems. The simulations show that the ESPC algorithm outperforms the FSPC algorithm at slow fading situations at the same signalling level.

The second contribution area is the application of Kalman filters in RRS and in the joining of RRS with smart antenna. Fixed rate and multi-rate power control algorithms have been proposed based on Kalman filters. Our motivation to use Kalman filter is the known fact that Kalman filter is the optimum linear tracking device on the basis of second order statistics. We have formulated the power control problem in state-space form. Kalman filter algorithm has been applied to estimate the optimum transmitted power.

A novel algorithm has been proposed in the adaptation of smart antenna weights. The algorithm is called General Minimum Variance Distortionless Response (GMVDR) algorithm. The GMVDR algorithm is a modification of the MVDR algorithm to be able to look at all directions of the multi-path signal. The upper channel capacity has been investigated in the presence of GMVDR algorithm.

The third part of this thesis is the joining procedure of the smart antenna and RRS. The cellular communication system performance has been investigated in the presence of MIMO smart antennas. General formulation of the optimization problem of joining RRS and smart antennas has been introduced. A simple algorithm based on Kalman filter has been proposed to join smart antennas and multi-rate power control. The influence of the smart antenna on the RRS performance in CDMA systems has been studied and analysed by simulations. The MODPRC is assumed for the RRS and the MVDR for the smart antenna. Multi-paths with different delays, slow fading, and fast fading have been assumed in the simulations. It is observed that smart antenna can clearly enhance the system performance in multi-path channels.

Many research issues can be continued to be studied. These include:

1. Application of analytical MO optimization in communication systems is very rich area and many algorithms can be proposed in different communication fields.
2. The design of the decision maker which selects the required solution from the Pareto optimal set has not been studied in this thesis. By studying this part one may find a more efficient way to tune the tradeoff parameters.
3. The applications of the proposed algorithms in infrastructureless systems such as ad hoc networks [114].
4. More analysis can be done for the applications of Kalman filters in radio resource schedulers to obtain more efficient algorithms.
5. Sub-optimal solutions can be obtained by solving the optimization problem in Section 5.3.
6. The ESPC algorithm (Section 2.4.7) performance can be considerably enhanced by using adaptive step size. Research activities are going on for this issue.
7. The performance of the derived GMVDR (Section 4.3.1) can be investigated by comparing it with other temporal-spatial algorithms for frequency selective channels.
8. Dropping algorithms (joined with adaptive antennas) which maximize the total throughput in CDMA cellular downlink is interesting topic to be continued [102],[117].

APPENDIX

1) INTRODUCTION TO MULTI-OBJECTIVE OPTIMIZATION TECHNIQUES

MO optimization is a method to find the best solution between different, usually conflicting objectives. In the MO optimization problem we have a vector of objective functions. Each objective function is a function in the decision (variable) vector. The mathematical formulation of the MO optimization problem is [77][96]:

Find

$$\begin{aligned} &\min \left\{ f_1(\mathbf{x}), f_2(\mathbf{x}), ..., f_m(\mathbf{x}) \right\} \\ &\text{subject to } \mathbf{x} \in \mathbf{S} \end{aligned} \tag{A.1}$$

where we have *m* (≥ 2) objective functions $f_i : \Re^n \to \Re$, $\mathbf{x}$ is the decision (variable) vector belonging to the (nonempty) feasible region (set) S, which is a subset of the decision variable space $\Re^n$. The abbreviation min means that we want to minimize all the objectives simultaneously. Usually the objectives are at least partially conflicting and possibly incommensurable. This means that, in general there is no single vector $\mathbf{x}$, which can minimize all the objectives simultaneously. Otherwise, there is no need to consider multiple objectives. Because of this, MO optimization is used to search for efficient solutions that can best compromise between the different objectives. Such solutions are called non-dominated or Pareto optimal solutions.

Definition 1 [77]

A decision vector $\mathbf{x}^* \in S$ is Pareto optimal, if there does not exist another decision vector $\mathbf{x} \in S$ such that $f_i(\mathbf{x}) \leq f_i(\mathbf{x}^*)$ for all i = 1,2,..,m and $f_j(\mathbf{x}) < f_j(\mathbf{x}^*)$ for at least one index j.

The Pareto optimal set is a set of all possible (infinite number) Pareto optimal solutions.

The condition of optimal Pareto set is rather strict and many MO algorithms can not guarantee to generate Pareto optimal solutions but only weak Pareto optimal solutions. Weak Pareto optimal solutions can be defined as follows:

Definition 2 [77]

A decision vector $\mathbf{x}^* \in S$ is a weakly Pareto optimal if there does not exist another decision vector $\mathbf{x} \in S$ such that $f_i(\mathbf{x}) < f_i(\mathbf{x}^*)$ for all i = 1,2,..,m.

The set of (weak) Pareto optimum solutions can be nonconvex and nonconnected.

Figure A.1 shows the geometric interpretation of Pareto optimal and weakly Pareto optimal solutions. Note that all points on the line segment between points A and B are weakly Pareto optimal solutions. All points on the curve between points B and C are Pareto optimal solutions. Also the following example illustrates the main concepts of Pareto optimal and weakly Pareto optimal solutions.

Example 1:

Table A.1 shows the results of MO optimization of three objectives. The objectives are minimizing BER, packet delay and the power consumption. It is clear that the first solution is dominated by any other solution. The BER of the 3rd solution is better than the BER of the 1st solution, but the packet delay as well as the power consumption of the 1st solution is better than that of the 3rd solution. In that sense all 1st, 2nd, and 3rd solutions are Pareto optimal. The 4th solution is weakly Pareto optimal. The 5th solution is not Pareto optimal solution because it is dominated by the 1st solution.

After the generation of the Pareto set, we are usually interested in one solution of this set. This solution is selected by the decision maker. In Example 1, the decision maker will select the 2nd solution, if the power consumption is the most important objective. If the objective is to select the solution with a low power consumption as well as low BER, then the 1st solution is preferred. The main point now is how to find the Pareto optimal or even weakly Pareto optimal solutions. There are many techniques to find the (weakly) Pareto optimal solutions [77]; [96]. Using soft-computing methods such as genetic algorithm is one way to solve this kind of problems [89]. In this appendix we will concentrate on the analytical solutions of the MO optimization problems. Most of the MO optimization methods are based on converting the MO functions to a single objective problem. Two different MO optimization techniques are discussed in this appendix. The first method is called the Weighting Method. The weighting method transforms the problem posed in (A.1) into

$$\min \sum_{i=1}^{m} \lambda_i f_i(\mathbf{x}) \quad \text{subject to } \mathbf{x} \in S \tag{A.2}$$

where the tradeoff factors λ_i satisfy the following $\lambda_i \geq 0$, $\forall i=1,..,m$ and $\sum_{i=1}^{m} \lambda_i = 1$.

Weakly Pareto optimal set can be obtained by solving the optimization problem (A.2) for different tradeoff factors values [77].

The second MO optimization technique is of special interest in the applications of MO optimization in RRS. It is the method of Weighted Metrics. If the global solutions of the objectives are known in advance, then problem (A.1) can be formulated as

$$\min \left(\sum_{i=1}^{m} \lambda_i \left| f_i(\mathbf{x}) - z_i^* \right|^p \right)^{1/p} \quad \text{subject to } \mathbf{x} \in S \tag{A.3}$$

where $1 \leq p \leq \infty$, z_i^* is the optimum solution of objective i, and the tradeoff factors satisfy the following

$$\lambda_i \geq 0 \text{ , } \forall i=1,..,m \text{ and } \sum_{i=1}^{m} \lambda_i = 1. \tag{A.4}$$

It is clear that (A.3) represents the minimization of the weighted p-norm distance. For p=2 the weighted Euclidean distance is obtained. With p=∞ the problem (A.3) is called weighted Tchebycheff or minmax problem [77][96]. The solutions of (A.3) depend on the p value.

The Tchebycheff problem is called minmax because it takes the form:

$$\min \left\{ \max_{i=1,..,m} \left(\lambda_i \left| f_i(\mathbf{x}) - z_i^* \right| \right) \right\} \quad \text{subject to } \mathbf{x} \in S \tag{A.5}$$

In (A.3), if p=1, the sum of weighted deviations is minimized (becomes equivalent to (A.2) if z_i^* is a global minimum). If p=2, the Euclidean distance is minimized. When p gets larger, the minimization of the largest deviation becomes more and more important [77].

Problem (A.5) is nondifferentiable, which makes the analytical solution not feasible. It can be solved in differentiable form as long as the objective and the constraint functions are differentiable:

$$\begin{aligned} &\min \ \alpha \\ &\text{subject to } \alpha \geq \mathrm{w}_i \left(f_i(\mathbf{x}) - z_i^* \right) \ \ \forall i = 1,...,m, and \\ &\qquad \mathbf{x} \in S \end{aligned} \tag{A.6}$$

We have indicated two simple and efficient methods to solve the MO optimization problems. There are many other methods to solve the MO optimization problems such as Goal Attainment method, Value Function method, Lexicographic ordering method, Interactive surrogate worth tradeoff method,…etc. Many packages to solve the MO optimizations problems are available. Some of them can be downloaded free from internet. Optimization toolbox in Matlab contains algorithms for MO optimization such as the Goal Attainment method.

Example 3:

A simple two objective optimization problem is given as follows

$$\min \left\{ f_1(\mathbf{x}), f_2(\mathbf{x}) \right\} \tag{A.7}$$

where

$$f_1(x) = x^2 - 10x + 26; \ f_2(x) = x^2 - 6x + 9 \tag{A.8}$$

We will show how to solve this with p=1,2, and ∞. The concept of the tradeoff factors is demonstrated as well. It is easy to find the minima of both objectives as $z_1^* = 1$ at x=5 ; $z_2^* = 0$ at x=3. Solving the MO optimization problem (A.3) with p=1 and $\lambda_2 = 1 - \lambda_1$ we obtain the following optimum solution

$$x^* = 2\lambda_1 + 3 \tag{A.9}$$

At $\lambda_1 = 1 \ (\lambda_2 = 0)$ we obtain the optimum solution of the first objective (x=5). As the importance of the second objective increases ($\lambda_2 > 0$) then the optimum solution will move toward the second objective. If both objectives have the same importance then the optimum solution (at p=1) is $x^* = 4$. It is clear that for non-dominated solution points an improvement in one objective requires degradation in the other objective.

Solving this simple example with (p=2 and p= ∞) and when both objectives have same importance, i.e. $\lambda_1 = \lambda_2 = \frac{1}{2}$, we obtain the same optimum solution $x^* = 4$.

Table A.1.

Solutions	BER	Packet delay [ms]	Power consumption [mW]
1	10^{-5}	0.45	176
2	10^{-4}	0.37	138
3	10^{-6}	0.85	286
4	10^{-5}	0.45	185
5	10^{-4}	0.87	179

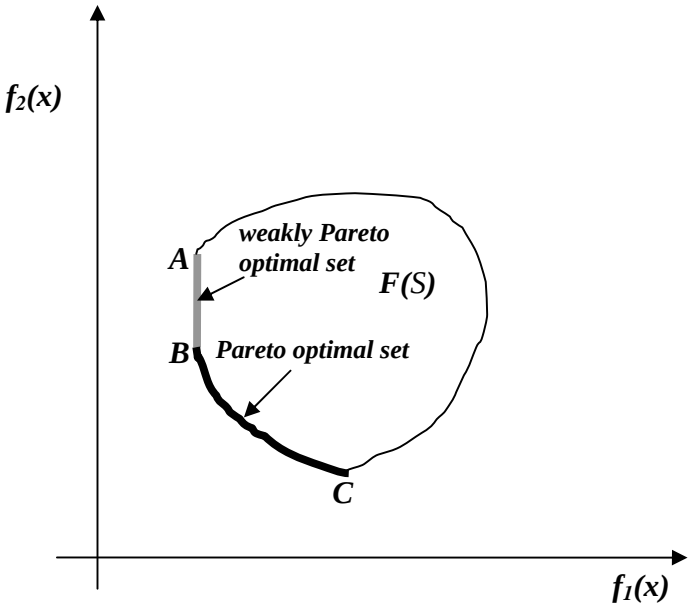

Figure A.1 Pareto and weakly Pareto optimal set

2) SPECTRAL RADIUS COMPARISONS

In this appendix we will prove the results of Section 2.5 in a different way. The result to be proved is $\mathbf{D}^{DBA} > \mathbf{D}^{DPC}$ which means that DPC algorithm is faster than DBA algorithm.

From Section 2.5 the strict convergence condition for any of the studied power control algorithm is

$$\rho\left(\mathbf{D}^{xxx}\right) < 1 \tag{A.10}$$

where $\rho(.)$ is the spectral radius, $\mathbf{D}^{xxx}$ refers to **D** matrix of any of the studied algorithms in Section 2.5.

From (2.136) and (2.137) one can say that

$$\mathbf{D}^{DBA} = \frac{\Gamma^T}{1+\Gamma^T}\left[\frac{1}{\Gamma^T}\mathbf{D}^{DPC} + \mathbf{I}\right] \tag{A.11}$$

It is well known that for any non-negative matrices **A** and **B**

$$\rho\left(\mathbf{A}+\mathbf{B}\right) \le \rho\left(\mathbf{A}\right) + \rho\left(\mathbf{B}\right) \tag{A.12}$$

and at **B**=*a***I,** (A.12) is held with equality such as

$$\rho\left(\mathbf{A}+a\mathbf{I}\right) = \rho\left(\mathbf{A}\right) + a \tag{A.13}$$

where *a* is a scalar.

Then from (A.11) and (A.12)

$$\rho\left(\mathbf{D}^{DBA}\right) = \frac{1}{1+\Gamma^T}\rho\left(\mathbf{D}^{DPC}\right) + \frac{\Gamma^T}{1+\Gamma^T} \tag{A.14}$$

Assume that

$$\rho\left(\mathbf{D}^{DBA}\right) = \varepsilon\rho\left(\mathbf{D}^{DPC}\right) \tag{A.15}$$

where

$$0 < \varepsilon \le 1 \tag{A.16}$$

Substitute (A.15) into (A.14) to obtain

$$\rho\left(\mathbf{D}^{DPC}\right) = \frac{\Gamma^T}{\varepsilon + \varepsilon\Gamma^T - 1} \tag{A.17}$$

To be restricted with convergence condition (A.10) then

$$\frac{\Gamma^T}{\varepsilon+\varepsilon\Gamma^T-1}<1 \tag{A.18}$$

It is clear that to achieve the inequality (A.18) then the value of ε should be greater than one (ε>1). This result contradicts with (A.16). This means that the spectral radius of DBA algorithm (at $\beta=\frac{\Gamma^T}{1+\Gamma^T}$) is always greater than the spectral radius of the DPC algorithm. This result is compatible with the obtained results in Section 2.5.

The same procedure can be followed to prove the other results.

BIBLIOGRAPHY

[1] J. Zander, "Distributed cochannel interference control in cellular radio systems," *IEEE Trans. Veh. Technol.,* vol. 41, pp. 305─311, Aug. 1992.

[2] S. Grandhi, R. Vijayan, and D. Goodman, "Distributed power control in cellular radio systems," *IEEE Trans. Commun.,* vol. 42, pp. 226─228, Feb.─Apr. 1994.

[3] T. Lee, and J. Lin, "A fully distributed power control algorithm for cellular mobile systems," *IEEE Trans. Commun.,* vol. 14, pp. 692─697, May 1996.

[4] G. Foschini, and Z. Miljanic, "A simple distributed autonomous power control algorithm and its convergence", *IEEE Trans. Veh. Technol.,* vol. 42, pp. 641─646, Nov. 1993.

[5] F. Gantmacher, *The Theory of Matrices*. Vol. 2, Chelsea Publishing Company, 1964.

[6] S. Grandhi, and J. Zander, "Constrained power control in cellular radio systems," in *Proc. IEEE Vehicular Technology Conf.,* vol. 2, Piscataway, USA, June 1994, pp. 824─828.

[7] R. Yates, "A framework for uplink power control in cellular radio systems," *IEEE J. Select. Areas Commun.,* vol. 13, pp. 1341─1347, Sep. 1995.

[8] A. El-Osery and C. Abdallah, "Distributed power control in CDMA cellular systems," *IEEE Antenna and Prop. Magazine*, vol. 42, pp. 152─159, Aug. 2000

[9] R. Jäntti and S. Kim, "Second-order power control with asymptotically fast convergence," ," *IEEE J. Select. Areas Commun.,* vol. 18, pp. 447─457, Mar. 2000.

[10] F. Farrokhi, L. Tassiulas, and K. Liu, "Joint optimal power control and beamforming in wireless networks using antenna arrays," *IEEE Trans. Commun.,* vol. 46, pp.1313─1324, Oct. 1998.

[11] L. Godara, "Application of antenna array to mobile communications, part II: beam-forming and direction of arrival considerations," *Proc. IEEE*, vol.85, pp.1195─1245, Aug.1997.

[12] J. Liberti, T. Rappaport, *Smart antennas for wireless communications*, Prentice Hall, 1999.

[13] R. Choi, K. Letaief,and R. Murch, "MIMO CDMA Antenna Systems," *in Proc. IEEE ICC*, New Orleans, USA, June 2000, pp. 990─994.

[14] Y. Liang, F. Chin, and K. Liu, "Downlink beamforming for DS-CDMA mobile radio with multimedia services," *IEEE Trans. Commun.,* vol. 49, pp.1288─1298, July 2001.

[15] K. Kim and S. Saunders, "New adaptive beamforming algorithm employing forward/backward averaging and signal enhancement scheme," *IEEE Commun. Lett.*, vol. 5, pp.98─100, Mar. 2001.

[16] M. Agrawal and S. Prasad, "Robust adaptive beamforming for wide-band moving and coherent jammers via uniform linear arrays", *IEEE Trans. Antennas Propagat*., vol. 47, pp. 1267─1275, Aug. 1999.

[17] S. Choi and D. Yun, "Design of an adaptive array for tracking the source of maximum power and its application to CDMA mobile communication," *IEEE Trans. Antennas Propagat*., vol. 45, pp. 1393─1404, Sep. 1997.

[18] A. Veen, F. Depraettere, and A. Swindlehurst, "Subspace-based signal analysis using singular value decomposition," *Proc. IEEE*, vol.81, pp. 1277─1308, Sep.1993.

[19] J. Candy, *Signal Processing- the modern approach*, McGraw-Hill, 1987.

[20] M. Grewal and A. Andrews, *Kalman Filtering*. Prentice Hall, 1993.

[21] S. Haykin, A. Sayed, J. Zeidler, P. Yee, and P. Wei," Adaptive tracking of linear time-variant systems by extended RLS algorithms," *IEEE Trans. Signal Processing,* vol. 45, pp. 1118─1128, May. 1997.

[22] Y. Chen and C. Chiang, "Adaptive beamforming using the constrained Kalman filter," *IEEE Trans. Antennas Propagat*., vol. 41, pp. 1576─1580, Nov. 1993.

[23] T. Lim, L. Rasmussen, and H. Sugimoto, "An asynchronous multiuser CDMA detector based on the Kalman filter," *IEEE J. Select. Areas Commun.*, vol. 16, pp. 1711─1722, May 1998.

[24] J. Proakis, *Digital Communications*, McGraw-Hill, 3rd ed. 1995.

[25] R. Yates, S. Gupta, C. Rose and S. Sohn, "Soft Dropping Power Control," in *Proc. IEEE Vehicular Technology Conf.,* Phoenix, USA , May 1997, pp.1694─1698

[26] F.Berggren, R. Jantti and S. Kim, " A generalized algorithm for constrained power control with capability of temporary removal," *IEEE Trans. Veh. Technol.*, vol. 50, pp. 1604─1612, Nov. 2001.

[27] C. Balanis, "Antenna theory: a review," *Proc. of the IEEE*, Vol. 80, pp. 7 –23, Jan. 1992.

[28] A. Naguib A.Paulraj,and T. Kailath, "Capacity improvement with base-station antenna arrays in cellular CDMA,", *IEEE Trans. Veh. Technol.*, vol. 43, pp.691─698, Aug. 1994.

[29] K. Bell, Y. Ephraim, H. Van Trees, "A Bayesian approach to robust adaptive beamforming," *IEEE Trans. Signal Processing,* vol. 48, pp. 386–398, Feb. 2000.

[30] Y. Wang and J.R. Cruz, "Adaptive antenna arrays for the reverse link of CDMA cellular communication systems," *IEE Electron. Lett.*, vol. 30, pp.1017─1018, Jun.1994.

[31] W. Youn and C. UN, "Eigenstructure method for robust array processing," *IEE Electron. Lett.*, vol. 26, pp.678─680, Jun.1990.

[32] S. Kwon, I. Oh, and S. Choi, "Adaptive beamforming from the generalized eigenvalue problem with a linear complexity for a wideband CDMA channel," in *Proc. IEEE Vehicular Technology Conf.,* Amsterdam, Netherlands, Sep. 1999, pp.1890 ─1894.

[33] J. Kim and J. Cioffi, "Spatial multiuser access with antenna diversity using singular value decomposition," *Proc. IEEE ICC*, New Orleans, USA, June 2000, pp. 1253─1257.

[34] A. Haimovich and Y. Bar-Ness, "An eigenanalysis interference canceler," *IEEE Trans. Signal Processing,* vol. 39, pp. 76─48, May 1991.

[35] L.Shang and E. Geraniotis, "An eigenvalue decomposition and interference cancellation array processing algorithm for low mobility CDMA communications," *in Proc. IEEE Signal Processing Workshop*, Paris, France, April 1997, pp. 205 ─ 208.

[36] Z. Rong, T. Rappaport, P. Petrus,and J. Reed, "Simulation of multitarget adaptive array algorithms for wireless CDMA systems" in *Proc. IEEE Vehicular Technology Conf.,* Phoenix, USA , May 1997, pp. 1─5.

[37] F. Farrokhi, G. Foschini, A. Lozano, and R. Valenzuela, "Link-optimal space-time processing with multiple transmit and receive antennas," *IEEE Commun. Lett.*, vol.5, pp. 85─87, Mar. 2001.

[38] P. Karaminas and A. Manikas, " Super-resolution broad null beamforming for cochannel interference cancellation in mobile radio networks", *IEEE Trans. Veh. Technol.,* vol. 49, pp. 689─696, May 2000.

[39] K. Leung, "Power control by Kalman filter with error margin for wireless IP networks," *in Proc. Wireless Commun. Networking Conf.*, Chicago, USA, Sep. 2000, pp.980─985.

[40] A. Mercado and K. Liu, "Adaptive QoS for mobile multimedia applications using power control and smart antenna," in *Proc. IEEE ICC*, New Orleans, USA, June 2000, pp. 60─64

[41] L. Milstein, "Wideband code division multiple access," *IEEE J. Select. Areas Commun.*, vol. 18, pp.1344─1354, Aug.2000

[42] P. Viswanath, V. Anantharam, and D. Tse, "Optimal sequences, power control, and user capacity of synchronous CDMA systems with linear MMSE multiuser receivers," *IEEE Trans. Inform. Theory*, vol.45, pp.1968─1983, Sep.1999

[43] A. Naguib, "Power control in wireless CDMA: performance with cell site antenna arrays," in *Proc. GLOBECOM*, Singapore , Nov. 1995, pp. 225─229

[44] S. Choi and D. Shim, "A novel adaptive beamforming algorithm for a smart antenna system in a CDMA mobile communication environment," *IEEE Trans. Veh. Technol.,* vol.49, pp. 1793─1806, Sep.2000

[45] S. Kandukuri and S. Boyd, "Optimal power control in interference-limited fading wireless channels with outage-probability specifications," *IEEE Trans. Wireless Commun.*, vol.1, pp. 46─55, Jan. 2002.

[46] C. Dietrich, W. Stutzman, B. Kim, and K. Dietze, "Smart antennas in wireless communications; base-station diversity and handset beamforming," IEEE Antenna and Prop. Mag., vol.42, No.5 pp. 142─151, Oct. 2000.

[47] C. Shannon, "A mathematical theory of communication," *Bell Sys. Tech. J.,* vol.27, pp. 379─423, 623─656, Jul.─Oct, 1948.

[48] G. Foschini and M. Gans, "On limits of wireless communications in a fading environment when using multiple antennas," *Wireless Personal Commun*., vol.6, pp. 311─335, Mar. 1998.

[49] A. Papoulis, *Probability, random variables, and stochastic processes*. New York: McGraw-Hill, 1991.

[50] S. Haykin, *Communication Systems*, Wily, 2001.

[51] S. Hanly and P. Whiting, "Information-theoretic capacity of multi-receiver networks," *Telecommun. Syst.*, vol. 1, pp. 1─42, 1993

[52] E. Telatar, "Capacity of multi-antenna Gaussian channels," *AT&T Bell labs Internal Tech. Memo*., June 1995

[53] S. Jafar, S. Vishwanath and A. Goldsmith, "Channel capacity and beamforming for multiple transmit and receive antennas with covariance feedback," in *Proc. IEEE ICC*, Helsinki, Finland, June 2001, pp. 2266─2270.

[54] E. Biglieri, J. Proakis and S. Shamai, "Fading channels: information-theoretic and communications aspects," *IEEE Trans. Inform. Theory,* vol.44, pp. 2619─2692, Oct. 1998.

[55] M. Elmusrati and H. Koivo, "A comparison study of smart antenna adaptation techniques for CDMA," in *Proc. URSI XXVI*, Tampere, Finland, Oct.2001.

[56] R. Jäntti., *Power control and transmission rate management in cellular radio systems*, PhD thesis, Control Engineering Laboratory, Helsinki University of Technology, Finland, 2001.

[57] Y. Liang, F. Chin, and A. Kot, "Adaptive beamforming and power control for DS-CDMA mobile radio communications," in *Proc. IEEE ICC*, Helsinki, Finland, June 2001, pp. 1441 ─1445.

[58] A. Yener, R. Yates, and S. Ulukus, "Interference management for CDMA systems through power control, multiuser detection, and beamforming," *IEEE Trans. Commun.*, vol.49, pp.1227─1239, July 2001.

[59] B. Suard, G. Xu, H. Liu, and T. Kailath, "Uplink channel capacity of space-dicision-multiple access schemes," *IEEE Trans. Inform. Theory*, vol.44, pp.1468─1476, July 1998.

[60] J. Chang, L. Tassiulas and F. Farrokhi, "Joint transmitter receiver diversity for efficient space division multiaccess," *IEEE Trans. Wireless Commun.*, vol.1, pp.16─27, Jan. 2002.

[61] S. Hanly and D. Tse, "Power control and capacity of spread spectrum wireless networks," *Automatica,* vol.35, pp. 1987─2012, Dec. 1999.

[62] C. Lee and R. Steele, "Closed loop power control in CDMA systems," *IEE Proc. Commun*., vol.143, pp.231─239, Aug. 1996.

[63] M. Honig, and M. Tsatsanis, "Adaptive techniques for multiuser CDMA receivers," *IEEE Signal Proc. Mag*azine, vol. 45, pp. 49─61, May 2000.

[64] *WCDMA for UMTS.* Ed's H. Holma and A. Toskala, Wiley 2000.

[65] B. Sklar, "Rayleigh fading channels in mobile digital communication systems part I: characterization," *IEEE Commun. Magazine,* vol. 35, pp. 136─146, Sep. 1997.

[66] M. Elmusrati and H. Koivo, "Multi-objective distributed power control algorithm," in *Proc. IEEE Vehicular Technology Conf.,* Vancouver, Canada, Sep. 2002, pp. 812 – 816.

[67] M. Elmusrati and H. Koivo, "Kalman distributed power control algorithm," in *Proc. Int. Wireless Opt. Commun*., IASTED, Banff, Canada, pp. 52─55, July 2002.

[68] M. Elmusrati and H. Koivo, "Performance Analysis of DS-CDMA Mobile communication systems with MIMO antenna system and Power Control," in *Proc. IEEE Int. Sym. Spread Spect. Techniques Applications*, Prague, Czech Republic, Sep. 2002, pp. 541─544.

[69] M. Elmusrati and H. Koivo, "Joining Power Control and Smart Antenna Using Kalman Algorithm in CDMA Communication Systems," *In Proc. the XXVIITH general assembly of URSI*, Maastricht, Netherlands, Aug. 2002.

[70] M. Elmusrati and H. Koivo, "Convergence rate comparison of distributed power control algorithms of wireless communication" in *Proc. IASTED Int. Conf. on Commun. Syst. Networks*, Malaga, Spain, Sep. 2003, pp. 98─100.

[71] M. Elmusrati and H. Koivo, "Multi-objective distributed power and rate control for wireless communications", in *Proc. IEEE ICC*, Alaska, USA, May 2001, pp. 1838─1842.

[72] D. Zhao, *Radio Resource Management in Cellular CDMA systems supporting heterogeneous services*, Ph.D. thesis, Electrical and Computer Engineering, University of Waterloo, Ontario, Canada, 2002.

[73] U. Mitra, "Comparative study of maximum likelihood detection for two multi-rate DS/CDMA systems," in *Proc. IEEE Int. Sym. Inform. Theory*, Ulm, Germany, July 1997, pp. 352.

[74] K. Chawla and X. Qiu, "Throughput performance of adaptive modulation in cellular systems," in *Proc. IEEE Int. Conf. Universal Person. Commun*., Florence, Italy, Oct. 1998, pp. 945─950.

[75] M. Elmusrati and H. Koivo, "Centralized algorithm for the tradeoff between total throughput maximization and total power minimization in cellular systems" in *Proc. IEEE Vehicular Technology Conf.,* Orlando, USA, Oct. 2003.

[76] M. Elmusrati and H. Koivo, "New power and rate control combining algorithm for wireless communications," in *Digest. IEEE XXVII Convention on Radio Science*, Helsinki, Finland , Oct.2002, pp. 120─122.

[77] K. Miettinen, *Nonlinear multiobjective optimization,* Boston: Kluwer Academic Publishers, 1998.

[78] A. Sampath, P. Kumar, and J. Holtzman, "Power control and resource management for a multimedia CDMA wireless system," in *Proc. IEEE PIMRC*, Toronto, Canada, Sep. 1995, pp. 21─25.

[79] H. Morikawa, T. Kajiya, T. Aoyama, and A. Campbell, "Distributed power control for various QoS in a CDMA wireless system," in *Proc. IEEE PIMRC*, Helsinki, Finland, Sep. 1997, pp. 903─907.

[80] S. Kim, Z. Rosberg, and J. Zander, "Combined power control and transmission rate selection in cellular networks," in *Proc. IEEE Vehicular Technology Conf.,* Amsterdam, Netherlands, Sep. 1999, pp. 1653─1657.

[81] R. Jäntti and S. Kim, "Selective power control and active link protection for combined rate and power management," in *Proc. IEEE Vehicular Technology Conf.,* Tokyo, Japan, May 2000, pp. 1960─1964.

[82] M. Moustafa, I. Habib, M. Naghshineh, and M. Guizani, "QoS-Enabled broadband mobile access to wireline network," *IEEE Commun. Magazine*, vol. 40, pp. 50─56, Apr. 2002.

[83] F. Berggren, *Power control, transmission rate control and scheduling in cellular radio systems*, Licentiate thesis, Royal Institute of Technology, Stockholm, Sweden, 2001.

[84] S.Ulukus and L. Greenstein, "Throughput maximization in CDMA uplinks using adaptive spreading and power control," in *Proc. IEEE Int. Sym. Spread Spect. Techniques Applications*, New Jersey, USA, Sep. 2000, pp. 565─569.

[85] L. Song and N. Mandayam, "Hierarchical SIR and rate control on the forward link for CDMA data users under delay and error constraints," *IEEE J. Select. Areas Commun.*,, vol. 19, pp. 1871─1882, Oct. 2001.

[86] A. Goldsmith, S. Jafar, N. Jindal, and S. Vishwanath, "Capacity limits of MIMO channels," *IEEE J. Select. Areas in Commun.*, vol. 21, pp. 684─702, June 2003.

[87] G. Dahlquist, *Numerical Methods*, Prentice-Hall 1974.

[88] M. Elmusrati and H. Koivo, *Radio resource scheduling in wireless communication systems*, Control Engineering Laboratory Report 134, Helsinki University of Technology, Helsinki, Finland 2003.

[89] C. Coello, "A short tutorial on evolutionary multiobjective optimization," *First Int. Conf. on Evolutionary Multi-Criterion Optimization,* Springer-Verlag, , Mar. 2001, pp. 21─40.

[90] J. Choi, "A receiver of simple structure for antenna array CDMA systems," *IEEE Trans. Veh. Technol.,* vol.48, pp. 1332─1340, Sep. 1999.

[91] M. Elmusrati and H. Koivo, "Multi-path smart antenna algorithm for frequency selective channels," in *Proc. Int. ITG-Conf. on Antennas*, Berlin, Germany, pp.369─371.

[92] M. Elmusrati, R. Jäntti and H. Koivo, "Multi-rate distributed power control algorithm using Kalman filters," in *Proc. IV Finnish Wireless Commun. Workshop*, Oulu, Finland, Oct. 2003, pp.205─208.

[93] M. Elmusrati, M. Rintamäki, I. Hartimo and H. Koivo, "Estimated step power control algorithm for wireless communication systems," in *Proc. Finnish Signal Processing Sym*., Tampere, Finland, May 2003, pp. 32─34.

[94] M. Elmusrati, M. Rintamäki, I. Hartimo and H. Koivo, "Fully distributed power control algorithm with one bit signaling and nonlinear error estimation," in *Proc. IEEE Vehicular Technology Conf.,* Orlando, USA, Oct. 2003.

[95] J. Zander, "Multirate resource management in wireless CDMA systems," published slides on the internet at address: http://www.s3.kth.se/%7Ejensz/MultirateCDMA00.pdf.

[96] G. Liu, J. Yang, and J. Whidborne, *Multiobjective optimisation and control.* Baldock: Research Studies Press LTD, 2003.

[97] M. Elmusrati and H. Koivo, "Multi-Objective approach of distributed power control in wireless communication" *submitted IEEE Trans. Veh. Technol.*

[98] M. Elmusrati and H. Koivo, "Applications of multi-objective optimization in radio resource management of wireless communication systems," *Submitted IEEE Trans. On Wireless Commun.*

[99] M. Elmusrati, R. Jäntti, and H. Koivo, "MAC layer design for intensive ad hoc networks with multi-channel coded UWB-TH-CDMA radio," *Submitted IEEE Int. Sym. Spread Spect. Techniques Applications,* Sydney, Australia.

[100] P. Ligdas and N. farvardin, "Optimizing the transmit power for slow fading channels," *IEEE Trans. On Inform. Theory,* vol. 46, pp. 265─276, Mar.2000.

[101] J. Chamberland and V. Veeravalli, "Decentralized dynamic power control for cellular CDMA systems," *IEEE Trans. On Wireless Commun.,* vol. 2, pp. 549─559, May 2003.

[102] M. Elmusrati, N. Tarhuni, R. Jäntti, and H. Koivo, "Distributed minimum outage removal algorithm for multi-rate CDMA wireless communication systems," *In Proc. 6th Nordic Signal Processing Sympisium NORSIG,* Espoo, Finland, June 9-11, 2004

[103] G. Janssen and J. Zander, "Power control and stepwise removal algorithms for a narrowband multiuser detector in a cellular system," in *Proc. IEEE ICC*, New York, USA, May 2002, pp. 345─350.

[104] T. Jiang, N. Sidiropoulos, and G. Giannakis, "Kalman filtering for power estimation in mobile communication," *IEEE Trans. On Wireless Commun*., vol. 2, pp. 151─161, Jan. 2003.

[105] K. Leung, "Power control by interference prediction for broadband wireless packet networks," IEEE Trans. On Wireless Communi., vol. 1, pp. 256─265 Apr. 2002.

[106] K. Shoarinejad, J. Speyer, and G. Pottie, "Integrated predictive power control and dynamic channel assignment in mobile radio systems," *IEEE Trans. Wireless Commun*., vol. 2, pp. 976─988, Sep. 2003.

[107] J. Cheng and N. Beaulieu, "Accurate DS-CDMA bit-error probability calculation in Rayleigh fading," *IEEE Trans. Wireless Commun.*, vol. 1, Jan. 2002.

[108] M. Elmusrati and H. Koivo, "Minimum variance power and rate control algorithm," *Accepted for publication in Int. Wireless Opt. Commun*., IASTED, Banff, Canada, July 2004.

[109] M. Elmusrati and H. Koivo, "Influence of Smart Antenna Systems on the Performance of Radio Resource Scheduling in CDMA Cellular Systems," *Accepted for publications in the International Symposium on Wireless Communication Systems, ISWCS 2004.*

[110] M. Elmusrati and R. Jäntti, "Comments on fast convergence distributed power algorithm for WCDMA systems," *submitted to IEE Proc. Commun.*

[111] R. Morrow, "Accurate CDMA BER calculations with low computational complexity," *IEEE Trans. On Commun*. Vol. 46, Nov. 1998.

[112] M. Elmusrati and H. Koivo, "Kalman Filters Applications in Radio Resource Scheduling of Wireless Communication," *Accepted for publication in IEEE Workshop on Signal Processing Advances in Wireless Communications* 2004

[113] M. Elmusrati and H. Koivo, "Maximum throughput beamforming algorithm," *To be submitted to IEEE ICC 2005*

[114] M. Elmusrati, N. Tarhuni, R. Jäntti, and H. Koivo, " Multi-channel coded UWB-TH-CDMA radio interference for sensor networks," *ready manuscript*.

[115] H. Shin and J. Lee, "Capacity of multiple-antenna fading channels: spatial fading correlation, double scattering, and keyhole," *IEEE Trans. Inform. Theory*, vol.49, pp.2636─2647, Oct. 2003.

[116] D. Palomar and M. Lagunas, "Joint transmit-receive space-time equalization in spatially correlated MIMO channels: a beamforming approach," *IEEE J. Select. Areas Commun.,* vol. 21, pp. 730─743, June 2003.

[117] M. Elmusrati, R. Jäntti, and H. Koivo, "Distributed removal algorithms for multi-rate CDMA wireless communication systems," *Accepted for publication in IEEE VTC- Fall 2004.*

HELSINKI UNIVERSITY OF TECHNOLOGY CONTROL ENGINEERING LABORATORY

Editor: H. Koivo

Report 129 Elmusrati, M. S.
Power Control and MIMO Beamforming in CDMA Mobile Communication Systems. August 2002.

Report 130 Pöyhönen, S., Negrea, M., Arkkio, A., Hyötyniemi, H.
Comparison of Reconstruction Schemes of Multiple SVM's Applied to Fault Classification of a Cage Induction Motor. August 2002.

Report 131 Pöyhönen, S.
Support Vector Machines in Fault Diagnostics of Electrical Motors. September 2002.

Report 132 Gadoura, I. A.
Design of Robust Controllers for Telecom Power Supplies. September 2002.

Report 133 Hyötyniemi, H.
On the Universality and Undecidability in Dynamic Systems. December 2002.

Report 134 Elmusrati, M. S., Koivo, H. N.
Radio Resource Scheduling in Wireless Communication Systems. January 2003.

Report 135 Blomqvist, E.
Security in Sensor Networks. February 2003.

Report 136 Zenger, K.
Modelling, Analysis and Controller Design of Time-Variable Flow Processes. March 2003.

Report 137 Hasu, V.
Adaptive Beamforming and Power Control in Wireless Communication Systems. August 2003.

Report 138 Haavisto, O., Hyötyniemi, H.
Simulation Tool of a Biped Walking Robot Model. March 2004.

Report 139 Halmevaara, K., Hyötyniemi, H.
Process Performance Optimization Using Iterative Regression Tuning. April 2004.

Report 140 Viitamäki, P.
Hybrid Modeling of Paper Machine Grade Changes. May 2004.

Report 141 Pöyhönen, S.
Support Vector Machine Based Classification in Condition Monitoring of Induction Motors. June 2004.

Report 142 Elmusrati, M. S.
Radio Resource Scheduling and Smart Antennas in Cellular CDMA Communication Systems. August 2004.

ISBN 951-22-7219-9

ISSN 0356-0872

Picaset Oy, Helsinki 2004